THESE

Pour l'obtention du grade de

DOCTEUR D'AIX MARSEILLE UNIVERSITE

Spécialité: MECANIQUE ET PHYSIQUE DES FLUIDES

Ecole Doctorale 353, Sciences pour l'Ingénieur: Mécanique, Physique, Micro et Nanoélectronique

DOMAINE DE RECHERCHE : MECANIQUE DES SOLIDES, ECOULEMENTS DIPHASIQUES

Présentée par

Serge NDANOU

Etude Mathématique et Numérique des Modèles Hyperélastiques et Visco-plastiques: Applications aux Impacts Hypervéloces

Directeur de thèse: M. Sergey GAVRILYUK

Co-directeur de thèse: M. Nicolas FAVRIE

JURY

M. Rémi ABGRALL	Professeur, Université de Zurich	Rapporteur
M. Bruno DESPRES	Professeur, Université de Paris 6	Rapporteur
M. Pierre-Henri MAIRE	Professeur, CEA-CESTA	Examinateur
M. Géry de SAXCE	Professeur, Université de Lille1	Examinateur
M. Jean-Paul VILA	Professeur, INSA Toulouse	Examinateur

Table des Matières

Chapitre 1

Introduction

1.1 Objectifs de la thèse

Le but de cette thèse est l'étude mathématique et numérique d'un solide déformable (ou d'un système de plusieurs solides déformables en interaction) soumis de grandes sollicitations dans un milieu compressible (gaz ou liquide). On peut citer comme exemple les déformations provoquées par l'impact d'un projectile sur une plaque (Figure 1.1) ou celui d'un débris spatial sur un satellite (Figure 1.2). Enfin, la catastrophe nucléaire de Tchernobyl est l'exemple des plus représentatifs d'interaction entres de multiples solides et fluides (Figure 1.3).

L'importance de ce sujet pour les applications civiles et militaires peut être démontrée sur l'exemple du projet américain PSAAP: Predictive Science Academic Alliance Program (http://www.psaap.caltech.edu). Ce projet regroupe les universités américaines les plus renommées (Caltech, Stanford, Texas, Michigan) et les laboratoires de la défense (Sandia National Laboratories, Los Alamos National Laboratory, Lawrence Livermore National Laboratory) dotés chacun d'environ 3.5M$ par an. Un des objectifs de PSAAP est, en particulier, le calcul numérique de la dynamique d'impacts hypervéloces directs et obliques (jusqu'à 10 km/s) de projectiles métalliques. Les phénomènes physiques qui apparaissent pendant l'impact sont multiples: transition de phase solide-liquide, déformations à grande vitesse, couplage thermo-mécanique, fissuration et fragmentation, écaillage, instabilités hydrodynamiques. A l'heure actuelle, aucun modèle ni code de calcul n'est capable de résoudre ces problèmes multi-physiques, multi-matériaux et multi-échelles en présence d'interfaces mobiles.

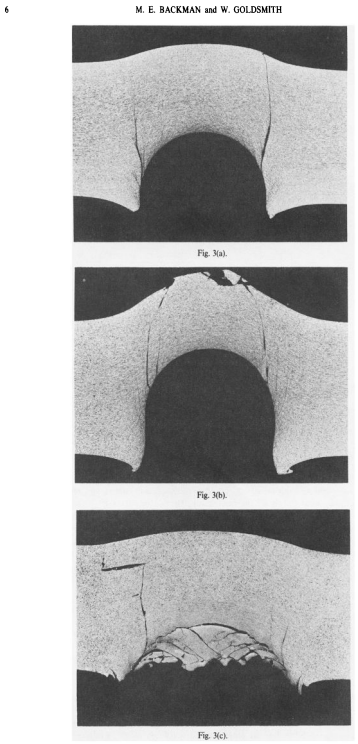

Figure 1.1: Impact d'un projectile sur une plaque (M. E. Backman & W. Goldsmith, 1978).

Figure 1.2: Impact d'un débris sur la paroi d'un satellite artificiel.

Figure 1.3: Explosion de la centrale nucléaire de Tchernobyl.

La formulation de modèles élastoplastiques en grandes déformations remonte aux années 50-60 (Taylor (1948), Wilkins (1964), etc.).

Les premiers développements de méthodes numériques dans ce cadre reposaient exclusivement sur l'utilisation de lois constitutives basées sur l'approche *hypoélastique*. Dans cette approche, les modèles élastoplastiques standards en petites déformations sont étendus aux grandes déformations en reformulant les équations d'évolution des contraintes au moyen de dérivées objectives dont la fonction est d'assurer l'invariance par changement de référentiel de la loi constitutive. Cette méthodologie a donné lieu à d'intenses débats et contreverses dans la communauté des mécaniciens portant non seulement sur la nature du choix de cette dérivée objective mais aussi sur les difficultés numériques à maintenir l'objectivité de la loi de comportement au niveau de la discrétisation en temps. En dépit de leur relative simplicité, les modèles élastoplastiques basés sur l'approche hypoélastique sont généralement incapables de prendre en compte un comportement réversible du matériau et ce, même en l'absence d'écoulement plastique. En d'autres termes, un comportement dissipatif peut être prédit dans les phases de comportement élastique. Ce défaut met en évidence l'inconsistance thermodynamique de cette approche vis-à-vis du second principe de la thermodynamique (non préservationde l'entropie dans les transformations réversibles d'un matériau) (Gavrilyuk *et al.* (2008), P.H. Maire *et al.* (2013)). Soulignons qu'en dépit de ces désavantages, les modèles basés sur l'approche hypoélastique sont massivement utilisés par les chercheurs et les ingénieurs et constituent bien souvent la seule option disponible dans les codes par 'éléments finis'

de production.

Pour pallier les difficultés précédemment évoquées, il est possible de recourir à une autre classe de modèles dits *hyperélastiques*. Ces modèles sont caractérisés par un tenseur des contraintes obtenu par la variation de l'énergie interne du solide. La formulation des équations se fait en déformations. Les modèles hyperélastiques connaissent un essor particulier ces derniers temps (Godunov (1978), Godunov & Romenskii (2003), Miller et Collela (2001), Gavrilyuk, Favrie & Saurel (2008, 2009), Kluth & Després (2008,) Godunov & Peshkov (2010), Gorsse, Iollo, Milcent & Telib (2014), etc.). Cette approche garantit l'invariance de la loi de comportement par changement de référentiel. De plus, la formulation mathématique correspondante est intrinsèquement conservative. Un seul bémol est l'hyperbolicité des équations qui est necéssaire pour que le modèle soit 'bien posé'.

Le critère de l'hyperbolicité est bien connu: l'énergie spécifique doit être une fonction convexe de rang un par rapport au gradient de déformation (Dafermos (2010)). Mais cette condition est difficile (voir impossible) à vérifier pour les équations d'états physiques 'classiques'. Par contre, pour une classe d'équations d'états sous forme 'séparable' où l'énergie spécifique est la somme d'une énergie 'hydrodynamique' qui ne dépend que de la densité et de l'entropie, et d'une énergie de 'cisaillement' qui ne dépend plus que du tenseur des déformations de Finger réduit, ce critère est plus facile à vérifier. Cette classe d'équations d'état sous forme séparable sera utilisée dans la thèse.

La mise en équations de phénomènes physiques comme la plasticité et l'écrouissage pour cette classe de modèles est présentée dans Miller & Collela (2001), Godunov & Romenskii (2003), Barton, Drikakis & Romenski (2010), Favrie & Gavrilyuk (2011), Barton, Deiterding, Meiron & Pullin (2013), etc.

Pour le traitement numérique de l'interaction solide-solide, fluide-solide ou fluide-fluide, de nombreuses méthodes existent. L'approche la plus fréquente est le couplage de deux ou plusieurs codes. Pour chaque composante, un code de calcul spécifique est utilisé et la difficulté consiste à faire transiter l'information d'un code à l'autre. Les codes ne fonctionnent pas simultanément mais successivement. Cette approche a été développée avec succès pour des applications en aéroélasticité (Farhat *et al.* (1998)), dans le domaine automobile (Le Tallec & Mouro (1996)). Les codes Abaqus et Fluent ont récemment été couplés par cette stratégie. Cette approche est très efficace en présence d'interfaces se déformant peu. Dans le cas des grandes

déformations ou en présence de sollicitations de grandes amplitudes, cette approche introduit des erreurs numériques importantes (pertes d'énergie à l'interface) qui peut être fatale pour la simulation des impacts [voir la discussion dans Piperno & Farhat (1997, 2000)].

Ces méthodes numériques ne permettent pas de traiter l'apparition dynamique d'interfaces, que ce soit dans les fluides (cavitation) ou dans les solides (fissuration et formation d'écailles). L'apparition dynamique d'interface peut malgré tout se faire par la Méthode de Transport Optimal (Li *et al.* (2010, 2012)) basée sur la discrétisation de l'action d'Hamilton pour les solides élastiques, où un algorithme spécifique de fragmentation du solide est ajouté. Une autre approche a été utilisée par Barton *et al.* (2013), où la fragmentation est régie par une régularisation dans une méthode 'level set'. Pour toutes ces raisons, nous avons choisi d'utiliser la méthode d'interfaces diffuses pour nos simulations numériques. La principale difficulté de ce type méthodes est le traitement des cellules de mélange situées sur l'interface entre les composantes, dans lesquelles il faut déterminer les propriétés thermodynamiques du mélange artificiel et satisfaire les conditions d'interface. Les premiers travaux sur ces mailles de mélanges, considérées comme 'interfaces diffuses' ont été menés pour les interfaces fluides-fluides par Karni (1994), Abgrall (1996), Saurel & Abgrall (1999), Abgrall & Karni (2001). Cette méthode a ensuite été largement utilisée dans l'équipe SMASH, dans laquelle cette thèse a été réalisé, pour traiter des problèmes plus complexes parmi lesquels nous pouvons citer: le traitement des réactions chimiques dans les fronts de détonation (Saurel & Le Metayer (2001)), les effets de tension de surface dans les fluides compressibles (Perigaud & Saurel (2005)), les transitions de phase (Saurel, Petipas & Abgrall (2008), Saurel, Petipas & Berry (2009)). L'approche des interfaces diffuses a été généralisée pour les interactions fluide-solide (Favrie, Gavrilyuk & Saurel (2009), Favrie & Gavrilyuk (2012)). Cette généralisation n'est pas triviale car le nombre d'équations pour le traitement des fluides et des solides n'est pas le même (5 equations pour le fluide et 14 quations pour le solide), et les conditions aux limites sur les interfaces sont différentes. L'avantage principal de cette approche est de résoudre les mêmes équations avec le même schéma numérique dans tout le domaine de calcul y compris au voisinage des interfaces. Les conditions aux limites aux interfaces sont incluses de façon naturelle dans la formulation.

Cette thèse est constituée principalement de deux parties:

- L'étude mathématique du modèle hyperélastique sous la forme pro-

posée par Gavrilyuk, Favrie & Saurel (2008). Plus précisément, les efforts ont porté sur les points suivants:

  - La formulation d'un critère de l'hyperbolicité pour ce modèle plus facile à vérifier 'en pratique'.
  - La résolution exacte du problème de Riemann associé à ce modèle qui servira comme solution de référence pour les codes de calcul;
  - Le développement d'une procédure de 'splitting' pour un meilleur traitement numérique de ce modèle.

- L'extension du modèle proposé par Favrie & Gavrilyuk (2012) pour l'interaction 'fluide' – 'solide visco-plastique' au cas de présence d'un nombre arbitraire de fluides et de solides, et l'application aux problèmes de type 'impacts hypervéloces'.

Les résultats obtenus au cours de ces travaux ont donné lieu à la rédaction et publication de plusieurs articles dans les revues internationales:

- Ndanou, Favrie & Gavrilyuk (2014a);
- Ndanou, Favrie & Gavrilyuk (2014b, papier soumis à Mathematics and Mechanics of Solids);
- Ndanou, Favrie & Gavrilyuk (2014c, papier soumis à Journal of Computational Physics);
- Favrie, Gavrilyuk & Ndanou (2014).

1.2 Étude mathématique du modèle hyperélastique

Nous rappelons ici le modèle hyperélastique conservatif (Gavrilyuk *et al.* (2008)):

$$\frac{\partial \rho}{\partial t} + div\left(\rho \mathbf{u}\right) = 0, \tag{1}$$

$$\frac{\partial (\rho \mathbf{u})}{\partial t} + div\left(\rho \mathbf{u} \otimes \mathbf{u} - \boldsymbol{\sigma}\right) = 0,$$

$$\frac{\partial \rho \left(e+\frac{1}{2}\left|\mathbf{u}\right|^{2}\right)}{\partial t}+div\left(\rho\left(e+\frac{1}{2}\left|\mathbf{u}\right|^{2}\right)\mathbf{u}-\boldsymbol{\sigma}\mathbf{u}\right)=0,$$

$$\frac{\partial \mathbf{e}^{\beta}}{\partial t}+\bigtriangledown\left(\mathbf{u}\cdot\mathbf{e}^{\beta}\right)=0,\quad \mathbf{rot}(\mathbf{e}^{\beta})=0,\qquad \beta=1,2,3.$$

Les opérateurs div, rot et $\bigtriangledown$ sont appliqués dans les coordonnées eulériennes $\mathbf{x}=(x,y,z)^{T}$. Ici, ρ est la densité du solide, $\mathbf{u}=(u,v,w)^{T}$ est le champ de vitesse, $\boldsymbol{\sigma}$ est le tenseur des contraintes de Cauchy défini par:

$$\boldsymbol{\sigma}=-2\rho\frac{\partial e}{\partial \mathbf{G}}\mathbf{G},$$

où

$$\mathbf{G}=\left(\mathbf{F}\mathbf{F}^{T}\right)^{-1}$$

est le tenseur de Finger, et $\mathbf{F}$ est le gradient des déformations. Dans le cas des solides isotropes, $\boldsymbol{\sigma}$ est symétrique. Les vecteurs $\mathbf{e}^{\beta}$ sont les colonnes de $\mathbf{F}^{-T}$:

$$\mathbf{F}^{-T}=\left(\mathbf{e}^{1},\mathbf{e}^{2},\mathbf{e}^{3}\right).$$

Les vecteurs $\mathbf{e}^{\beta}$ sont les gradients des coordonnées de Lagrange. L'équation $rot(\mathbf{e}^{\beta})=0$ est donc une condition de compatibilité. Cette condition est invariante par rapport au temps: si elle est vérifiée initialement, alors elle est vérifiée quel que soit le temps $t>t_{0}$, avec t_{0} le temps initiale (Miller & Collela, (2001), Gavrilyuk *et al.* (2008)). L'énergie interne spécifique e est une fonction des invariants de $\mathbf{G}$. Nous la prenons sous une forme séparable (Flory (1961)):

$$e=e^{h}\left(\rho,\eta\right)+e^{e}\left(\mathbf{g}\right),$$

où e^{h} represente l'énergie interne hydrodynamique, e^{e} l'énergie interne élastique et,

$$\rho=\rho_{0}\left|\mathbf{G}\right|^{1/2},\qquad \left|\mathbf{G}\right|=\det\mathbf{G},\qquad \mathbf{g}=\frac{\mathbf{G}}{\left|\mathbf{G}\right|^{1/3}}.$$

Ici ρ_{0} est la densité initiale et η est l'entropie spécifique. Pour simplifier la présentation, nous allons considérer le cas où ρ_{0} est homogène. Cette forme nous permet d'écrire:

$$\boldsymbol{\sigma}=-p\mathbf{I}+\mathbf{S},\qquad tr\left(\mathbf{S}\right)=0,$$

avec

$$p=\rho^{2}\frac{\partial e^{h}(\rho,\eta)}{\partial \rho}$$

$$\mathbf{S} = -2\rho \frac{\partial e^e}{\partial \mathbf{G}} \mathbf{G}$$

Remarquons que la pression p est uniquement déterminée par la partie hydrodynamique de l'énergie e^h. Pour les solides isotropes, l'énergie de cisaillement e^e peut être écrite comme une fonction des deux invariants de $\mathbf{g}$:

$$e^e(\mathbf{g}) = e^e(j_1, j_2)$$

où

$$j_1 = tr(\mathbf{g}) = \frac{J_1}{|\mathbf{G}|^{1/3}}, \quad j_2 = tr(\mathbf{g}^2) = \frac{J_2}{|\mathbf{G}|^{2/3}}, \; J_i = tr\left(\mathbf{G}^i\right), \; i = 1, 2.$$

Cela implique:

$$\mathbf{S} = -2\rho \frac{\partial e^e}{\partial \mathbf{G}} \mathbf{G} = -2\rho \left(\frac{\partial e^e}{\partial j_1} \left(\mathbf{g} - \frac{j_1}{3} \mathbf{I} \right) + 2 \frac{\partial e^e}{\partial j_2} \left(\mathbf{g}^2 - \frac{j_2}{3} \mathbf{I} \right) \right).$$

Pour les applications, nous prenons:

$$e^h(\rho, \eta) = \frac{A \exp\left(\frac{\eta - \eta_0}{c_v}\right) \rho^\gamma + (\gamma - 1) p_\infty}{(\gamma - 1)\rho}, \tag{2}$$

$$e^e(\mathbf{g}) = \frac{\mu}{4\rho_0} (j_2 - 2j_1 + 3). \tag{3}$$

Ici, A, η_0, $p_\infty(Pa)$, $\gamma > 1$, $c_v(J \cdot kg^{-1} \cdot K^{-1})$, $\mu(Pa)$, et $\rho_0(Kg/m^3)$ sont des constantes. En particulier, à la limite des petites déformations, cette loi permet de retrouver la loi de Hooke. Dans le cas des grandes sollicitations, la partie isochore de l'énergie e^e est négligeable par rapport à la partie hydrodynamique e^h, c'est-à-dire que le tenseur des contraintes est presque sphérique.

Le tenseur de Finger peut aussi s'écrire:

$$\mathbf{G} = \sum_{\beta=1}^{3} \mathbf{e}^\beta \otimes \mathbf{e}^\beta$$

Dans la base cartésienne $(\mathbf{i}, \mathbf{j}, \mathbf{k})$, les vecteurs $\mathbf{e}^\beta$ ont les composantes $\left(a^\beta, b^\beta, c^\beta\right)^T$, $\beta = 1, 2, 3$. Introduisons les vecteurs $\mathbf{a} = (a^1, a^2, a^3)^T$, $\mathbf{b} = (b^1, b^2, b^3)^T$, $\mathbf{c} = (c^1, c^2, c^3)^T$. Evidemment:

$$F^{-1} = (\mathbf{a}, \mathbf{b}, \mathbf{c}), \qquad F^{-T} = \begin{pmatrix} \mathbf{a}^T \\ \mathbf{b}^T \\ \mathbf{c}^T \end{pmatrix}$$

Le tenseur $\mathbf{G}$ est donc la matrice de Gram des vecteurs $\mathbf{a}$, $\mathbf{b}$, $\mathbf{c}$:

$$\mathbf{G} = F^{-T}F^{-1} = \begin{pmatrix} \|\mathbf{a}\|^2 & \mathbf{a}\cdot\mathbf{b} & \mathbf{a}\cdot\mathbf{c} \\ \mathbf{a}\cdot\mathbf{b} & \|\mathbf{b}\|^2 & \mathbf{b}\cdot\mathbf{c} \\ \mathbf{a}\cdot\mathbf{c} & \mathbf{b}\cdot\mathbf{c} & \|\mathbf{c}\|^2 \end{pmatrix}.$$

1.2.1 Critère d'hyperbolicité

Ceci correspond au chapitre 2 de la thèse

L'hyperbolicité est une propriété importante pour les modèles hyperélastiques car elle permet de garantir, au moins localement, que le problème de Cauchy que l'on résout est bien posé. Le critère d'hyperbolicité de l'hyperélasticité est connu sous le nom de condition de Legendre-Hadamard (voir Dafermos (2010)). Elle s'écrit:

$$\sum_{i,j=1}^{d}\sum_{\alpha,\beta,=1}^{d}\frac{\partial^2 e\left(\mathbf{F},\eta\right)}{\partial F_{i\alpha}\partial F_{j\beta}}\nu_\alpha\nu_\beta\xi_i\xi_j > 0, \qquad \text{pour tout } \boldsymbol{\nu} \text{ et } \boldsymbol{\xi} \text{ dans } \Omega^{d-1}, \tag{4}$$

où d est la dimension de l'espace $\mathbf{R}^d$, e est l'énergie interne spécifique et Ω^{d-1} la sphère unité de $\mathbf{R}^d$. Ce critère est aussi appelé, en quasi statique, critère d'ellipticité (Ball (1977), Wang & Aron (1996), Dacarogna (2001), Sfyris (2011), Tommasi *et al.* (2012)), mais ces conditions restent difficiles à vérifier même pour un modèle où l'énergie interne s'écrit sous forme séparable.

Nous proposons dans ce travail un nouveau critère d'hyperbolicité pour une équation d'état donnée sous forme séparable. Il s'énonce de la façon suivante.

Nous notons $\Delta = det(\mathbf{F}^{-1}) = \mathbf{a}.(\mathbf{b}\wedge\mathbf{c}) > 0$. Introduisons l'énergie volumique de cisaillement $E = \Delta e^e$. Soit E'' la matrice Hessienne de E par rapport au vecteur $\mathbf{a}$.

Supposons que

- $$c^2 = \frac{\partial p}{\partial \rho} > 0, \qquad \frac{\partial p}{\partial \eta} > 0,$$
- $\mathbf{M} = \Delta^{-1}\mathbf{F}^{-T}E''\mathbf{F}^{-1}$ *défini positif sur toutes les surfaces* (S_α), $0 \leq \alpha < 1$ *définies par*:

$$(S_\alpha) : X^2 + Y^2 + Z^2 - 2XYZ - \alpha = 0,$$

avec,

$$X = \frac{\mathbf{a}^{'} \cdot \mathbf{b}^{'}}{||\mathbf{a}^{'}||||\mathbf{b}^{'}||}, \quad Y = \frac{\mathbf{a}^{'} \cdot \mathbf{c}^{'}}{||\mathbf{a}^{'}||||\mathbf{c}^{'}||}, \quad Z = \frac{\mathbf{b}^{'} \cdot \mathbf{c}^{'}}{||\mathbf{b}^{'}||||\mathbf{c}^{'}||}$$

où

$$\mathbf{a}^{'} = \frac{\mathbf{a}}{\Delta^{\frac{1}{3}}}, \quad \mathbf{b}^{'} = \frac{\mathbf{b}}{\Delta^{\frac{1}{3}}}, \quad \mathbf{c}^{'} = \frac{\mathbf{c}}{\Delta^{\frac{1}{3}}}.$$

Alors le modèle est hyperbolique.

Nous avons proposé une loi qui vrifie ce critère:

$$e^e(\mathbf{g}) = \frac{\mu}{8\rho_0}(j_2 - 3). \tag{5}$$

A la limite des petites déformations, on retrouve la loi de Hooke. Le modèle est hyperbolique quelles que soient les déformations. C'est cette loi qui sera utilisée pour nos applications numériques.

Une extension de cette loi (avec une preuve numérique) est donnée par:

$e^e(\mathbf{g}) = \frac{\mu}{4\rho_0}(aj_2+(2-4a)j_1+3(3a-2)), \quad a$ étant dans un voisinage de $0,5$.

Cette famille d'équations d'états vérifie les propriétés suivantes:

- La loi de Hooke est retrouvée dans la limite des petites déformations.
- Le modèle est hyperbolique quelles que soient les déformations.

Le paramètre 'a' a une influence sur la non-linéarité de la partie déviatorique du tenseur des contraintes $\mathbf{S}$. Si on prend $a = 1$, on retrouve l'équation d'état utilisée par Gavrilyuk *et al.* (2008). Si on prend $a = 0.5$, on retrouve l'équation d'état (5) qui sera utilisée pour les applications numériques.

1.2.2 Le problème du piston en hyperélasticité

Ceci correspond au chapitre 3 de la thèse

Dans le but de valider les résultats obtenus par la résolution numérique, il est nécessaire d'avoir des solutions de 'références'. Nous utiliserons des solutions exactes de problèmes de Riemann. Pour les équations d'Euler des fluides compressibles, la résolution du problème de Riemann est assez

simple. Dans le cas de l'élasticité, le nombre et la structure des ondes (2 ondes longitudinales, 4 ondes transversales et une discontinuité de contact) rendent le problème de Riemann impossible à résoudre analytiquement dans le cas général. Pour cette raison, nous avons résolu un problème plus simple appelé le 'problème du piston' (ou demi-problème de Riemann) (voir Figure 1.4).

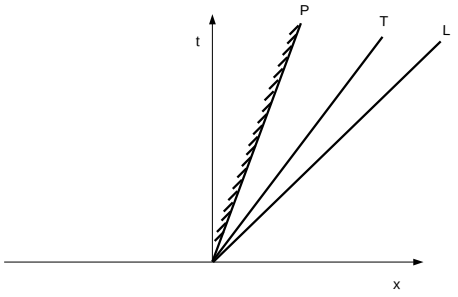

Figure 1.4: Le piston (P) est initialement positionné à $x = 0$ et 'collé' à un solide élastique au repos, libre de contraintes, situé à $x > 0$. Le piston commence à se déplacer à l'instant $t = 0$ avec un champ de vitesse imposé (u_p, v_p). Deux ondes vont ainsi se propager dans le solide: une onde longitudinale plus rapide (L), suivie d'une onde transversale moins rapide (T). Le problème du piston consiste à déterminer les valeurs des variables physiques après le passage de chacune de ces ondes.

La résolution du problème de Riemann dans le cadre de l'élasticité a donné lieu à de nombreux travaux: Kulikovskii & E. Sveshnikova (1995), Kulikovskii & Chugainova (2000), Garaizar (1991), Barton *et al.* (2009).

Il permet entre autres l'étude de la structure des différents types d'ondes présentes dans le modèle, ce qui débouche sur la construction de solveurs robustes et efficaces que nous utilisons dans les codes.

Les vitesses d'ondes sont données explicitement:

- $\nu_L = u \pm \sqrt{\frac{tr(\mathbf{K})+\sqrt{\Delta}}{2}}$
- $\nu_T = u \pm \sqrt{\frac{tr(\mathbf{K})-\sqrt{\Delta}}{2}}$

- $\nu_C = u$

où 'L', 'T' et 'C' signifient respectivement 'longitudinale', 'transversale', et 'discontinuité de contact' avec:

$$\mathbf{K} = \begin{pmatrix} c^2 & 0 \\ 0 & 0 \end{pmatrix} + \mathbf{M},$$

$$\mathbf{M} = \begin{pmatrix} \dfrac{\partial e^e}{\partial \mathbf{a}} \cdot \mathbf{a} + \dfrac{\partial}{\partial \mathbf{a}} \left(\dfrac{\partial e^e}{\partial \mathbf{a}} . \mathbf{a} \right) \cdot \mathbf{a} & \dfrac{\partial e^e}{\partial \mathbf{a}} \cdot \mathbf{b} + \dfrac{\partial}{\partial \mathbf{a}} \left(\dfrac{\partial e^e}{\partial \mathbf{a}} \cdot \mathbf{b} \right) \cdot \mathbf{a} \\ \dfrac{\partial e^e}{\partial \mathbf{a}} \cdot \mathbf{b} + \dfrac{\partial}{\partial \mathbf{a}} \left(\dfrac{\partial e^e}{\partial \mathbf{a}} \cdot \mathbf{b} \right) \cdot \mathbf{a} & \dfrac{\partial}{\partial \mathbf{a}} \left(\dfrac{\partial e^e}{\partial \mathbf{a}} \cdot \mathbf{b} \right) \cdot \mathbf{b} \end{pmatrix},$$

$$\Delta = (tr(\mathbf{K}))^2 - 4det(\mathbf{K}) = (K_{11} - K_{22})^2 + 4K_{12}^2,$$

$\mathbf{a} = (a^1, a^2)^T$ et $\mathbf{b} = (0, 1)^T$.

Les ondes longitudinales sont semblables aux ondes de pression en dynamique des gaz. Par contre, le champ associé à l'onde transversale (voir Figure 3.1) n'est pas vraiment non-linéaire au sens de Lax. Ce résultat est concordant avec des résultats de Miller & Collela (2003).

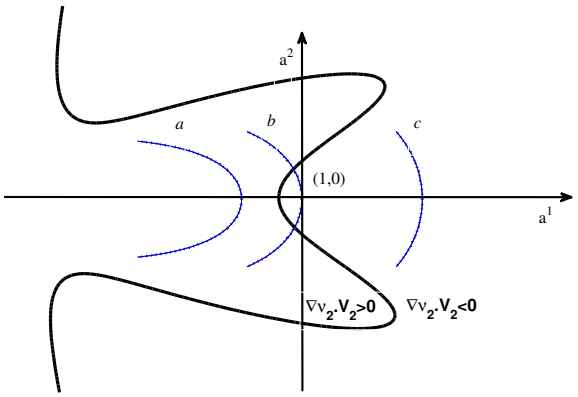

Figure 1.5: La courbe où $\nabla\nu_2.\mathbf{V}_2\big|_{\rho=\rho_0 a^1} = 0$ est représentée en trait gras ('2' correspond au signe 'moins' dans l'expression pour la vitesse ν_T. Les courbes en pointillé correspondent aux lignes de niveau de l'invariant de Riemann correspondant.

Un résultat remarquable de cette étude est la présence d'ondes de choc transversales de 'détente': à travers ces ondes, la densité diminue de manière discontinue.

1.2.3 Une procédure de splitting en hyperélasticité

Ceci correspond au chapitre 4 de la thèse

L'utilisation du solveur HLLC (Toro (2009)) permet de capturer à la fois les ondes longitudinales et les ondes de cisaillement. Ces dernières ont en général une petite amplitude. En conséquence, ces ondes transversales sont très diffusées (voir Gavrilyuk *et al.* (2008)). Pour réduire cette diffusion numérique, une procédure de splitting a été établie. Ceci a été possible grâce à la forme non conservative des équations de la cobase $\mathbf{e}^\beta, \beta = 1, 2, 3$ qui s'écrit:

$$\frac{D\mathbf{e}^\beta}{Dt} + \left(\frac{\partial \mathbf{u}}{\partial \mathbf{x}}\right) \mathbf{e}^\beta = 0, \quad \beta = 1, 2, 3. \tag{6}$$

La procédure de splitting consiste en la résolution numérique de 3 sous-modèles. Chacun des sous-modèles contient un seul type d'onde (soit une onde longitudinale, soit une onde transversale). Ces modèles vérifient aussi les propriétés suivantes :

- les sous-systèmes sont hyperboliques si le système complet est hyperbolique.
- les sous-systèmes sont thermodynamiquement compatibles.
- les vitesses d'ondes sont données sous forme explicite.
- les sous-systèmes ont une structure similaire aux équations d'Euler (isentropique ou pas).

Les différents sous-modèles s'écrivent (dans le cas $1D$):

- Sous-modèle 1

$$\begin{cases} \dfrac{\partial \rho}{\partial t} + \dfrac{\partial(\rho u)}{\partial x} = 0, \\ \dfrac{\partial (\rho u)}{\partial t} + \dfrac{\partial(\rho u^2 + p - S_{11})}{\partial x} = 0, \\ \dfrac{\partial (\rho v)}{\partial t} + \dfrac{\partial(\rho uv)}{\partial x} = 0, \quad \dfrac{\partial (\rho w)}{\partial t} + \dfrac{\partial(\rho uw)}{\partial x} = 0, \\ \dfrac{\partial a^\beta}{\partial t} + \dfrac{\partial \left(u a^\beta\right)}{\partial x} = 0, \quad \beta = 1,2,3 \\ \dfrac{Db^\beta}{Dt} = 0, \quad \dfrac{Dc^\beta}{Dt} = 0, \quad \beta = 1,2,3 \\ \dfrac{D\eta}{Dt} = 0. \end{cases} \tag{7}$$

Les vitesses d'ondes associées sont:

$$\begin{cases} \lambda = u \pm \sqrt{\dfrac{\partial p}{\partial \rho} - \dfrac{\partial S_{11}}{\partial \rho} - \dfrac{1}{\rho}\left(\dfrac{\partial S_{11}}{\partial \mathbf{a}} \cdot \mathbf{a}\right)} \\ \lambda = u \end{cases}$$

- Sous-modèle 2

$$\begin{cases} \dfrac{\partial \rho}{\partial t} = 0, \quad \dfrac{\partial (\rho u)}{\partial t} = 0, \\ \dfrac{\partial (\rho v)}{\partial t} + \dfrac{\partial(-S_{12})}{\partial x} = 0, \quad \dfrac{\partial (\rho w)}{\partial t} = 0, \\ \dfrac{\partial a^\beta}{\partial t} + b^\beta \dfrac{\partial v}{\partial x} = 0, \quad \beta = 1,2,3 \\ \dfrac{\partial b^\beta}{\partial t} = 0, \quad \dfrac{\partial c^\beta}{\partial t} = 0, \quad \beta = 1,2,3 \\ \dfrac{\partial \eta}{\partial t} = 0 \end{cases} \tag{8}$$

Les vitesses d'ondes associées sont:

$$\begin{cases} \lambda = u \pm \sqrt{-\frac{1}{\rho}\frac{\partial S_{12}}{\partial \mathbf{a}} \cdot \mathbf{b}} \\ \\ \lambda = u \end{cases}$$

- Sous-modèle 3

$$\begin{cases} \dfrac{\partial \rho}{\partial t} = 0, \quad \dfrac{\partial (\rho u)}{\partial t} = 0, \quad \dfrac{\partial (\rho v)}{\partial t} = 0, \\ \dfrac{\partial (\rho w)}{\partial t} + \dfrac{\partial (-S_{13})}{\partial x} = 0, \\ \dfrac{\partial a^\beta}{\partial t} + c^\beta \dfrac{\partial w}{\partial x} = 0, \quad \beta = 1,2,3 \\ \dfrac{\partial b^\beta}{\partial t} = 0, \quad \dfrac{\partial c^\beta}{\partial t} = 0, \quad \beta = 1,2,3 \\ \dfrac{\partial \eta}{\partial t} = 0 \end{cases} \tag{9}$$

Les vitesses d'ondes associées sont:

$$\begin{cases} \lambda = u \pm \sqrt{-\frac{1}{\rho}\frac{\partial S_{13}}{\partial \mathbf{a}} \cdot \mathbf{c}} \\ \\ \lambda = u \end{cases}$$

La simplicité de chaque sous-modèle permet l'utilisation d'un solveurs de type HLLC (solveur à 3 ondes). Ceci réduit la diffusion numérique. Un autre avantage est la possibilité d'utiliser des solveurs exacts pour chaque sous-modèle pour une meilleure précision. Cette procédure de splitting se généralise facilement dans le cas multi-D. Un test difficile a été proposé pour déterminer si la procédure de splitting vérifie la condition $\mathbf{rot}(\mathbf{e}^\beta) = 0$, $\beta = 1,2,3$. On applique le champ de vitesse (de rotation) suivant dans le cas plan (voir Figure 1.6):

$$\left.\begin{pmatrix} u \\ v \end{pmatrix}\right|_{t=0} = \begin{cases} \begin{pmatrix} -\omega y \\ \omega x \end{pmatrix}, & \text{if} \quad x^2+y^2 < R^2 \\ \\ \begin{pmatrix} 0 \\ 0 \end{pmatrix}, & \text{if} \quad x^2+y^2 \geq R^2. \end{cases} \tag{10}$$

On suppose que le tenseur des contraintes est initialement sphérique: $\boldsymbol{\sigma} = -p_0\mathbf{I}$, $p_0 = constante$. Ceci correspond initialement à un cisaillement dans le domaine : $x^2 + y^2 \leq R^2$. Pour les applications numériques, nous avons choisi: $\omega = 4000s^{-1}$, $R = 0.05$m, $p_0 = 10^5$ Pa. Les résultats sont présentés à l'instant $5\mu s$. Plus précisément, ce test correspond à un cisaillement fort au bord $x^2 + y^2 = R^2$ où nous avons un saut de la vitesse tangentielle de $2000m/s$ à $0m/s$. Un tel saut produira deux ondes de cisaillement se propageant à l'intérieur et à l'extérieur du cercle $x^2+y^2 = R^2$. Les résultats de ce test sont visibles sur la Figure 4.10 où nous avons com-

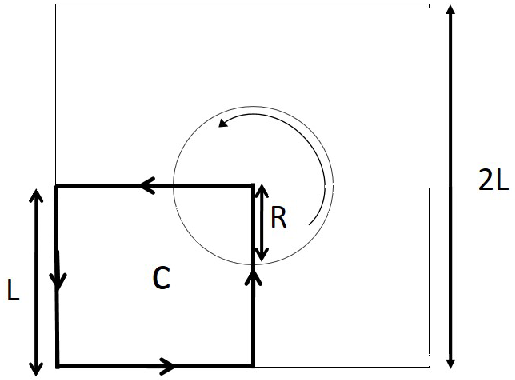

Figure 1.6: Configuration initiale et définition du contour C où la circulation du champ e^β le long du contour C est évaluée.

paré les résultats donnés par la procédure de splitting à ceux donnés par le schéma de type Lax Friedrichs qui conserve la contrainte $\mathbf{rot}(\mathbf{e}^\beta) = 0$, $\beta = 1, 2, 3$.

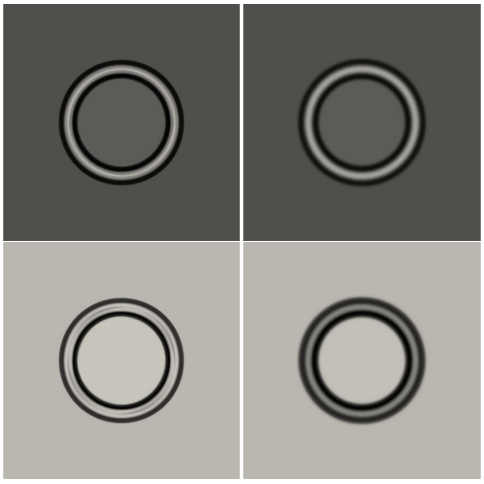

Figure 1.7: Sur cette figure sont représentées la densité (au dessus) et la pression (en dessous). La région foncée correspond à une densité élevée. Les résultats numériques en rapport avec la procédure de splitting sont présentés à gauche et ceux en rapport avec le schéma de Lax-Friedrichs sont présentés sur la droite. Le maillage utilisé est de 1500×1500. Les résultats obtenus par la procédure de splitting sont clairement moins diffusés.

La Figure 4.9 montre que cette condition est vérifiée pour la procédure de splitting à l'ordre 1.

1.3 Extension du modèle d'interaction solide-fluide

Ceci correspond au chapite 5 de la thèse

Nous proposons une extension du modèle traitant l'interaction fluide–solide (Favrie & Gavrilyuk (2012)) au cas de l'interaction de N solides. Le modèle proposé est le suivant:

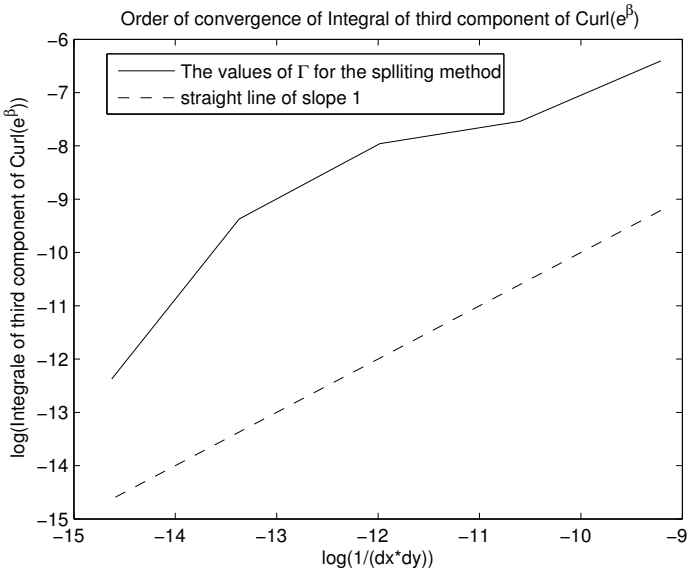

Figure 1.8: Courbe de convergence de la circulation de $\vec{\mathbf{e}}^{\beta}$ sur le contour C de la partie inférieure gauche de la figure 1.6. Nous avons utilisé des maillages de 100×100, 200×200, 400×400, 800×800, 1500×1500 cellules pour tracer cette courbe. Ce résultat nous montre la convergence à l'ordre 1 pour ce test difficile.

$$\begin{cases} \frac{D\mathbf{e}_l^\beta}{Dt} + \left(\frac{\partial \mathbf{v}}{\partial \mathbf{x}}\right)^T \mathbf{e}_l^\beta = \frac{a\mathbf{S}_l \mathbf{e}_l^\beta}{\tau_{rel,l}} \\ \frac{\partial \alpha_l \rho_l}{\partial t} + div\left(\alpha_l \rho_l \mathbf{v}\right) = 0 \\ p = p_1 = ... = p_N, \quad \sum_{l=1}^N \alpha_l = 1 \\ \frac{\partial \rho}{\partial t} + div\left(\rho \mathbf{v}\right) = 0, \\ \frac{\partial (\rho \mathbf{v})}{\partial t} + div(\rho \mathbf{v} \otimes \mathbf{v} - \boldsymbol{\sigma}) = 0 \\ \frac{D\eta_l}{Dt} = f_l \end{cases} \tag{11}$$

où ρ_l est la densité de chaque composant l, α_l est sa fraction volumique. La densité du mélange est définie comme: $\rho = \sum_{l=1}^N \alpha_l \rho_l$, $\mathbf{v}$ est le champ de vitesse, p est la pression. $\boldsymbol{\sigma} = \sum_{l=1}^N \alpha_l \boldsymbol{\sigma}_l$ est le tenseur des contraintes de Cauchy du mélange, $\mathbf{S}_l$ représente la partie déviatorique du tenseur des contraintes $\boldsymbol{\sigma}_l$, η_l est l'entropie du composant l, $\mathbf{e}_l^\beta$ est la cobase du composant l. e_l représente l'énergie interne de chaque composante l. L'énergie interne spécifique du mélange e est définie comme: $e = \sum_{l=1}^N Y_l e_l$ où Y_l est la fraction massique: $Y_l = \dfrac{\alpha_l \rho_l}{\rho}$ du composant L.

L'énergie e_l est prise sous forme séparable (Flory (1961), Hartmann et Neff (2003), Gavrilyuk *et al.* (2008)) :

$$e_l = e_l^h\left(\rho_l, \eta_l\right) + e_l^e\left(\mathbf{g}_l\right),$$

où η_l est l'entropie spécifique et

$$\mathbf{g}_l = \frac{\mathbf{G}_l}{|\mathbf{G}_l|^{\frac{1}{3}}}, \qquad |\mathbf{G}_l| = \det\left(\mathbf{G}_l\right).$$

avec $\mathbf{G}_l$ le tenseur de Finger.

Le second membre f_l est choisi de telle sorte que le modèle vérifie le second principe de la thermodynamique. $\tau_{rel,l}$ est le temps de relaxation défini par:

$$\frac{1}{\tau_{rel,l}} = \begin{cases} \frac{1}{\tau_{0,l}} \left(\frac{\sum_\alpha \left(S_{\alpha,l}\right)^2 - \frac{2}{3}\sigma_{Y,l}^2}{\mu_l^2} \right)^{n_l}, & \text{si } \sum_\alpha \left(S_{\alpha,l}\right)^2 - \frac{2}{3}\sigma_{Y,l}^2 > 0 \\ 0 \quad \text{si } \sum_\alpha \left(S_{\alpha,l}\right)^2 - \frac{2}{3}\sigma_{Y,l}^2 \leq 0 \end{cases} \tag{12}$$

a est une constante ayant la dimension d'une contrainte, $\tau_{0,l}$ et n_l désignant respectivement le temps caractéristique de relaxation et l'exposant de relaxation, $\sigma_{Y,l}$ est la limite d'élasticité de chaque solide et $S_{\alpha,l}$ sont les contraintes principales de la partie déviatorique du tenseur des contraintes du composant l. L'expression du temps de relaxation (13) est une adaptation du modèle de Perzyna en visco-plasticité (Lemaitre, Chaboche, Benallal, Desmond (2003)). Les termes f_l doivent être déterminés de telle sorte que:

- ils sont compatibles avec l'équation d'énergie totale;
- ils sont compatibles avec l'inégalité entropie.

Le choix de N cobases locales $\mathbf{e}_l^\beta$ se justifie car le processus de relaxation est spécifique à chaque solide et agit sur sa cobase locale.

La partie hydrodynamique de l'énergie e_l^h peut être prise sous la forme:

$$e_l^h(\rho_l, p_l) = \frac{p_l + \gamma_l p_{\infty,l}}{(\gamma_l - 1)\rho_l}, \quad \gamma_l > 1, \quad p_{\infty,l} > 0, \tag{13}$$

avec

$$\frac{p_l + p_{\infty,l}}{\rho_l^{\gamma_l}} = A_l(\eta_l) > 0, \quad \frac{dA_l}{d\eta_l} > 0.$$

La partie élastique de l'énergie e_l^e pour les solides isotropes est une fonction des invariants de $\mathbf{g}_l$:

$$e_l^e(\mathbf{g}_l) = e_l^e(j_{1,l}, j_{2,l}), \quad j_{1,l} = tr(\mathbf{g}_l), \quad j_{2,l} = tr\left(\mathbf{g}_l^2\right), \quad i = 1, 2.$$

Pour les applications, nous prenons:

$$e_l^e(\mathbf{g}_l) = \frac{\mu_l}{8\rho_{0,l}}(j_{2,l} - 3) \tag{14}$$

Une importante remarque est la suivante: si le module de cisaillement μ_l du composant l s'annule, on retrouve les équations d'Euler des fluides compressibles. Ainsi, nous n'avons pas besoin de séparer les N composants en 'solides' et 'fluides'.

Bien que le nombre d'équations soit important, nous avons montré que le modèle est hyperbolique et vérifie le second principe de la thermodynamique. La preuve de l'hyperbolicité est basée sur l'étude de la matrice $\mathbf{M}_w + \sum_{l=1}^N Y_l \mathbf{M}_l$ avec

$$\mathbf{M}_w = \begin{pmatrix} c_w^2 & 0 & 0 \\ 0 & 0 & 0 \\ 0 & 0 & 0 \end{pmatrix} \quad et \quad \mathbf{M}_l = \Delta_l^{-1} \mathbf{F}_l^{-T} E_l'' \mathbf{F}_l^{-1},$$

où c_w est la vitesse du son de Wood et les matrices $\mathbf{M}_l$ sont définies comme dans la section précédente. Si chaque sous-modèle de solide pur est hyperbolique, alors le modèle de mélange est hyperbolique.

Ce résultat, bien que simple, est loin d'être trivial. Il provient d'une utilisation optimale de la structure des équations et de la preuve de l'hyperbolicité dans le cas d'un seul composant solide.

La résolution numérique du problème d'équilibre de pression pose un problème important car c'est une équation algébrique reliant toutes les pression p_l. Pour contourner ce problème, on introduit un modèle en déséquilibre des pressions qui est également hyperbolique et thermodynamiquement bien posé (Favrie et Gavrilyuk (2012)). On remplace la condition d'équilibre de pression par des équations algébriques sur la fraction volumique de chaque composant l:

$$\frac{D\alpha_l}{Dt} = \lambda_l \left(p_l - p_I \right)$$

où les $\lambda_l > 0$ sont des coefficients très grands qu'on fera tendre vers l'infini, et p_I est la pression interfaciale définie comme:

$$p_I = \sum_{l=1}^{N} \beta_l p_l, \quad \beta_l > 0, \quad \sum_{l=1}^{N} \beta_l = 1.$$

Nous avons montré de la même manière que ce que ce nouveau modèle est hyperbolique et thermodynamiquement bien posé.

Une condition sous-caractéristique 'faible' similaire à celle de Whitham (1975) a été établie entre le modèle d'équilibre de pressions 'E' et le modèle hors d'équilibre de pressions 'HE'. Plus précisément, nous avons montré que:

- $\lambda_E^{max} \leq \lambda_{HE}^{max}$
- $\lambda_E^{min} \leq \lambda_{HE}^{min}$

λ^{max}, λ^{min} désignant respectivement la plus grande et la plus petite vitesse d'onde du système correspondant.

Comme applications de ce modèle, nous avons présenté deux résultats. Le premier est celui d'un exemple d'écaillage (voir Figure 5.16). Le second est celui d'un impact hypervéloce (voir Figure 5.18)

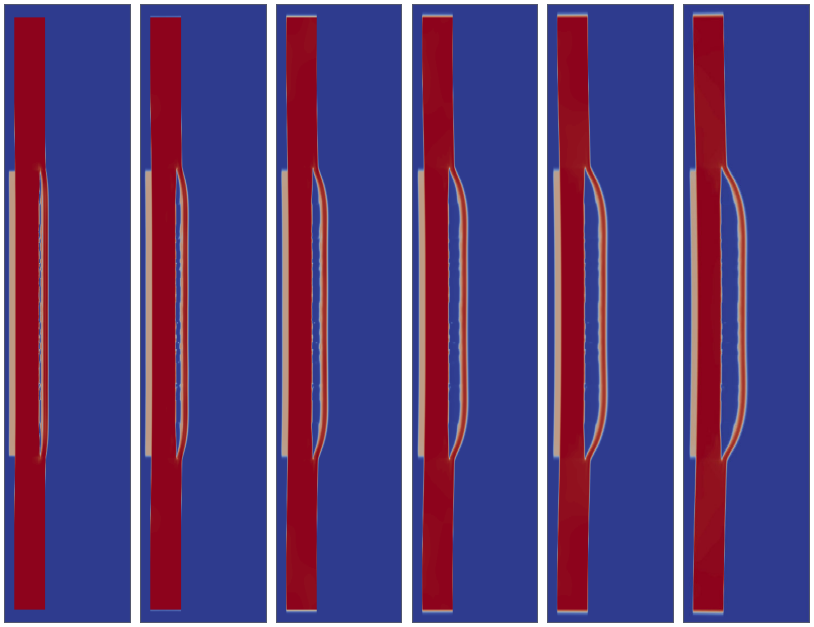

Figure 1.9: Une plaque d'aluminium impacte une plaque de titane à une vitesse de $700m/s$. Nous observons la formation d'une fracture dans la plaque de titane. Les instants où les simulations sont présentées sont respectivement de $50\mu s$, $100\mu s$, $150\mu s$, $200\mu s$, $250\mu s$ and $290\mu s$.

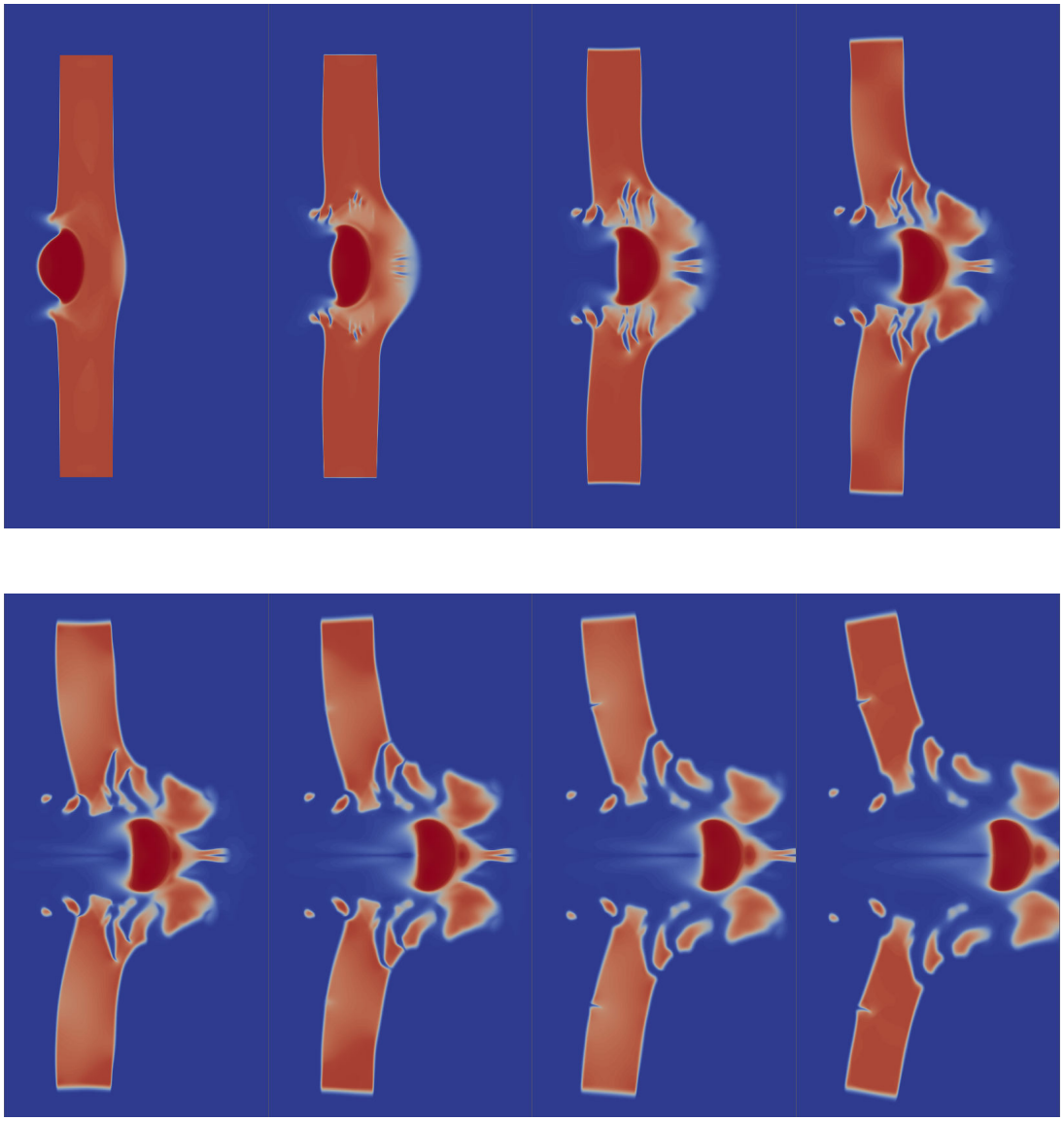

Figure 1.10: Un disque de fer impacte une plaque d'aluminium à la vitesse de $1000m/s$. Des fissures apparaissent au cours de la pénétration. Il en résulte finalement une fragmentation de la plaque d'aluminium.

1.4 Conclusion

Un modèle mathématique d'interfaces diffuses pour l'interaction de N solides élasto-plastiques a été construit. C'une extension du modèle développé par Favrie & Gavrilyuk (2012) pour l'interaction d'un fluide et d'un solide. En dépit du grand nombre d'équations présentes dans ce modèle, deux propriétés remarquables ont été démontrées: ce modèle est hyperbolique (quelles que soient les déformations admissibles) et il vérifie le second principe de la thermodynamique. L'énergie interne de chaque solide est prise sous forme séparable: c'est la somme d'une énergie hydrodynamique qui ne dépend que de la densité et de l'entropie, et d'une énergie de cisaillement. L'équation d'état de chaque solide est telle que si nous prenons le module de cisaillement du solide égal à zéro, on retrouve les équations de la mécanique des fluides. Ce modèle permet, en particulier, de:

- prédire les déformations de solides élasto-plastiques en petites déformations et en très grandes déformations.
- prédire l'interaction d'un nombre arbitraire de solides élasto-plastiques et de fluides.

L'aptitude de ce modèle à résoudre des problèmes complexes a été démontrée. Sans être exhaustif, on peut citer:

- le phénomène d'écaillage dans les solides.
- la fracturation et la fragmentation dans les solides.

Les perspectives de ces travaux sont nombreuses. On peut citer, par exemple:

- La prise en compte du glissement entre composantes.
- Le développement d'une méthode de raidissement d'interface diffuse pour traiter une dynamique moins rapide. Cela ouvrira de nombreuses applications en médecine.
- L'ajout d'écrouissage dynamique pour chaque composant du milieu.
- L'ajout de la transition de phase dans les solides pour le traitement de problèmes physiques encore plus complexes tel que le soudage par explosif.

1.5 Références

Abgrall, R. (1996) How to prevent pressure oscillations in multi-component flow calculations: A quasi conservative approach. Journal of Computational Physics, Vol. 125, pp. 150-160.

Abgrall, R. & Karni, (2001) Ghost-fluids for the poor: A single fluid algorithm for multi-fluids. International series of numerical mathematics. Vol. 140, pp. 1-10.

Backman, M. E., & Goldsmith, W. (1978) The mechanics of penetration of projectiles into targets. International Journal of Engineering Science, Vol. 16(1), pp. 1-99.

Ball, J.M. (1977) Convexity conditions and existence theorems in non-linear elasticity. Archive for Rational Mechanics and Analysis, Vol. 63, pp. 337-403.

Barton, P.T., Drikakis, D., Romenski, E. & Titarev, V.A. (2009) Exact and approximate solutions of Riemann problems in non-linear elasticity. Journal of Computational Physics, Vol. 228, pp. 7046-7068.

Barton, P.T., Drikakis, D. & Romenskii, E.I. (2010) An Eulerian scheme for large elastoplastic deformations in solids. Int. J. Numer. Meth. Engng, Vol. 81, pp. 453-484.

Barton, P.T. Deiterding, R. Meiron, D. & Pullin, D. (2013) Eulerian adaptive finite-difference method for high-velocity impact and penetration problems, Journal of Computational Physics, Vol. 240, pp. 76-99.

Dacorogna, B. (2001) Necessary and sufficient conditions for strong ellipticity of isotropic functions in any dimension. Discrete and Continuous Dynamical Systems - Series B, Vol. 1, pp. 257-263.

Dafermos, C.M. (2010) Hyperbolic Conservation Laws in Continuum Mechanics (third ed.), Springer.

De Tommasi, D., Puglisi, G. & Zurlo, G. (2012) A note on the strong ellipticity in two-dimensional isotropic elasticity. Journal of Elasticity, Vol. 109, pp. 67-74.

Farhat, C., Lesoinne, M., & Le Tallec, P. (1998) Load and motion transfer algorithms for fluid/structure interaction problems with non-matching discrete interfaces: Momentum and energy conservation, optimal discretization and application to aeroelasticity. Computer methods in applied mechanics and engineering, Vol. 157(1), pp. 95-114.

Favrie, N., Gavrilyuk, S.L. & Saurel, R. (2009) Solid-fluid diffuse interface model in cases of extreme deformations. J. Computational Physics, Vol. 228, pp. 6037-6077.

Favrie, N. & Gavrilyuk, S.L. (2011) Mathematical and numerical model for nonlinear visco-plasticity. Phil. Trans. R. Soc. A, Vol. 369, pp. 2864-2880.

Favrie, N. & Gavrilyuk, S.L. (2012) Diffuse interface model for compressible fluid-compressible elastic-plastic solid interaction. J. Computational Physics, vol. 231, pp. 2695-2723.

Favrie, N., Gavrilyuk & S. Ndanou (2014) A thermodynamically compatible splitting procedure in hyperelasticity. J. Computational Physics, Vol. 270, pp. 300-324.

Flory, R.J. (1961) Thermodynamic relations for highly elastic materials. Transactions of the Faraday Society, Vol. 57, pp. 829-838.

Garaizar, X. (1991) Solution of a Riemann problem for elasticity. Journal of Elasticity, Vol. 26, pp. 43-63.

Gavrilyuk, S.L., Favrie, N., & Saurel, R. (2008) Modeling wave dynamics of compressible elastic materials. Journal of Computational Physics, Vol 227, pp. 2941-2969.

Godunov, S.K (1978) Elements of Continuum Mechanics, Nauka, Moscow (in russian).

Godunov, S.K & Romenskii, E.I. (2003) Elements of Continuum Mechanics and Conservation Laws. Kluwer Academic Plenum Publishers, NY.

Godunov, S.K. & Peshkov, I.M. (2010) Thermodynamically consistent nonlinear model of an elasto-plastic Maxwell medium. Computational Mathematics and Mathematical Physics, Vol. 50, pp. 1481-1498.

Gorsse, Y., Iollo, A., Milcent, T. & Telib, H. (2014) A simple Cartesian scheme for compressible multimaterials. Journal of Computational Physics, Vol. 272, pp. 772-798.

Hartmann, S. & Neff, P. (2003) Polyconvexity of generalized polynomial-type hyperelastic strain energy functions for nearly incompressibility. Int. J. Solid and Structures, Vol. 40, pp. 2767-2791.

Karni, S. (1994). Multicomponent flow calculations by a consistent primitive algorithm. Journal of Computational Physics. Vol. 112, pp. 31-43.

Kluth, G. & Desprès, B. (2008) Perfect plasticity and hyperelastic models for isotropic materials. Continuum Mechanics and Thermodynamics, Vol. 20, pp. 173-192.

Kulikovskii, A. & Sveshnikova, E. (1995) Nonlinear waves in elastic media. CRC Press Book.

Kulikovskii, A.G. & Chugainova, A.P. (2000) The Stability of Quasi-

transverse Shock Waves in Anisotropic Elastic Media. Prikl. Mat. Mekh., Vol 64, pp. 1020-1026.

Lemaitre, J., Chaboche, J.L., Benallal, A. & Desmorat, R., (2009) Mécanique des matérieux solides. Dunod.

Le Tallec, P. & Mouro, J. (1996) Structures en grands déplacements couplées à des fluides en mouvement. Rapport INRIA 2961.

Li, B., Habbal, F. & Ortiz, M. (2010) Optimal transportation meshfree approximation schemes for fluid an plastic flows. International Journal of for Numerical Methods in Engineering, Vol. 83, pp. 1541-1579.

Li, B., Kidane, A., Ravichandran, G. & Ortiz, M., (2012) Verification and validation of the Optimal Transportation Meshfree (OTM) simulation of terminal ballistics. International Journal of Impact Engineering, Vol. 42, pp. 25-36.

Maire, P.H., Abgrall, R., Breil, J., Loubère, R. & Rebourcet,B., (2013) A nominally second-order cell-centered Lagrangian scheme for simulating elastic-plastic flows on two-dimensional unstructured grids. Journal of Computational Physics, Vol. 235, pp. 626-665.

Miller, G.H. & Colella, P. (2001) A high order Eulerian Godunov method for elastic plastic flow in solids. Journal of Computational Physics, Vol. 167, pp. 131-176.

Miller, G.H. & Colella, P. (2003) An iterative Riemann solver for systems of hyperbolic conservation laws, with application to hyperelastic solid mechanics. Journal of Computational Physics, Vol. 193, pp. 198-225.

Ndanou, S., Favrie, N. & Gavrilyuk, S.L. (2014a) Criterion of hyperbolicity in hyperelasticity in the case of the stored energy in separable form. Journal of Elasticity. Vol 115, pp. 1-25.

Ndanou, S., Favrie ,N. & Gavrilyuk, S. (2014b) The piston problem in hyper-elasticity with the stored energy in separable form, http://hal.archives-ouvertes.fr/hal-00917961.

Ndanou, S., Favrie, N. & Gavrilyuk, S.L. (2014c) Multi-solid and multi-fluid diffuse interface model : applications to dynamic fracture and fragmentation. Journal of Computational Physics (soumis).

Perigaud, G. & Saurel, R. (2005) A compressible flow model with capillary effects. Journal of Computational Physics, Vol 209(1), pp. 139-178.

Piperno, S. & Farhat, C. (1997) Design and Evaluation of Staggered Partitioned Procedures for the transcient solution of aeroelastic probnlems, Rapport de recherche INRIA 3241.

Piperno, S. & Farhat, C. (2000) Design of efficient partitioned procedures

for the transient solution of aeroélastic problems. Revue Européenne des Eléments finis, Vol. 9(6-7), pp. 655-680.

Romenski, E., Drikakis, D. & Toro, E. (2009) Conservative Models and Numerical Methods for Compressible Two-Phase Flow. Journal of Computational Physics, Vol. 42, pp. 68-95.

Saurel, R., Petitpas, F. & Abgrall, R. (2008) Modelling phase transition in metastable liquids: application to cavitating and flashing flows. Journal of Fluid Mechanics, Vol. 607, pp. 313-350.

Saurel, R., Petitpas, F. & Berry, R. A. (2009) Simple and efficient relaxation methods for interfaces separating compressible fluids, cavitating flows and shocks in multiphase mixtures. Journal of Computational Physics, Vol. 228(5), pp. 1678-1712.

Saurel, R. & Abgrall, R. (1999) A multiphase Godunov method for multifluid and multiphase flows. Journal of Computational Physics, Vol. 150, pp. 425-467.

Saurel, R. & Le Metayer, O. (2001) A multiphase model for interfaces, shocks, detonation waves and cavitation. Journal of Fluid Mechanics, Vol. 431, pp. 239-271.

Sfyris, D. (2011) The strong ellipticity condition under changes in the current and reference configuration. Journal of Elasticity, vol. 103, pp. 281-287.

Taylor, G.I. (1948) The use of flat ended projectiles for determining yield stress. I. Theoretical considerations, Proc. R. Soc. A, Vol. 194, pp. 289-299.

Toro, E.F. (2009) Riemann Solvers and Numerical Methods for Fluid Dynamics: A Practical Introduction (third ed.). Springer-Verlag.

Wang, Y.& Aron, M. (1996) A reformulation of the strong ellipticity conditions for unconstrained hyperelastic media. Journal of Elasticity, Vol. 44, pp. 89-96.

Wilkins, M.L. (1964) Calculation of elastic-plastic flow. Methods Comput. Phys., Vol. 3, pp. 211-263.

Whitham, G.B. (1974) Linear and Nonlinear Waves. John Wiles& Sons.

Chapitre 2

Critère de l'hyperbolicité

Ce chapitre correspond à l'article S. Ndanou and N. Favrie and S. L. Gavrilyuk, Criterion of hyperbolicity in hyperelasticity in the case of the stored energy in separable form, Journal of Elasticity, 115 (2014) 1-25.

2.1 Introduction

The criterion of hyperbolicity of the non-stationary hyperelasticity is the rank-one convexity of the specific energy e as a function of the deformation gradient $\mathbf{F}$ (see, for example, Dafermos, 2000). In statics, the rank-one convexity is also called 'strong ellipticity' condition (Ball 1977, Dacorogna 2001, Sfyris 2011, etc.). This condition is not easy to verify even in the case of isotropic elastic materials, where the specific energy depends only on the invariants of the right Cauchy-Green deformation tensor $\mathbf{C} = \mathbf{F}^T\mathbf{F}$ or the left Cauchy-Green deformation tensor $\mathbf{B} = \mathbf{F}\mathbf{F}^T$. The literature on this subject is vast. We will give here just a few references concerning the general case of isotropic solids, because our aim is to study this condition in a specific case which will be precised below.

The necessary and sufficient conditions of strong ellipticity for two-dimensional isotropic hyperelastic materials were proposed by Knowles & Sternberg (1977), Davies (1991), Aubert (1995) and Dacorogna (2001). Recently, De Tommasi *et al.* (2012) used a special linear combination of the invariants of $\mathbf{C}$ to derive a single scalar condition which guarantees the strong ellipticity for plane equilibrium deformations. In the 3D case, the necessary and sufficient conditions were proposed, for example, in Simpson

& Spector (1983), Wang & Aron (1996) and Dacorogna (2001). Simple sufficient conditions are proposed in Dacorogna (2001) (Proposition 7 in that paper). The necessary and sufficient conditions formulated in that paper are difficult to apply directly (Theorem 5).

An alternative approach to the hyperbolicity study was proposed by Godunov (see Godunov & Romenskii, 2003). It consists in rewriting the equations of isotropic elastic materials as a symmetric t-hyperbolic in the sense of Friedrichs system. Such a transformation allows us to assure hyperbolicity of the governing equations and a possibility to calculate the eigenvalues in terms of symmetric matrices, which is a wellposed numerical problem. The last approach is not direct, because it needs to use the Legendre transform of the stored energy function.

In practice, it is important to guarantee the hyperbolicity in all domain of $\mathbf{F}$ having positive determinant. The domain of large deformations occurs, in particular, in studying of rubber-like materials (Horgan, 1995, Sendova & Walton, 2004). The rank-one convexity condition can be violated for these models in the limit of large strains. Another application of large deformations hyperelasticity comes from the numerical treatment of mathematical models of elastic-plastic solids where one usually uses a splitting procedure : the 'elastic' step is followed by the 'plastic' relaxation step (Miller & Collela (2001), Godunov & Romenskii (2003), Godunov & Peshkov (2010), Barton *et al.* (2010), Favrie & Gavrilyuk (2011, 2012)). It is necessary to assure the hyperbolicity condition at each 'elastic' step. Indeed, the hyperbolicity is a necessary condition for the wellposdness of the Cauchy problem and the corresponding numerical Godunov-type methods.

We will consider the Eulerian formulation of the hyperelasticity for isotropic solids. The Eulerian formulation is important in applications involving large deformations. These equations are invariant under rotation group $SO\,(3)$. The consequence of that are immediate : for hyperbolicity it is sufficient to consider only 1D case. Indeed, the normal characteristic direction can always be transformed by rotation to the one of Cartesian basis vectors (we have to use three composed rotations defined by the Euler angles between the Cartesian basis and a natural local basis on characteristic surface). So, the problem to assure the hyperbolicity of the one-dimensional system for arbitrary strains and shears becomes the basic one. This 1D problem stays complex because the number of unknowns involved in such a formulation is large (14 scalar partial differential equations).

We will concentrate on a particular class of elastic materials described

by a stored energy e taken in separable form (Flory, 1961) :

$$e = e^h\left(|\mathbf{G}|, \eta\right) + e^e\left(\mathbf{g}\right),$$

where $\mathbf{G} = \mathbf{B}^{-1}$ is the Finger tensor, $\mathbf{g} = \mathbf{G}\,|\mathbf{G}|^{-1/3}$, and $|\mathbf{G}|$ is the determinant of $\mathbf{G}$. The choice of the Finger tensor is more natural for the Eulerian description of isotropic solids. The energy $e^h\left(|\mathbf{G}|, \eta\right)$ is the hydrodynamic part of the energy, depending only on the determinant of $\mathbf{G}$ and the entropy η, and $e^e\left(\mathbf{g}\right)$ is the shear elastic energy. The shear part of the energy is unaffected by the volume change. Such a decomposition into purely volumetric and isochoric deformation is, in particular, useful for description of nearly incompressible isotropic hyperelasticity (see Hartmann & Neff, 2003). This implies that the Cauchy stress tensor is also in separable form :

$$\sigma = -p\mathbf{I} + \mathbf{S},$$

where p is the pressure calculated only by the hydrodynamic part of the energy, $\mathbf{I}$ is the identity tensor, and the deviatoric part $\mathbf{S}$ is calculated only by the shear energy. Under a classical hypothesis about the pressure behavior (the hydrodynamic sound speed should be positive), we reduce the problem of hyperbolicity to a simpler one : show that a symmetric 3x3 matrix (determined in terms of the shear energy e^e only) is positive definite on a one-parameter family of unit-determinant deformation gradient compact surfaces. Some explicit forms of the stored energy are then tested.

2.2 Eulerian formulation of the hyperelasticity

The Eulerian formulation of the hyperelasticity can be found, for example, in Godunov & Romenskii (2003) and Miller & Collela (2001). We follow Gavrilyuk *et al.* (2008) for a modified conservative formulation of the model, which is easier to analyze. The model can be written as follows:

$$\frac{\partial \rho}{\partial t} + div\left(\rho \mathbf{u}\right) = 0, \tag{1}$$

$$\frac{\partial (\rho \mathbf{u})}{\partial t} + div\left(\rho \mathbf{u} \otimes \mathbf{u} - \boldsymbol{\sigma}\right)) = 0,$$

$$\frac{\partial \rho \left(e+\frac{1}{2}\left|\mathbf{u}\right|^2\right)}{\partial t}+div\left(\rho\left(e+\frac{1}{2}\left|\mathbf{u}\right|^2\right)\mathbf{u}-\boldsymbol{\sigma}\mathbf{u}\right)=0,$$

$$\frac{\partial \mathbf{e}^{\beta}}{\partial t}+\bigtriangledown\left(\mathbf{u}\cdot\mathbf{e}^{\beta}\right)=0,\quad rot(\mathbf{e}^{\beta})=0,\qquad \beta=1,2,3.$$

The operators div, rot and $\bigtriangledown$ are applied in the Eulerian coordinates $\mathbf{x}=(x,y,z)^T$. Here ρ is the solid density, $\mathbf{u}=(u,v,w)^T$ is the velocity, $\boldsymbol{\sigma}$ is the Cauchy stress tensor defined as

$$\boldsymbol{\sigma}=-2\rho\frac{\partial e}{\partial \mathbf{G}}\mathbf{G},$$

where

$$\mathbf{G}=\mathbf{B}^{-1}=\left(\mathbf{F}\mathbf{F}^T\right)^{-1}$$

is the Finger tensor, and $\mathbf{F}$ is the deformation gradient. Obviously, in the case of isotropic solids $\boldsymbol{\sigma}$ is symmetric. The vectors $\mathbf{e}^{\beta}$ are the columns of $\mathbf{F}^{-T}$:

$$\mathbf{F}^{-T}=\left(\mathbf{e}^1,\mathbf{e}^2,\mathbf{e}^3\right).$$

Since $\mathbf{e}^{\beta}$ are gradients of the Lagrangian coordinates, the equation $rot(\mathbf{e}^{\beta})=0$ is a compatibility condition. The condition is time invariant : if it is verified initially, it will be verified for any time (Miller & Collela, 2001, Gavrilyuk *et al.*, 2008). The energy e is the function of invariants of $\mathbf{G}$. We take it in the following separable form (Flory, 1961):

$$e=e^h\left(\rho,\eta\right)+e^e\left(\mathbf{g}\right),$$

where

$$\rho=\rho_0\left|\mathbf{G}\right|^{1/2},\qquad \left|\mathbf{G}\right|=\det\mathbf{G},\qquad \mathbf{g}=\frac{\mathbf{G}}{\left|\mathbf{G}\right|^{1/3}}.$$

Here ρ_0 is the reference density. For simplicity, we will consider the case where ρ_0 is a constant, even if it is not necessary. Such a form allows us to write :

$$\boldsymbol{\sigma}=-p\mathbf{I}+\mathbf{S},\qquad tr\left(\mathbf{S}\right)=0$$

with

$$p=\rho^2\frac{\partial e^h(\rho,\eta)}{\partial \rho},$$

$$\mathbf{S}=-2\rho\frac{\partial e^e}{\partial \mathbf{G}}\mathbf{G}.$$

Let us remark that the pressure p is determined only by the hydrodynamic part of the energy e^h. For isotropic solids, the shear energy e^e can be written as a function of only two invariants of $\mathbf{g}$:

$$e^e(\mathbf{g}) = e^e(j_1, j_2)$$

which are taken as

$$j_1 = tr(\mathbf{g}) = \frac{J_1}{|\mathbf{G}|^{1/3}}, \quad j_2 = tr(\mathbf{g}^2) = \frac{J_2}{|\mathbf{G}|^{2/3}}, \; J_i = tr\left(\mathbf{G}^i\right), \; i = 1, 2.$$

It implies :

$$\mathbf{S} = -2\rho\frac{\partial e^e}{\partial \mathbf{G}}\mathbf{G} = -2\rho\left(\frac{\partial e^e}{\partial j_1}\left(\mathbf{g} - \frac{j_1}{3}\mathbf{I}\right) + 2\frac{\partial e^e}{\partial j_2}\left(\mathbf{g}^2 - \frac{j_2}{3}\mathbf{I}\right)\right).$$

Particular forms of the equations of state used in applications are (Gavrilyuk *et al.* (2008), Favrie & Gavrilyuk (2011, 2012)) :

$$e^h(\rho, \eta) = \frac{A\exp\left(\frac{\eta-\eta_0}{c_v}\right)\rho^\gamma + (\gamma-1)\,p_\infty}{(\gamma-1)\,\rho}, \tag{2}$$

$$e^e(\mathbf{g}) = \frac{\mu}{4\rho_0}\left((2-4a)j_1 + aj_2 + 3\,(3a-2)\right). \tag{3}$$

Here A, η_0, p_∞, $\gamma > 1$, c_v , μ, ρ_0 and a are constants. In particular, in the limit of small deformations the Hooke law is recovered. In the case of large-amplitude compressive stress-wave propagation the solid behaves as a fluid. Indeed, in this case the stress tensor will be nearly spherical because the isochoric part of the energy e^e is negligible with respect to the hydrodynamic part e^h. The parameter a is a new nonlinearity material parameter. The deviatoric part of the stress tensor is sensible to the choice of a. Experimental data are needed for its identification. In particular, $a = 1$ was a resonable value for the study of impacts of jelly-like materials (Favrie *et al.* 2009).

The Finger tensor can also be written as

$$\mathbf{G} = \sum_{\beta=1}^{3} \mathbf{e}^\beta \otimes \mathbf{e}^\beta.$$

In the Cartesian basis $(\mathbf{i},\mathbf{j},\mathbf{k})$ the vectors $\mathbf{e}^\beta$ have the components $\left(a^\beta,b^\beta,c^\beta\right)^T$, $\beta=1,2,3$. Let us introduce the vectors $\mathbf{a}=\left(a^1,a^2,a^3\right)^T$, $\mathbf{b}=\left(b^1,b^2,b^3\right)^T$, $\mathbf{c}=\left(c^1,c^2,c^3\right)^T$. Obviously,

$$F^{-1}=(\mathbf{a},\mathbf{b},\mathbf{c}),\qquad F^{-T}=\begin{pmatrix}\mathbf{a}^T\\ \mathbf{b}^T\\ \mathbf{c}^T\end{pmatrix}$$

The tensor $\mathbf{G}$ is then the Gram matrix for the vectors $\mathbf{a}$, $\mathbf{b}$, $\mathbf{c}$:

$$\mathbf{G}=F^{-T}F^{-1}=\begin{pmatrix}\|\mathbf{a}\|^2 & \mathbf{a}\cdot\mathbf{b} & \mathbf{a}\cdot\mathbf{c}\\ \mathbf{a}\cdot\mathbf{b} & \|\mathbf{b}\|^2 & \mathbf{b}\cdot\mathbf{c}\\ \mathbf{a}\cdot\mathbf{c} & \mathbf{b}\cdot\mathbf{c} & \|\mathbf{c}\|^2\end{pmatrix}.$$

Its determinant is :

$$|\mathbf{G}|=|\mathbf{a}\cdot(\mathbf{b}\wedge\mathbf{c})|^2.$$

A non-conservative system following from (2) is :

$$\begin{aligned}\frac{\partial\rho}{\partial t}+\bigtriangledown\rho\cdot\mathbf{u}+&\rho div\mathbf{u}=0,\\ \frac{\partial\mathbf{e}^\beta}{\partial t}+\frac{\partial\mathbf{e}^\beta}{\partial\mathbf{x}}\mathbf{u}+&\left(\frac{\partial\mathbf{u}}{\partial\mathbf{x}}\right)^T\mathbf{e}^\beta=0,\\ \frac{\partial\mathbf{u}}{\partial t}+\frac{\partial\mathbf{u}}{\partial\mathbf{x}}\mathbf{u}+&\frac{\bigtriangledown p}{\rho}-\frac{div\mathbf{S}}{\rho}=0,\\ \frac{\partial\eta}{\partial t}+&\bigtriangledown\eta\cdot\mathbf{u}=0\end{aligned}\tag{4}$$

with

$$p=\rho^2\frac{\partial e^h(\rho,\eta)}{\partial\rho},\qquad \mathbf{S}=-2\rho\left(\frac{\partial e^e}{\partial j_1}\left(\mathbf{g}-\frac{j_1}{3}\mathbf{I}\right)+2\frac{\partial e^e}{\partial j_2}\left(\mathbf{g}^2-\frac{j_2}{3}\mathbf{I}\right)\right).\tag{5}$$

To obtain the equation for $\mathbf{e}^\beta$, we used the compatibility condition

$$\frac{\partial\mathbf{e}^\beta}{\partial\mathbf{x}}=\left(\frac{\partial\mathbf{e}^\beta}{\partial\mathbf{x}}\right)^T.$$

Also, we replaced the energy equation by an equivalent equation expressing the conservation of the entropy. We have finally the system (4) for 14 unknowns

$$\mathbf{U}=\left(\rho,a^1,a^2,a^3,b^1,b^2,b^3,c^1,c^2,c^3,u,v,w,\eta\right)^T.$$

Theorem 1 *Equations (4) are invariant under rotations :*

$$t' = t, \qquad \mathbf{x}' = O\mathbf{x}, \qquad \mathbf{u}' = O\mathbf{u}, \qquad \rho' = \rho, \qquad \left(\mathbf{e}^{\beta}\right)' = O\mathbf{e}^{\beta}, \qquad \eta' = \eta, \tag{6}$$

where O is any element of $SO(3)$.

Proof. The proof is a standard exercise in continuum mechanics.

The system (4) is equivalent to the system (2) under the restriction $rot(\mathbf{e}^{\beta}) = 0$ on the initial data. The evolution equation for $\mathbf{e}^{\beta}$ then ensures that $rot(\mathbf{e}^{\beta}) = 0$ holds for $t > 0$.

2.3 Hyperbolicity

The evolution equations (4) for the unknowns $\mathbf{U}$ can be written in a generic form :

$$\frac{\partial \mathbf{U}}{\partial t} + \mathbf{D}_x \frac{\partial \mathbf{U}}{\partial x} + \mathbf{D}_y \frac{\partial \mathbf{U}}{\partial y} + \mathbf{D}_z \frac{\partial \mathbf{U}}{\partial z} = 0, \tag{7}$$

where $\mathbf{D}_x, \mathbf{D}_y, \mathbf{D}_z$ are 14x14 matrices. Let us consider a smooth hypersurface $h\,(t, x, y, z) = 0$. We denote

$$\tau = \frac{\partial h}{\partial t}, \xi = \frac{\partial h}{\partial x}, \eta = \frac{\partial h}{\partial y}, \varsigma = \frac{\partial h}{\partial z}.$$

The following definitions can be found in Serre (1999) and Dafermos (2000).

The hypersurface is *characteristic* if

$$det\,(\tau \mathbf{I} + \xi \mathbf{D}_x + \eta \mathbf{D}_y + \varsigma \mathbf{D}_z) = 0.$$

The system (7) is $t-$*hyperbolic*, if the eigenvalues τ are real and the matrix $\xi \mathbf{D}_x + \eta \mathbf{D}_y + \varsigma \mathbf{D}_z$ is diagonalizable for any $(\xi,\eta,\varsigma)^T$.

Thanks to Theorem 1, the normal characteristic direction $(\xi,\eta,\varsigma)^T$ can always be transformed by rotation to the one of the Cartesian basis vectors (we have to use three composed rotations defined by Euler angles between the Cartesian basis and a natural right local basis on the characteristic surface). Hence, the unit normal vector $\frac{(\xi,\eta,\varsigma)^T}{\sqrt{\xi^2+\eta^2+\varsigma^2}}$ can always be transformed to $(1,0,0)^T$. The solution is then transformed according to (6). Hence, for the hyperbolicity it will be sufficient to study the 1D case :

$$\frac{\partial \mathbf{U}}{\partial t} + \mathbf{D}_x \frac{\partial \mathbf{U}}{\partial x} = 0. \tag{8}$$

The explicit form of (8) is :

$$\frac{\partial \rho}{\partial t} + u\frac{\partial \rho}{\partial x} + \rho\frac{\partial u}{\partial x} = 0,$$

$$\frac{\partial a^1}{\partial t} + u\frac{\partial a^1}{\partial x} + a^1\frac{\partial u}{\partial x} + b^1\frac{\partial v}{\partial x} + c^1\frac{\partial w}{\partial x} = 0,$$

$$\frac{\partial a^2}{\partial t} + u\frac{\partial a^2}{\partial x} + a^2\frac{\partial u}{\partial x} + b^2\frac{\partial v}{\partial x} + c^2\frac{\partial w}{\partial x} = 0,$$

$$\frac{\partial a^3}{\partial t} + u\frac{\partial a^3}{\partial x} + a^3\frac{\partial u}{\partial x} + b^3\frac{\partial v}{\partial x} + c^3\frac{\partial w}{\partial x} = 0,$$

$$\frac{\partial b^1}{\partial t} + u\frac{\partial b^1}{\partial x} = 0, \quad \frac{\partial b^2}{\partial t} + u\frac{\partial b^2}{\partial x} = 0, \quad \frac{\partial b^3}{\partial t} + u\frac{\partial b^3}{\partial x} = 0,$$

$$\frac{\partial c^1}{\partial t} + u\frac{\partial c^1}{\partial x} = 0, \quad \frac{\partial c^2}{\partial t} + u\frac{\partial c^2}{\partial x} = 0, \quad \frac{\partial c^3}{\partial t} + u\frac{\partial c^3}{\partial x} = 0$$

$$\frac{\partial u}{\partial t} + \frac{\left(c^2 - \frac{\partial S_{11}}{\partial \rho}\right)}{\rho}\frac{\partial \rho}{\partial x}$$

$$-\frac{1}{\rho}\frac{\partial S_{11}}{\partial a^1}\frac{\partial a^1}{\partial x} - \frac{1}{\rho}\frac{\partial S_{11}}{\partial a^2}\frac{\partial a^2}{\partial x} - \frac{1}{\rho}\frac{\partial S_{11}}{\partial a^3}\frac{\partial a^3}{\partial x}$$

$$-\frac{1}{\rho}\frac{\partial S_{11}}{\partial b^1}\frac{\partial b^1}{\partial x} - \frac{1}{\rho}\frac{\partial S_{11}}{\partial b^2}\frac{\partial b^2}{\partial x} - \frac{1}{\rho}\frac{\partial S_{11}}{\partial b^3}\frac{\partial b^3}{\partial x}$$

$$-\frac{1}{\rho}\frac{\partial S_{11}}{\partial c^1}\frac{\partial c^1}{\partial x} - \frac{1}{\rho}\frac{\partial S_{11}}{\partial c^2}\frac{\partial c^2}{\partial x} - \frac{1}{\rho}\frac{\partial S_{11}}{\partial c^3}\frac{\partial c^3}{\partial x}$$

$$+u\frac{\partial u}{\partial x} + \frac{\partial p}{\partial \eta}\frac{\partial \eta}{\partial x} = 0,$$

$$\frac{\partial v}{\partial t} - \frac{1}{\rho}\frac{\partial S_{12}}{\partial \rho}\frac{\partial \rho}{\partial x}$$

$$-\frac{1}{\rho}\frac{\partial S_{12}}{\partial a^1}\frac{\partial a^1}{\partial x} - \frac{1}{\rho}\frac{\partial S_{12}}{\partial a^2}\frac{\partial a^2}{\partial x} - \frac{1}{\rho}\frac{\partial S_{12}}{\partial a^3}\frac{\partial a^3}{\partial x}$$

$$-\frac{1}{\rho}\frac{\partial S_{12}}{\partial b^1}\frac{\partial b^1}{\partial x} - \frac{1}{\rho}\frac{\partial S_{12}}{\partial b^2}\frac{\partial b^2}{\partial x} - \frac{1}{\rho}\frac{\partial S_{12}}{\partial b^3}\frac{\partial b^3}{\partial x}$$

$$-\frac{1}{\rho}\frac{\partial S_{12}}{\partial c^1}\frac{\partial c^1}{\partial x}-\frac{1}{\rho}\frac{\partial S_{12}}{\partial c^2}\frac{\partial c^2}{\partial x}-\frac{1}{\rho}\frac{\partial S_{12}}{\partial c^3}\frac{\partial c^3}{\partial x}$$

$$+u\frac{\partial v}{\partial x}=0$$

$$\frac{\partial w}{\partial t}-\frac{1}{\rho}\frac{\partial S_{13}}{\partial \rho}\frac{\partial \rho}{\partial x}$$

$$-\frac{1}{\rho}\frac{\partial S_{13}}{\partial a^1}\frac{\partial a^1}{\partial x}-\frac{1}{\rho}\frac{\partial S_{13}}{\partial a^2}\frac{\partial a^2}{\partial x}-\frac{1}{\rho}\frac{\partial S_{13}}{\partial a^3}\frac{\partial a^3}{\partial x}$$

$$-\frac{1}{\rho}\frac{\partial S_{13}}{\partial b^1}\frac{\partial b^1}{\partial x}-\frac{1}{\rho}\frac{\partial S_{13}}{\partial b^2}\frac{\partial b^2}{\partial x}-\frac{1}{\rho}\frac{\partial S_{13}}{\partial b^3}\frac{\partial b^3}{\partial x}$$

$$-\frac{1}{\rho}\frac{\partial S_{13}}{\partial c^1}\frac{\partial c^1}{\partial x}-\frac{1}{\rho}\frac{\partial S_{13}}{\partial c^2}\frac{\partial c^2}{\partial x}-\frac{1}{\rho}\frac{\partial S_{13}}{\partial c^3}\frac{\partial c^3}{\partial x}$$

$$+u\frac{\partial w}{\partial x}=0,$$

$$\frac{\partial \eta}{\partial t}+u\frac{\partial \eta}{\partial x}=0.$$

Here $c^2=\dfrac{\partial p\left(\rho,\eta\right)}{\partial \rho}$ is the squared sound velocity, and S_{ij} are the components of the deviatoric part of the stress tensor. In the following, we omit the index x of $\mathbf{D}_x$. The matrix $\mathbf{D}$ is then :

$$\mathbf{D}=\begin{pmatrix}\mathbf{A} & \mathbf{T}\\ \mathbf{O}_{1,13} & u\end{pmatrix}.$$

Here $\mathbf{O}_{m,n}$ is the zero matrix with m rows and n columns,

$$\mathbf{T}=\begin{pmatrix}0 & 0 & 0 & 0 & 0 & 0 & 0 & 0 & 0 & 0 & \dfrac{\partial p}{\partial \eta} & 0 & 0\end{pmatrix}^T,$$

$$\mathbf{A}=\begin{pmatrix}u\mathbf{I}_{10} & \mathbf{B}_1\\ \mathbf{C}_1 & u\mathbf{I}_3\end{pmatrix},$$

$$\mathbf{B}_1 = \begin{pmatrix} \rho & 0 & 0 \\ a^1 & b^1 & c^1 \\ a^2 & b^2 & c^2 \\ a^3 & b^3 & c^3 \\ 0 & 0 & 0 \\ 0 & 0 & 0 \\ 0 & 0 & 0 \\ 0 & 0 & 0 \\ 0 & 0 & 0 \\ 0 & 0 & 0 \end{pmatrix},$$

$$\mathbf{C}_1 = \begin{pmatrix} \frac{c^2 - \frac{\partial S_{11}}{\partial \rho}}{\rho} & -\frac{1}{\rho}\frac{\partial S_{11}}{\partial \mathbf{a}} & -\frac{1}{\rho}\frac{\partial S_{11}}{\partial \mathbf{b}} & -\frac{1}{\rho}\frac{\partial S_{11}}{\partial \mathbf{c}} \\ -\frac{1}{\rho}\frac{\partial S_{12}}{\partial \rho} & -\frac{1}{\rho}\frac{\partial S_{12}}{\partial \mathbf{a}} & -\frac{1}{\rho}\frac{\partial S_{12}}{\partial \mathbf{b}} & -\frac{1}{\rho}\frac{\partial S_{12}}{\partial \mathbf{c}} \\ -\frac{1}{\rho}\frac{\partial S_{13}}{\partial \rho} & -\frac{1}{\rho}\frac{\partial S_{13}}{\partial \mathbf{a}} & -\frac{1}{\rho}\frac{\partial S_{13}}{\partial \mathbf{b}} & -\frac{1}{\rho}\frac{\partial S_{13}}{\partial \mathbf{c}} \end{pmatrix}.$$

The vector $\mathbf{T}$ is nontrivial, if

$$\frac{\partial p}{\partial \eta} > 0.$$

This is a classical inequality in fluid dynamics. In particular, it is verified for the hydrodynamic energy in the form (2). We need to calculate the eigenvalues ν of the matrix $\mathbf{D}$. We have:

$$\mathbf{D} - \nu\mathbf{I} = \begin{pmatrix} \mathbf{A} - \nu\mathbf{I}_{13} & \mathbf{T} \\ \mathbf{O}_{1,13} & u - \nu \end{pmatrix}.$$

$$\det(\mathbf{D} - \nu\mathbf{I}) = (u - \nu)\det(\mathbf{A} - \nu\mathbf{I}_{13}). \tag{9}$$

Then we have to solve the characteristic equation

$$\det(\mathbf{A} - \nu\mathbf{I}_{13}) = \det\begin{pmatrix} (u - \nu)\mathbf{I}_{10} & \mathbf{B}_1 \\ \mathbf{C}_1 & (u - \nu)\mathbf{I}_3 \end{pmatrix} = 0. \tag{10}$$

Let us consider the first case : $\nu = u$. We will show that there are 7 eigenvectors of the matrix $\mathbf{A}$ corresponding to this eigenvalue. Let $\mathbf{r}$ be a right eigenvector of $\mathbf{A}$ corresponding to $\nu = u$:

$$\mathbf{r} = (r_1, ..., r_{13})^T = \left(\mathbf{r}'^T, \mathbf{r}''^T\right)$$

where

$$\mathbf{r}' = (r_1, ..., r_{10})^T, \mathbf{r}'' = (r_{11}, r_{12}, r_{13})^T.$$

The equation for the eigenvectors is :

$$\begin{pmatrix} \mathbf{O}_{10,10} & \mathbf{B}_1 \\ \mathbf{C}_1 & \mathbf{O}_{3,3} \end{pmatrix} \mathbf{r} = \mathbf{0}.$$

Obviously, $\mathbf{r}'' = 0$, because

$$\det \begin{pmatrix} a^1 & b^1 & c^1 \\ a^2 & b^2 & c^2 \\ a^3 & b^3 & c^3 \end{pmatrix} = \det \mathbf{F}^{-1} > \mathbf{0}.$$

In particular, it implies that $rank\,(\mathbf{B}_1) = 3$. To have 7 independent eigenvectors $\mathbf{r}'$ we need to prove that

$$rank\,(\mathbf{C}_1) = 3.$$

Theorem 2 *$rank\,(\mathbf{C}_1) \geq rank\,(\mathbf{C}_1\mathbf{B}_1)$. If $rank\,(\mathbf{C}_1\mathbf{B}_1) = 3$, then $rank\,(\mathbf{C}_1) = 3$.*

Proof. *Indeed, $rank\,(\mathbf{C}_1\mathbf{B}_1) \leq \min(rank\,(\mathbf{C}_1), rank\,(\mathbf{B}_1)) =$*
$\min(rank\,(\mathbf{C}_1), 3) = rank\,(\mathbf{C}_1)$. If $rank\,(\mathbf{C}_1\mathbf{B}_1) = 3$, then $rank\,(\mathbf{C}_1) \geq 3$. But $rank\,(\mathbf{C}_1) \leq 3$. Hence, $rank\,(\mathbf{C}_1) = 3$.

Finally, if $rank\,(\mathbf{C}_1\mathbf{B}_1) = 3$, the matrix $\mathbf{D}$ has 8 multiple eigenvalues $\nu = u$ and a corresponding system of 8 linearly independent right eigenvectors.

Theorem 3 *If $\nu \neq u$, then the eigenvalues of (2) are given by*

$$\det\left((u-\nu)^2\mathbf{I}_3 - \mathbf{K}\right) = 0,$$

where $\mathbf{K} = \mathbf{C}_1\mathbf{B}_1$. In particular, if $\mathbf{K}$ is symmetric and positive definite, then (2) has 6 real eigenvalues $\nu \neq u$ corresponding to 6 independent eigenvectors.

Proof. *Consider now the case where $\nu \neq u$. The characteristic polynomial (2) can be transformed as:*

$$\det \begin{pmatrix} (u-\nu)\,\mathbf{I}_{10} & \mathbf{B}_1 \\ \mathbf{C}_1 & (u-\nu)\,\mathbf{I}_3 \end{pmatrix} = \det \begin{pmatrix} \mathbf{I}_{10} & \mathbf{O}_{10,3} \\ \mathbf{C}_1(u-\nu)^{-1} & \mathbf{I}_3 \end{pmatrix} \times$$

$$det \begin{pmatrix} (u-\nu)\mathbf{I}_{10} & \mathbf{B}_1 \\ \mathbf{O}_{3,10} & (u-\nu)\mathbf{I}_3 - (u-\nu)^{-1}\mathbf{C}_1\mathbf{B}_1 \end{pmatrix}$$

$$= \det \begin{pmatrix} (u-\nu)\mathbf{I}_{10} & \mathbf{B}_1 \\ \mathbf{O}_{3,10} & (u-\nu)\mathbf{I}_3 - (u-\nu)^{-1}\mathbf{C}_1\mathbf{B}_1 \end{pmatrix}$$

$$= (u-\nu)^7 \det\left((u-\nu)^2\mathbf{I}_3 - \mathbf{C}_1\mathbf{B}_1\right)$$

$$= (u-\nu)^7 \det\left((u-\nu)^2\mathbf{I}_3 - \mathbf{K}\right)$$

If $\mathbf{K} = \mathbf{C}_1\mathbf{B}_1$ *is symmetric and positive definite, the eigenvalues* ν *are all real. Now, consider the corresponding eigenvectors.*

$$\begin{pmatrix} (u-\nu)\,\mathbf{I}_{10} & \mathbf{B}_1 \\ \mathbf{C}_1 & (u-\nu)\,\mathbf{I}_3 \end{pmatrix} \mathbf{r} = \mathbf{0}.$$

Then

$$(u-\nu)\,\mathbf{r}' + \mathbf{B}_1\mathbf{r}'' = 0, \qquad \mathbf{C}_1\mathbf{r}' + (u-\nu)\,\mathbf{r}'' = 0.$$

It implies

$$\left(\mathbf{K} - (u-\nu)^2\,\mathbf{I}_3\right)\mathbf{r}'' = 0. \tag{11}$$

If $\mathbf{K}$ *is symmetric and positive definite, the system has three independent eigenvectors* $\mathbf{r}''$*. Finally,*

$$\mathbf{r}' = -\frac{\mathbf{B}_1\mathbf{r}''}{u-\nu}$$

form a system of 6 linearly independent eigenvectors, because $u-\nu$ *can have opposite signs. Hence, the total number of linearly independent vectors* $\mathbf{r}$ *is also* 6*. The theorem is proved.*

Remark The fact that the characteristic polynomial (11) depends only on $u-\nu$ is the property of the invariance of the governing equations with respect to the Galilean group of transformations.

2.4 Sufficient criterion of hyperbolicity

The explicit form of $\mathbf{K}$ (*we used here the fact that* $S_{ij}\,(\rho, \mathbf{a}, \mathbf{b}, \mathbf{c})$ *given by (5)are linear with respect to* ρ) is :

$$\mathbf{K} = \begin{pmatrix} c^2 - \dfrac{S_{11}}{\rho} - \dfrac{1}{\rho}\dfrac{\partial S_{11}}{\partial \mathbf{a}}\cdot\mathbf{a} & -\dfrac{1}{\rho}\dfrac{\partial S_{11}}{\partial \mathbf{a}}\cdot\mathbf{b} & -\dfrac{1}{\rho}\dfrac{\partial S_{11}}{\partial \mathbf{a}}\cdot\mathbf{c} \\ -\dfrac{S_{12}}{\rho} - \dfrac{1}{\rho}\dfrac{\partial S_{12}}{\partial \mathbf{a}}\cdot\mathbf{a} & -\dfrac{1}{\rho}\dfrac{\partial S_{12}}{\partial \mathbf{a}}\cdot\mathbf{b} & -\dfrac{1}{\rho}\dfrac{\partial S_{12}}{\partial \mathbf{a}}\cdot\mathbf{c} \\ -\dfrac{S_{13}}{\rho} - \dfrac{1}{\rho}\dfrac{\partial S_{13}}{\partial \mathbf{a}}\cdot\mathbf{a} & -\dfrac{1}{\rho}\dfrac{\partial S_{13}}{\partial \mathbf{a}}\cdot\mathbf{b} & -\dfrac{1}{\rho}\dfrac{\partial S_{13}}{\partial \mathbf{a}}\cdot\mathbf{c} \end{pmatrix}.$$

Lemma *For* $\mathbf{S}$ *defined by* (5)*, its components are given by the formulas:*

$$S_{11} = -\rho\frac{\partial e^e}{\partial \mathbf{a}}\cdot\mathbf{a}, \quad S_{12} = -\rho\frac{\partial e^e}{\partial \mathbf{a}}\cdot\mathbf{b} = -\rho\frac{\partial e^e}{\partial \mathbf{b}}\cdot\mathbf{a}, \quad S_{13} = -\rho\frac{\partial e^e}{\partial \mathbf{a}}\cdot\mathbf{c} = -\rho\frac{\partial e^e}{\partial \mathbf{c}}\cdot\mathbf{a},$$

$$S_{22} = -\rho\frac{\partial e^e}{\partial \mathbf{b}}\cdot\mathbf{b}, \quad S_{23} = -\rho\frac{\partial e^e}{\partial \mathbf{b}}\cdot\mathbf{c} = -\rho\frac{\partial e^e}{\partial \mathbf{c}}\cdot\mathbf{b}, \quad S_{33} = -\rho\frac{\partial e^e}{\partial \mathbf{c}}\cdot\mathbf{c}.$$

Proof *See Appendix A for the proof.*

The matrix $\mathbf{K}$ is symmetric if

$$\begin{aligned} S_{12} + \frac{\partial S_{12}}{\partial \mathbf{a}}\cdot\mathbf{a} &= \frac{\partial S_{11}}{\partial \mathbf{a}}\cdot\mathbf{b}, \\ S_{13} + \frac{\partial S_{13}}{\partial \mathbf{a}}\cdot\mathbf{a} &= \frac{\partial S_{11}}{\partial \mathbf{a}}\cdot\mathbf{c}, \\ \frac{\partial S_{13}}{\partial \mathbf{a}}\cdot\mathbf{b} &= \frac{\partial S_{12}}{\partial \mathbf{a}}\cdot\mathbf{c}. \end{aligned} \tag{12}$$

Obviously, the Lemma implies the identities (12), and hence the symmetry condition : $\mathbf{K} = \mathbf{K}^T$.

It remains to understand when $\mathbf{K}$ is positive definite. Using the Lemma, we can transform $\mathbf{K}$ to the following form :

$$\mathbf{K} = \begin{pmatrix} c^2 + \frac{\partial e^e}{\partial \mathbf{a}}\cdot\mathbf{a} + \frac{\partial}{\partial \mathbf{a}}\left(\frac{\partial e^e}{\partial \mathbf{a}}\cdot\mathbf{a}\right)\cdot\mathbf{a} & \frac{\partial e^e}{\partial \mathbf{a}}\cdot\mathbf{b} + \frac{\partial}{\partial \mathbf{a}}\left(\frac{\partial e^e}{\partial \mathbf{a}}\cdot\mathbf{b}\right)\cdot\mathbf{a} & \frac{\partial e^e}{\partial \mathbf{a}}\cdot\mathbf{c} + \frac{\partial}{\partial \mathbf{a}}\left(\frac{\partial e^e}{\partial \mathbf{a}}\cdot\mathbf{c}\right)\cdot\mathbf{a} \\ \frac{\partial e^e}{\partial \mathbf{a}}\cdot\mathbf{b} + \frac{\partial}{\partial \mathbf{a}}\left(\frac{\partial e^e}{\partial \mathbf{a}}\cdot\mathbf{b}\right)\cdot\mathbf{a} & \frac{\partial}{\partial \mathbf{a}}\left(\frac{\partial e^e}{\partial \mathbf{a}}\cdot\mathbf{b}\right)\cdot\mathbf{b} & \frac{\partial}{\partial \mathbf{a}}\left(\frac{\partial e^e}{\partial \mathbf{a}}\cdot\mathbf{b}\right)\cdot\mathbf{c} \\ \frac{\partial e^e}{\partial \mathbf{a}}\cdot\mathbf{c} + \frac{\partial}{\partial \mathbf{a}}\left(\frac{\partial e^e}{\partial \mathbf{a}}\cdot\mathbf{c}\right)\cdot\mathbf{a} & \frac{\partial}{\partial \mathbf{a}}\left(\frac{\partial e^e}{\partial \mathbf{a}}\cdot\mathbf{b}\right)\cdot\mathbf{c} & \frac{\partial}{\partial \mathbf{a}}\left(\frac{\partial e^e}{\partial \mathbf{a}}\cdot\mathbf{c}\right)\cdot\mathbf{c} \end{pmatrix} \tag{13}$$

$$= \begin{pmatrix} c^2 & 0 & 0 \\ 0 & 0 & 0 \\ 0 & 0 & 0 \end{pmatrix} +$$

$$\begin{pmatrix} \frac{\partial e^e}{\partial \mathbf{a}}\cdot\mathbf{a} + \frac{\partial}{\partial \mathbf{a}}\left(\frac{\partial e^e}{\partial \mathbf{a}}\cdot\mathbf{a}\right)\cdot\mathbf{a} & \frac{\partial e^e}{\partial \mathbf{a}}\cdot\mathbf{b} + \frac{\partial}{\partial \mathbf{a}}\left(\frac{\partial e^e}{\partial \mathbf{a}}\cdot\mathbf{b}\right)\cdot\mathbf{a} & \frac{\partial e^e}{\partial \mathbf{a}}\cdot\mathbf{c} + \frac{\partial}{\partial \mathbf{a}}\left(\frac{\partial e^e}{\partial \mathbf{a}}\cdot\mathbf{c}\right)\cdot\mathbf{a} \\ \frac{\partial e^e}{\partial \mathbf{a}}\cdot\mathbf{b} + \frac{\partial}{\partial \mathbf{a}}\left(\frac{\partial e^e}{\partial \mathbf{a}}\cdot\mathbf{b}\right)\cdot\mathbf{a} & \frac{\partial}{\partial \mathbf{a}}\left(\frac{\partial e^e}{\partial \mathbf{a}}\cdot\mathbf{b}\right)\cdot\mathbf{b} & \frac{\partial}{\partial \mathbf{a}}\left(\frac{\partial e^e}{\partial \mathbf{a}}\cdot\mathbf{b}\right)\cdot\mathbf{c} \\ \frac{\partial e^e}{\partial \mathbf{a}}\cdot\mathbf{c} + \frac{\partial}{\partial \mathbf{a}}\left(\frac{\partial e^e}{\partial \mathbf{a}}\cdot\mathbf{c}\right)\cdot\mathbf{a} & \frac{\partial}{\partial \mathbf{a}}\left(\frac{\partial e^e}{\partial \mathbf{a}}\cdot\mathbf{b}\right)\cdot\mathbf{c} & \frac{\partial}{\partial \mathbf{a}}\left(\frac{\partial e^e}{\partial \mathbf{a}}\cdot\mathbf{c}\right)\cdot\mathbf{c} \end{pmatrix}$$

$$= \begin{pmatrix} c^2 & 0 & 0 \\ 0 & 0 & 0 \\ 0 & 0 & 0 \end{pmatrix} + \frac{1}{\Delta}\begin{pmatrix} \mathbf{a}^T E''\mathbf{a} & \mathbf{a}^T E''\mathbf{b} & \mathbf{a}^T E''\mathbf{c} \\ \mathbf{a}^T E''\mathbf{b} & \mathbf{b}^T E''\mathbf{b} & \mathbf{b}^T E''\mathbf{c} \\ \mathbf{a}^T E''\mathbf{c} & \mathbf{b}^T E''\mathbf{c} & \mathbf{c}^T E''\mathbf{c} \end{pmatrix} = \begin{pmatrix} c^2 & 0 & 0 \\ 0 & 0 & 0 \\ 0 & 0 & 0 \end{pmatrix} + \mathbf{M},$$

where

$$\mathbf{M} = \frac{1}{\Delta}\mathbf{F}^{-T} E'' \mathbf{F}^{-1}, \tag{14}$$

E is the volume shear energy (determined up to a multiplicative constant ρ_0) :

$$E = \mathbf{a}\cdot(\mathbf{b}\wedge\mathbf{c})\, e^e = \Delta e^e,$$
$$\Delta = \det\left(\mathbf{F}^{-1}\right) = \mathbf{a}\cdot(\mathbf{b}\wedge\mathbf{c}) > 0,$$

and

$$E'' = \frac{\partial^2 E}{\partial \mathbf{a}^2}.$$

Indeed, one has

$$\frac{\partial \Delta}{\partial \mathbf{a}} = \mathbf{b}\wedge\mathbf{c}.$$

Then

$$\frac{\partial E}{\partial \mathbf{a}} = \Delta\frac{\partial e^e}{\partial \mathbf{a}} + e^e \mathbf{b}\wedge\mathbf{c}, \qquad E'' = \frac{\partial^2 E}{\partial \mathbf{a}^2} = \Delta\frac{\partial^2 e^e}{\partial \mathbf{a}^2} + (\mathbf{b}\wedge\mathbf{c})\otimes\frac{\partial e^e}{\partial \mathbf{a}} + \frac{\partial e^e}{\partial \mathbf{a}}\otimes(\mathbf{b}\wedge\mathbf{c}).$$

Hence

$$\mathbf{a}^T E''\mathbf{a} = \Delta\mathbf{a}^T\frac{\partial^2 e^e}{\partial \mathbf{a}^2}\mathbf{a} + 2\Delta\frac{\partial e^e}{\partial \mathbf{a}}\mathbf{a} = \boldsymbol{\Delta}\left(\frac{\partial}{\partial \mathbf{a}}\left(\frac{\partial e^e}{\partial \mathbf{a}}\cdot\mathbf{a}\right)\cdot\mathbf{a} + \frac{\partial e^e}{\partial \mathbf{a}}\cdot\mathbf{a}\right),$$

$$\mathbf{a}^T E''\mathbf{b} = \mathbf{a}^T\left(\Delta\frac{\partial^2 e^e}{\partial \mathbf{a}^2} + (\mathbf{b}\wedge\mathbf{c})\otimes\frac{\partial e^e}{\partial \mathbf{a}} + \frac{\partial e^e}{\partial \mathbf{a}}\otimes(\mathbf{b}\wedge\mathbf{c})\right)\mathbf{b}$$
$$= \Delta\left(\frac{\partial e^e}{\partial \mathbf{a}}\cdot\mathbf{b} + \frac{\partial}{\partial \mathbf{a}}\left(\frac{\partial e^e}{\partial \mathbf{a}}\cdot\mathbf{b}\right)\cdot\mathbf{a}\right).$$

The proof of other relations is analogous.

The matrix $\mathbf{M}$ defined by (14) is positive definite for all $\mathbf{F}$ such that $\det\mathbf{F} > \mathbf{0}$ is equivalent to E'' is positive definite for all $\mathbf{F}$ such that $\det\mathbf{F} > \mathbf{0}$. In particular, it implies that $\mathbf{K} > \mathbf{0}$ if the squared sound velocity c^2 is positive and $\mathbf{M}$ is positive definite (see (13)). We will precise now the condition of positive definiteness of $\mathbf{M}$.

Consider the invariants j_1, j_2 given by (1), (2) (see Appendix A) :

$$j_1 = tr\,(\mathbf{g}) = \frac{\|\mathbf{a}\|^2 + \|\mathbf{b}\|^2 + \|\mathbf{c}\|^2}{|\mathbf{a}\cdot(\mathbf{b}\wedge\mathbf{c})|^{2/3}},$$
$$j_2 = tr\left(\mathbf{g}^2\right) = \frac{\|\mathbf{a}\|^4 + \|\mathbf{b}\|^4 + \|\mathbf{c}\|^4 + 2(\mathbf{a}\cdot\mathbf{b})^2 + 2(\mathbf{b}\cdot\mathbf{c})^2 + 2(\mathbf{a}\cdot\mathbf{c})^2}{|\mathbf{a}\cdot(\mathbf{b}\wedge\mathbf{c})|^{4/3}}.$$

Obviously, they are homogeneous functions of degree zero of $\mathbf{a}, \mathbf{b}, \mathbf{c}$:

$$j_i(\lambda\mathbf{a},\lambda\mathbf{b},\lambda\mathbf{c}) = j_i(\mathbf{a},\mathbf{b},\mathbf{c}),\ i = 1,2,\ \lambda > 0.$$

The same property of homogeneity is then valid for the elements of the matrix $\mathbf{M}$. In particular, it implies that the study of the positive definiteness of $\mathbf{M}$ for all $\mathbf{F}$ with $\det \mathbf{F} > \mathbf{0}$ can be reduced to the study of positive definiteness of $\mathbf{M}$ in the space of the unit-determinant deformation gradients. For this, it is sufficient to introduce the homogeneous stretched variables

$$\mathbf{a}' = \frac{\mathbf{a}}{\Delta^{1/3}}, \qquad \mathbf{b}' = \frac{\mathbf{b}}{\Delta^{1/3}}, \qquad \mathbf{c}' = \frac{\mathbf{b}}{\Delta^{1/3}}$$

Hence,

$$\mathbf{a}'\cdot(\mathbf{b}'\wedge\mathbf{c}') = 1. \tag{15}$$

In the following, we omit the primes. The relation (15) implies the inequality

$$\|\mathbf{a}\|^2 \|\mathbf{b}\|^2 \|\mathbf{c}\|^2 \geq 1 \tag{16}$$

Let us introduce the angles between vectors :

$$\frac{\mathbf{a}\cdot\mathbf{b}}{\|\mathbf{a}\|\,\|\mathbf{b}\|} = X, \ \frac{\mathbf{a}\cdot\mathbf{c}}{\|\mathbf{a}\|\,\|\mathbf{c}\|} = Y, \ \frac{\mathbf{b}\cdot\mathbf{c}}{\|\mathbf{b}\|\,\|\mathbf{c}\|} = Z.$$

Since

$$\mathbf{b}\wedge\mathbf{c} = \left(\|\mathbf{b}\|^2\|\mathbf{c}\|^2 - (\mathbf{b}\cdot\mathbf{c})^2\right)\mathbf{a} + \left((\mathbf{b}\cdot\mathbf{c})(\mathbf{a}\cdot\mathbf{c}) - (\mathbf{a}\cdot\mathbf{b})\|\mathbf{c}\|^2\right)\mathbf{b}$$
$$+ \left((\mathbf{a}\cdot\mathbf{b})(\mathbf{b}\cdot\mathbf{c}) - (\mathbf{a}\cdot\mathbf{c})\|\mathbf{b}\|^2\right)\mathbf{c},$$

the relation

$$\mathbf{a}\cdot(\mathbf{b}\wedge\mathbf{c}) = 1$$

gives us

$$1 = \left(\|\mathbf{b}\|^2\|\mathbf{c}\|^2 - (\mathbf{b}\cdot\mathbf{c})^2\right)\|\mathbf{a}\|^2 + \left((\mathbf{b}\cdot\mathbf{c})(\mathbf{a}\cdot\mathbf{c}) - (\mathbf{a}\cdot\mathbf{b})\|\mathbf{c}\|^2\right)(\mathbf{a}\cdot\mathbf{b})$$
$$+ \left((\mathbf{a}\cdot\mathbf{b})(\mathbf{b}\cdot\mathbf{c}) - (\mathbf{a}\cdot\mathbf{c})\|\mathbf{b}\|^2\right)(\mathbf{a}\cdot\mathbf{c}).$$

Or :

$$X^2 + Y^2 + Z^2 - 2XYZ = \alpha, \tag{17}$$

where

$$0 \leq \alpha = 1 - \frac{1}{\|\mathbf{a}\|^2\|\mathbf{b}\|^2\|\mathbf{c}\|^2} < 1.$$

The coefficient α is positive due to (16). For each $0 \leq \alpha < 1$, the surface S_α determined by (17) is a compact surface contained in the cube

$$-1 \leq X \leq 1, -1 \leq Y \leq 1, -1 \leq Z \leq 1.$$

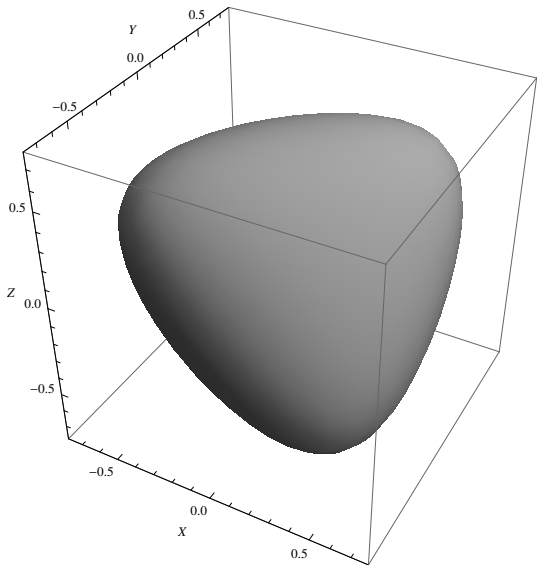

Figure 2.1: The surface $X^2 + Y^2 + Z^2 - 2XYZ = \alpha$ is shown in the case $\alpha = 0.5$. When $\alpha \to 0$, the surface vanishes.

It is homeomorphic to a sphere (see Figure 2.1). The positive definiteness of $\mathbf{M}$ defined by (14) at each surface S_α determined by (17) is equivalent to the positive definiteness of $\mathbf{M}$ in the domain Ω defined by

$$X^2 + Y^2 + Z^2 - 2XYZ < 1, \tag{18}$$

$$-1 \leq X \leq 1, -1 \leq Y \leq 1, -1 \leq Z \leq 1$$

The point $X = Y = Z = 0$ of Ω corresponds to the choice of orthogonal vectors $\mathbf{a}, \mathbf{b}, \mathbf{c}$. In this case $\alpha = 0$. The condition of positive definiteness of $\mathbf{M}$ in Ω defined by (18) can be weakened. Suppose that $\mathbf{M}$ is positive definite for $(\mathbf{a}, \mathbf{b}, \mathbf{c}) = (\mathbf{i}, \mathbf{j}, \mathbf{k})$. If $det\mathbf{M} > \mathbf{0}$ in Ω defined by (18), the matrix $\mathbf{M}$ is then positive definite everywhere in Ω. Indeed, if the matrix $\mathbf{M}$ is positive definite at a point of Ω, it will be positive definite in the vicinity of that point. If one of the eigenvalues of $\mathbf{M}$ vanishes, the determinant also vanishes.

Remark *The third order surface*

$$X^2 + Y^2 + Z^2 - 2XYZ = 1$$

which is the boundary of Ω defined by (18) is called Cayley's cubic surface. For

$$-1 \leq X \leq 1, -1 \leq Y \leq 1, -1 \leq Z \leq 1$$

this surface can be parametrized as

$$X = \cos u, \quad Y = \cos v, \quad Z = \cos(u + v).$$

It is worth noting that Cayley's surface also appears in the study of the strong ellipticity of anisotropic linearly elastic materials (Chiriţă et al. 2007). In particular, for a class of rhombic elastic materials the strong ellipticity condition can be expressed as a number of inequalities involving points at Cayley's surface satisfying some restrictions (see Theorem 1 in Chiriţă et al. 2007).

Finally, the criterion of hyperbolicity of (4) is :

Theorem 4 *Consider isotropic solids with the specific store energy in separable form*

$$e\left(\mathbf{G}, \eta\right) = e^h\left(\rho, \eta\right) + e^e\left(j_1, j_2\right)$$

where ρ is the density, η is the specific entropy,

$$j_i = tr\left(\frac{\mathbf{G}^i}{|\mathbf{G}|^{i/3}}\right), \qquad i = 1, 2,$$

where $\mathbf{G} = (\mathbf{F}\mathbf{F}^T)^{-1}$ is the Finger tensor, and $\mathbf{F}$ is the deformation gradient. We present $\mathbf{F}$ in the form

$$\mathbf{F}^{-1} = (\mathbf{a}, \mathbf{b}, \mathbf{c}),$$

i.e. $\mathbf{a}, \mathbf{b}, \mathbf{c}$ are the columns of $\mathbf{F}^{-1}$. We denote

$$\Delta = \det\left(\mathbf{F}^{-1}\right) = \mathbf{a} \cdot (\mathbf{b} \wedge \mathbf{c}) > 0.$$

and introduce the volume shear energy

$$E = \Delta e^e.$$

Let E'' be the Hessian matrix of E with respect to $\mathbf{a}$, and

$$p = \rho^2 \frac{\partial e^h}{\partial \rho}$$

be the pressure. Suppose that

- $$c^2 = \frac{\partial p}{\partial \rho} > 0, \qquad \frac{\partial p}{\partial \eta} > 0,$$

- $\mathbf{M} = \Delta^{-1}\mathbf{F}^{-T}E''\mathbf{F}^{-1}$ *is positive definite on a one-parameter family of unit-determinant deformation gradient surfaces determined by (17).*

Then the equations (4) are hyperbolic.

2.5 Applications

Consider the stored energy defined by (2), (3). Obviously, the inequalities $c^2 > 0$, $\frac{\partial p}{\partial \eta} > 0$ are verified. We need only to study positive definiteness of $\mathbf{M}$.

2.5.1 The case $a = 0.5$

Consider the shear energy defined by (3) for $a = 0.5$:

$$e^e = \frac{\mu}{8\rho_0}\left(j_2 - 3\right).$$

First, let us show that a sufficient criterion of the rank-one convexity proposed in Dacorogna (2001) is not satisfied for such a choice of e^e. For that, we have to express the energy in terms of the singular values λ_i of $\mathbf{F}$, which are square roots of the eigenvalues of $\mathbf{C}$ or $\mathbf{B}$. Obviously,

$$j_2 = \frac{tr\left(\mathbf{G}^2\right)}{\Delta^{4/3}} = \frac{\frac{1}{\lambda_1^4} + \frac{1}{\lambda_2^4} + \frac{1}{\lambda_3^4}}{\left(\frac{1}{\lambda_1}\frac{1}{\lambda_2}\frac{1}{\lambda_3}\right)^{4/3}} = \frac{\left(\lambda_2\lambda_3\right)^{4/3}}{\lambda_1^{8/3}} + \frac{\left(\lambda_1\lambda_3\right)^{4/3}}{\lambda_2^{8/3}} + \frac{\left(\lambda_1\lambda_2\right)^{4/3}}{\lambda_3^{8/3}}.$$

Then, the calculation of one of the conditions of the Proposition 7 (inequality (22) in Dacorogna (2001)) gives us :

$$\frac{\sqrt{\frac{\partial^2 j_2}{\partial \lambda_1^2}\frac{\partial^2 j_2}{\partial \lambda_2^2}}}{2} + \frac{\partial^2 j_2}{\partial \lambda_1 \partial \lambda_2} + \frac{\frac{\partial j_2}{\partial \lambda_1} - \frac{\partial j_2}{\partial \lambda_2}}{\lambda_1 - \lambda_2} =$$

$$4\frac{(3\lambda_1^3\lambda_2\lambda_3^4 + 3\lambda_1^2\lambda_2^2\lambda_3^4 + 3\lambda_1\lambda_2^3\lambda_3^4 + 2\lambda_2^4\lambda_3^4 + 2\lambda_1^4\lambda_3^4 - \lambda_1^4\lambda_2^4)}{3\lambda_1^{11/3}\lambda_2^{11/3}\lambda_3^{11/3}}.$$

Obviously, if λ_3 is finite, and λ_1 , λ_2 are large, this expression can be negative, while it should be positive to assure the rank-one convexity.

The necessary and sufficient conditions of the rank-one convexity were recently proposed in the 2D case by De Tommasi *et al.* (2012). Instead of variables λ_1, λ_2 they used the variables (u, d) , $u > d > 0$:

$$\lambda_1 = \sqrt{u} + \sqrt{d}, \quad \lambda_2 = \sqrt{u} - \sqrt{d}$$

and formulated the criterion of the rank-one convexity in terms of the stored energy as a function of (u, d). In the 2D case the invariant j_2 is defined as :

$$j_2 = \frac{\lambda_1^2}{\lambda_2^2} + \frac{\lambda_2^2}{\lambda_1^2} = \frac{\left(\sqrt{u} + \sqrt{d}\right)^2}{\left(\sqrt{u} - \sqrt{d}\right)^2} + \frac{\left(\sqrt{u} - \sqrt{d}\right)^2}{\left(\sqrt{u} + \sqrt{d}\right)^2}. \tag{19}$$

It can easily be proved that necessary and sufficient conditions proposed in De Tommasi *et al.* (2012) are satisfied for the energy given by (19). In particular, this function verifies the conditions (III), (IV) of the Theorem 2 in that paper.

However, our aim is the general 3D case involving also the hydrodynamic part of the energy. This is why we will apply directly the Theorem 4 giving the criterium of hyperbolicity in 3D case in terms of the positive definiteness of the matrix $\mathbf{M}$ given by :

$$\mathbf{M} = \frac{1}{\Delta}\mathbf{F}^{-T}E''\mathbf{F}^{-1} = \frac{1}{\Delta}\begin{pmatrix} \mathbf{a}^T E''\mathbf{a} & \mathbf{a}^T E''\mathbf{b} & \mathbf{a}^T E''\mathbf{c} \\ \mathbf{a}^T E''\mathbf{b} & \mathbf{b}^T E''\mathbf{b} & \mathbf{b}^T E''\mathbf{c} \\ \mathbf{a}^T E''\mathbf{c} & \mathbf{b}^T E''\mathbf{c} & \mathbf{c}^T E''\mathbf{c} \end{pmatrix}.$$

Since $\mu/(8\rho_0) > 0$, we take it one, and denote

$$E = \Delta j_2 = \frac{\|\mathbf{a}\|^4 + \|\mathbf{b}\|^4 + \|\mathbf{c}\|^4 + 2\left(\mathbf{b}\cdot\mathbf{c}\right)^2 + 2\left(\mathbf{a}\cdot\mathbf{b}\right)^2 + 2\left(\mathbf{a}\cdot\mathbf{c}\right)^2}{\Delta^{1/3}}.$$

Then

$$\frac{\partial E}{\partial \mathbf{a}} = \frac{4\|\mathbf{a}\|^2\mathbf{a} + 4\left(\mathbf{a}\cdot\mathbf{b}\right)\mathbf{b} + 4\left(\mathbf{a}\cdot\mathbf{c}\right)\mathbf{c}}{\Delta^{1/3}}$$

$$-\frac{1}{3}\left(\frac{\|\mathbf{a}\|^4 + \|\mathbf{b}\|^4 + \|\mathbf{c}\|^4 + 2\left(\mathbf{b}\cdot\mathbf{c}\right)^2 + 2\left(\mathbf{a}\cdot\mathbf{b}\right)^2 + 2\left(\mathbf{a}\cdot\mathbf{c}\right)^2}{\Delta^{4/3}}\right)\left(\mathbf{b}\wedge\mathbf{c}\right),$$

$$\frac{\partial^2 E}{\partial \mathbf{a}^2} = \frac{4\|\mathbf{a}\|^2\mathbf{I} + 8\mathbf{a}\otimes\mathbf{a} + 4\mathbf{b}\otimes\mathbf{b} + 4\mathbf{c}\otimes\mathbf{c}}{\Delta^{1/3}}$$

$$-\frac{1}{3}\left(\frac{4\left\|\mathbf{a}\right\|^2\mathbf{a}+4\left(\mathbf{a}\cdot\mathbf{b}\right)\mathbf{b}+4\left(\mathbf{a}\cdot\mathbf{c}\right)\mathbf{c}}{\Delta^{4/3}}\right)\otimes\left(\mathbf{b}\wedge\mathbf{c}\right)$$

$$-\frac{1}{3}\left(\mathbf{b}\wedge\mathbf{c}\right)\otimes\left(\frac{4\left\|\mathbf{a}\right\|^2\mathbf{a}+4\left(\mathbf{a}\cdot\mathbf{b}\right)\mathbf{b}+4\left(\mathbf{a}\cdot\mathbf{c}\right)\mathbf{c}}{\Delta^{4/3}}\right)$$

$$+\frac{4}{9}\left(\frac{\left\|\mathbf{a}\right\|^4+\left\|\mathbf{b}\right\|^4+\left\|\mathbf{c}\right\|^4+2\left(\mathbf{b}\cdot\mathbf{c}\right)^2+2\left(\mathbf{a}\cdot\mathbf{b}\right)^2+2\left(\mathbf{a}\cdot\mathbf{c}\right)^2}{\Delta^{7/3}}\right)\left(\mathbf{b}\wedge\mathbf{c}\right)\otimes\left(\mathbf{b}\wedge\mathbf{c}\right).$$

The elements of the matrix are :

$$\mathbf{a}^T E''\mathbf{a}=\left(\frac{12\left\|\mathbf{a}\right\|^4+4\left(\mathbf{a}\cdot\mathbf{b}\right)^2+4\left(\mathbf{a}\cdot\mathbf{c}\right)^2}{\Delta^{1/3}}-\frac{2}{3}\left(\frac{4\left\|\mathbf{a}\right\|^4+4\left(\mathbf{a}\cdot\mathbf{b}\right)^2+4\left(\mathbf{a}\cdot\mathbf{c}\right)^2}{\Delta^{1/3}}\right)\right)$$

$$+\frac{4}{9}\left(\frac{\left\|\mathbf{a}\right\|^4+\left\|\mathbf{b}\right\|^4+\left\|\mathbf{c}\right\|^4+2\left(\mathbf{b}\cdot\mathbf{c}\right)^2+2\left(\mathbf{a}\cdot\mathbf{b}\right)^2+2\left(\mathbf{a}\cdot\mathbf{c}\right)^2}{\Delta^{1/3}}\right)$$

$$=\frac{\frac{88}{9}\left\|\mathbf{a}\right\|^4+\frac{4}{9}\left\|\mathbf{b}\right\|^4+\frac{4}{9}\left\|\mathbf{c}\right\|^4+\frac{20}{9}\left(\mathbf{a}\cdot\mathbf{b}\right)^2+\frac{20}{9}\left(\mathbf{a}\cdot\mathbf{c}\right)^2+\frac{8}{9}\left(\mathbf{b}\cdot\mathbf{c}\right)^2}{\Delta^{1/3}},$$

$$\mathbf{a}^T E''\mathbf{b}=\frac{12\left\|\mathbf{a}\right\|^2\left(\mathbf{a}\cdot\mathbf{b}\right)+4\left\|\mathbf{b}\right\|^2\left(\mathbf{a}\cdot\mathbf{b}\right)+4\left(\mathbf{a}\cdot\mathbf{c}\right)\left(\mathbf{b}\cdot\mathbf{c}\right)}{\Delta^{1/3}}$$

$$-\frac{1}{3}\left(\frac{4\left\|\mathbf{a}\right\|^2\left(\mathbf{a}\cdot\mathbf{b}\right)+4\left(\mathbf{a}\cdot\mathbf{b}\right)\left\|\mathbf{b}\right\|^2+4\left(\mathbf{a}\cdot\mathbf{c}\right)\left(\mathbf{b}\cdot\mathbf{c}\right)}{\Delta^{1/3}}\right)$$

$$=\frac{1}{3}\left(\frac{32\left\|\mathbf{a}\right\|^2\left(\mathbf{a}\cdot\mathbf{b}\right)+8\left\|\mathbf{b}\right\|^2\left(\mathbf{a}\cdot\mathbf{b}\right)+8\left(\mathbf{a}\cdot\mathbf{c}\right)\left(\mathbf{b}\cdot\mathbf{c}\right)}{\Delta^{1/3}}\right),$$

$$\mathbf{a}^T E''\mathbf{c}=\frac{\mathbf{8}\left\|\mathbf{a}\right\|^{\mathbf{2}}\left(\mathbf{a}\cdot\mathbf{c}\right)}{\Delta^{2/3}}+\frac{1}{3}\left(\frac{4\left\|\mathbf{a}\right\|^2\left(\mathbf{a}\cdot\mathbf{c}\right)+4\left(\mathbf{a}\cdot\mathbf{b}\right)\left(\mathbf{b}\cdot\mathbf{c}\right)+4\left(\mathbf{a}\cdot\mathbf{c}\right)\left\|\mathbf{c}\right\|^2}{\Delta^{2/3}}\right),$$

$$=\frac{1}{3}\left(\frac{32\left\|\mathbf{a}\right\|^2\left(\mathbf{a}\cdot\mathbf{c}\right)+8\left(\mathbf{a}\cdot\mathbf{b}\right)\left(\mathbf{b}\cdot\mathbf{c}\right)+8\left(\mathbf{a}\cdot\mathbf{c}\right)\left\|\mathbf{c}\right\|^2}{\Delta^{1/3}}\right),$$

$$\mathbf{b}^T E''\mathbf{c}=\frac{4\left\|\mathbf{a}\right\|^2\left(\mathbf{b}\cdot\mathbf{c}\right)+8\left(\mathbf{a}\cdot\mathbf{b}\right)\left(\mathbf{a}\cdot\mathbf{c}\right)+4\left\|\mathbf{b}\right\|^2\left(\mathbf{b}\cdot\mathbf{c}\right)+4\left\|\mathbf{c}\right\|^2\left(\mathbf{b}\cdot\mathbf{c}\right)}{\Delta^{1/3}},$$

$$\mathbf{b}^T E''\mathbf{b} = \frac{4\|\mathbf{a}\|^2\|\mathbf{b}\|^2 + 8(\mathbf{a}\cdot\mathbf{b})^2 + 4\|\mathbf{b}\|^4 + 4(\mathbf{b}\cdot\mathbf{c})^2}{\Delta^{1/3}},$$

$$\mathbf{c}^T E''\mathbf{c} = \frac{4\|\mathbf{a}\|^2\|\mathbf{c}\|^2 + \mathbf{8}(\mathbf{a}\cdot\mathbf{c})^{\mathbf{2}} + 4(\mathbf{b}\cdot\mathbf{c})^2 + 4\|\mathbf{c}\|^4}{\Delta^{1/3}}.$$

Finally, the matrix $\mathbf{M}$ can be written as :

$$\mathbf{M} = \mathbf{D}\mathbf{N}\mathbf{D}^T$$

where

$$\mathbf{N} = \begin{pmatrix} \frac{22\|\mathbf{a}\|^4+\|\mathbf{b}\|^4+\|\mathbf{c}\|^4+5(\mathbf{a}\cdot\mathbf{b})^2+5(\mathbf{a}\cdot\mathbf{c})^2+2(\mathbf{b}\cdot\mathbf{c})^2}{\Delta^{4/3}} & 2\left(\frac{\left(4\|\mathbf{a}\|^2+\|\mathbf{b}\|^2\right)(\mathbf{a}\cdot\mathbf{b})+(\mathbf{a}\cdot\mathbf{c})(\mathbf{b}\cdot\mathbf{c})}{\Delta^{4/3}}\right) \\ 2\left(\frac{\left(4\|\mathbf{a}\|^2+\|\mathbf{b}\|^2\right)(\mathbf{a}\cdot\mathbf{b})+(\mathbf{a}\cdot\mathbf{c})(\mathbf{b}\cdot\mathbf{c})}{\Delta^{4/3}}\right) & \frac{\|\mathbf{a}\|^2\|\mathbf{b}\|^2+\|\mathbf{b}\|^4+2(\mathbf{a}\cdot\mathbf{b})^2+(\mathbf{b}\cdot\mathbf{c})^2}{\Delta^{4/3}} \\ 2\left(\frac{\left(4\|\mathbf{a}\|^2+\|\mathbf{c}\|^2\right)(\mathbf{a}\cdot\mathbf{c})+(\mathbf{a}\cdot\mathbf{b})(\mathbf{b}\cdot\mathbf{c})}{\Delta^{4/3}}\right) & \frac{\left(\|\mathbf{a}\|^2+\|\mathbf{c}\|^2+\|\mathbf{b}\|^2\right)(\mathbf{b}\cdot\mathbf{c})+2(\mathbf{a}\cdot\mathbf{b})(\mathbf{a}\cdot\mathbf{c})}{\Delta^{4/3}} \end{pmatrix}$$

$$\begin{pmatrix} 2\left(\frac{\left(4\|\mathbf{a}\|^2+\|\mathbf{c}\|^2\right)(\mathbf{a}\cdot\mathbf{c})+(\mathbf{a}\cdot\mathbf{b})(\mathbf{b}\cdot\mathbf{c})}{\Delta^{4/3}}\right) \\ \frac{\left(\|\mathbf{a}\|^2+\|\mathbf{c}\|^2+\|\mathbf{b}\|^2\right)(\mathbf{b}\cdot\mathbf{c})+2(\mathbf{a}\cdot\mathbf{b})(\mathbf{a}\cdot\mathbf{c})}{\Delta^{4/3}} \\ \frac{\|\mathbf{a}\|^2\|\mathbf{c}\|^2+\|\mathbf{c}\|^4+\mathbf{2}(\mathbf{a}\cdot\mathbf{c})^{\mathbf{2}}+(\mathbf{b}\cdot\mathbf{c})^2}{\Delta^{4/3}} \end{pmatrix},$$

and

$$\mathbf{D} = \mathbf{D}^T = \begin{pmatrix} \frac{2}{3} & 0 & 0 \\ 0 & 2 & 0 \\ 0 & 0 & 2 \end{pmatrix}.$$

As we have mentioned above, the elements of $\mathbf{M}$ are homogeneous functions of degree zero of $\mathbf{a}, \mathbf{b}, \mathbf{c}$ because e^e is a homogeneous function of degree zero. The positive definiteness of $\mathbf{M}$ is equivalent to the positive definiteness of the matrix $\mathbf{N}$ (which is a reduced form of $\mathbf{M}$) :

$$\mathbf{N} = \begin{pmatrix} 22A^4 + B^4 + C^4 + 5A^2B^2X^2 + 5A^2C^2Y^2 + 2B^2C^2Z^2 & 2AB\left(\left(4A^2+B^2\right)X + C^2YZ\right) \\ 2AB\left(\left(4A^2+B^2\right)X + C^2YZ\right) & B^2\left(A^2+B^2+2A^2X^2+C^2Z^2\right) \\ 2AC\left(\left(4A^2+C^2\right)Y + B^2XZ\right) & BC\left(\left(A^2+B^2+C^2\right)Z + 2A^2XY\right) \end{pmatrix}$$

$$\begin{pmatrix} 2AC\left(\left(4A^2+C^2\right)Y + B^2XZ\right) \\ BC\left(\left(A^2+B^2+C^2\right)Z + 2A^2XY\right) \\ C^2\left(A^2+C^2+2A^2Y^2+B^2Z^2\right) \end{pmatrix}$$

for any A, B, C, X, Y, Z satisfying (17) and (16). Here we have denoted

$$A = \|\mathbf{a}\|, \qquad B = \|\mathbf{b}\|, \qquad C = \|\mathbf{c}\|.$$

Let us show that the matrix is positive definite. Estimating $\mathbf{N}$ in the Cartesian basis (corresponding to $X = Y = Z = 0$ and $A = B = C = 1$) we get

$$\mathbf{N} = \begin{pmatrix} 24 & 0 & 0 \\ 0 & 2 & 0 \\ 0 & 0 & 2 \end{pmatrix}.$$

Hence, $\mathbf{N}$ is positive definite at this point. It is now sufficient to show that the determinant of $\mathbf{N}$ is positive at each surface S_α determined by (17). The determinant of $\mathbf{N}$ is :

$$\begin{aligned}
\det \mathbf{N} = {} & A^8B^2C^2\left(22 - 20\alpha - 2Z^2\right) \\
& + A^6B^4C^2\left(3X^2\left(\alpha - Z^2\right) + (1-\alpha)\left(20 - 7X^2\right) + 2\left(1 - Z^2\right)\right) \\
& + A^6B^2C^4(3Y^2\left(\alpha - Z^2\right) + (1-\alpha)\left(20 - 7Y^2\right) + 2\left(1 - Z^2\right)) \\
& + A^4B^6C^2(2\left(X^2Z - XY\right)^2 + 2\left(X^2 - 2XYZ + Y^2\right) + X^2\left(1 - Z^2\right) + 1 - Z^2) \\
& + A^4B^4C^4(\left(X^2 - Y^2\right)^2 + X^2\left(1 - Z^2\right) + Y^2\left(1 - Z^2\right) - 3Z^4 - 14Z^2(1-\alpha) + 9\alpha^2 - 28\alpha + 22) \\
& + A^4B^2C^6(2\left(Y^2Z - XY\right)^2 + 2\left(X^2 - 2XYZ + Y^2\right) + Y^2\left(1 - Z^2\right) + 1 - Z^2) \\
& + A^2B^8C^2((2XZ - Y)^2 + 1 - Z^2) \\
& + A^2B^6C^4(4\left(XZ^2 - YZ\right)^2 + 2(X - YZ)^2 + X^2\left(Z^2 - 1\right)^2 - 2Z^4 + Z^2 + 1) \\
& + A^2B^4C^6(4\left(XZ - YZ^2\right)^2 + 2(XZ - Y)^2 + Y^2\left(Z^2 - 1\right)^2 - 2Z^4 + Z^2 + 1) \\
& + A^2B^2C^8(2(X - YZ)^2 + 1 - Z^2) \\
& + B^8C^4\left(Z^2 - 1\right)^2 \\
& + 2B^6C^6Z^2\left(Z^2 - 1\right)^2 \\
& + B^4C^8\left(Z^2 - 1\right)^2.
\end{aligned}$$

Let us show that each coefficient of $A^kB^lC^s$ is positive at S_α, $0 \le \alpha < 1$. First, we have

$$X^2 - 2XYZ + Y^2 \ge X^2 + Y^2 - 2|X||Y| = \left(|X| - |Y|\right)^2. \qquad (20)$$

(20) implies, in particular :

$$\alpha = X^2 + Y^2 + Z^2 - 2XYZ \ge Z^2 + \left(|X| - |Y|\right)^2.$$

Hence,

$$Z^2 \leq \alpha. \tag{21}$$

Moreover,

$$-2Z^4 + Z^2 + 1 \geq -2Z^4 + Z^4 + 1 = 1 - Z^4 \geq 1 - \alpha^2 > 0. \tag{22}$$

Finally, using (21) we obtain

$$-3Z^4 - 14Z^2(1-\alpha) + 9\alpha^2 - 28\alpha + 22 \geq -3\alpha^2 - 14\alpha(1-\alpha) + 9\alpha^2 - 28\alpha + 22 \tag{23}$$

$$= 20\alpha^2 - 42\alpha + 22 = 20(\alpha - 1)\left(\alpha - \frac{22}{20}\right) > 0.$$

Inequalities (20)–(23) imply that $\det \mathbf{N} > 0$.

2.5.2 The case $a = 0$

Consider now the limit case of (3) where $a = 0$. Taking

$$E = \Delta j_1 = (||\mathbf{a}||^2 + ||\mathbf{b}||^2 + ||\mathbf{c}||^2)\Delta^{1/3},$$

we obtain

$$E' = 2\mathbf{a}\Delta^{1/3} + \frac{\mathbf{a}^2 + \mathbf{b}^2 + \mathbf{c}^2}{3\Delta^{2/3}}(\mathbf{b} \wedge \mathbf{c}),$$

$$E'' = 2\Delta^{1/3}\mathbf{I} + \frac{2}{3\Delta^{2/3}}\mathbf{a}\otimes(\mathbf{b}\wedge\mathbf{c}) + \frac{2}{3\Delta^{2/3}}(\mathbf{b}\wedge\mathbf{c})\otimes\mathbf{a} - \frac{2}{9\Delta^{5/3}}(||\mathbf{a}||^2 + ||\mathbf{b}||^2 + ||\mathbf{c}||^2)(\mathbf{b}\wedge\mathbf{c})\otimes(\mathbf{b}\wedge\mathbf{c}),$$

and the matrix $\mathbf{M}$ is :

$$\mathbf{M} = \frac{\mathbf{F}^{-T}E''\mathbf{F}^{-1}}{\Delta} = \frac{1}{\Delta^{2/3}}\begin{pmatrix} \frac{10}{3}\mathbf{a}^2 - \frac{2}{9}(||\mathbf{a}||^2 + ||\mathbf{b}||^2 + ||\mathbf{c}||^2) & \frac{8}{3}\mathbf{a}^T\mathbf{b} & \frac{8}{3}\mathbf{a}^T\mathbf{c} \\ \frac{8}{3}\mathbf{a}^T\mathbf{b} & 2||\mathbf{b}||^2 & 2\mathbf{b}^T\mathbf{c} \\ \frac{8}{3}\mathbf{a}^T\mathbf{c} & 2\mathbf{b}^T\mathbf{c} & 2||\mathbf{c}||^2 \end{pmatrix}.$$

In stretched variables the matrix $\mathbf{M}$ is :

$$\mathbf{M} = \begin{pmatrix} \frac{10}{3}A^2 - \frac{2}{9}(A^2 + B^2 + C^2) & \frac{8}{3}ABX & \frac{8}{3}ACY \\ \frac{8}{3}ABX & 2B^2 & 2BCZ \\ \frac{8}{3}ACY & 2BCZ & 2C^2 \end{pmatrix}.$$

Its determinant is :

$$\det \mathbf{M} =$$

$$\frac{384A^2B^2C^2\left(1-\alpha\right)-24B^2C^2\left(1-Z^2\right)\left(C^2+B^2+2A^2\right)}{27}>\frac{24\left(1-\alpha\right)B^2C^2\left(14A^2-\left(C^2+B^2\right)\right)}{27}.$$

If $14A^2-(C^2+B^2)>0$ with $A^2B^2C^2>1$, the equations are hyperbolic. This is obviously true in the vicinity of the equilibrium where $A=B=C=1$, $X=Y=Z=0$. However, for large strains $\det\mathbf{M}$ becomes negative and the equations become elliptic.

2.5.3 General case

The choice of the parameter a in (3) is very important : if a is small, the corresponding matrix $\mathbf{M}$ can not be positive definite for large strains. To find the domain of positive definiteness for $a\neq 0.5$, we parametrized the surface S_α defined by (17) as :

$$X=r\sin\theta\cos\varphi,\qquad Y=r\sin\theta\sin\varphi,\qquad Z=r\cos\theta$$

$$0\leq\theta\leq\pi,\qquad 0\leq\varphi\leq 2\pi$$

where $r\left(\theta,\varphi,\alpha\right)$ is the minimal positive root of the equation (corresponding to (17)) :

$$r^2-r^3\sin^2\theta\cos\theta\sin\left(2\varphi\right)-\alpha=0,\qquad \alpha=1-\frac{1}{A^2B^2C^2}.$$

This root satisfies the relation

$$r\left(\theta,\varphi,0\right)=0,$$

i.e. the surface S_α vanishes as $\alpha\to 0$. We considered the following domain of finite deformations :

$$0<A,B,C<2,\qquad ABC>1. \tag{24}$$

For each value of A,B,C from (24), we verified numerically the condition $\det\mathbf{M}>\mathbf{0}$ where the matrix $\mathbf{M}$ was a linear combination of the corresponding matrices calculated for the energies Δj_1 and Δj_2. If

$$0.45\leq a\leq 0.75,$$

the determinant was always positive. Let us also recall that the positivity of the hydrodynamic squared sound velocity c^2 can only make larger the hyperbolicity region (for hyperbolicity, we need the positive definiteness of the matrix $\mathbf{K}$ defined by (13)). So, in applications the parameter a could be even larger than one.

2.6 Conclusion

We studied the Eulerian equations of hyperelasticity for isotropic solids in a special case of equations of state in separable form : the specific stored energy is a sum of two functions. The first one, the hydrodynamic part of the energy, depends only on the solid density and the entropy, and the second one, the shear energy, depends on the invariants of the Finger tensor in such a way that it is unaffected by the volume change, i.e. it is a homogeneous function of degree zero of the deformation gradient **F**. We formulated a new sufficient criterion of hyperbolicity for such a system. Under natural hypothesis about the hydrodynamic part of the energy (the sound velocity should be real), a symmetric 3x3 matrix (determined in terms of the shear energy e^e) is positive definite on a one-parameter family of unit-determinant deformation gradient surfaces. This criterion was applied to a specific equation of state used in the dynamics of elastic-plastic solids.

2.7 References

Aubert, G. : Necessary and sufficient conditions for isotropic rank one functions in dimension 2. J. Elasticity, **39,** 31 –46 (1995)

Ball, J. M. : Convexity conditions and existence theorems in nonlinear elasticity. Archive for Rational Mechanics and Analysis **63,** 337 – 403 (1977)

Barton, P. T., Drikakis, D. and Romenskii, E. I. : An Eulerian scheme for large elastoplastic deformations in solids. Int. J. Numer. Meth. Engng, **81**, 453 – 484 (2010)

Chiriţă, S., Danescu, A. and Ciarletta, M. : On the strong ellipticity of the anisotropic linearly elastic materials, J. Elasticity, **87,** 1 – 27 (2007)

Davies, P. J. : A simple derivation of necessary and sufficient conditions for the strong ellipticity of isotropic hyperelastic materials in plane strain. J. Elasticity **26**, 291–296 (1991)

Dacorogna, B. : Necessary and sufficient conditions for strong ellipticity of isotropic functions in any dimension. Discrete and Continuous Dynamical Systems - Series B, **1**, N 2, 257 – 263 (2001)

Dafermos, C. M. : Hyperbolic Conservation Laws in Continuum Mechanics, Springer (2000)

De Tommasi, D., Puglisi, G. and Zurlo, G. : A note on the strong ellipticity in two-dimensional isotropic elasticity. J. Elasticity, **109,** 67 –74

(2012)

Favrie, N., Gavrilyuk, S. L. and Saurel, R. : Solid-fluid diffuse interface model in cases of extreme deformations. J. Computational Physics, **228**, 6037-6077 (2009)

Favrie, N. and Gavrilyuk, S. L. : Mathematical and numerical model for nonlinear viscoplasticity. Phil. Trans. R. Soc. A, **369**, 2864 – 2880 (2011)

Favrie, N. and Gavrilyuk, S. L. : Diffuse interface model for compressible fluid-compressible elastic-plastic solid interaction. J. Computational Physics, **231**, 2695 – 2723 (2012)

Flory, R. J. : Thermodynamic relations for highly elastic materials. Transactions of the Faraday Society, **57**, 829 – 838 (1961)

Gavrilyuk, S. L., Favrie, N. and Saurel, R. : Modeling wave dynamics of compressible elastic materials. Journal of Computational Physics, **227**, 2941 – 2969 (2008).

Godunov, S. K. and Romenskii, E. I. : Elements of Continuum Mechanics and Conservation Laws, Kluwer Academic Plenum Publishers, NY (2003)

Godunov, S. K. and Peshkov, I. M. : Thermodynamically consistent nonlinear model of an elastoplastic Maxwell medium. Computational Mathematics and Mathematical Physics, **50**, 1481 – 1498 (2010)

Hartmann, S. and Neff, P. : Polyconvexity of generalized polynomial-type hyperelastic strain energy functions for nearly incompressibility. Int. J. Solid and Structures, **40,** 2767 – 2791 (2003)

Horgan, C. O. : Remarks on ellipticity for the generalized Blatz-Ko constitutive model for a compressible nonlinearly elastic solid. J. Elasticity **42,** 165 – 176 (1995)

Knowles, J. K. and Sternberg, E. : On the failure of ellipticity of the equations for finite elastostatic plane strain. Arch. Rational Mech. Anal. **63**, 321–336 (1977)

Miller, G. H. and Colella, P. : A high order Eulerian Godunov method for elastic plastic flow in solids Journal of Computational Physics, **167**, 131 – 176 (2001)

Sendova, T. and Walton, J. R. : On strong ellipticity for isotropic hyperelastic materials based upon logarithmic strain. International J. Non-Linear Mechanics **40,** 195 – 212 (2005)

Sfyris, D. The strong ellipticity condition under changes in the current and reference configuration. J. Elasticity **103**, 281–287 (2011)

Simpson, H. C., Spector, S. J. : On copositive matrices and strong

ellipticity for isotropic elastic materials. Arch. Rational Mech. Anal. **84,** 55–68 (1983)

Serre, D. : Systems of conservation laws (I), Cambridge University Press (1999).

Wang, Y., Aron, M. : A reformulation of the strong ellipticity conditions for unconstrained hyperelastic media. J. Elasticity **44** , 89-96 (1996)

Appendices

Appendix A

Appendices

A.1 Lemma

If S is defined by (5) *then*

$$S_{11} = -\rho \frac{\partial e^e}{\partial \mathbf{a}} \cdot \mathbf{a}, \quad S_{12} = -\rho \frac{\partial e^e}{\partial \mathbf{a}} \cdot \mathbf{b} = -\rho \frac{\partial e^e}{\partial \mathbf{b}} \cdot \mathbf{a}, \quad S_{13} = -\rho \frac{\partial e^e}{\partial \mathbf{a}} \cdot \mathbf{c} = -\rho \frac{\partial e^e}{\partial \mathbf{c}} \cdot \mathbf{a},$$

$$S_{22} = -\rho \frac{\partial e^e}{\partial \mathbf{b}} \cdot \mathbf{b}, \quad S_{23} = -\rho \frac{\partial e^e}{\partial \mathbf{b}} \cdot \mathbf{c} = -\rho \frac{\partial e^e}{\partial \mathbf{c}} \cdot \mathbf{b}, \quad S_{33} = -\rho \frac{\partial e^e}{\partial \mathbf{c}} \cdot \mathbf{c}.$$

Proof Let $\mathbf{i}, \mathbf{j}, \mathbf{k}$ be the Cartesian basis. We will first calculate the component $S_{11} = \mathbf{i}^T \mathbf{S}\ \mathbf{i}$. For this, we need explicit expressions for the invariants j_1 and j_2 :

$$j_1 = tr\left(\mathbf{g}\right) = tr\left(\frac{\mathbf{G}}{|\mathbf{G}|^{1/3}}\right) = \frac{\sum_{\alpha=1}^{3} \mathbf{e}^\alpha \cdot \mathbf{e}^\alpha}{|\mathbf{G}|^{1/3}} = \frac{\|\mathbf{a}\|^2 + \|\mathbf{b}\|^2 + \|\mathbf{c}\|^2}{|\mathbf{a} \cdot (\mathbf{b} \wedge \mathbf{c})|^{2/3}}, \quad (1)$$

$$j_2 = tr\left(\mathbf{g}^2\right) = tr\left(\frac{\mathbf{G}^2}{|\mathbf{G}|^{2/3}}\right) = \frac{\|\mathbf{a}\|^4 + \|\mathbf{b}\|^4 + \|\mathbf{c}\|^4 + 2\left(\mathbf{a} \cdot \mathbf{b}\right)^2 + 2\left(\mathbf{b} \cdot \mathbf{c}\right)^2 + 2\left(\mathbf{a} \cdot \mathbf{c}\right)^2}{|\mathbf{a} \cdot (\mathbf{b} \wedge \mathbf{c})|^{4/3}}. \quad (2)$$

The proof of (1) is direct. Let us prove (2) :

$$tr\left(\mathbf{G}^2\right) = \mathbf{i}^T \mathbf{G}^2 \mathbf{i} + \mathbf{j}^T \mathbf{G}^2 \mathbf{j} + \mathbf{k}^T \mathbf{G}^2 \mathbf{k} = \|\mathbf{G}\mathbf{i}\|^2 + \|\mathbf{G}\mathbf{j}\|^2 + \|\mathbf{G}\mathbf{k}\|^2$$

$$= \left\| \sum_{\alpha=1}^{3} a^\alpha \mathbf{e}^\alpha \right\|^2 + \left\| \sum_{\alpha=1}^{3} b^\alpha \mathbf{e}^\alpha \right\|^2 + \left\| \sum_{\alpha=1}^{3} c^\alpha \mathbf{e}^\alpha \right\|^2$$

$$
\begin{aligned}
&= \|\mathbf{a}\|^4 + (\mathbf{a}\cdot\mathbf{b})^2 + (\mathbf{a}\cdot\mathbf{c})^2 \\
&+ \|\mathbf{b}\|^4 + (\mathbf{a}\cdot\mathbf{b})^2 + (\mathbf{b}\cdot\mathbf{c})^2 \\
&+ \|\mathbf{c}\|^4 + (\mathbf{a}\cdot\mathbf{c})^2 + (\mathbf{b}\cdot\mathbf{c})^2 .
\end{aligned}
$$

Since

$$
\mathbf{i}^T\mathbf{g}\mathbf{i} = \frac{\mathbf{i}^T\mathbf{G}\mathbf{i}}{|\mathbf{G}|^{1/3}} = \frac{\|\mathbf{a}\|^2}{|\mathbf{a}\cdot(\mathbf{b}\wedge\mathbf{c})|^{2/3}},
$$

$$
\mathbf{i}^T\mathbf{g}^2\mathbf{i} = \frac{\mathbf{i}^T\mathbf{G}^2\mathbf{i}}{|\mathbf{G}|^{2/3}} = \frac{\|\mathbf{a}\|^4 + (\mathbf{a}\cdot\mathbf{b})^2 + (\mathbf{a}\cdot\mathbf{c})^2}{|\mathbf{a}\cdot(\mathbf{b}\wedge\mathbf{c})|^{4/3}},
$$

we finally obtain (see the definition (5) of $\mathbf{S}$) :

$$
S_{11} = \mathbf{i}^T\mathbf{S}\mathbf{i} = -2\rho\left(\frac{\partial e^e}{\partial j_1}\left(\mathbf{i}^T\mathbf{g}\mathbf{i} - \frac{j_1}{3}\right) + 2\frac{\partial e^e}{\partial j_2}\left(\mathbf{i}^T\mathbf{g}^2\mathbf{i} - \frac{j_2}{3}\right)\right) \qquad (3)
$$

$$
= -2\rho\left(\frac{\partial e^e}{\partial j_1}\left(\frac{\|\mathbf{a}\|^2}{|\mathbf{a}\cdot(\mathbf{b}\wedge\mathbf{c})|^{2/3}} - \frac{j_1}{3}\right) + 2\frac{\partial e^e}{\partial j_2}\left(\frac{\|\mathbf{a}\|^4 + (\mathbf{a}\cdot\mathbf{b})^2 + (\mathbf{a}\cdot\mathbf{c})^2}{|\mathbf{a}\cdot(\mathbf{b}\wedge\mathbf{c})|^{4/3}} - \frac{j_2}{3}\right)\right).
$$

Let us show that the expression of S_{11} given by (3) coinciders with that given in the Lemma. For that, consider e^e as a function of $\mathbf{a},\mathbf{b},\mathbf{c}$:

$$
e^e(\mathbf{a},\mathbf{b},\mathbf{c}) = e^e\left(j_1(\mathbf{a},\mathbf{b},\mathbf{c}), j_2(\mathbf{a},\mathbf{b},\mathbf{c})\right).
$$

For any positive λ we define

$$
\tilde{e}^e(\lambda,\mathbf{a},\mathbf{b},\mathbf{c}) = e^e(\lambda\mathbf{a},\mathbf{b},\mathbf{c}) = e^e\left(j_1(\lambda\mathbf{a},\mathbf{b},\mathbf{c}), j_2(\lambda\mathbf{a},\mathbf{b},\mathbf{c})\right)
$$

Differentiating this equality with respect to λ and evaluating it for $\lambda = 1$, we get

$$
\left.\frac{\partial\tilde{e}^e(\lambda,\mathbf{a},\mathbf{b},\mathbf{c})}{\partial\lambda}\right|_{\lambda=1} = \frac{\partial e^e}{\partial\mathbf{a}}\mathbf{a} = \frac{\partial e^e}{\partial j_1}\left.\frac{\partial j_1}{\partial\lambda}\right|_{\lambda=1} + \frac{\partial e^e}{\partial j_2}\left.\frac{\partial j_2}{\partial\lambda}\right|_{\lambda=1}.
$$

We will prove that

$$
\left.\frac{\partial j_1(\lambda\mathbf{a},\mathbf{b},\mathbf{c})}{\partial\lambda}\right|_{\lambda=1} = 2\left(\frac{\|\mathbf{a}\|^2}{|\mathbf{a}\cdot(\mathbf{b}\wedge\mathbf{c})|^{2/3}} - \frac{j_1(\mathbf{a},\mathbf{b},\mathbf{c})}{3}\right), \qquad (4)
$$

$$
\left.\frac{\partial j_2(\lambda\mathbf{a},\mathbf{b},\mathbf{c})}{\partial\lambda}\right|_{\lambda=1} = 4\left(\frac{\|\mathbf{a}\|^4 + (\mathbf{a}\cdot\mathbf{b})^2 + (\mathbf{a}\cdot\mathbf{c})^2}{|\mathbf{a}\cdot(\mathbf{b}\wedge\mathbf{c})|^{4/3}} - \frac{j_2(\mathbf{a},\mathbf{b},\mathbf{c})}{3}\right).
$$

Indeed,

$$j_1(\lambda\mathbf{a},\mathbf{b},\mathbf{c}) = \frac{\lambda^{4/3}\|\mathbf{a}\|^2 + \lambda^{-2/3}\left(\|\mathbf{b}\|^2 + \|\mathbf{c}\|^2\right)}{|\mathbf{a}\cdot(\mathbf{b}\wedge\mathbf{c})|^{2/3}},$$

$$j_2(\lambda\mathbf{a},\mathbf{b},\mathbf{c}) = \frac{\lambda^{8/3}\|\mathbf{a}\|^4 + \lambda^{-4/3}\left(\|\mathbf{b}\|^4 + \|\mathbf{c}\|^4 + 2(\mathbf{b}\cdot\mathbf{c})^2\right)}{|\mathbf{a}\cdot(\mathbf{b}\wedge\mathbf{c})|^{4/3}}.$$

$$+\frac{2\lambda^{2/3}\left((\mathbf{a}\cdot\mathbf{b})^2 + (\mathbf{a}\cdot\mathbf{c})^2\right)}{|\mathbf{a}\cdot(\mathbf{b}\wedge\mathbf{c})|^{4/3}}.$$

Then

$$\left.\frac{\partial j_1(\lambda\mathbf{a},\mathbf{b},\mathbf{c})}{\partial\lambda}\right|_{\lambda=1} = \frac{\frac{4}{3}\|\mathbf{a}\|^2 - \frac{2}{3}\left(\|\mathbf{b}\|^2 + \|\mathbf{c}\|^2\right)}{|\mathbf{a}\cdot(\mathbf{b}\wedge\mathbf{c})|^{2/3}} = 2\left(\frac{\frac{2}{3}\|\mathbf{a}\|^2 - \frac{1}{3}\left(\|\mathbf{b}\|^2 + \|\mathbf{c}\|^2\right)}{|\mathbf{a}\cdot(\mathbf{b}\wedge\mathbf{c})|^{2/3}}\right),$$

$$\left.\frac{\partial j_2(\lambda\mathbf{a},\mathbf{b},\mathbf{c})}{\partial\lambda}\right|_{\lambda=1} = \left(\frac{\frac{8}{3}\|\mathbf{a}\|^4 - \frac{4}{3}\left(\|\mathbf{b}\|^4 + \|\mathbf{c}\|^4 + 2(\mathbf{b}\cdot\mathbf{c})^2\right) + \frac{4}{3}\left((\mathbf{a}\cdot\mathbf{b})^2 + (\mathbf{a}\cdot\mathbf{c})^2\right)}{|\mathbf{a}\cdot(\mathbf{b}\wedge\mathbf{c})|^{4/3}}\right).$$

This proves (4). Hence, we have proved that

$$S_{11} = -\rho\frac{\partial e^e}{\partial\mathbf{a}}\cdot\mathbf{a}.$$

The definition of S_{12} is :

$$S_{12} = \mathbf{i}^T\mathbf{S}\mathbf{j} = -2\rho\left(\frac{\partial e^e}{\partial j_1}\left(\mathbf{i}^T\mathbf{g}\mathbf{j}\right) + 2\frac{\partial e^e}{\partial j_2}\left(\mathbf{i}^T\mathbf{g}^2\mathbf{j}\right)\right)$$

But

$$\mathbf{i}^T\mathbf{g}\mathbf{j} = \frac{\mathbf{a}\cdot\mathbf{b}}{|\mathbf{G}|^{1/3}}, \qquad \mathbf{i}^T\mathbf{g}^2\mathbf{j} = \frac{(\mathbf{G}\mathbf{i})^T\mathbf{G}\mathbf{j}}{|\mathbf{G}|^{2/3}} = \frac{\left(\sum_{\alpha=1}^{3} a^\alpha\mathbf{e}^\alpha\right)^T\left(\sum_{\alpha=1}^{3} b^\alpha\mathbf{e}^\alpha\right)}{|\mathbf{G}|^{2/3}}$$

$$= \frac{\left(\|\mathbf{a}\|^2 + \|\mathbf{b}\|^2\right)(\mathbf{a}\cdot\mathbf{b}) + (\mathbf{a}\cdot\mathbf{c})(\mathbf{b}\cdot\mathbf{c})}{|\mathbf{G}|^{2/3}}$$

Hence

$$S_{12} = \mathbf{i}^T\mathbf{S}\mathbf{j} = -2\rho\left(\frac{\partial e^e}{\partial j_1}\frac{\mathbf{a}\cdot\mathbf{b}}{|\mathbf{G}|^{1/3}} + 2\frac{\partial e^e}{\partial j_2}\frac{\left(\|\mathbf{a}\|^2 + \|\mathbf{b}\|^2\right)(\mathbf{a}\cdot\mathbf{b}) + (\mathbf{a}\cdot\mathbf{c})(\mathbf{b}\cdot\mathbf{c})}{|\mathbf{G}|^{2/3}}\right)$$

We will show that

$$S_{12} = -\rho \frac{\partial e^e}{\partial \mathbf{a}} \cdot \mathbf{b}.$$

Consider the function

$$\tilde{e}^e(\lambda, \mathbf{a}, \mathbf{b}, \mathbf{c}) = e^e(\mathbf{a}\cos\lambda + \mathbf{b}\sin\lambda, \mathbf{b}, \mathbf{c})$$

$$= e^e\left(j_1(\mathbf{a}\cos\lambda + \mathbf{b}\sin\lambda, \mathbf{b}, \mathbf{c}), j_2(\mathbf{a}\cos\lambda + \mathbf{b}\sin\lambda, \mathbf{b}, \mathbf{c})\right).$$

If $\lambda = 0$, we have

$$\tilde{e}^e(0, \mathbf{a}, \mathbf{b}, \mathbf{c}) = e^e(\mathbf{a}, \mathbf{b}, \mathbf{c}) = e^e\left(j_1(\mathbf{a}, \mathbf{b}, \mathbf{c}), j_2(\mathbf{a}, \mathbf{b}, \mathbf{c})\right)$$

Then its derivative with respect to λ evaluated at $\lambda = 0$ is :

$$\left.\frac{\partial \tilde{e}^e(\lambda, \mathbf{a}, \mathbf{b}, \mathbf{c})}{\partial \lambda}\right|_{\lambda=0} = \frac{\partial e^e}{\partial \mathbf{a}} \cdot \mathbf{b}.$$

From the other side, taking into accont that

$$j_1(\mathbf{a}\cos\lambda + \mathbf{b}\sin\lambda, \mathbf{b}, \mathbf{c}) = \frac{\|\mathbf{a}\cos\lambda + \mathbf{b}\sin\lambda\|^2 + \|\mathbf{b}\|^2 + \|\mathbf{c}\|^2}{(\cos\lambda)^{2/3}\left|\mathbf{a}\cdot(\mathbf{b}\wedge\mathbf{c})\right|^{2/3}}$$

$$j_2(\mathbf{a}\cos\lambda + \mathbf{b}\sin\lambda, \mathbf{b}, \mathbf{c})$$

$$= \frac{\|\mathbf{a}\cos\lambda + \mathbf{b}\sin\lambda\|^4 + \|\mathbf{b}\|^4 + \|\mathbf{c}\|^4 + 2(\mathbf{b}\cdot\mathbf{c})^2}{(\cos\lambda)^{4/3}\left|\mathbf{a}\cdot(\mathbf{b}\wedge\mathbf{c})\right|^{4/3}},$$

$$+\frac{2\left((\mathbf{a}\cos\lambda + \mathbf{b}\sin\lambda)\cdot\mathbf{b}\right)^2 + 2\left((\mathbf{a}\cos\lambda + \mathbf{b}\sin\lambda)\cdot\mathbf{c}\right)^2}{(\cos\lambda)^{4/3}\left|\mathbf{a}\cdot(\mathbf{b}\wedge\mathbf{c})\right|^{4/3}},$$

we get

$$-\rho\left(\left.\frac{\partial \tilde{e}^e}{\partial \lambda}\right|_{\lambda=0}\right) = -\rho\left(\left.\frac{\partial \tilde{e}^e}{\partial j_1}\frac{\partial j_1}{\partial \lambda}\right|_{\lambda=0} + \left.\frac{\partial \tilde{e}^e}{\partial j_2}\frac{\partial j_2}{\partial \lambda}\right|_{\lambda=0}\right)$$

$$= -2\rho\left(\frac{\partial e^e}{\partial j_1}\frac{(\mathbf{a}\cdot\mathbf{b})}{\left|\mathbf{a}\cdot(\mathbf{b}\wedge\mathbf{c})\right|^{2/3}} + 2\frac{\partial e^e}{\partial j_2}\left(\frac{\|\mathbf{a}\|^2(\mathbf{a}\cdot\mathbf{b}) + \|\mathbf{b}\|^2(\mathbf{a}\cdot\mathbf{b}) + 4(\mathbf{a}\cdot\mathbf{c})(\mathbf{b}\cdot\mathbf{c})}{\left|\mathbf{a}\cdot(\mathbf{b}\wedge\mathbf{c})\right|^{4/3}}\right)\right)$$

$$= S_{12}$$

Hence, we have proved that

$$S_{12} = -\rho \frac{\partial e^e}{\partial \mathbf{a}} \cdot \mathbf{b}.$$

In the same manner,

$$S_{13} = -\rho \frac{\partial e^e}{\partial \mathbf{a}} \cdot \mathbf{c}.$$

Let us now prove that

$$\frac{\partial e^e}{\partial \mathbf{a}} \cdot \mathbf{b} = \frac{\partial e^e}{\partial \mathbf{b}} \cdot \mathbf{a}.$$

Let

$$\Delta = \mathbf{a} \cdot (\mathbf{b} \wedge \mathbf{c}).$$

Then

$$\frac{\partial \Delta}{\partial \mathbf{a}} = \mathbf{b} \wedge \mathbf{c},$$
$$\frac{\partial \Delta}{\partial \mathbf{b}} = \mathbf{c} \wedge \mathbf{a},$$
$$\frac{\partial \Delta}{\partial \mathbf{c}} = \mathbf{a} \wedge \mathbf{b}.$$

Hence

$$\frac{\partial j_1}{\partial \mathbf{a}} = \frac{2\mathbf{a}}{\Delta^{2/3}} - \frac{2}{3}\left(\frac{\|\mathbf{a}\|^2 + \|\mathbf{b}\|^2 + \|\mathbf{c}\|^2}{\Delta^{5/3}}\right)(\mathbf{b} \wedge \mathbf{c}) = \frac{2\mathbf{a}}{\Delta^{2/3}} - \frac{2}{3} j_1 \frac{(\mathbf{b} \wedge \mathbf{c})}{\Delta},$$

$$\frac{\partial j_1}{\partial \mathbf{b}} = \frac{2\mathbf{b}}{\Delta^{2/3}} - \frac{2}{3}\left(\frac{\|\mathbf{a}\|^2 + \|\mathbf{b}\|^2 + \|\mathbf{c}\|^2}{\Delta^{5/3}}\right)(\mathbf{c} \wedge \mathbf{a}) = \frac{2\mathbf{b}}{\Delta^{2/3}} - \frac{2}{3} j_1 \frac{(\mathbf{c} \wedge \mathbf{a})}{\Delta},$$

$$\frac{\partial j_2}{\partial \mathbf{a}} = \frac{4\|\mathbf{a}\|^2 \mathbf{a} + 4(\mathbf{a} \cdot \mathbf{b})\mathbf{b} + 4(\mathbf{a} \cdot \mathbf{c})\mathbf{c}}{\Delta^{4/3}}$$
$$-\frac{4}{3}\left(\frac{\|\mathbf{a}\|^4 + \|\mathbf{b}\|^4 + \|\mathbf{c}\|^4 + 2(\mathbf{b} \cdot \mathbf{c})^2 + 2(\mathbf{a} \cdot \mathbf{b})^2 + 2(\mathbf{a} \cdot \mathbf{c})^2}{\Delta^{4/3}}\right)\frac{(\mathbf{b} \wedge \mathbf{c})}{\Delta}$$
$$= \frac{4\|\mathbf{a}\|^2 \mathbf{a} + 4(\mathbf{a} \cdot \mathbf{b})\mathbf{b} + 4(\mathbf{a} \cdot \mathbf{c})\mathbf{c}}{\Delta^{4/3}} - \frac{4}{3} j_2 \frac{(\mathbf{b} \wedge \mathbf{c})}{\Delta},$$

$$\frac{\partial j_2}{\partial \mathbf{b}} = \frac{4\|\mathbf{b}\|^2 \mathbf{b} + 4(\mathbf{b} \cdot \mathbf{c})\mathbf{c} + 4(\mathbf{a} \cdot \mathbf{b})\mathbf{a}}{\Delta^{4/3}}$$
$$-\frac{4}{3}\left(\frac{\|\mathbf{a}\|^4 + \|\mathbf{b}\|^4 + \|\mathbf{c}\|^4 + 2(\mathbf{b} \cdot \mathbf{c})^2 + 2(\mathbf{a} \cdot \mathbf{b})^2 + 2(\mathbf{a} \cdot \mathbf{c})^2}{\Delta^{4/3}}\right)\frac{(\mathbf{c} \wedge \mathbf{a})}{\Delta},$$

It implies

$$\frac{\partial j_1}{\partial \mathbf{a}} \cdot \mathbf{b} = \frac{2\mathbf{a} \cdot \mathbf{b}}{\Delta^{2/3}} = \frac{\partial j_1}{\partial \mathbf{b}} \cdot \mathbf{a},$$

$$\frac{\partial j_2}{\partial \mathbf{a}}\cdot\mathbf{b} = \frac{4\left\|\mathbf{a}\right\|^2(\mathbf{a}\cdot\mathbf{b}) + 4(\mathbf{a}\cdot\mathbf{b})\left\|\mathbf{b}\right\|^2 + 4(\mathbf{a}\cdot\mathbf{c})(\mathbf{c}\cdot\mathbf{b})}{\Delta^{4/3}}$$
$$= \frac{\partial j_2}{\partial \mathbf{b}}\cdot\mathbf{a} = \frac{4\left\|\mathbf{b}\right\|^2(\mathbf{a}\cdot\mathbf{b}) + 4(\mathbf{b}\cdot\mathbf{c})(\mathbf{a}\cdot\mathbf{c}) + 4(\mathbf{a}\cdot\mathbf{b})\left\|\mathbf{a}\right\|^2}{\Delta^{4/3}}.$$

Consequently,

$$S_{12} = -\rho\frac{\partial e^e}{\partial \mathbf{a}}\cdot\mathbf{b} = -\rho\left(\frac{\partial e^e}{\partial j_1}\frac{\partial j_1}{\partial \mathbf{a}}\cdot\mathbf{b} + \frac{\partial e^e}{\partial j_2}\frac{\partial j_2}{\partial \mathbf{a}}\cdot\mathbf{b}\right) = -\rho\left(\frac{\partial e^e}{\partial j_1}\frac{\partial j_1}{\partial \mathbf{b}}\cdot\mathbf{a} + \frac{\partial e^e}{\partial j_2}\frac{\partial j_2}{\partial \mathbf{b}}\cdot\mathbf{a}\right)$$
$$= -\rho\frac{\partial e^e}{\partial \mathbf{b}}\cdot\mathbf{a}.$$

In the same manner, one can prove that

$$S_{13} = -\rho\frac{\partial e^e}{\partial \mathbf{a}}\cdot\mathbf{c} = -\rho\left(\frac{\partial e^e}{\partial j_1}\frac{\partial j_1}{\partial \mathbf{a}}\cdot\mathbf{c} + \frac{\partial e^e}{\partial j_2}\frac{\partial j_2}{\partial \mathbf{a}}\cdot\mathbf{c}\right) = -\rho\left(\frac{\partial e^e}{\partial j_1}\frac{\partial j_1}{\partial \mathbf{c}}\cdot\mathbf{a} + \frac{\partial e^e}{\partial j_2}\frac{\partial j_2}{\partial \mathbf{c}}\cdot\mathbf{a}\right)$$
$$= -\rho\frac{\partial e^e}{\partial \mathbf{c}}\cdot\mathbf{a},$$
$$S_{23} = -\rho\frac{\partial e^e}{\partial \mathbf{b}}\cdot\mathbf{c} = -\rho\left(\frac{\partial e^e}{\partial j_1}\frac{\partial j_1}{\partial \mathbf{b}}\cdot\mathbf{c} + \frac{\partial e^e}{\partial j_2}\frac{\partial j_2}{\partial \mathbf{b}}\cdot\mathbf{c}\right) = -\rho\left(\frac{\partial e^e}{\partial j_1}\frac{\partial j_1}{\partial \mathbf{c}}\cdot\mathbf{b} + \frac{\partial e^e}{\partial j_2}\frac{\partial j_2}{\partial \mathbf{c}}\cdot\mathbf{b}\right)$$
$$= -\rho\frac{\partial e^e}{\partial \mathbf{c}}\cdot\mathbf{b}.$$

The expressions for S_{22} and S_{33} are also direct consequences of the isotropy hypothesis and the formula for S_{11}. The Lemma is proved.

Chapitre 3

Le problème du piston en hyperélasticité

Ce chapitre correspond à l'article Ndanou, S., Favrie ,N. & Gavrilyuk, S.(2014) The piston problem in hyper-elasticity with the stored energy in separable form sous Mathematics and Mechanics of Solids

3.1 Introduction

An Eulerian hyperelastic hyperbolic conservative model is studied (Miller and Colella [26], Godunov and Romenskii [15] and others). We use here an equivalent formulation better adapted to the numerical study in the Eulerian coordinates (Gavrilyuk, Favrie and Saurel [3]). We consider the case of isotropic elastic solids where the stored energy is a function of the invariants of the Finger tensor (inverse of the left Cauchy-Green tensor). The hyperelastic hyperbolic model can also be extended to deal with visco-plasticity (Favrie and Gavrilyuk [4]). Recently, we proposed a criterion of hyperbolicity of the equations of hyperelasticity in the case where the stored energy is taken in separable form : it is the sum of the energy depending only on the density and the entropy (hydrodynamic part), and the energy depending only on a the invariants of a reduced Finger tensor having unit determinant (isochoric part). In this paper, we study the piston problem for such a model. More exactly, we study auto-similar solutions appearing when the velocity is prescribed at the boundary of a non-deformed elastic half-space ('piston' problem). The fact that the elastic half-space is initially

free of shear stresses allows us to simplify the solution. In particular, we constructed solutions containing transverse shocks in which the solid density after the shock is lower then that before the shock (this discontinuity is thus a 'rarefaction' shock). This is a consequence of the fact that the eigenfields corresponding to transverse waves (shear waves) of the governing equations of hyperelasticity are not genuinely non-linear in the sense of Lax (Godlewski and Raviart [5], Lax [6], LeFloch [7], Serre [8]).

The paper is organized as follows: in section 2 we present the governing equations and the hyperbolicity study; in section 3 we study the eigenfields; in section 4 the piston problem is solved.

3.2 Governing Equations and Hyperbolicity

3.2.1 Governing equations of isotropic solids

The general hyperelasticity model in the case of isotropic solids can be written as follows (Miller and Colella [26], Godunov and Romenskii [15], Gavrilyuk, Favrie and Saurel [3]):

$$\begin{cases} \dfrac{\partial \rho}{\partial t} + div(\rho \mathbf{u}) = 0, \\ \dfrac{\partial (\rho \mathbf{u})}{\partial t} + div\left(\rho \mathbf{u} \otimes \mathbf{u} - \boldsymbol{\sigma}\right) = 0, \\ \dfrac{\partial \left(\rho e + \frac{1}{2}\rho \mathbf{u}^2\right)}{\partial t} + div\left(\left(\rho e + \frac{1}{2}\rho \mathbf{u}^2\right)\mathbf{u} - \boldsymbol{\sigma}\mathbf{u}\right) = 0, \\ \dfrac{\partial \mathbf{e}^\beta}{\partial t} + \boldsymbol{\nabla}_{\mathbf{x}}(\mathbf{u}.\mathbf{e}^\beta) = 0, \quad \mathbf{curl}(\mathbf{e}^\beta) = 0, \quad \beta = 1,2,3. \end{cases} \tag{1}$$

The operators div, $\mathbf{curl}$ and $\boldsymbol{\nabla}$ are applied in the Eulerian coordinates $\mathbf{x} = (x, y, z)^T$. Here ρ is the solid density, $\mathbf{u} = (u, v, w)^T$ is the velocity field, $e\,(\mathbf{G},\eta)$ is the internal energy, η is the specific entropy, $\mathbf{G} = (\mathbf{F}\mathbf{F}^T)^{-1}$ is the Finger tensor, $\mathbf{F}$ is the deformation gradient, $\boldsymbol{\sigma}$ is the Cauchy stress tensor defined as

$$\boldsymbol{\sigma} = -2\rho \frac{\partial e}{\partial \mathbf{G}} \mathbf{G}, \tag{2}$$

$\boldsymbol{\sigma}$ is symmetric, because we deal with isotropic solids. The vectors $\mathbf{e}^\beta = (a^\beta, b^\beta, c^\beta)^T$ are the columns of $\mathbf{F}^{-T} = (\mathbf{e}^1, \mathbf{e}^2, \mathbf{e}^3)$. Since $\mathbf{e}^\beta$ are gradients of the Lagrangian coordinates, necessarily, the compatibility condition is $\mathbf{curl}(\mathbf{e}^\beta) = 0$. This condition is time invariant : if it is satisfied initially, then it is satisfied for all the time.

We take the internal energy e in separable form (Flory [13]) : $e = e^h(\rho,\eta) + e^e(\mathbf{g})$, where η is the specific entropy, $\rho = \rho_0|\mathbf{G}|^{\frac{1}{2}}$, $|\mathbf{G}| = det(\mathbf{G})$, ρ_0 is a reference density, $\mathbf{g} = \dfrac{\mathbf{G}}{|\mathbf{G}|^{\frac{1}{3}}}$ is a reduced Finger tensor. The stress tensor is also in separable form

$$\boldsymbol{\sigma} = -p\mathbf{I} + \mathbf{S}, \quad p = \rho^2 \frac{\partial e^h(\rho,\eta)}{\partial \rho}, \quad \mathbf{S} = -2\rho \frac{\partial e^e}{\partial \mathbf{G}}\mathbf{G}, \quad tr(\mathbf{S}) = 0. \tag{3}$$

The hydrodynamic sound speed c is defined as

$$c^2 = \frac{\partial p}{\partial \rho}.$$

We will suppose that the following natural inequalities are satisfied :

$$\frac{\partial p}{\partial \rho} > 0, \ \frac{\partial p}{\partial \eta} > 0. \tag{4}$$

The following particular forms of the energy can be used in applications :

$$e^h(\rho,\eta) = \frac{p + \gamma p_\infty}{(\gamma - 1)\,\rho}, \quad p = f(\eta)\rho^\gamma, \tag{5}$$

$$e^e(\mathbf{g}) = \frac{\mu}{8\rho_0}\left(tr(\mathbf{g}^2) - 3\right). \tag{6}$$

Here $f(\eta)$ is a function of entropy, and p_∞, $\gamma > 1$, μ are material constants. In the limit of small deformations these equations of state give us Hooke's law. If $df/d\eta > 0$, the hydrodynamic part of the energy satisfies inequalities (4).

A non-conservative form of (1) is :

$$\begin{cases} \dfrac{\partial \rho}{\partial t} + \mathbf{u}\cdot\nabla\rho + \rho div\,(\mathbf{u}) = 0, \\ \dfrac{\partial \mathbf{u}}{\partial t} + \dfrac{\partial \mathbf{u}}{\partial \mathbf{x}}\mathbf{u} + \dfrac{\nabla p}{\rho} - \dfrac{div\,(\mathbf{S})}{\rho} = 0, \\ \dfrac{\partial \eta}{\partial t} + \mathbf{u}\cdot\nabla\eta = 0, \\ \dfrac{\partial \mathbf{e}^\beta}{\partial t} + \dfrac{\partial \mathbf{e}^\beta}{\partial \mathbf{x}}\mathbf{u} + \left(\dfrac{\partial \mathbf{u}}{\partial \mathbf{x}}\right)^T \mathbf{e}^\beta = 0, \quad \beta = 1,2,3. \end{cases} \tag{7}$$

These equations are invariant under the transformation group

$$t' = t, \quad \mathbf{x}' = O\mathbf{x}, \quad \mathbf{u}' = O\mathbf{u}, \quad \mathbf{e}^{\beta\prime} = O\mathbf{e}^\beta, \quad \rho' = \rho, \quad \eta' = \eta,$$

where O is any element of $SO(3)$. In particular, it allows us to reduce the hyperbolicity study of the multi-dimensional system (7) to the hyperbolicity study of the corresponding 1D system (see for detail [27]). For the case (5), (6), equations (7) are hyperbolic for any deformations. In particular, this will imply the hyperbolicity of the system (1) because the system (7) contains (1) in a particular case where $\mathbf{curl}(\mathbf{e}^\beta) = 0$. The proof of hyperbolicity of (7) is based on the following technical Lemma.

Lemma 3.2.1 *(Ndanou, Favrie and Gavrilyuk [27]). Let the energy $e^e(\mathbf{g})$ be an isotropic function of $\mathbf{g} = \dfrac{\mathbf{G}}{|\mathbf{G}|^{\frac{1}{3}}}$, i.e. $e^e(\mathbf{g}) = e^e(j_1, j_2)$, where $j_i = tr(\mathbf{g}^i)$, $i = 1, 2$. Let us introduce the vectors $\mathbf{a} = (a^\alpha)$, $\mathbf{b} = (b^\alpha)$ and $\mathbf{c} = (c^\alpha)$, $\alpha = 1, 2, 3$. Then the deviatoric part of the stress tensor can be expressed as :*

$$\mathbf{S} = -2\rho\frac{\partial e^e}{\partial \mathbf{G}}\mathbf{G} = -\rho\begin{pmatrix} \frac{\partial e^e}{\partial \mathbf{a}}\mathbf{a} & \frac{\partial e^e}{\partial \mathbf{a}}\mathbf{b} & \frac{\partial e^e}{\partial \mathbf{a}}\mathbf{c} \\ \frac{\partial e^e}{\partial \mathbf{a}}\mathbf{b} & \frac{\partial e^e}{\partial \mathbf{b}}\mathbf{b} & \frac{\partial e^e}{\partial \mathbf{c}}\mathbf{b} \\ \frac{\partial e^e}{\partial \mathbf{a}}\mathbf{c} & \frac{\partial e^e}{\partial \mathbf{c}}\mathbf{b} & \frac{\partial e^e}{\partial \mathbf{c}}\mathbf{c} \end{pmatrix}. \tag{8}$$

Moreover,

$$\frac{\partial e^e}{\partial \mathbf{a}}\mathbf{b} = \frac{\partial e^e}{\partial \mathbf{b}}\mathbf{a}, \quad \frac{\partial e^e}{\partial \mathbf{a}}\mathbf{c} = \frac{\partial e^e}{\partial \mathbf{c}}\mathbf{a}, \quad \frac{\partial e^e}{\partial \mathbf{b}}\mathbf{c} = \frac{\partial e^e}{\partial \mathbf{c}}\mathbf{b},$$

In particular, the lemma 3.2.1 guarantees the symmetry of $\mathbf{S}$.

Consider the 1D case where all the variables depend only on (t, x). Moreover, $\mathbf{u} = (u, v, w)^T = (u, v, 0)^T$, $a^3 = 0$, $b^1 = 0$, $b^2 = 1$, $b^3 = 0$, $c^1 = 0$, $c^2 = 0$, $c^3 = 1$. The corresponding system of equations is as follows :

$$\begin{cases} \dfrac{\partial \rho}{\partial t} + u\dfrac{\partial \rho}{\partial x} + \rho\dfrac{\partial u}{\partial x} = 0, \\ \dfrac{\partial a^1}{\partial t} + u\dfrac{\partial a^1}{\partial x} + a^1\dfrac{\partial u}{\partial x} = 0, \\ \dfrac{\partial a^2}{\partial t} + u\dfrac{\partial a^2}{\partial x} + a^2\dfrac{\partial u}{\partial x} + \dfrac{\partial v}{\partial x} = 0, \\ \dfrac{\partial u}{\partial t} + u\dfrac{\partial u}{\partial x} + \left(\dfrac{c^2}{\rho} - \dfrac{1}{\rho}\dfrac{\partial S_{11}}{\partial \rho}\right)\dfrac{\partial \rho}{\partial x} - \dfrac{1}{\rho}\dfrac{\partial S_{11}}{\partial a^1}\dfrac{\partial a^1}{\partial x} - \dfrac{1}{\rho}\dfrac{\partial S_{11}}{\partial a^2}\dfrac{\partial a^2}{\partial x} + \dfrac{\partial p}{\partial \eta}\dfrac{\partial \eta}{\partial x} = 0, \\ \dfrac{\partial v}{\partial t} + u\dfrac{\partial v}{\partial x} - \dfrac{1}{\rho}\dfrac{\partial S_{12}}{\partial \rho}\dfrac{\partial \rho}{\partial x} - \dfrac{1}{\rho}\dfrac{\partial S_{12}}{\partial a^1}\dfrac{\partial a^1}{\partial x} - \dfrac{1}{\rho}\dfrac{\partial S_{12}}{\partial a^2}\dfrac{\partial a^2}{\partial x} = 0, \\ \dfrac{\partial \eta}{\partial t} + u\dfrac{\partial \eta}{\partial x} = 0. \end{cases} \tag{9}$$

If we set $\mathbf{U} = (\rho, a^1, a^2, u, v, \eta)^T$, the system can be written as follows

$$\frac{\partial \mathbf{U}}{\partial t} + \mathbf{A}\frac{\partial \mathbf{U}}{\partial x} = 0, \tag{10}$$

with

$$\mathbf{A} = \begin{pmatrix} u & 0 & 0 & \rho & 0 & 0 \\ 0 & u & 0 & a^1 & 0 & 0 \\ 0 & 0 & u & a^2 & 1 & 0 \\ \frac{c^2}{\rho} - \frac{1}{\rho}\frac{\partial S_{11}}{\partial \rho} & -\frac{1}{\rho}\frac{\partial S_{11}}{\partial a^1} & -\frac{1}{\rho}\frac{\partial S_{11}}{\partial a^2} & u & 0 & \frac{\partial p}{\partial \eta} \\ -\frac{1}{\rho}\frac{\partial S_{12}}{\partial \rho} & -\frac{1}{\rho}\frac{\partial S_{12}}{\partial a^1} & -\frac{1}{\rho}\frac{\partial S_{12}}{\partial a^2} & 0 & u & 0 \\ 0 & 0 & 0 & 0 & 0 & u \end{pmatrix} \tag{11}$$

Lemma 3.2.2 *The eigenvalues $\nu_6 > \nu_5 > v_4 = \nu_3 > \nu_2 > \nu_1$ of the matrix A are given by :*

$$\nu_{1,6} = u \pm \sqrt{\frac{tr(\mathbf{K}) + \sqrt{\Delta}}{2}},$$

$$\nu_{2,5} = u \pm \sqrt{\frac{tr(\mathbf{K}) - \sqrt{\Delta}}{2}},$$

$$\nu_{3,4} = u,$$

where

$$\mathbf{K} = \begin{pmatrix} c^2 & 0 \\ 0 & 0 \end{pmatrix} + \mathbf{M},$$

$$\mathbf{M} = \begin{pmatrix} \frac{\partial e^e}{\partial \mathbf{a}} \cdot \mathbf{a} + \frac{\partial}{\partial \mathbf{a}}\left(\frac{\partial e^e}{\partial \mathbf{a}}.\mathbf{a}\right) \cdot \mathbf{a} & \frac{\partial e^e}{\partial \mathbf{a}} \cdot \mathbf{b} + \frac{\partial}{\partial \mathbf{a}}\left(\frac{\partial e^e}{\partial \mathbf{a}} \cdot \mathbf{b}\right) \cdot \mathbf{a} \\ \frac{\partial e^e}{\partial \mathbf{a}} \cdot \mathbf{b} + \frac{\partial}{\partial \mathbf{a}}\left(\frac{\partial e^e}{\partial \mathbf{a}} \cdot \mathbf{b}\right) \cdot \mathbf{a} & \frac{\partial}{\partial \mathbf{a}}\left(\frac{\partial e^e}{\partial \mathbf{a}} \cdot \mathbf{b}\right) \cdot \mathbf{b} \end{pmatrix},$$

$$\Delta = (tr(\mathbf{K}))^2 - 4det(\mathbf{K}) = (K_{11} - K_{22})^2 + 4K_{12}^2,$$

$\mathbf{a} = (a^1, a^2)^T$ *and* $\mathbf{b} = (0, 1)^T$.

The proof of the Lemma 3.2.2 is direct. The Lemma 3.2.1 was used to obtain a symmetric form of $\mathbf{K}$.

Note that $\mathbf{M}$ is positive definite for the equation of state (6) [27]. Since $c^2 > 0$, $\mathbf{K}$ is also positive definite. In particular, the eigenvalues ν_i, $i = 1, ..., 6$ are real. We find now the corresponding right eigenvectors of $\mathbf{A}$.

The eigenvectors $\mathbf{V}_3 = (1,0,0,0,0,0)^T$ and $\mathbf{V}_4 = (0,0,0,0,0,1)^T$ correspond to the eigenvalues $\nu_3 = \nu_4 = u$. For the eigenvalues ν_i, $i = 1, 6$ corresponding to longitudinal waves the eigenvectors are :

$$\mathbf{V}_i = \left(\frac{\rho}{(\nu_i - u)}, \frac{a^1}{(\nu_i - u)}, \frac{2a^2 K_{12} + K_{22} - K_{11} + \sqrt{\Delta}}{2K_{12}(\nu_i - u)}, 1, \frac{K_{22} - K_{11} + \sqrt{\Delta}}{2K_{12}}, 0 \right).$$

Since

$$(K_{22} - K_{11}) + \sqrt{\Delta} = \frac{(K_{22} - K_{11})^2 - \Delta}{(K_{22} - K_{11}) - \sqrt{\Delta}} = \frac{-4K_{12}^2}{(K_{22} - K_{11}) + \sqrt{\Delta}}.$$

the eigenvectors are not singular when K_{12} vanishes.

For the eigenvalues ν_i, $i = 2, 5$ corresponding to transverse waves the eigenvectors are :

$$\mathbf{V}_i = \left(\frac{\rho}{(\nu_i - u)}, \frac{a^1}{(\nu_i - u)}, \frac{2a^2 K_{12} + K_{22} - K_{11} - \sqrt{\Delta}}{2K_{12}(\nu_i - u)}, 1, \frac{K_{22} - K_{11} - \sqrt{\Delta}}{2K_{12}}, 0 \right).$$

The eigenvalues can be ordered :

$$\nu_1 > \nu_2 > \nu_3 = \nu_4 > \nu_5 > \nu_6.$$

ν_1 and ν_6 are longitudinal wave speeds, ν_2 and ν_5 are transverse wave speeds, and ν_3 or ν_4 are speeds of contact characteristics. Let us also remark that the equation of the density can be integrated in the form

$$\rho = \rho_0 a^1. \tag{12}$$

Here ρ_0 is a constant. In general, ρ_0 can also be a function of time and space which is conserved along trajectories.

3.3 Study of eigenfields

3.3.1 Eigenfields associated to $\nu_3 = \nu_4 = u$

Obviously, these fields are linearly degenerate : $\boldsymbol{\nabla}\nu_3.\mathbf{V}_3 = \boldsymbol{\nabla}\nu_4.\mathbf{V}_4 = 0$.

3.3.2 Eigenfields associated to ν_1 and ν_6

These fields corresponding to longitudinal waves and estimated on the variety (12) are genuinely non-linear in the sense of Lax :

$$\nabla\nu_1.\mathbf{V}_1|_{\rho=\rho_0 a^1} > 0$$

This result can easily be checked analytically in the vicinity of the equilibrium ($a^1 = 1$, $a^2 = 0$), and numerically out of equilibrium.

Simple waves

We are looking for the solution of (10) in the form :

$$\mathbf{U}(t,x) = \mathbf{U}\left(\frac{x}{t}\right) = \mathbf{U}(\xi).$$

Then $\mathbf{U}$ verifies the following system:

$$(\mathbf{A}-\xi\mathbf{I})\frac{d\mathbf{U}}{d\xi} = 0.$$

Hence, ξ is an eigenvalue of $\mathbf{A}$, and $\dfrac{d\mathbf{U}}{d\xi}$ is the corresponding right eigenvector. In particular, for the field ν_1 one has

$$\frac{d\mathbf{U}}{d\xi} = \frac{\mathbf{V}_1}{\boldsymbol{\nabla}\nu_1.\mathbf{V}_1}.$$

Or, in developed form :

$$\begin{aligned}
\frac{d\rho}{d\xi} &= \frac{\rho}{(\nu_1-u)\,\boldsymbol{\nabla}\nu_1.\mathbf{V}_1},\\
\frac{da^1}{d\xi} &= \frac{a^1}{(\nu_1-u)\,\boldsymbol{\nabla}\nu_1.\mathbf{V}_1},\\
\frac{da^2}{d\xi} &= \frac{2a^2K_{12}+K_{22}-K_{11}+\sqrt{\Delta}}{2K_{12}\,(\nu_1-u)\,\boldsymbol{\nabla}\nu_1.\mathbf{V}_1}\\
&= \frac{a^2}{(\nu_1-u)\,\boldsymbol{\nabla}\nu_1.\mathbf{V}_1} + \frac{2K_{12}}{\Big(K_{11}-K_{22})+\sqrt{\Delta}\Big)\,(\nu_1-u)\,\boldsymbol{\nabla}\nu_1.\mathbf{V}_1},\\
\frac{du}{d\xi} &= \frac{1}{\boldsymbol{\nabla}\nu_1.\mathbf{V}_1},
\end{aligned} \tag{13}$$

$$\frac{dv}{d\xi} = \frac{K_{22} - K_{11} + \sqrt{\Delta}}{2K_{12}\boldsymbol{\nabla}\nu_1.\mathbf{V}_1},$$

$$\frac{d\eta}{d\xi} = 0.$$

One can prove that in the case

$$e^e(\mathbf{g}) = \frac{\mu}{8\rho_0}\left(j_2 - 3\right),$$

K_{12} is proportional to a^2. Indeed,

$$K_{12} = \frac{\mu}{8\rho_0}\left(\frac{\partial j_2}{\partial \mathbf{a}}\cdot\mathbf{b} + \frac{\partial}{\partial \mathbf{a}}\left(\frac{\partial j_2}{\partial \mathbf{a}}\cdot\mathbf{b}\right)\cdot\mathbf{a}\right)$$

$$= \frac{\mu}{8\rho_0}\left(\frac{4a^2\left(\left(a^1\right)^2 + \left(a^2\right)^2 + 1\right)}{\left(a^1\right)^{4/3}} + a^1\frac{\partial}{\partial a^1}\left(\frac{4a^2\left(\left(a^1\right)^2 + \left(a^2\right)^2 + 1\right)}{\left(a^1\right)^{4/3}}\right)\right.$$

$$\left. + a^2\frac{\partial}{\partial a^2}\left(\frac{4a^2\left(\left(a^1\right)^2 + \left(a^2\right)^2 + 1\right)}{\left(a^1\right)^{4/3}}\right)\right).$$

Hence, if initially (a^2) was zero, it will stay zero. The equation for the vertical velocity v also gives the solution $v = 0$ if it was initially zero. In particular, the equations admit the following Riemann invariant corresponding to the right facing waves where we have to replace $\rho = \rho_0 a^1$:

$$u - \int^{a^1} \frac{\sqrt{\frac{tr(\mathbf{K}) + \sqrt{\Delta}}{2}}}{a^1} da^1 = const.$$

The study of the field ν_6 gives another invariant corresponding to the left facing waves :

$$u + \int^{a^1} \frac{\sqrt{\frac{tr(\mathbf{K}) + \sqrt{\Delta}}{2}}}{a^1} da^1 = const.$$

Since

$$\nabla\nu_{1,6}.\mathbf{V}_{1,6}\big|_{\rho=\rho_0 a^1} > 0$$

the longitudinal simple waves are always rarefaction waves (in which the density decreases). These invariants are reminiscent of those for the Euler equations of compressible fluids.

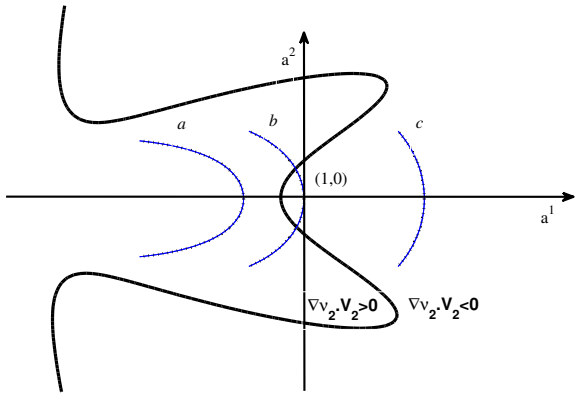

Figure 3.1: The curve where $\nabla\nu_2.\mathbf{V}_2|_{\rho=\rho_0 a^1} = 0$ is shown in bold line. Different invariant curves associated to the eigenfield ν_2 are shown by dashed lines.

3.3.3 Eigenfields associated to ν_2 or ν_5

These eigenvalues correspond to the transverse waves. Obviously, $\boldsymbol{\nabla}\nu_2.\mathbf{V}_2 = -\boldsymbol{\nabla}\nu_5.\mathbf{V}_5$. Hence, it is sufficient to study only the field ν_2. Figure 3.1 shows that these fields estimated at the variety $\rho = \rho_0 a^1$ are not genuinely nonlinear in the sense of Lax. The curve where $\nabla\nu_2.\mathbf{V}_2|_{\rho=\rho_0 a^1}$ vanishes is shown in bold line.

Simple waves

The equations corresponding to the eigenvalue ν_2 are :

$$\frac{d\rho}{d\xi} = \frac{\rho}{(\nu_2 - u)\,(\boldsymbol{\nabla}\nu_2.\mathbf{V}_2)},$$

$$\frac{da^1}{d\xi} = \frac{a^1}{(\nu_2 - u)\,(\boldsymbol{\nabla}\nu_2.\mathbf{V}_2)},$$

$$\frac{da^2}{d\xi} = \frac{2a^2K_{12} + K_{22} - K_{11} - \sqrt{\Delta}}{2K_{12}\,(\nu_2 - u)\,(\boldsymbol{\nabla}\nu_2.\mathbf{V}_2)},$$

$$\frac{du}{d\xi} = \frac{1}{(\boldsymbol{\nabla}\nu_2.\mathbf{V}_2)},$$

$$\frac{dv}{d\xi} = \frac{K_{22} - K_{11} - \sqrt{\Delta}}{2K_{12}\left(\boldsymbol{\nabla}\nu_2.\mathbf{V}_2\right)},$$

$$\frac{ds}{d\xi} = 0.$$

$$\mathbf{V}_i = \left(\frac{\rho}{(\nu_i - u)}, \frac{a^1}{(\nu_i - u)}, \frac{2a^2K_{12} + K_{22} - K_{11} - \sqrt{\Delta}}{2K_{12}\left(\nu_i - u\right)}, 1, \frac{K_{22} - K_{11} - \sqrt{\Delta}}{2K_{12}}, 0\right)^T.$$

The Riemann invariant for the right facing transverse waves (corresponding to ν_2) is

$$u - \int^{a^1} \frac{\sqrt{\dfrac{tr(\mathbf{K}) - \sqrt{\Delta}}{2}}}{a^1} da^1 = const.$$

For for the left facing transverse waves the corresponding Riemann invariant is :

$$u + \int^{a^1} \frac{\sqrt{\dfrac{tr(\mathbf{K}) - \sqrt{\Delta}}{2}}}{a^1} da^1 = const,$$

In these formulas a^2 should be replaced as a function of a^1 as the solution of the following Cauchy problem (always calculated for $\rho = \rho_0 a^1$) :

$$\frac{da^2}{da^1} = \frac{a^2}{a^1} + \frac{2K_{12}}{a^1\left(K_{11} - K_{22} + \sqrt{\Delta}\right)},$$

$$a^2\big|_{a^1 = a^1_*} = 0.$$

Here a^1_* is a state obtained from the state a^1 by a simple longitudinal wave which is always rarefaction wave, or by the longitudinal shock (see the discussion below about Rankine- Hugoniot relations). In the vicinity of the state $(a^1 = 1, a^2 = 0)$ the expression $\nabla\nu_2.\mathbf{V}_2|_{\rho=\rho_0 a^1}$ is negative. Hence, if the longitudinal rarefaction waves (where a^1 is decreasing) are not too strong (i.e. $\nabla\nu_2.\mathbf{V}_2|_{\rho=\rho_0 a^{1}*}$ is negative at $(a^1_*,\ a^2 = 0)$), the eigenvalue ν_2 has a minimum along each simple wave passing by that point. Hence, the simple transverse waves does not exist in this case. In the case of strong longitudinal rarefaction waves transforming the state $(a^1 = 1, a^2 = 0)$ into $(a^1_* < 1, a^2 = 0)$ where $\nabla\nu_2.\mathbf{V}_2|_{\rho=\rho_0 a^{1}*}$ is positive (a curve a in Figure 3.1) one can have simple transverse waves which are also rarefaction waves (the density will decrease).

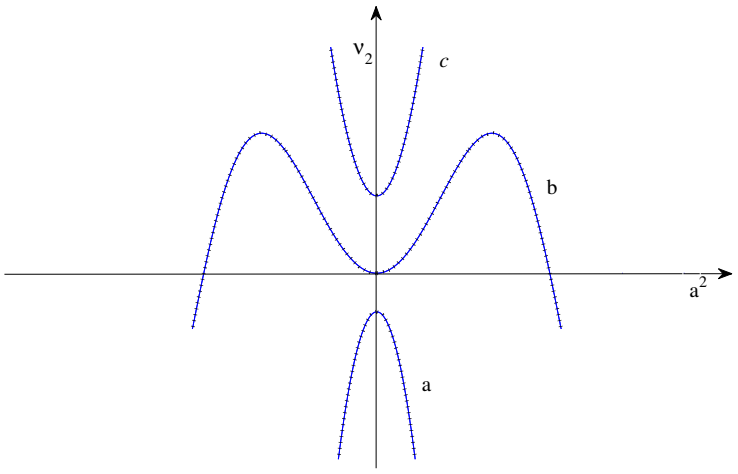

Figure 3.2: The behavior of characteristic speed ν_2 along transverse waves is shown. The first case (a) corresponds to the rarefaction curve containing in the domain $\nabla\nu_2.\mathbf{V}_2|_{\rho=\rho_0 a^1} > 0$ (see Figure 3.1). The transverse rarefaction waves are thus possible. In the cases (b) and (c) the continuous rarefaction waves do not exist.

3.4 Rankine-Hugoniot relations

For any variable X, we denote $[X] = X^r - X^l$ (the difference between right and left values at the discontinuity). The Rankine-Hugoniot relations coming from the conservative system (1) in the case where $a^3 = 0, \quad w = 0, \quad b^1 = 0, \quad b^2 = 1, \quad b^3 = 0, \quad c^1 = 0, \quad c^2 = 0, \quad c^3 = 1$, can be written as :

$$\begin{cases} [\rho\,(u-D)] = [m] = 0 \\ m\,[u] = [\sigma_{11}]\,, \\ m\,[v] = [\sigma_{12}]\,, \\ m\left[e + \dfrac{1}{2}\,(u^2+v^2)\right] = [\sigma_{11}u + \sigma_{12}v]\,, \\ m\left[\dfrac{a^1}{\rho}\right] = 0, \\ m\left[\dfrac{a^2}{\rho}\right] + [v] = 0. \end{cases} \tag{14}$$

Here we denoted $m = \rho\,(u-D)$ where D is the velocity of the discontinuity. They are equivalent to :

$$\begin{cases} [\rho\,(u-D)] = 0 \\ m\,[u] = [\sigma_{11}]\,, \\ m\,[v] = [\sigma_{12}]\,, \\ m[e] = m\dfrac{\sigma_{11}^l + \sigma_{11}^r}{2}[\tau] - m\dfrac{\sigma_{12}^r + \sigma_{12}^l}{2}[a^2\tau], \\ m\left[\dfrac{a^1}{\rho}\right] = 0, \\ m\left[\dfrac{a^2}{\rho}\right] + [v] = 0, \end{cases} \tag{15}$$

where $\tau = 1/\rho$ is the specific volume.

Through the *contact discontinuities* where $m = 0$ we get $u_r = D = u_l$, $[\sigma_{11}] = 0$, $[\sigma_{12}] = 0$ and $[v] = 0$. For *shocks* where $m \neq 0$, we will distinguish two types of shocks : *longitudinal and transverse ones.*

3.4.1 Longitudinal shock waves

We suppose in this part that $m \neq 0$. Obviously, $[v] = 0 \Leftrightarrow [\sigma_{12}] = 0 \Leftrightarrow [a^2\tau] = 0, \quad \tau = \dfrac{1}{\rho}$. *Longitudinal shock waves* are defined by $[a^2\tau] = 0$.

The Rankine-Hugoniot relations for longitudinal waves are written as :

$$\begin{cases} D = \dfrac{u_r\rho_r - u_l\rho_l}{\rho_r - \rho_l}, \\ [a^2\tau] = 0, \\ [u]^2 = [\sigma_{11}]\,[\tau]\,, \\ [e] = \dfrac{\sigma_{11}^l + \sigma_{11}^r}{2}[\tau]. \\ [v] = 0, \\ [\sigma_{12}] = 0. \end{cases} \tag{16}$$

a^2 vanishes after the shock if it was zero before the shock. The same statement is valid for the transversal velocity v.

3.4.2 Transverse shock waves

Consider now transverse shock waves. In this case $[a^2\tau] \neq 0$ This give us:

$$\begin{cases} D = \dfrac{u_r\rho_r - u_l\rho_l}{\rho_r - \rho_l}, \\ m\,[u] = [\sigma_{11}]\,, \\ m\,[v] = [\sigma_{12}]\,, \\ [e] = \dfrac{\sigma_{11}^l + \sigma_{11}^r}{2}[\tau] - \dfrac{\sigma_{12}^r + \sigma_{12}^l}{2}[a^2\tau], \\ \left[\dfrac{a^1}{\rho}\right] = 0, \\ m\,[a^2\tau] + [v] = 0 \end{cases} \tag{17}$$

Since $[u] = m\,[\tau]$, $m\,[u] = [\sigma_{11}]$, $m^2\,[\tau] = [\sigma_{11}]$ and $m^2\,[v]^2 = [\sigma_{12}]^2$, we finally get :

$$\begin{cases} D = \dfrac{u_r\rho_r - u_l\rho_l}{\rho_r - \rho_l}, \\ m\,[u] = [\sigma_{11}]\,, \\ m\,[v] = [\sigma_{12}]\,, \\ [e] = \dfrac{\sigma_{11}^l + \sigma_{11}^r}{2}[\tau] - \dfrac{\sigma_{12}^r + \sigma_{12}^l}{2}[a^2\tau], \\ [u]^2 = [\sigma_{11}]\,[\tau]\,, \\ [v]^2 = \dfrac{[\sigma_{12}]^2\,[\tau]}{[\sigma_{11}]}, \\ \left[\dfrac{a^1}{\rho}\right] = 0, \\ [\sigma_{11}]\,[a^2\tau] + [\sigma_{12}]\,[\tau] = 0. \end{cases} \tag{18}$$

3.5 The piston problem

3.5.1 A special piston problem

Consider a piston (an infinite plane described initially as $x = 0$) which is sticked to an elastic solid at rest situated at $x > 0$. Initially, the elastic solid is free of shear stresses. The variables in this state will be denoted by index '0'. So, $a_0^1 = 1$, $a_0^2 = 0$, $u_0 = v_0 = 0$. The piston becomes to move at time $t = 0$ with a given velocity (u_p, v_p). In the case of $v_p = 0$ the solution is simple. If $u_p > 0$ then we have a longitudinal shock wave. If $u_p < 0$, the solution is the longitudinal rarefaction wave. Consider the case where $u_p > 0$ and v_p takes any value (not too large to stay in the domain where $\nabla\nu_2.\mathbf{V}_2|_{\rho=\rho_0 a^1} < 0$). The state '0' will be transformed by a longitudinal shock wave into the state '*' where $a_*^1 > 1$, $a_*^2 = a_0^2 = 0$ following by a transverse shock (see Figure 3.3, the first case). The transverse shock is always a rarefaction shock (i.e. the solid density will decrease after the transverse shock). In the Figure the classical different configurations that we can have.

However, in the case where u_p is negative, the solution depends on the value of v_p. One can have several different situations. The longitudinal rarefaction wave (LR) transforms the state '0' into a state '*' where we have always $\nabla\nu_2.\mathbf{V}_2|_{\rho=\rho_0 a^1 *} < 0$. Then it will followed by the transverse shock TS (the second case in Figure 3.3). The transverse wave can also be a characteristic shock, i. e. the wave can be followed by a rarefaction continuous transverse wave (the fourth case). Very large longitudinal rarefaction waves can also be followed by a transverse rarefaction wave (RT).

We ask now the following question : what is the relation between u_p and v_p allowing us to have a solution containing only one transverse shock relating the state '0' to a state 'P' where the velocity is prescribed : $(u, v)_p = (u_p, v_p)$ (see Figure 3.4). In a sense, this limiting curve will separate the the first basic configuration $LS \to TS$ (which can happen also for negative horizontal piston velocities when the vertical velocities are quite large), from the other three configurations (see Figure 3.3). This degenerate configuration is shown in Figure 3.5. We wish to connect the equilibrium state "0" with a state "P" by transverse shock wave. The Rankine-Hugoniot relations are :

$$(u_P)^2 = ((\sigma_{11})_P - (\sigma_{11})_0)(\tau_P - \tau_0), \tag{19}$$

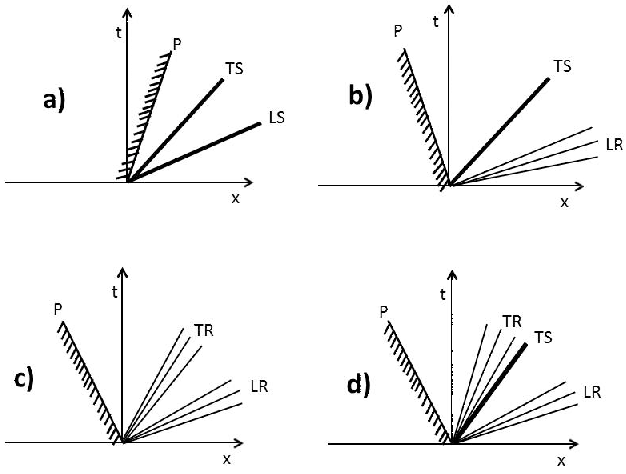

Figure 3.3: We have four different general configurations for the piston problem where the initial state is in equilibrium: The first case : a longitudinal shock wave (LS) is followed by a transverse shock wave (TS). This configuration can appear not only in the case where the horizontal piston velocity is positive. The other three cases can appear only if the horizontal piston velocity is negative. The second case : a longitudinal rarefaction wave (LR) is followed by a transverse shock wave (TS). The third case: a longitudinal rarefaction wave (LR) is followed by a transverse rarefaction wave (TR). The fourth case : a longitudinal rarefaction wave (LR) is followed by a transverse characteristic shock wave (TS) to which a transverse rarefaction wave (TR) is sticked.

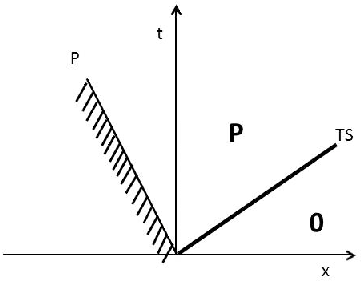

Figure 3.4: Solution with a unique transverse wave

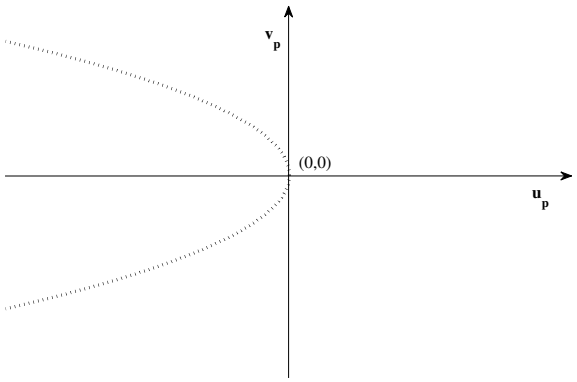

Figure 3.5: When the piston velocity takes the values belonging to the limit curve shown by dashed line, the only solution is the TS wave. Outside this curve we have a two-wave configuration $LS \rightarrow TS$. Inside this curve, the three other configurations can occur.

$$(v_P)^2 = \frac{((\sigma_{12})_P)^2}{((\sigma_{11})_P - (\sigma_{11})_0)} (\tau_P - \tau_0), \tag{20}$$

$$0 = ((\sigma_{12})_P)(\tau_P - \tau_0) + \left(\left(a^2\tau\right)_P\right)((\sigma_{11})_P - (\sigma_{11})_0), \tag{21}$$

$$(e_P - e_0) = \frac{1}{2}((\sigma_{11})_P + (\sigma_{11})_0)(\tau_P - \tau_0) + \frac{1}{2}((\sigma_{12})_P)\left(\left(a^2\tau\right)_P\right). \tag{22}$$

We have four relations for three unknowns a_P^1, a_P^2 and η_P. Hence, it allows us to relate the parameters u_P and v_P.

3.6 Conclusion

The piston problem for a hyperelastic hyperbolic conservative model where the stored energy is given in separable form is studied. Such an exact solution is very useful to evaluate the convergence of numerical schemes. The eigenfields corresponding to the hyperbolic system are of three types : linearly degenerate fields (corresponding to the contact characteristics), the fields which are genuinely nonlinear in the sense of Lax (corresponding to longitudinal waves), and nonlinear fields which are not genuinely nonlinear (corresponding to transverse waves). Taking the initial state free of stresses, we presented possible auto-similar solutions to the piston problem. In particular, we have shown that the equations admit transverse shock waves having a remarkable property : the density is decreasing through such a shock.

For numerical applications, the solution of the general Riemann problem is needed. However, such a problem is much more complicated because its solution depends on the choice of the equations of state (see, for example, Kulikovskii and Sveshnikova [11] for the study of the Riemann problem in the case of a polynomial equation of state).

3.7 Reference

Bibliography

[1] G. H. Miller and P. Colella, A high order Eulerian Godunov method for elastic plastic flow in solids, Journal of Computational Physics, 167, 131-176, 2001.

[2] S.K. Godunov, E. I. Romenskii, Elements of Continuum Mechanics and Conservation Laws, Kluwer Academic Publishers, N. Y., 2003.

[3] S. L. Gavrilyuk, N. Favrie & R. Saurel, Modeling wave dynamics of compressible elastic materials, Journal of Computational Physics, 227, 2941-2969, 2008.

[4] N. Favrie & S.Gavrilyuk, Mathematical and numerical model for nonlinear viscoplastictity, Phil. Trans. R. Soc. A, 369, 2864-2880, 2011.

[5] E. Godlewski & P.-A. Raviart, Hyperbolic systems of conservation laws Mathematics and Applications (Paris). Ellipses, vol. 3/4, 1991.

[6] P.D. Lax, Hyperbolic Partial Differential Equations Lecture notes, Courant Institute of Mathematical Sciences, American Mathematical Society, 2006.

[7] P.G. LeFloch, Hyperbolic Systems of Conservation Laws, The Theory of Classical and Nonclassical Shock Waves, Lectures in Mathematics, Birkhä user, 2002

[8] D. Serre, Systmes de lois de conservation I. Fondations. Diderot Editeur, Paris, 1996.

[9] R. J. Flory, Thermodynamic relations for highly elastic materials Transactions of Faraday Society ,57, 829-838, 1981

[10] S. Ndanou, N. Favrie & S. Gavrilyuk, Criterion of hyperbolicity in hyperelasticity in the case of the stored energy in separable form, J. Elasticity 2014, v. 115, pp. 1-25.

[11] A. Kulikovskii & E. Sveshnikova, Nonlinear waves in elastic media, CRC Press, Boca Raton, FL, 1995.

Chapitre 4

Une procédure de splitting en hyperélasticité

Ce chapitre correspond à l'article Favrie, N., Gavrilyuk & S. Ndanou (2014) A thermodynamically compatible splitting procedure in hyperelasticity. J. Computational Physics, Vol. 270, pp. 300-324

4.1 Introduction

The Eulerian formulation of the hyperelasticity can be found, for example, in Godunov and Romenskii (2003), and Miller and Collela (2001). We follow Gavrilyuk, Favrie and Saurel (2008) for a modified conservative formulation of the model in the case of isotropic solids. In the last reference, a particular class of elastic materials was studied. They are characterized by a specific stored energy e in separable form (Flory, 1961) :

$$e\left(\mathbf{G},\eta\right)=e^{h}\left(\left|\mathbf{G}\right|,\eta\right)+e^{e}\left(\mathbf{g}\right), \tag{1}$$

where $\mathbf{G}=\mathbf{B}^{-1}$ is the Finger tensor, $\mathbf{B}=\mathbf{F}\mathbf{F}^{T}$ is the left Cauchy-Green deformation tensor, $\mathbf{F}$ is the deformation gradient, $\mathbf{g}=\mathbf{G}\left|\mathbf{G}\right|^{-1/3}$, $\left|\mathbf{G}\right|$ is the determinant of $\mathbf{G}$, and η is the specific entropy. The energy $e^{h}\left(\left|\mathbf{G}\right|,\eta\right)$ is the hydrodynamic part of the energy, depending only on the determinant of $\mathbf{G}$ and the entropy η, and $e^{e}\left(\mathbf{g}\right)$ is the shear elastic energy. The shear part of the energy is unaffected by the volume change.

Such a decomposition into purely volumetric and isochoric deformation is useful, in particular, for description of nearly incompressible isotropic

hyperelasticity (Hartmann and Neff, 2003, Pence, 2013). A numerical advantage of giving the energy in separable form is that the numerical codes of hyperelasticity can directly be used for fluids (it is sufficient to take $e^e = 0$). Also, such a separable form allows us to prove easier the hyperbolicity of governing equations. The hyperbolicity property is a necessary condition for the wellposedness of the Cauchy problem and the corresponding numerical Godunov-type methods. Even if the criterion of hyperbolicity in hyperelasticity is well known (the energy e should be an one-rank convex function of the deformation gradient $\mathbf{F}$, Dafermos, 2000), it is extremely difficult, if not impossible, to verify it in practice even in the case of isotropic elastic materials (see Davies, 1991, Horgan, 1995, Dacorogna, 2001, De Tommasi, Puglisi and Zurlo, 2012 for the rank-one convexity study). Recently, in the case of isotropic solids with the equation of state in separable form, we have proposed a criterion of hyperbolicity in multi-dimensional case which is easier to verify (Ndanou, Favrie and Gavrilyuk, 2014).

When a general 3D problem is considered, a spatial splitting is usually used to reduce the numerical problem to three 1D problems. Hence, a reliable 1D Riemann solver is needed based on exact or approximate solutions of the Riemann problem. The Riemann problem has been intensively studied in Kulikovskii and Sveshnikova (1995) for a weakly anisotropic media where the elastic potential (volume energy) was a polynomial of the deformation tensor. In Ndanou, Favrie and Gavrilyuk (2013), the solution of the piston problem in the case of equation of state in separable form is given. The solution of the general Riemann problem is quite complex. Indeed, 7 waves are present in such a solution : 2 longitudinal waves, 4 shear waves, and a contact discontinuity. For numerical purposes, an approximate HLLC Riemann solver dealing with only 3 waves can be used (Gavrilyuk, Favrie and Saurel, 2008). The solver is capable to show up the 7-wave structure of the solution. However, the solver presents a large numerical diffusion of shear waves.

An Eulerian Riemann solver for isotropic solids was recently proposed in Titarev *et al.* (2008) and Barton *et al.* (2009). These authors highlighted difficulties of numerical solving hyperelastic models when seven characteristic fields are present. They compared the choice of different approximate Riemann solvers. In particular, the extension to a higher order scheme (WENO-5) is presented there. But even with such an expensive numerical method, the diffusion of shear waves was important.

In this paper, we study a non-conservative formulation of hyperelastic-

ity. We propose a special splitting of each 1D model into three sub-models. The first sub-model deals with longitudinal waves and a contact discontinuity. The equations of the model describe traction - compression of the solid and are similar in a sense to the Euler equations of compressible fluids. The two other sub-models describe shear waves. All the three sub-models are hyperbolic. Also, the mass, the momentum and the energy equations are satisfied for each sub-system. Such a splitting procedure is thus thermodynamically compatible. Moreover, each model has only 3 waves (and not 7 ones), and the corresponding eigenvalues are given in explicit form. Hence, the solution of the Riemann problem can be found explicitly for each sub-model. In particular, we show that the Riemann problem for shear waves can be reduced to the equations of the barotropic gas. A numerical scheme based on such a splitting allows us to obtain an important reduction of the numerical diffusion for shear waves. Indeed, in multiple applications, one deals with the strong longitudinal waves and weak shear waves. If the longitudinal waves can be well captured by any Riemann solver, a better accuracy is needed to capture the shear waves.

The splitting approach is also extended to 2D case. In particular, we compared the 2D splitting approach proposed for the non-conservative equations of hyperelasticity with a Lax-Friedrichs type scheme built for the conservative equations of hyperelasticity. The Lax-Friedrichs type scheme was built to assure the conservation of natural stationary constraints of the model (some variables must be spatial gradients). A numerical test involving a very strong shear is proposed. The numerical results show that the stationary constraints are also conserved by the splitting approach, and its numerical solution is less diffusive.

This paper is organized as follows. In Section 2, we recall the equations of hyperelasticity and give explicit examples of the specific store energy in separable form. In Section 3, the three sub-models are presented and their mathematical properties are studied. In Section 4, numerical methods are presented. Numerical tests and comparison with exact solutions are given in Section 5. The discussion of the results obtained is given in Section 6. Technical details are given in Appendices.

4.2 Presentation of the model

Consider the Eulerian formulation of hyperelasticity for isotropic solids (Godunov and Romenskii (2003), Miller and Collela (2001) and others). We

follow Gavrilyuk, Favrie and Saurel (2008) for a modified presentation of these equations :

$$\begin{cases} \dfrac{\partial \rho}{\partial t} + div\left(\rho \mathbf{u}\right) = 0, \\ \dfrac{\partial \left(\rho \mathbf{u}\right)}{\partial t} + div\left(\rho \mathbf{u} \otimes \mathbf{u} - \boldsymbol{\sigma}\right) = 0, \\ \dfrac{\partial \left(\rho \left(e + \dfrac{1}{2}|\mathbf{u}|^2\right)\right)}{\partial t} + div\left(\rho \mathbf{u} \left(e + \dfrac{1}{2}|\mathbf{u}|^2\right) - \boldsymbol{\sigma}\mathbf{u}\right) = 0, \\ \dfrac{\partial \mathbf{e}^\beta}{\partial t} + \boldsymbol{\nabla}(\mathbf{u} \cdot \mathbf{e}^\beta) = 0, \quad \text{curl } \mathbf{e}^\beta = 0, \quad \beta = 1, 2, 3. \end{cases} \tag{2}$$

The operators div, curl and $\boldsymbol{\nabla}$ are applied in the Eulerian coordinates $\mathbf{x} = (x, y, z)^T$. Here ρ is the solid density, $\mathbf{u} = (u, v, w)^T$ is the velocity, $\boldsymbol{\sigma}$ is the Cauchy stress tensor. For the specific store energy (1) it is given as :

$$\boldsymbol{\sigma} = -2\rho \frac{\partial e}{\partial \mathbf{G}} \mathbf{G}. \tag{3}$$

The tensor (3) is symmetric in the case of isotropic solids where the energy e is a function of eigenvalues of $\mathbf{G}$. The density ρ can be expressed as

$$\rho = \rho_0 |\mathbf{G}|^{\frac{1}{2}}.$$

Here ρ_0 is the reference density. For simplicity, we will consider the case where ρ_0 is a constant.

The vectors $\mathbf{e}^\beta$ are the columns of the $\mathbf{F}^{-T}$:

$$\mathbf{F}^{-T} = (\mathbf{e}^1, \mathbf{e}^2, \mathbf{e}^3).$$

Then

$$\mathbf{G} = \sum_{\beta=1}^{3} \mathbf{e}^\beta \otimes \mathbf{e}^\beta.$$

Since $\mathbf{e}^\beta$ are the gradients of the Lagrangian coordinates, the equation curl $\mathbf{e}^\beta = 0$ is a compatibility condition. This condition is time invariant: if it is verified initially, it will be verified for any time (Miller and Colella, 2001; Godunov and Romenskii, 2003; Gavrilyuk, Favrie and Saurel, 2008).

The separable form (1) allows us to write:

$$\boldsymbol{\sigma} = -p\mathbf{I} + \mathbf{S}, \quad tr(\mathbf{S}) = 0,$$

with

$$p = \rho^2 \frac{\partial e^h(\rho,\eta)}{\partial \rho}, \quad \mathbf{S} = -2\rho \frac{\partial e^e}{\partial \mathbf{G}}\mathbf{G}. \tag{4}$$

Let us remark that the pressure p is determined by only the hydrodynamic part of the energy e^h, while the deviatoric part of the stress tensor $\mathbf{S}$ is determined only by the shear part of the energy e^e. For isotropic solids, the shear energy e^e can be written as a function of only two invariants of $\mathbf{g}$:

$$e^e(\mathbf{g}) = e^e(j_1, j_2), \quad j_1 = tr(\mathbf{g}), \quad j_2 = tr(\mathbf{g}^2).$$

It implies :

$$\mathbf{S} = -2\rho \frac{\partial e^e}{\partial \mathbf{G}}\mathbf{G} = -2\rho \left(\frac{\partial e^e}{\partial j_1}\left(\mathbf{g} - \frac{j_1}{3}\mathbf{I}\right) + 2\frac{\partial e^e}{\partial j_2}\left(\mathbf{g}^2 - \frac{j_2}{3}\mathbf{I}\right)\right).$$

Concerning the hydrodynamic part e^h, any equation of state which is convex with respect to $\tau = 1/\rho$ and η can be used. In particular, for numerical applications we will use the stiffened gas equation of state :

$$e^h(\rho, p) = \frac{p + \gamma p_\infty}{(\gamma - 1)\rho}, \quad \frac{p + p_\infty}{\rho^\gamma} = A(\eta). \tag{5}$$

For the shear part of the internal energy e^e, we take the equation of state in the form

$$e^e(\mathbf{g}) = \frac{\mu}{8\rho_0}\left(j_2 - 3\right). \tag{6}$$

Here $A(\eta)$ is any increasing function of η, $p_\infty > 0, \gamma > 1, \mu > 0$ and $\rho_0 > 0$ are constants. For small deformations, Hooke's law can be recovered from (5) and (6).

Let $\mathbf{e}^\beta = (a^\beta, b^\beta, c^\beta)^T$ in the Cartesian basis $(\mathbf{i}, \mathbf{j}, \mathbf{k})$. Introducing $\mathbf{a} = (a^1, a^2, a^3)^T$, $\mathbf{b} = (b^1, b^2, b^3)^T$, $\mathbf{c} = (c^1, c^2, c^3)^T$, we have for the inverse deformation gradient :

$$\mathbf{F}^{-1} = (\mathbf{a}, \mathbf{b}, \mathbf{c}), \quad \mathbf{F}^{-T} = \begin{pmatrix} \mathbf{a}^T \\ \mathbf{b}^T \\ \mathbf{c}^T \end{pmatrix}, \quad \mathbf{G} = \begin{pmatrix} ||\mathbf{a}||^2 & \mathbf{a}\cdot\mathbf{b} & \mathbf{a}\cdot\mathbf{c} \\ \mathbf{a}\cdot\mathbf{b} & ||\mathbf{b}||^2 & \mathbf{b}\cdot\mathbf{c} \\ \mathbf{a}\cdot\mathbf{c} & \mathbf{b}\cdot\mathbf{c} & ||\mathbf{c}||^2 \end{pmatrix}.$$

The non-conservative form of (2) is :

$$\begin{cases} \dfrac{\partial \rho}{\partial t} + \boldsymbol{\nabla}\rho.\mathbf{u} + \rho div(\mathbf{u}) = 0, \\ \dfrac{\partial \mathbf{u}}{\partial t} + \dfrac{\boldsymbol{\nabla} p}{\rho} - \dfrac{div(\mathbf{S})}{\rho} = 0, \\ \dfrac{\partial \eta}{\partial t} + \boldsymbol{\nabla}\eta \cdot \mathbf{u} = 0, \\ \dfrac{\partial \mathbf{e}^\beta}{\partial t} + \left(\dfrac{\partial \mathbf{e}^\beta}{\partial x}\right)\mathbf{u} + \left(\dfrac{\partial \mathbf{u}}{\partial x}\right)^{\mathbf{T}} \mathbf{e}^\beta = 0, \quad \beta = 1,2,3. \end{cases} \tag{7}$$

When the smooth solutions are studied, the systems (2) and (7) are equivalent. Indeed, they conserve the condition curl $\mathbf{e}^\beta = 0$ which is the condition on the initial data. A criterion of hyperbolicity of (7) was proposed in Ndanou, Favrie and Gavrilyuk (2014). In particular, the authors proved that for the shear energy in the form (6) the equations are hyperbolic.

The 1D system (projection in x-direction of (7)) is :

$$\frac{\partial \rho}{\partial t} + u\frac{\partial \rho}{\partial x} + \rho\frac{\partial u}{\partial x} = 0, \tag{8}$$

$$\frac{\partial u}{\partial t} + u\frac{\partial u}{\partial x} + \frac{\left(c^2 - \frac{\partial S_{11}}{\partial \rho}\right)}{\rho}\frac{\partial \rho}{\partial x} + \frac{\partial p}{\partial \eta}\frac{\partial \eta}{\partial x}$$

$$-\frac{1}{\rho}\sum_{\alpha=1}^{3}\frac{\partial S_{11}}{\partial a^\alpha}\frac{\partial a^\alpha}{\partial x} - \frac{1}{\rho}\sum_{\alpha=1}^{3}\frac{\partial S_{11}}{\partial b^\alpha}\frac{\partial b^\alpha}{\partial x} - \frac{1}{\rho}\sum_{\alpha=1}^{3}\frac{\partial S_{11}}{\partial c^\alpha}\frac{\partial c^\alpha}{\partial x} = 0,$$

$$\frac{\partial v}{\partial t} + u\frac{\partial v}{\partial x} - \frac{1}{\rho}\frac{\partial S_{12}}{\partial \rho}\frac{\partial \rho}{\partial x}$$

$$-\frac{1}{\rho}\sum_{\alpha=1}^{3}\frac{\partial S_{12}}{\partial a^\alpha}\frac{\partial a^\alpha}{\partial x} - \frac{1}{\rho}\sum_{\alpha=1}^{3}\frac{\partial S_{12}}{\partial b^\alpha}\frac{\partial b^\alpha}{\partial x} - \frac{1}{\rho}\sum_{\alpha=1}^{3}\frac{\partial S_{12}}{\partial c^\alpha}\frac{\partial c^\alpha}{\partial x} = 0,$$

$$\frac{\partial w}{\partial t} + u\frac{\partial w}{\partial x} - \frac{1}{\rho}\frac{\partial S_{13}}{\partial \rho}\frac{\partial \rho}{\partial x}$$

$$-\frac{1}{\rho}\sum_{\alpha=1}^{3}\frac{\partial S_{13}}{\partial a^\alpha}\frac{\partial a^\alpha}{\partial x} - \frac{1}{\rho}\sum_{\alpha=1}^{3}\frac{\partial S_{13}}{\partial b^\alpha}\frac{\partial b^\alpha}{\partial x} - \frac{1}{\rho}\sum_{\alpha=1}^{3}\frac{\partial S_{13}}{\partial c^\alpha}\frac{\partial c^\alpha}{\partial x} = 0,$$

$$\frac{\partial a^1}{\partial t} + u\frac{\partial a^1}{\partial x} + a^1\frac{\partial u}{\partial x} + b^1\frac{\partial v}{\partial x} + c^1\frac{\partial w}{\partial x} = 0,$$

$$\frac{\partial a^2}{\partial t} + u\frac{\partial a^2}{\partial x} + a^2\frac{\partial u}{\partial x} + b^2\frac{\partial v}{\partial x} + c^2\frac{\partial w}{\partial x} = 0,$$

$$\frac{\partial a^3}{\partial t} + u\frac{\partial a^3}{\partial x} + a^3\frac{\partial u}{\partial x} + b^3\frac{\partial v}{\partial x} + c^3\frac{\partial w}{\partial x} = 0,$$

$$\frac{\partial b^1}{\partial t} + u\frac{\partial b^1}{\partial x} = 0, \quad \frac{\partial b^2}{\partial t} + u\frac{\partial b^2}{\partial x} = 0, \quad \frac{\partial b^3}{\partial t} + u\frac{\partial b^3}{\partial x} = 0,$$

$$\frac{\partial c^1}{\partial t} + u\frac{\partial c^1}{\partial x} = 0, \quad \frac{\partial c^2}{\partial t} + u\frac{\partial c^2}{\partial x} = 0, \quad \frac{\partial c^3}{\partial t} + u\frac{\partial c^3}{\partial x} = 0,$$

$$\frac{\partial \eta}{\partial t} + u\frac{\partial \eta}{\partial x} = 0.$$

Here $c^2 = \dfrac{\partial p(\rho,\eta)}{\partial \rho}$ is the squared hydrodynamic sound velocity, and S_{ij} are the components of the deviatoric part of the stress tensor given by (4). S_{ij} are linear functions of ρ and non-linear functions of $\mathbf{a}$, $\mathbf{b}$, $\mathbf{c}$ defined for isotropic solids by the following expressions (Ndanou, Favrie and Gavrilyuk, 2014) :

$$S_{11} = -\rho\frac{\partial e^e}{\partial \mathbf{a}} \cdot \mathbf{a}, \tag{9}$$

$$S_{12} = -\rho\frac{\partial e^e}{\partial \mathbf{a}} \cdot \mathbf{b} = -\rho\frac{\partial e^e}{\partial \mathbf{b}} \cdot \mathbf{a},$$

$$S_{13} = -\rho\frac{\partial e^e}{\partial \mathbf{a}} \cdot \mathbf{c} = -\rho\frac{\partial e^e}{\partial \mathbf{c}} \cdot \mathbf{a},$$

$$S_{23} = -\rho\frac{\partial e^e}{\partial \mathbf{b}} \cdot \mathbf{c} = -\rho\frac{\partial e^e}{\partial \mathbf{c}} \cdot \mathbf{b}.$$

The system (8) is a hyperbolic system of 14 scalar equations with seven characteristic directions: two longitudinal waves, four shear waves and a contact discontinuity (see Figure 4.1).

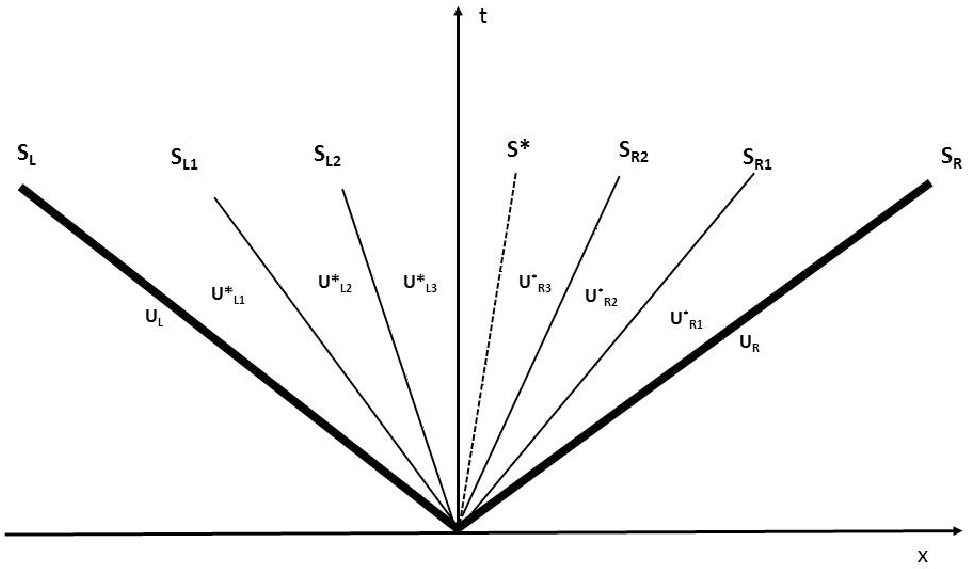

Figure 4.1: The solution of the Riemann problem to the general 1D system containing seven waves.

4.3 Sub-system's decomposition

In this part, the system (8) will be decomposed into 3 sub-systems. These systems must have the following properties.

- To be hyperbolic
- To be conservative
- Admit the energy equation compatible with the entropy equation
- They should solve the full system (8)

4.3.1 Sub-system 1

Consider the following sub-system (called 'sub-system 1'):

$$\begin{cases} \dfrac{\partial \rho}{\partial t} + \dfrac{\partial(\rho u)}{\partial x} = 0, \\ \dfrac{\partial (\rho u)}{\partial t} + \dfrac{\partial(\rho u^2 + p - S_{11})}{\partial x} = 0, \\ \dfrac{\partial (\rho v)}{\partial t} + \dfrac{\partial(\rho uv)}{\partial x} = 0, \quad \dfrac{\partial (\rho w)}{\partial t} + \dfrac{\partial(\rho uw)}{\partial x} = 0, \\ \dfrac{\partial a^\beta}{\partial t} + \dfrac{\partial \left(u a^\beta\right)}{\partial x} = 0, \quad \beta = 1,2,3 \\ \dfrac{Db^\beta}{Dt} = 0, \quad \dfrac{Dc^\beta}{Dt} = 0, \quad \beta = 1,2,3 \\ \dfrac{D\eta}{Dt} = 0. \end{cases} \tag{10}$$

Compatibility between the mass conservation and equations for a^β, b^β and c^β

Equations for a^β, b^β, c^β are compatible with the mass conservation law :

$$\rho = \rho_0 |\mathbf{G}|^{\frac{1}{2}} = \rho_0 \mathbf{a} \cdot (\mathbf{b} \wedge \mathbf{c}),$$

where:

$$\frac{D\rho_0}{Dt} = 0.$$

Indeed,

$$\frac{\partial\left(\rho_0|\mathbf{G}|^{\frac{1}{2}}\right)}{\partial t} + \frac{\partial\left(\rho_0|\mathbf{G}|^{\frac{1}{2}}u\right)}{\partial x} = \rho_0\left(\frac{\partial|\mathbf{G}|^{\frac{1}{2}}}{\partial t} + \frac{\partial|\mathbf{G}|^{\frac{1}{2}}u}{\partial x}\right)$$

$$= \rho_0\left(\frac{\partial\mathbf{a}\cdot(\mathbf{b}\wedge\mathbf{c})}{\partial t} + \frac{\partial\mathbf{a}\cdot(\mathbf{b}\wedge\mathbf{c})\,u}{\partial x}\right)$$

$$= \rho_0\left(\frac{\partial\mathbf{a}}{\partial t} + \frac{\partial(u\mathbf{a})}{\partial x}\right)\cdot(\mathbf{b}\wedge\mathbf{c}) + \rho_0\mathbf{a}\cdot\left(\frac{\partial\mathbf{b}\wedge\mathbf{c}}{\partial t} + u\frac{\partial\mathbf{b}\wedge\mathbf{c}}{\partial x}\right) = 0.$$

Compatibility with the energy equation

The system (10) admits the energy conservation law :

$$\frac{\partial\rho\left(e^h + e^e + \frac{1}{2}(u^2+v^2+w^2)\right)}{\partial t} + \frac{\partial\rho u\left(e^h + e^e + \frac{1}{2}(u^2+v^2+w^2) + pu - S_{11}u\right)}{\partial x} = 0.$$

Indeed,

$$\frac{\partial\rho\left(e^h + e^e + \frac{1}{2}(u^2+v^2+w^2)\right)}{\partial t} + \frac{\partial\rho u\left(e^h + e^e + \frac{1}{2}(u^2+v^2+w^2) + pu - S_{11}u\right)}{\partial x}$$

$$= \rho\frac{D\left(e^h + e^e + \frac{1}{2}(u^2+v^2+w^2)\right)}{Dt} + \frac{\partial(pu - S_{11}u)}{\partial x}$$

$$= \rho\frac{De^e}{Dt} + (-S_{11})\frac{\partial u}{\partial x}$$

$$= \rho\left(\frac{\partial e^e}{\partial a^1}\frac{Da^1}{Dt} + \frac{\partial e^e}{\partial a^2}\frac{Da^2}{Dt} + \frac{\partial e^e}{\partial a^3}\frac{Da^3}{Dt}\right) + (-S_{11})\frac{\partial u}{\partial x}$$

$$= -\rho\left(a^1\frac{\partial e^e}{\partial a^1} + a^2\frac{\partial e^e}{\partial a^2} + a^3\frac{\partial e^e}{\partial a^3}\right)\frac{\partial u}{\partial t} + (-S_{11})\frac{\partial u}{\partial x} = 0$$

$$= -\rho\left(\frac{\partial e^e}{\partial\mathbf{a}}\cdot\mathbf{a}\right)\frac{\partial u}{\partial x} + (-S_{11})\frac{\partial u}{\partial x} = 0.$$

The last expression vanishes because of the symmetry relations (9).

Hyperbolicity

The system (10) can be rewritten in the following form:

$$\mathbf{W}_t + \mathbf{A}_1 \mathbf{W}_x = 0,$$

with

$$\mathbf{W} = \begin{pmatrix} \rho & u & v & w & a^1 & a^2 & a^3 & b^1 & b^2 & b^3 & c^1 & c^2 & c^3 & \eta \end{pmatrix}^T,$$

where

$$A_1 = \begin{pmatrix} A_{11} & A_{12} \\ A_{21} & A_{22} \end{pmatrix},$$

with

$$A_{11} = \begin{pmatrix} u & \rho \\ \frac{1}{\rho}\left(\frac{\partial p}{\partial \rho} - \frac{\partial S_{11}}{\partial \rho}\right) & u \end{pmatrix},$$

$$A_{12} = \begin{pmatrix} 0 & 0 & \mathbf{o}_3^T & \mathbf{o}_3^T & \mathbf{o}_3^T & 0 \\ 0 & 0 & -\frac{1}{\rho}\frac{\partial S_{11}}{\partial \mathbf{a}} & -\frac{1}{\rho}\frac{\partial S_{11}}{\partial \mathbf{b}} & -\frac{1}{\rho}\frac{\partial S_{11}}{\partial \mathbf{c}} & \frac{1}{\rho}\frac{\partial p}{\partial \eta} \end{pmatrix},$$

$$A_{21} = \begin{pmatrix} 0 & 0 \\ 0 & 0 \\ \mathbf{o}_3 & \mathbf{a} \\ 0 & 0 \\ 0 & 0 \\ 0 & 0 \\ 0 & 0 \\ 0 & 0 \\ 0 & 0 \\ 0 & 0 \end{pmatrix},$$

$$A_{22} = u\, I_{12\times 12}.$$

Here $\mathbf{o}_k$ is k-dimensional zero vector, and $I_{m\times m}$ is the unit square matrix of dimension n. The sound characteristics are:

$$\nu_1 = u - c_l < \nu_2 = u + c_l,$$

where

$$c_l = \sqrt{\frac{\partial p}{\partial \rho} - \frac{\partial S_{11}}{\partial \rho} - \frac{1}{\rho}\left(\frac{\partial S_{11}}{\partial \mathbf{a}} \cdot \mathbf{a}\right)}.$$

The eigenvalue $\nu_3 = u$ is of multiplicity 12. To have real eigenvalues we need (a sufficient condition) that

$$\frac{\partial p}{\partial \rho} > 0, \quad -\frac{\partial S_{11}}{\partial \rho} - \frac{1}{\rho}\left(\frac{\partial S_{11}}{\partial \mathbf{a}} \cdot \mathbf{a}\right) = \frac{\partial e^e}{\partial \mathbf{a}} \cdot \mathbf{a} + \frac{\partial}{\partial \mathbf{a}}\left(\frac{\partial e^e}{\partial \mathbf{a}} \cdot \mathbf{a}\right) \cdot \mathbf{a} > 0.$$

The second inequality admits the following interperetation (Ndanou, Favrie and Gavrilyuk, 2014). Consider the shear energy per unit volume $E = \Delta e^e(\mathbf{a}, \mathbf{b}, \mathbf{c})$ (defined up to the multiplier ρ_0) where $\Delta = \det(\mathbf{F}^{-1}) = \mathbf{a} \cdot (\mathbf{b} \wedge \mathbf{c}) > 0$. We denote

$$E'' = \frac{\partial^2 E}{\partial \mathbf{a}^2}, \quad (e^e)'' = \frac{\partial^2 e^e}{\partial \mathbf{a}^2}.$$

Then

$$\frac{\partial E}{\partial \mathbf{a}} = \Delta \frac{\partial e^e}{\partial \mathbf{a}} + (\mathbf{b} \wedge \mathbf{c})\, e^e, \quad E'' = \Delta\,(e^e)'' + \frac{\partial e^e}{\partial \mathbf{a}} \otimes (\mathbf{b} \wedge \mathbf{c}) + (\mathbf{b} \wedge \mathbf{c}) \otimes \frac{\partial e^e}{\partial \mathbf{a}}. \tag{11}$$

Hence

$$-\frac{\partial S_{11}}{\partial \rho} - \frac{1}{\rho}\left(\frac{\partial S_{11}}{\partial \mathbf{a}} \cdot \mathbf{a}\right) = \frac{\partial e^e}{\partial \mathbf{a}} \cdot \mathbf{a} + \frac{\partial}{\partial \mathbf{a}}\left(\frac{\partial e^e}{\partial \mathbf{a}} \cdot \mathbf{a}\right) \cdot \mathbf{a} = \frac{\mathbf{a}^T E'' \mathbf{a}}{\Delta}.$$

In particular, if E'' is positive definite and $\dfrac{\partial p}{\partial \rho} > 0$, (10) is hyperbolic. Such a criterion was formulated in Ndanou, Favrie and Gavrilyuk (2014) in the general case. In particular, the equation of state (6) satisfies the condition $E'' > 0$.

The right eigenvectors for the sonic waves ν_1 and ν_2 are, respectively :

$$\left(\rho, -c_l, 0, 0, a^1, a^2, a^2, 0, 0, 0, 0, 0, 0, 0\right)^T, \quad \left(\rho, c_l, 0, 0, a^1, a^2, a^2, 0, 0, 0, 0, 0, 0, 0\right)^T$$

For the contact discontinuity, the right eigenvectors are:

$$\left(\frac{\partial p}{\partial \eta}, 0, 0, 0, 0, 0, 0, 0, 0, 0, 0, 0, 0, 0, -\frac{\partial p}{\partial \rho}\right)^T, \quad (0, 0, 1, 0, 0, 0, 0, 0, 0, 0, 0, 0, 0, 0)^T$$
$$(0, 0, 0, 1, 0, 0, 0, 0, 0, 0, 0, 0, 0, 0)^T \quad \left(0, 0, 0, 0, \frac{\partial p}{\partial \eta}, 0, 0, 0, 0, 0, 0, 0, 0, -\frac{\partial S_{11}}{\partial a^1}\right)^T$$
$$\left(0, 0, 0, 0, 0, \frac{\partial p}{\partial \eta}, 0, 0, 0, 0, 0, 0, 0, -\frac{\partial S_{11}}{\partial a^2}\right)^T \quad \left(0, 0, 0, 0, 0, 0, \frac{\partial p}{\partial \eta}, 0, 0, 0, 0, 0, 0, -\frac{\partial S_{11}}{\partial a^3}\right)^T,$$
$$\left(0, 0, 0, 0, 0, 0, 0, 0, \frac{\partial p}{\partial \eta}, 0, 0, 0, 0, 0, -\frac{\partial S_{11}}{\partial b^1}\right)^T, \quad \left(0, 0, 0, 0, 0, 0, 0, 0, 0, \frac{\partial p}{\partial \eta}, 0, 0, 0, 0, -\frac{\partial S_{11}}{\partial b^2}\right)^T$$
$$\left(0, 0, 0, 0, 0, 0, 0, 0, 0, 0, \frac{\partial p}{\partial \eta}, 0, 0, 0, -\frac{\partial S_{11}}{\partial b^3}\right)^T \quad \left(0, 0, 0, 0, 0, 0, 0, 0, 0, 0, 0, \frac{\partial p}{\partial \eta}, 0, 0, -\frac{\partial S_{11}}{\partial c^1}\right)^T$$
$$\left(0, 0, 0, 0, 0, 0, 0, 0, 0, 0, 0, 0, \frac{\partial p}{\partial \eta}, 0, -\frac{\partial S_{11}}{\partial c^2}\right)^T \quad \left(0, 0, 0, 0, 0, 0, 0, 0, 0, 0, 0, 0, 0, \frac{\partial p}{\partial \eta}, -\frac{\partial S_{11}}{\partial c^3}\right)^T.$$

The eigenfields corresponding to longitudinal waves are genuinely non-linear in the sense of Lax, while the contact eigenfields are linearly degenerate in the sense of Lax. The structure of the subsystem 1 is reminiscent of the Euler equations of compressible fluids with multiple transport equations.

4.3.2 Sub-system 2

Consider the following sub-system (called 'sub-system 2') :

$$\begin{cases} \dfrac{\partial \rho}{\partial t} = 0, \quad \dfrac{\partial (\rho u)}{\partial t} = 0, \\ \dfrac{\partial (\rho v)}{\partial t} + \dfrac{\partial (-S_{12})}{\partial x} = 0, \quad \dfrac{\partial (\rho w)}{\partial t} = 0, \\ \dfrac{\partial a^\beta}{\partial t} + b^\beta \dfrac{\partial v}{\partial x} = 0, \quad \beta = 1, 2, 3 \\ \dfrac{\partial b^\beta}{\partial t} = 0, \quad \dfrac{\partial c^\beta}{\partial t} = 0, \quad \beta = 1, 2, 3 \\ \dfrac{\partial \eta}{\partial t} = 0 \end{cases} \tag{12}$$

Compatibility with the mass conservation law

Differentiating the density with respect to time we obtain :

$$\frac{\partial \rho}{\partial t} = \frac{\partial \rho_0 |\mathbf{G}|^{\frac{1}{2}}}{\partial t} = \rho_0 \frac{\partial |\mathbf{G}|^{\frac{1}{2}}}{\partial t} = \rho_0 \frac{\partial \mathbf{a} \cdot (\mathbf{b} \wedge \mathbf{c})}{\partial t} = \rho_0 \frac{\partial \mathbf{a}}{\partial t} \cdot (\mathbf{b} \wedge \mathbf{c}) = -\rho_0 \frac{\partial v}{\partial x} \mathbf{b} \cdot (\mathbf{b} \wedge \mathbf{c}) = 0.$$

Compatibility with the energy conservation law

Let us show that the equations (12) imply the conservation of energy :

$$\frac{\partial \left(\rho e^h + \rho e^e + \frac{1}{2} \left(\rho u^2 + \rho v^2 + \rho w^2 \right) \right)}{\partial t} + \frac{\partial \left(-S_{12} v \right)}{\partial x} = 0.$$

Indeed:

$$\frac{\partial \left(\rho \left(e^h + e^e + \frac{1}{2} \left(u^2 + v^2 + w^2 \right) \right) \right)}{\partial t} + \frac{\partial \left(-S_{12} v \right)}{\partial x} = \rho \frac{\partial \left(e^e + \frac{1}{2} w^2 \right)}{\partial t} + \frac{\partial \left(-S_{12} v \right)}{\partial x}$$

$$= \rho \left(\frac{\partial e^e}{\partial a^1} \frac{\partial a^1}{\partial t} + \frac{\partial e^e}{\partial a^2} \frac{\partial a^2}{\partial t} + \frac{\partial e^e}{\partial a^3} \frac{\partial a^3}{\partial t} + v \frac{\partial v}{\partial t} \right) + (-S_{12}) \frac{\partial v}{\partial x} + v \frac{\partial \left(-S_{12} \right)}{\partial x}$$

$$= -\rho \left(b^1 \frac{\partial e^e}{\partial a^1} + b^2 \frac{\partial e^e}{\partial a^1} + b^3 \frac{\partial e^e}{\partial a^1} \right) \frac{\partial v}{\partial x} + \left(-S_{12} \right) \frac{\partial v}{\partial x} = 0.$$

The last expression vanishes because of the symmetry relations (9). Let us now prove the hyperbolicity of sub-system 2.

Hyperbolicity

Consider the vector of unknowns

$$\mathbf{W} = \left(\begin{array}{cccccccccccccc} \rho & u & v & w & a^1 & a^2 & a^3 & b^1 & b^2 & b^3 & c^1 & c^2 & c^3 & \eta \end{array} \right)^T$$

The system (12) can be written in the form

$$\mathbf{W}_t + \mathbf{A}_2 \mathbf{W}_x = 0,$$

where

$$A_2 = \left(\begin{array}{cc} B_{11} & B_{12} \\ B_{21} & B_{22} \end{array} \right),$$

with

$$B_{11} = O_{3\times 3}$$

$$B_{12} = \begin{pmatrix} 0 & \mathbf{o}_3^T & \mathbf{o}_3^T & \mathbf{o}_3^T & 0 \\ 0 & \mathbf{o}_3^T & \mathbf{o}_3^T & \mathbf{o}_3^T & 0 \\ 0 & -\frac{1}{\rho}\frac{\partial S_{12}}{\partial \mathbf{a}} & -\frac{1}{\rho}\frac{\partial S_{12}}{\partial \mathbf{b}} & -\frac{1}{\rho}\frac{\partial S_{12}}{\partial \mathbf{c}} & 0 \end{pmatrix},$$

$$B_{21} = \begin{pmatrix} 0 & 0 & 0 \\ \mathbf{o}_3 & \mathbf{o}_3 & \mathbf{b} \\ \mathbf{o}_7 & \mathbf{o}_7 & \mathbf{o}_7 \end{pmatrix}.$$

$$B_{22} = O_{11\times 11}$$

Here $O_{m\times m}$ is the zero square matrix of dimension m. The eigenvalues of A_2 are :

$$\nu_1 = -\sqrt{-\frac{1}{\rho}\frac{\partial S_{12}}{\partial \mathbf{a}}\cdot\mathbf{b}}, \quad \nu_2 = \sqrt{-\frac{1}{\rho}\frac{\partial S_{12}}{\partial \mathbf{a}}\cdot\mathbf{b}}, \quad \nu_3 = 0.$$

The eigenvalue $\nu_3 = 0$ is of multiplicity 12. The right eigenvectors corresponding to the sound characteristics ν_1 and ν_2 are, respectively :

$$\left(0, 0, -\sqrt{-\frac{1}{\rho}\frac{\partial S_{12}}{\partial \mathbf{a}}\cdot\mathbf{b}}, 0, b^1, b^2, b^3, 0, 0, 0, 0, 0, 0, 0\right)^T, \tag{13}$$

$$\left(0, 0, \sqrt{-\frac{1}{\rho}\frac{\partial S_{12}}{\partial \mathbf{a}}\cdot\mathbf{b}}, 0, b^1, b^2, b^3, 0, 0, 0, 0, 0, 0, 0\right)^T. \tag{14}$$

For $\nu_3 = 0$, the right eigenvectors are:

$$(1,0,0,0,0,0,0,0,0,0,0,0,0,0,0)^T, \qquad (0,1,0,0,0,0,0,0,0,0,0,0,0,0)^T$$

$$(0,0,0,1,0,0,0,0,0,0,0,0,0,0,0)^T, \qquad \left(0,0,0,0,\frac{\partial S_{12}}{\partial c^3},0,0,0,0,0,0,0,-\frac{\partial S_{12}}{\partial a^1},0\right)^T,$$

$$\left(0,0,0,0,0,\frac{\partial S_{12}}{\partial c^3},0,0,0,0,0,0,-\frac{\partial S_{12}}{\partial a^2},0\right)^T, \quad \left(0,0,0,0,0,0,\frac{\partial S_{12}}{\partial c^3},0,0,0,0,0,-\frac{\partial S_{12}}{\partial a^3},0\right)^T,$$

$$\left(0,0,0,0,0,0,0,\frac{\partial S_{12}}{\partial c^3},0,0,0,0,-\frac{\partial S_{12}}{\partial b^1},0\right)^T, \quad \left(0,0,0,0,0,0,0,0,\frac{\partial S_{12}}{\partial c^3},0,0,0,-\frac{\partial S_{12}}{\partial b^2},0\right)^T,$$

$$\left(0,0,0,0,0,0,0,0,0,\frac{\partial S_{12}}{\partial c^3},0,0,-\frac{\partial S_{12}}{\partial b^3},0\right)^T, \quad \left(0,0,0,0,0,0,0,0,0,0,\frac{\partial S_{12}}{\partial c^3},0,-\frac{\partial S_{12}}{\partial c^1},0\right)^T,$$

$$\left(0,0,0,0,0,0,0,0,0,0,0,\frac{\partial S_{12}}{\partial c^3},-\frac{\partial S_{12}}{\partial c^2},0\right)^T, \quad (0,0,0,0,0,0,0,0,0,0,0,0,0,1)^T.$$

The system is hyperbolic if

$$-\frac{1}{\rho}\frac{\partial S_{12}}{\partial \mathbf{a}}\cdot\mathbf{b}=\frac{\partial}{\partial \mathbf{a}}\left(\frac{\partial e^e}{\partial \mathbf{a}}\cdot\mathbf{b}\right)\cdot\mathbf{b}=\mathbf{b}^T\left(e^e\right)''\mathbf{b}=\frac{\mathbf{b}^T E''\mathbf{b}}{\Delta}>0.$$

The eigenfields associated to the zero eigenvalue are linearly degenerate in the sense of Lax. The eigenfields associated to the sound characteristics are not genuinely nonlinear in the sense of Lax. The analysis of auto-similar solutions and Rankine-Hugoniot relations of subsystem 2 (12) is given in Appendices B.1 and B.2.

4.3.3 Sub-system 3

Consider the following sub-system (called "sub-system 3"):

$$\begin{cases} \dfrac{\partial \rho}{\partial t}=0, \quad \dfrac{\partial(\rho u)}{\partial t}=0, \quad \dfrac{\partial(\rho v)}{\partial t}=0, \\ \dfrac{\partial(\rho w)}{\partial t}+\dfrac{\partial(-S_{13})}{\partial x}=0, \\ \dfrac{\partial a^\beta}{\partial t}+c^\beta\dfrac{\partial w}{\partial x}=0, \quad \beta=1,2,3 \\ \dfrac{\partial b^\beta}{\partial t}=0, \quad \dfrac{\partial c^\beta}{\partial t}=0, \quad \beta=1,2,3 \\ \dfrac{\partial \eta}{\partial t}=0 \end{cases} \tag{15}$$

We can show in the same way as for (12) that (15) is compatible with the mass conservation law. One can also show that it admits the energy conservation law in the form :

$$\frac{\partial\left(\rho e^h+\rho e^e+\frac{1}{2}\left(\rho u^2+\rho v^2+\rho w^2\right)\right)}{\partial t}+\frac{\partial\left(-S_{13}w\right)}{\partial x}=0$$

For hyperbolicity, we need:

$$-\frac{1}{\rho}\left(\frac{\partial S_{13}}{\partial \mathbf{a}}\cdot\mathbf{c}\right)=\frac{\partial}{\partial \mathbf{a}}\left(\frac{\partial e^e}{\partial \mathbf{a}}\cdot\mathbf{c}\right)\cdot\mathbf{c}=\mathbf{c}^T\left(e^e\right)''\mathbf{c}=\frac{\mathbf{c}^T E''\mathbf{c}}{\Delta}>0.$$

4.3.4 General remark on the hyperbolicity of subsystems 1–3

If (7) is hyperbolic, then each subsystem (10), (12), (15) is hyperbolic. Indeed, as it was mentioned before, a sufficient condition for hyperbolicity of (7) is the positivity of the squared hydrodynamic sound speed $c^2 = \frac{\partial p}{\partial \rho}$ and the convexity of the shear energy per unit volume $E = \Delta e^e$ with respect to $\mathbf{a}$. In particular, for the equation of state (6) this condition is verified and hence each sub-system is hyperbolic for any deformations. A question appears whether it is possible to propose a family of equations of state that guarantees the hyperbolicity of the general system for any deformations (and, hence, the hyperbolicity of each sub-system). Such an example is given below :

$$e^e = \frac{\mu}{4\rho_0}\left(aj_2 + \frac{1-2a}{3}j_1^2 + 3\,(a-1)\right). \tag{16}$$

Here a can be viewed as a new material parameter. With such an energy, the equations are hyperbolic for any deformations, if $0 \leq a \leq 0.5$ (see Appendix B.3 for the proof). The case $a = 0.5$ corresponds to (6). We present now the numerical treatment of each sub-system.

4.4 Numerical treatment

In this section, we derive a second-order Godunov scheme with an approximate Riemann solver for each subsystem 1–3, and propose its generalization to 2D case.

4.4.1 Numerical treatment of sub-system 1

This system is similar to the Euler equations of compressible fluids with multiple transport equations along the particle trajectories. It is therefore legitimate to use a HLLC type solver (see Toro, 2009) because it is easy to implement and it is less "expensive" than the exact solver. The different states to be determined are shown in Figure 4.2.

Shock jump relations

Jump relations for physical variables

The Rankine-Hugoniot relations across each wave (D_L, D_R, D_*) read:

$$\mathbf{H}_L^* - D_L\mathbf{W}_L^* = \mathbf{H}_L - D_L\mathbf{W}_L,$$

$$\mathbf{H}_R^* - D_R\mathbf{W}_R^* = \mathbf{H}_R - D_R\mathbf{H}_R,$$

$$\mathbf{H}_L^* - D_*\mathbf{H}_L^* = \mathbf{H}_R^* - D_*\mathbf{H}_R^*,$$

where $\mathbf{W} = (\rho, \rho u, \rho v, \rho w, \rho E)^T$ is the vector of conservative variables and $\mathbf{H} = (\rho u, \rho u^2 + p - \sigma_{11}, \rho uv, \rho uw, \rho Eu + pu - S_{11}u)^T$ is the corresponding flux vector. The meaning of indices is shown in Figure 4.2.

Jump relations for geometric variables

The equations for geometric variables a^β, b^β and c^β, $\beta = 1, 2, 3$, are:

$$\frac{\partial a^\beta}{\partial t} + \frac{\partial\left(a^\beta u\right)}{\partial x} = 0,$$

$$\frac{\partial b^\beta}{\partial t} + u\frac{\partial b^\beta}{\partial x} = 0,$$

$$\frac{\partial c^\beta}{\partial t} + u\frac{\partial c^\beta}{\partial x} = 0.$$

We can deduce that $[a^\beta(u-D)] = 0$, $[b^\beta] = 0$ and $[c^\beta] = 0$ for shocks moving with the velocity D_L or D_R.

Interface relations

The interface relations are :

$$u_L^* = u_R^* = D_*, \quad \sigma_{11L}^* = \sigma_{11R}^*.$$

HLLC Riemann solver

The extreme wave speeds are approximated by Davis approximation (Davis, 1988) :

$$D_R = max(u_L + c_{lL}, u_R + c_{lR})$$

$$D_L = min(u_L - c_{lL}, u_R - c_{lR})$$

where $c_{lL,R}$ are the sound speeds of the system. The speed of the contact discontinuity is computed using the following explicit formula :

$$u^* = D_* = \frac{(\rho u^2 - \sigma_{11})_L - (\rho u^2 - \sigma_{11})_R - D_L(\rho u)_L + D_R(\rho u)_R}{(\rho u)_L - (\rho u)_R - D_L\rho_L + D_R\rho_R}.$$

From these wave speeds, the conservative state variables in the "star regions" are determined by :

$$\rho_L^* = \rho_L \frac{D_L - u_L}{D_L - D_*},$$

$$\rho_R^* = \rho_R \frac{D_R - u_R}{D_R - D_*},$$

$$\sigma_{11}^* = \sigma_{11R} - \rho_R u_R(u_R - D_R) + \rho_R^* D_*(D_* - D_R),$$

or

$$\sigma_{11}^* = \sigma_{11L} - \rho_L u_L(u_L - D_L) + \rho_L^* D_*(D_* - D_L),$$

$$v_R^* = v_R,$$

$$v_L^* = v_L,$$

$$w_R^* = w_R,$$

$$w_L^* = w_L,$$

$$a_L^{\beta *} = a_L^\beta \frac{D_L - u_L}{D_L - D_*}, \quad a_R^{\beta *} = a_R^\beta \frac{D_R - u_R}{D_R - D_*},$$

$$b_R^{\beta *} = b_R^\beta, \quad b_L^{\beta *} = b_L^\beta,$$

$$c_R^{\beta *} = c_R^\beta, \quad c_L^{\beta *} = c_L^\beta.$$

Second order Godunov type methods

The second-order Godunov type method used for the computation in the forthcoming section follows MUSCL-Hancock method. The sub-system 1 can be rewritten in the following form :

$$\frac{\partial \mathbf{U}}{\partial t} + \frac{\partial \mathbf{F}}{\partial x} + \mathbf{K}_u \frac{\partial u}{\partial x} + \mathbf{K}_v \frac{\partial v}{\partial x} + \mathbf{K}_w \frac{\partial w}{\partial x} = 0 \tag{17}$$

with $\mathbf{U} = (\rho,\ \rho u,\ \rho v, \rho w, \rho E,\ a^\beta,\ b^\beta,\ c^\beta)^T$,

$\mathbf{F} = (\rho u,\ \rho u^2,\ \rho v u,\ \rho w u, \rho E u,\ a^\beta u,\ b^\beta u,\ c^\beta u)^T$,

$\mathbf{K}_u = (0, 0, 0, 0, 0, 0, 0, 0, -b^\beta,\ -c^\beta)^T$, $\mathbf{K}_v = \mathbf{0}$ and $\mathbf{K}_w = \mathbf{0}$. The vectors $\mathbf{K}_v$ and $\mathbf{K}_w$ are useless in the case of the sub-model 1. However, they are kept here to introduce a general scheme used also for other sub-systems. The flow variables are characterized by their mean value $\mathbf{U}_i^n$ and a slope $\delta\mathbf{U}_i^n$ The slopes are computed with conservative variables $\mathbf{U}$, but other options are possible. The conservative variables at the cell boundary are

given by: $\mathbf{U}^n_{i+1/2,+} = \mathbf{U}^n_{i+1/2} + \frac{1}{2}\delta\mathbf{U}^n_i$ and $\mathbf{U}^n_{i-1/2,-} = \mathbf{U}^n_{i-1/2} - \frac{1}{2}\delta\mathbf{U}^n_i$. These cell boundary variables are then evolved over a half-time step by :

$$\begin{aligned}
\mathbf{U}^{n+1/2}_{i+1/2,-} &= \mathbf{U}^n_{i+1/2,-} - \frac{\Delta t}{2\Delta x}\left(\begin{array}{l}\mathbf{F}_{i+1/2,-} - \mathbf{F}_{i-1/2,+} + \mathbf{K}^n_{u,i}\left(u_{i+1/2,-} - u_{i-1/2,+}\right)\\ +\mathbf{K}^n_{v,i}\left(v_{i+1/2,-} - v_{i-1/2,+}\right) + \mathbf{K}^n_{w,i}\left(w_{i+1/2,-} - w_{i-1/2,+}\right).\end{array}\right)\\
\mathbf{U}^{n+1/2}_{i-1/2,+} &= \mathbf{U}^n_{i-1/2,+} - \frac{\Delta t}{2\Delta x}\left(\begin{array}{l}\mathbf{F}_{i+1/2,-} - \mathbf{F}_{i-1/2,+} + \mathbf{K}^n_{u,i}\left(u_{i+1/2,-} - u_{i-1/2,+}\right)\\ +\mathbf{K}^n_{v,i}\left(v_{i+1/2,-} - v_{i-1/2,+}\right) + \mathbf{K}^n_{w,i}\left(w_{i+1/2,-} - w_{i-1/2,+}\right).\end{array}\right)
\end{aligned} \tag{18}$$

Here $u_{i+1/2,\mp} = (\rho u)_{i+1/2,\mp}/\rho_{i+1/2,\mp}$ etc. The Riemann problem under HLLC approximation is then solved with the cell boundary states $\mathbf{U}^{n+1/2}_{i\pm1/2,+}$ and $\mathbf{U}^{n+1/2}_{i\pm1/2,-}$ as initial data. The solution is then evolved over the time step :

$$\mathbf{U}^{n+1}_i = \mathbf{U}^n_i - \tag{19}$$

$$\frac{\Delta t}{\Delta x}\left(\begin{array}{l}\mathbf{F}^{HLLC}\left(\mathbf{U}^{n+1/2}_{i+1/2,-}, \mathbf{U}^{n+1/2}_{i+1/2,+}\right) - \mathbf{F}^{HLLC}\left(\mathbf{U}^{n+1/2}_{i-1/2,-}, \mathbf{U}^{n+1/2}_{i-1/2,+}\right)\\ +\mathbf{K}^{n+1/2}_{u,i}\left(u^{HLLC}\left(\mathbf{U}^{n+1/2}_{i+1/2,-}, \mathbf{U}^{n+1/2}_{i+1/2,+}\right) - u^{HLLC}\left(\mathbf{U}^{n+1/2}_{i-1/2,-}, \mathbf{U}^{n+1/2}_{i-1/2,+}\right)\right)\\ +\mathbf{K}^{n+1/2}_{v,i}\left(v^{HLLC}\left(\mathbf{U}^{n+1/2}_{i+1/2,-}, \mathbf{U}^{n+1/2}_{i+1/2,+}\right) - v^{HLLC}\left(\mathbf{U}^{n+1/2}_{i-1/2,-}, \mathbf{U}^{n+1/2}_{i-1/2,+}\right)\right)\\ +\mathbf{K}^{n+1/2}_{w,i}\left(w^{HLLC}\left(\mathbf{U}^{n+1/2}_{i+1/2,-}, \mathbf{U}^{n+1/2}_{i+1/2,+}\right) - w^{HLLC}\left(\mathbf{U}^{n+1/2}_{i-1/2,-}, \mathbf{U}^{n+1/2}_{i-1/2,+}\right)\right).\end{array}\right).$$

Here the upper index $HLLC$ is for variables computed with HLLC solver.

4.4.2 Numerical treatment of sub-system 2

The sub-system 2 is reminiscent of the Euler equations of barotropic gas with a non-convex equation of state behavior. An exact Riemann solver can be derived (see Appendices B.1 and B.2 for detailed description). For a computational cost reason, an approximate Riemann solver is more suitable. The scheme will be again decomposed into two steps: first, the HLLC approximate solver (Toro, 2009) is used. Then the flow variables evolve by using the MUSCL-Hancock approach as in solving the sub-system 1 with obvious changements in the vector $\mathbf{F}$, $\mathbf{K}_u$, $\mathbf{K}_v$ and $\mathbf{K}_w$

The HLLC configuration is shown in Figure 4.2. Two shock waves and a contact discontinuity with zero velocity ($u^* = 0$) are present. The Rankine-

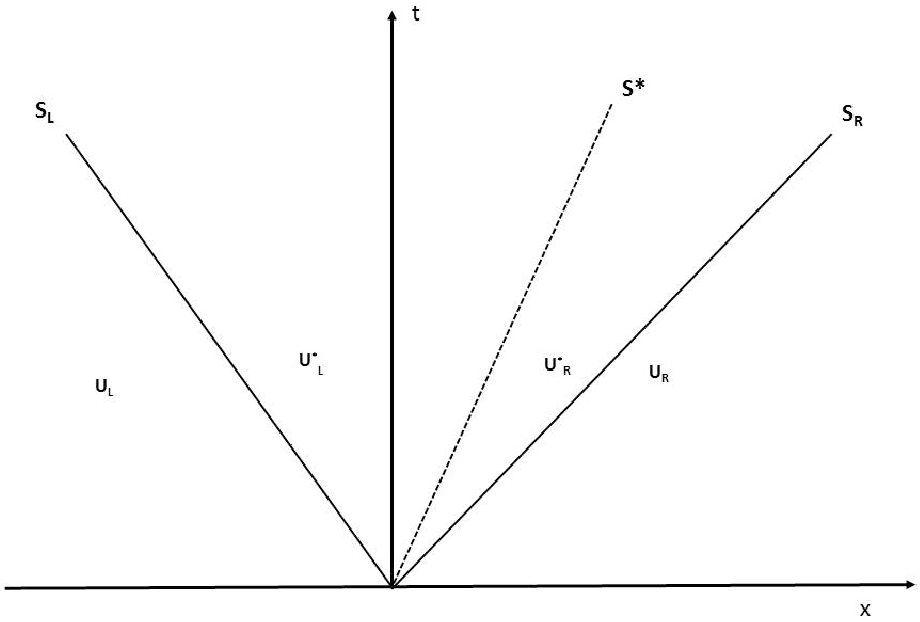

Figure 4.2: The different states which should be determined by the HLLC approximate Riemann solver are shown.

Hugoniot relations for this system are :

$$\begin{cases} \sigma_{12,R} - \sigma_{12}^* + S_R\rho_R(v_R - v^*) = 0, \\ \sigma_{12}^* - \sigma_{12,L} + S_L\rho_L(v^* - v_L) = 0, \\ b_R^\beta(v^* - v_R) + S_R(a^{\beta *}_R - a_R^\beta) = 0, \\ b_L^\beta(v^* - v_L) + S_L(a^{\beta *}_L - a_L^\beta) = 0, \\ (\sigma_{12,R}v_R - \sigma_{12}^* v^*) + S_R\rho_R(E_R - E_R^*) = 0, \\ (\sigma_{12}^* v^* - \sigma_{12,L}v_L) + S_L\rho_L(E_L^* - E_L) = 0. \end{cases} \tag{20}$$

It implies :

$$\begin{cases} v^* = \dfrac{\sigma_{12,L} - \sigma_{12,R} + (\rho_L S_L v_L - \rho_R S_R v_R)}{(\rho_L S_L - \rho_R S_R)}, \\ \sigma_{12}^* = \sigma_{12,L} + \rho_L S_L \left(v_L - v_*\right) \\ a^{\beta *}{}_R = a_R^\beta + b_R^\beta \dfrac{v_R - v^*}{S_R} \\ a^{\beta *}{}_L = a_L^\beta + b_L^\beta \dfrac{v_L - v^*}{S_L} \\ E_R^* = E_R + \dfrac{\sigma_{12,R} v_R - \sigma_{12}^* v^*}{S_R \rho_R} \\ E_L^* = E_L + \dfrac{\sigma_{12,L} v_L - \sigma_{12}^* v^*}{S_R \rho_R}. \end{cases} \tag{21}$$

4.4.3 Numerical treatment of sub-system 3

The resolution of system 3 is the same as for the sub-system 2. We have just to permute v and w, and b^β and c^β.

4.4.4 Numerical treatment in 2D case

In the multi-dimensional case we use an analogous finite volume splitting procedure. Moreover, we will show numerically that such a splitting conserves up to the first order with respect to the space discretization the stationary constraint curl $\mathbf{e}^\beta = 0$.

In 2D case the numerical procedure involves two principal steps. The first step is to solve the system describing the traction - compression of the solid that is a natural extension of (10) (sub-system 1) :

$$\frac{\partial \mathbf{U}}{\partial t} + \frac{\partial \mathbf{F}^x}{\partial x} + \frac{\partial \mathbf{F}^y}{\partial y} + \mathbf{K}_u^x \frac{\partial u}{\partial x} + \mathbf{K}_v^y \frac{\partial v}{\partial y} = 0 \tag{22}$$

with

$$\begin{array}{lcl} \mathbf{U} & = & (\rho,\, \rho u,\, \rho v, \rho E,\, a^\beta,\, b^\beta)^T, \\ \mathbf{F}^x & = & (\rho u,\, \rho u^2 - \sigma_{11},\, \rho v u,\, \rho E u - \sigma_{11} u,\, a^\beta u,\, b^\beta u)^T, \\ \mathbf{F}^y & = & (\rho v,\, \rho u v, \rho v^2 - \sigma_{22}, \rho E v - \sigma_{22} v,\, a^\beta v,\, b^\beta v)^T, \\ \mathbf{K}_u^x & = & (0,0,0,0,0,0,0,0,-b^\beta)^T, \\ \mathbf{K}_v^y & = & (0,0,0,0,0,0,0,-a^\beta,0)^T. \end{array} \tag{23}$$

The application of a finite volume method to (22), (23) needs the calculation of fluxes in x and y direction. These fluxes are in fact exactly the same as the ones coming from (10) (the sub-system 1) written in x-direction, and an analogous system in y-direction (the last system is obtained by permutation of u and v, x and y, a^β and b^β, σ_{11} and σ_{22}).

The second step will be to describe shear effects. The corresponding 2D system is a natural generalization of (12) (sub-system 2) :

$$\frac{\partial \mathbf{V}}{\partial t} + \frac{\partial \mathbf{G}^x}{\partial x} + \frac{\partial \mathbf{G}^y}{\partial y} + \mathbf{W}_u^y \frac{\partial u}{\partial y} + \mathbf{W}_v^x \frac{\partial v}{\partial x} = 0 \tag{24}$$

with

$$\begin{array}{lcl} \mathbf{V} & = & (\rho,\, \rho u,\, \rho v, \rho E,\, a^\beta,\, b^\beta)^T, \\ \mathbf{G}^x & = & (0,\, 0,\, -\sigma_{12},\, -\sigma_{12} v,\, 0,\, 0)^T, \\ \mathbf{G}^y & = & (0,\, -\sigma_{12}, 0, -\sigma_{12} u,\, 0,\, 0)^T, \\ \mathbf{W}_v^x & = & (0,0,0,0,0,0,0,b^\beta,0)^T, \\ \mathbf{W}_u^y & = & (0,0,0,0,0,0,0,0,a^\beta)^T. \end{array} \tag{25}$$

The application of a finite volume method for (24, 25) needs the computation of fluxes in x and y direction. These fluxes are in fact exactly the same as the ones coming from (12) (sub-system 2) written in x-direction, and an analogous system in y-direction (the last system is obtained by permutation of of u and v, x and y, a^β and b^β).

4.5 Numerical Results

In this section, we will compare the numerical results obtained by the splitting procedure to the numerical results for the system (8), and the exact solution proposed in Ndanou, Favrie and Gavrilyuk (2013). The results are obtained for the following material parameters (corresponding to aluminum): $\gamma = 3.4$, $p_\infty = 21.5\, GPa$, $\mu = 26\, GPa$, $\rho_0 = 2700\, kg/m^3$.

4.5.1 Shear Test

Initially, the normal speed is zero everywhere, the pressure is atmosperic : $p_0 = 10^5\, Pa$, the shear stress is zero, the tangential velocity is $500\, m/s$ at the left, and $-500\, m/s$ at the right. The initial discontinuity is located at $x = 0.5\, m$. The entire domain is of $1\, m$ long. The results are presented at time instant $t = 50\, \mu s$. In Figure 4.3, the solution is computed by using the first order version of the Godunov type method. The calculation domain contains 200 computing cells. The exact solution is shown by line. The numerical solution obtained by the splitting procedure is shown by squares, the solution of the full system (8) is shown by circles. For both numerical approaches we used the same CFL number equal to 0.5. The diffusion of shear waves is smaller in the case of splitting procedure. Consider now the same test case by using the second order Godunov type method. The results are obtained by using Minmod limiter for the full system (8), Minmod limiter for sub-system 1 (10), and van Leer limiter for sub-system 2 (12). The results are shown in Figure 4.4 by squares for the splitting approach, and by circles for the full system (8) at time instant $t = 50\, \mu s$ on a 200 computing cells. The agreement with the exact solution represented by a continuous line is much more better. The diffusion of the shear waves is represented by 10 circles and only by 6 squares. The splitting model is thus less diffusive.

4.5.2 Impact+Shear Test

In the following test problems, the Riemann problem with two colliding materials subjected to strong shear is considered. The normal velocity is $100\, m/s$ at the left and $-100\, m/s$ at the right, the transverse velocities were chosen as in the previous example. The initial discontinuity is located at $0.5\, m$, the entire domain is $1\, m$ long. No shear stress is initially presented. The results are shown at time $t = 50\, \mu s$. The calculation domain was divided into 200 calculating cells. In Figure 4.5, the solution is computed by using the first order version of the Godunov type method. The splitting model solution is represented by squares, the solution of the full system is shown by circles. The same CFL number equal to 0.5 is used. The exact solution is represented with lines. The results are in good agreement. The diffusion of the shear waves is smaller in the case of the splitting approach.

The numerical results obtained by using a second order scheme on 200 calculating cells are shown in Figure 4.6. The results are in perfect agree-

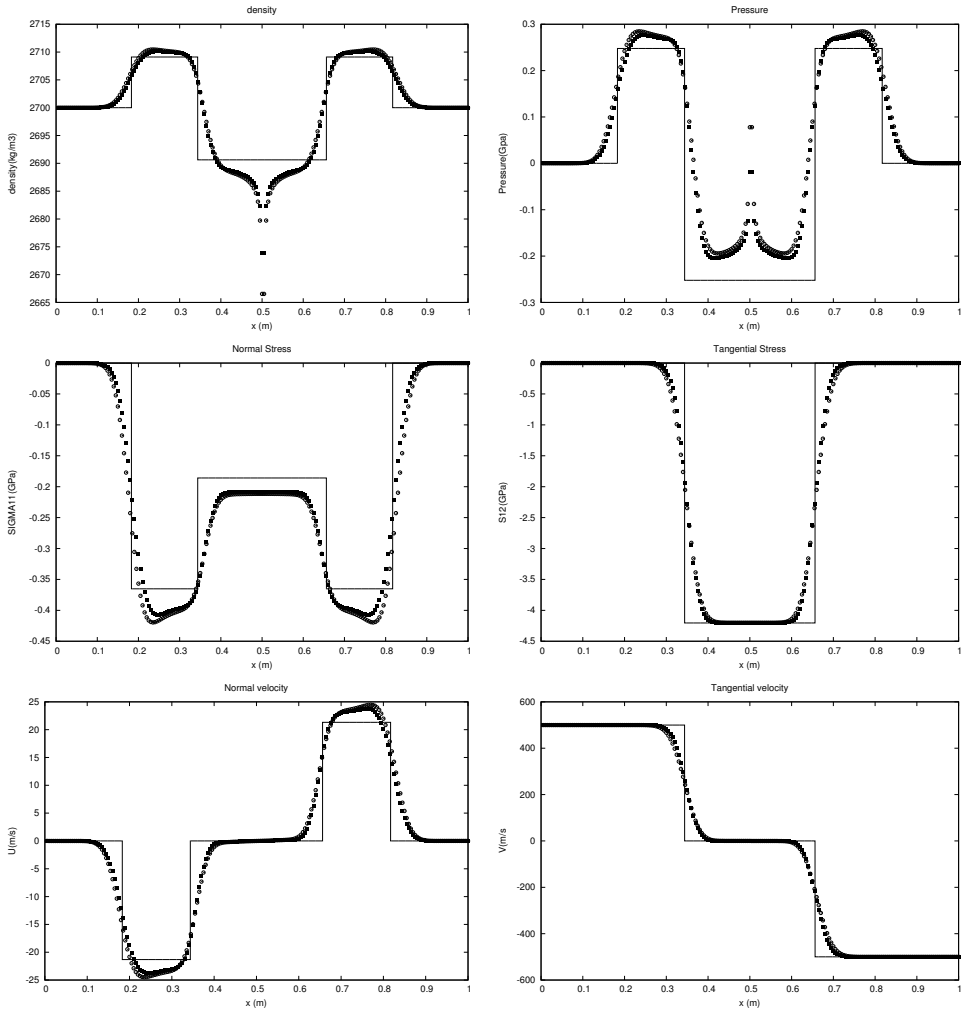

Figure 4.3: Shear test problem : initially, the discontinuity of the tangential velocity is imposed. The exact solution (shown by a continuous line) is a symmetric with respect to x and represents left-and right longitudinal shocks followed by shear 'rarefaction shocks' (see Ndanou, Favrie, Gavrilyuk 2013 for details). The numerical solution obtained by the splitting procedure is shown by squares, the solution of the full system (8) is shown by circles. The numerical results are obtained by using a first order Godunov type scheme on a 200 cells grid. The diffusion of the shear waves is smaller in the case of the splitting approach.

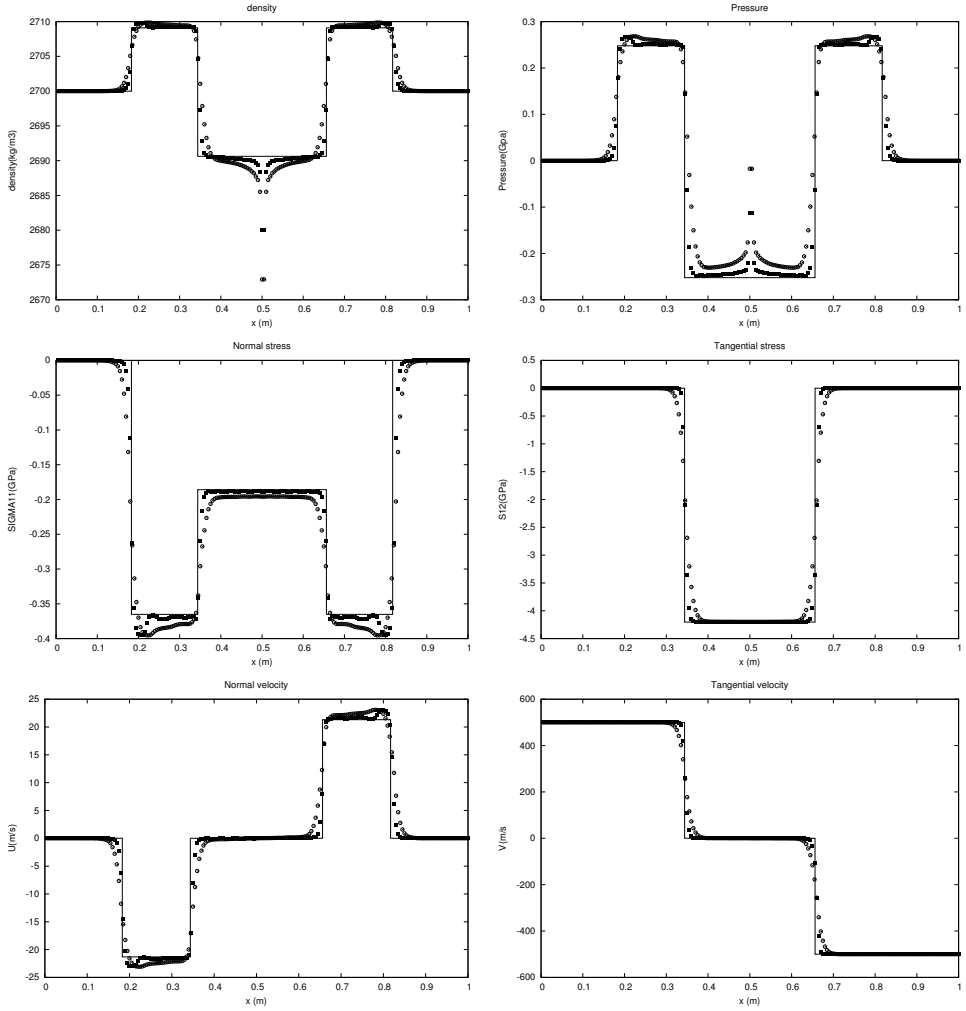

Figure 4.4: The same shear test as in Figure 4.3 is treated by using the MUSCL extension of Godunov method with Van Leer limiter. The numerical diffusion of shear waves is again much smaller in the case of the splitting approach.

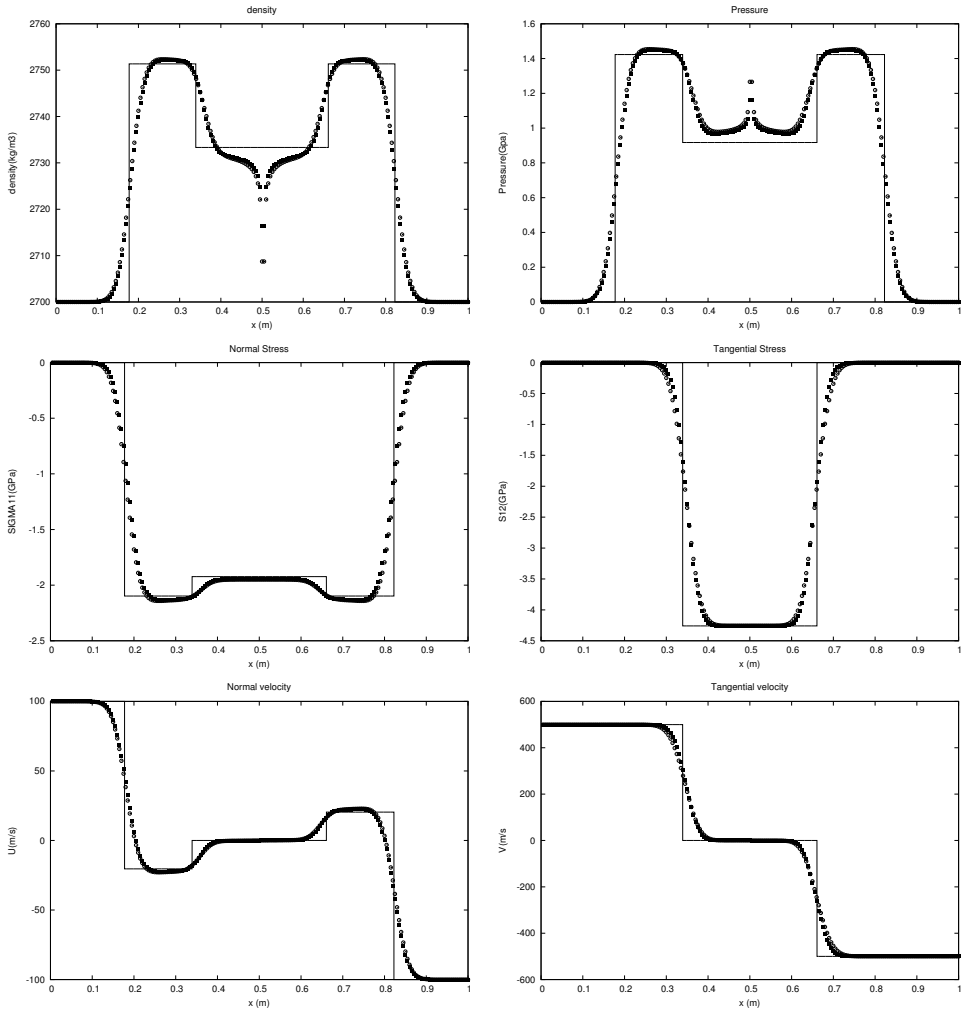

Figure 4.5: Impact-shear test problem : initially, the normal and the tangential velocity discontinuity is imposed. The exact solution is represented by a continuous line. The numerical solution obtained by the splitting procedure is represented by squares, the solution of the full system (8) is shown by circles. The numerical results are obtained by using a first order Godunov type scheme on a 200 cells grid. The diffusion of the shear waves is smaller in the case of the splitting approach.

ment with the exact solution. The diffusion is reduced in the split model.

4.5.3 Convergence test

We consider now the same "impact + shear" test for the split system by using the first order Godunov type method. The solution for 100, 1000 and 10 000 computing cells is shown in Figure 4.7 by crosses, triangles and points, respectively. The exact solution is represented by continuous line. The convergence is clearly visible.

4.5.4 2D test case

In this section, we present a numerical simulation of a 2D problem The initial configuration is shown in Figure 4.8. The initial velocity field is given by :

$$\left.\begin{pmatrix} u \\ v \end{pmatrix}\right|_{t=0} = \begin{cases} \begin{pmatrix} -\omega y \\ \omega x \end{pmatrix}, & \text{if} \quad x^2+y^2 < R^2 \\ \\ \begin{pmatrix} 0 \\ 0 \end{pmatrix}, & \text{if} \quad x^2+y^2 \geq R^2. \end{cases} \tag{26}$$

The initial stress tensor is spherical: $\boldsymbol{\sigma} = -p_0\mathbf{I}$, $p_0 = const$. For numerical applications, we have chosen $\omega = 40000\,s^{-1}$, $R = 0.05\,m$, $p_0 = 10^5\,Pa$. The material parameters are the same as in 1D case. The results are shown at time instant $t = 5\,\mu s$. This test corresponds to a strong shear at the boundary $x^2 + y^2 = R^2$ where the tangential velocity jumps from $2000\,m/s$ to $0\,m/s$. This produces, both inside and outside the circle $x^2 + y^2 = R^2$, a longitudinal shock followed by a transverse shock. The transverse shocks are "rarefaction shocks", i.e. the density behind them decreases. We compared the results obtained by our scheme for the non-conservative formulation to the results obtained by the Lax-Friedrichs type scheme for the conservative formulation. The Lax-Friedrichs scheme was modified to conserve the stationary constraint $\mathrm{curl}\mathbf{e}^\beta = 0$ at the discrete level (see Appendix D). The property of conservation of the vorticity constraint for the splitting approach was proved numerically. For this, we determined the circulation of

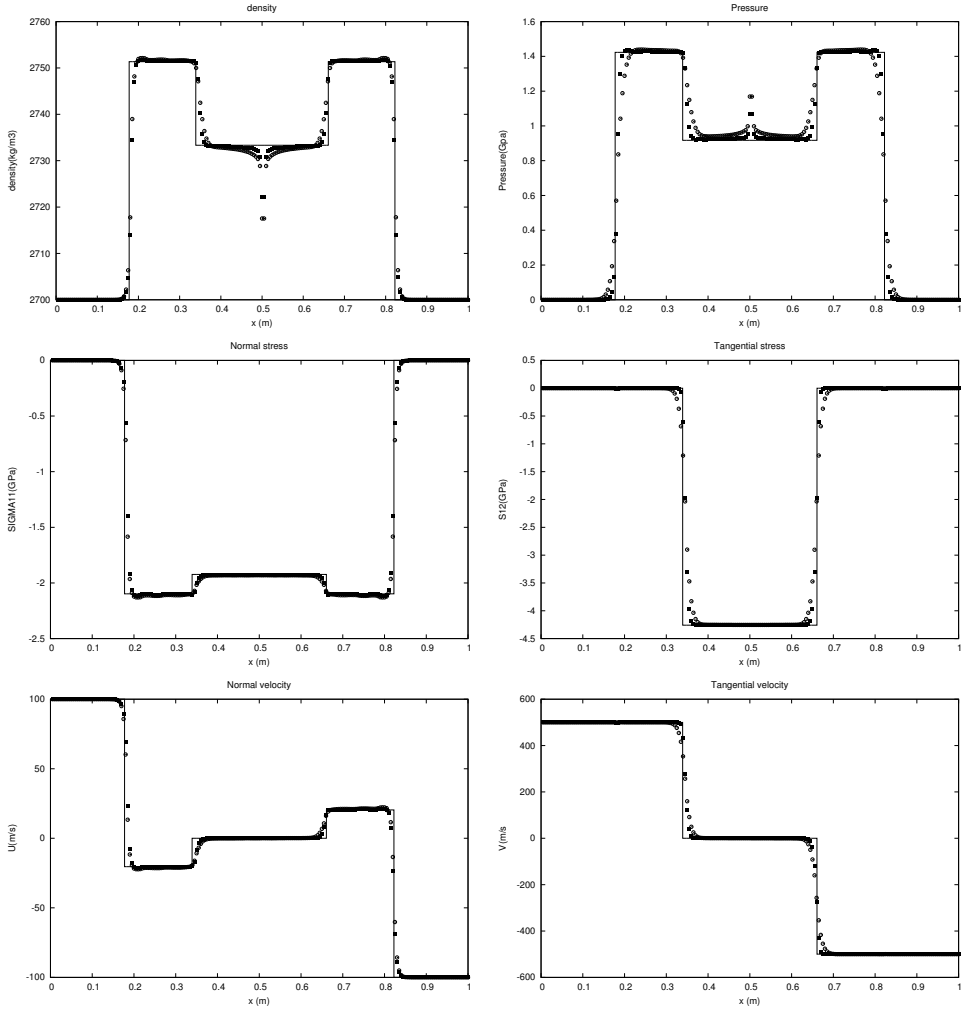

Figure 4.6: The same impact-shear test as in Figure 4.5 is treated by using the MUSCL extension of Godunov method with Van Leer limiter. The numerical diffusion of shear waves is again much smaller in the case of the splitting approach.

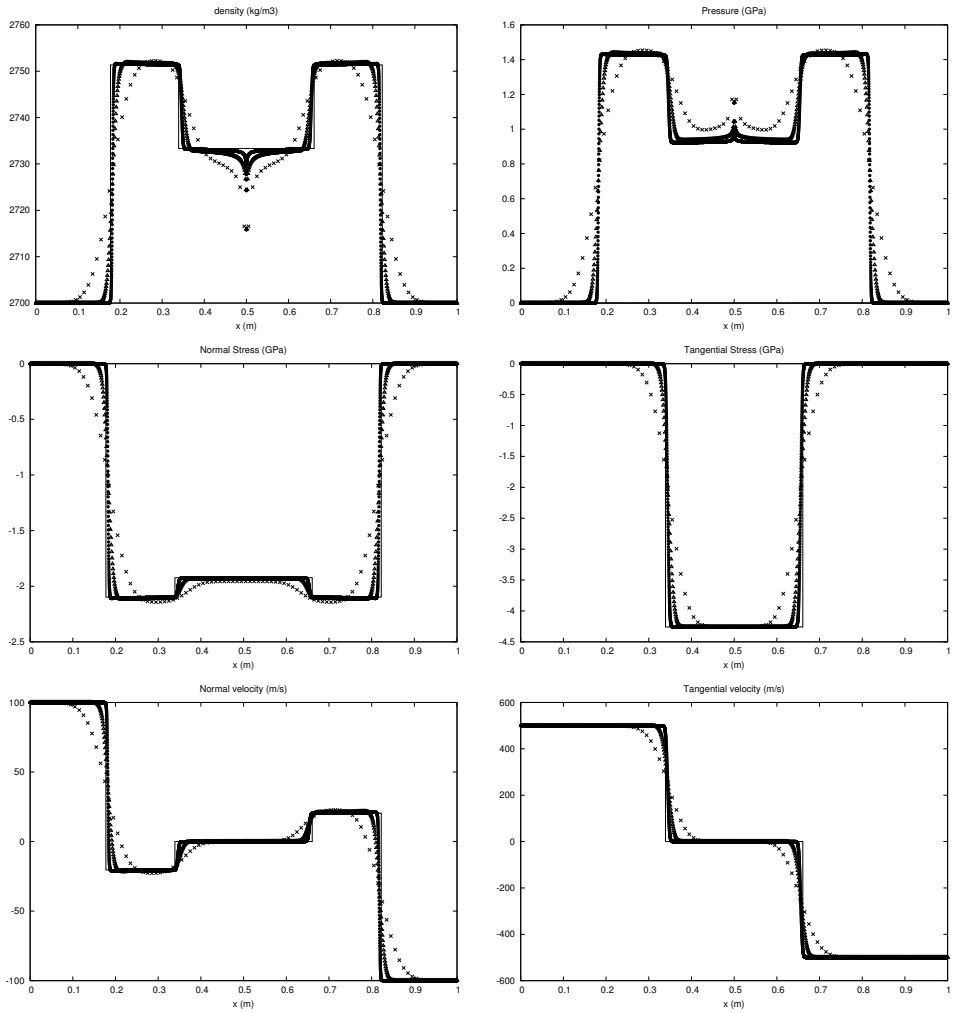

Figure 4.7: The same impact with shear test as in Figure 4.5 is treated for different meshes (100 cells, 1000 cells, 10000 cells) using the splitting procedure. The convergence to the exact solution is highlighted.

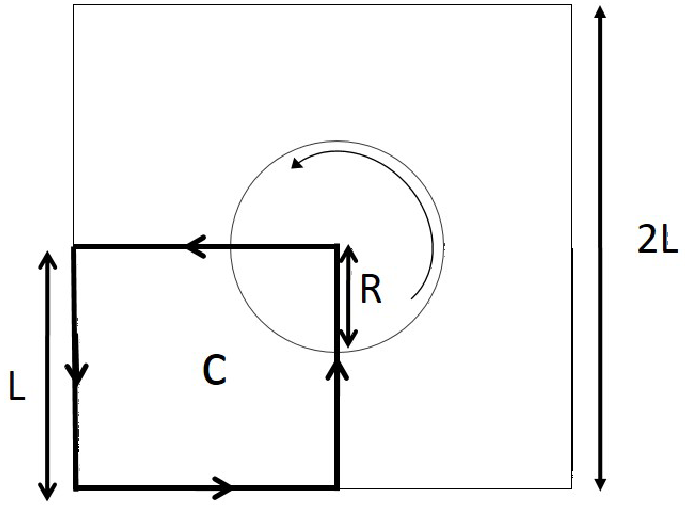

Figure 4.8: The initial configuration is shown. Outside the circle of radius R the solid is initially at rest, while inside the circle the initial velocity field corresponds to the solid rotation with constant angular velocity. The contour C along which the circulation Γ is calculated, is a square of length L (shown by arrows).

the vector $\mathbf{e}^\beta$ along a closed contour C that is the boundary of the domain D. For definiteness, we took only the vector $\mathbf{e}^1$ and denoted :

$$\Gamma = \oint_C a^1 dx + b^1 dy = \int\int_D \left(\frac{\partial b^1}{\partial x} - \frac{\partial a^1}{\partial y} \right) dx\, dy$$

The closed contour C along which the circulation Γ is calculated is a square of of length $L = 1m$ (shown by arrows in Figure 4.8). The value of $\log|\Gamma|$ as a function on the grid cell size is shown in Figure 4.9. Different regular Cartesian grids (100×100,200×200, 400×400, 800×800, 1500×1500 cells) were used. The order of convergence was always about 1 (see Figure 4.9). This test shows that the splitting procedure respects the vorticity constraint in the first order.

The numerical results obtained by the two schemes are shown in Figure 4.10 on a 1500×1500 Cartesian grid at time instant $t = 5\,\mu s$. The results are qualitatively and quantitatively similar but the splitting model is clearly less diffusive.

4.6 Conclusion

We consider the equations of hyperelasticity for isotropic solids in the Eulerian coordinates in a special case where the specific stored energy is the sum of two functions. The first one, the hydrodynamic specific energy, depends only on the density and the entropy. The second one, the shear energy, depends only on invariants of the Finger tensor in such a way that it is unaffected by the volume change. We proposed a new splitting method which has at least two advantages with respect to numerical methods without splitting.

First, one deals always with simple subsystems containing only three waves : two acoustic waves and one material wave, while the full 1D system contains seven waves. The subsystems are hyperbolic if the full system is hyperbolic. Moreover, the corresponding eigenvalues are explicitly given for each sub-system, while it is not the case for the full system. Such a three-wave structure of a split model simplifies the development of conventional high order schemes (WENO, ADER, etc.) because of the similarity with the Euler system of compressible fluids.

Second, for a given order of numerical scheme, this splitting approach reduces significantly the numerical diffusion of shear waves. Even if the

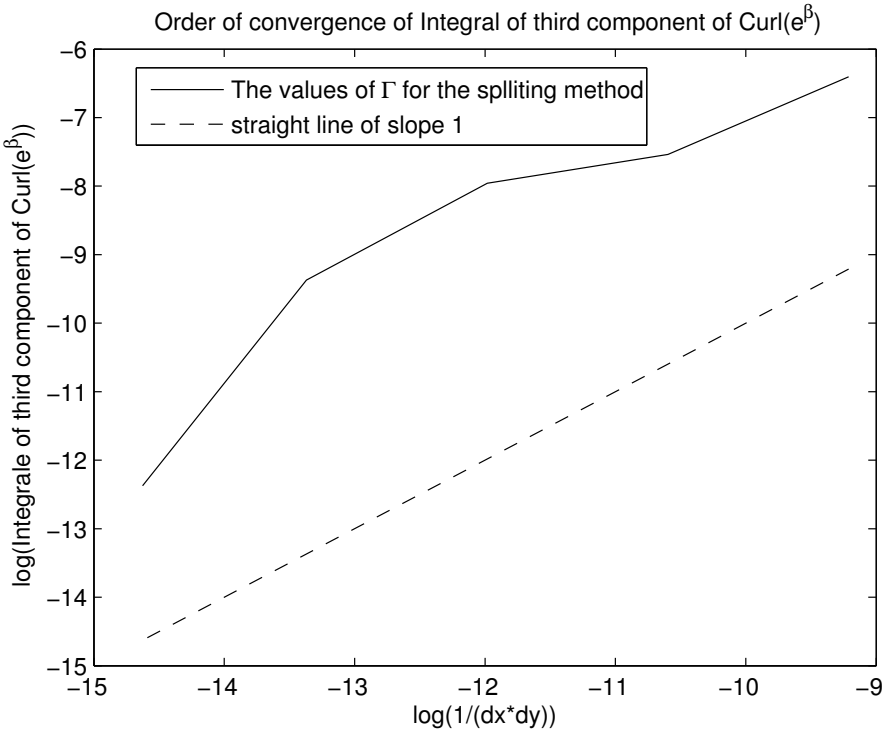

Figure 4.9: The convergence curve $\log|\Gamma|$ as a function of the grid cell size is shown (continuous line). The number of grid cells was 100×100, 200×200, 400×400, 800×800 and 1500×1500. The dashed line corresponds to the convergence order equal to 1. The results obtained show the convergence about of order 1 for this difficult test case. The dimensionless variables Γ/L, $\Delta x/L$ and $\Delta y/L$ where used. This test shows the ability of the splitting procedure to preserve the zero vorticity condition in the first order.

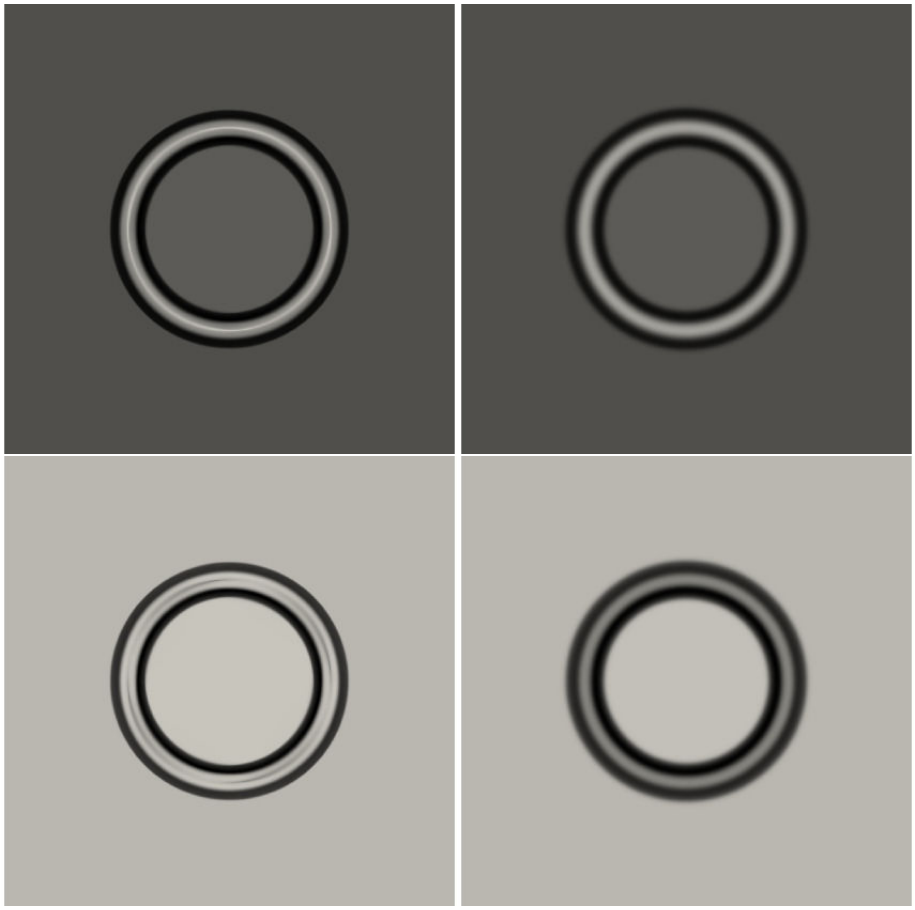

Figure 4.10: At the top, we represented at time instant $5\,\mu s$ the values of density, and at the bottom, those of the pressure. Dark regions correspond to higher values. The results based on the splitting procedure are shown on the left, and those obtained by the Lax-Friedrichs type scheme are shown on the right. The results are qualitatively and quantitatively similar but the splitting model is clearly less diffusive. The number of cells was 1500×1500.

numerical treatment of this splitting is a little bit 'more expensive' than the treatment of the full model, it is easier to compute than the full model.

The case of equation of state in separable form with a constant value of shear modulus considered in this paper can easily be generalized to the case where the shear modulus is a function of entropy. It allows us to model real materials where the dependence on the entropy (and hence, indirectly on the pressure and temperature) is crucial.

Moreover, the splitting approach can also be applied to any equation of state for isotropic solids expressed in the form:

$$e = e\left(\rho, j_1, j_2, \eta\right). \tag{27}$$

The presentation implies that the Cauchy stress tensor can be written in the form :

$$\sigma = -p\mathbf{I} + \mathbf{S},$$

with $\mathbf{I}$ being the identity tensor, $p = \rho^2 \dfrac{\partial e}{\partial \rho}$ being the pressure, and

$$\mathbf{S} = -2\rho \left(\frac{\partial e}{\partial j_1} \frac{\partial j_1}{\partial \mathbf{G}} + \frac{\partial e}{\partial j_2} \frac{\partial j_2}{\partial \mathbf{G}} \right) \mathbf{G}$$

being the deviatoric part of the stress tensor. However, the main difficulty will be to assure the hyperbolicity of the full system and each subsystem.

The splitting procedure can also be extended to deal with elasto–plastic solids interacting with compressible fluids by using the diffuse interface models developed in Favrie, Gavrilyuk and Saurel (2009), and Favrie and Gavrilyuk (2011, 2012).

4.7 References

Barton, B., Drikakis, D., Romenski, E. I. and Titarev, V. A. : Exact and approximate solutions of Riemann problems in non-linear elasticity. J. Comp. Physics, **228**, 7046–7068 (2009)

Davies, P. J. : A simple derivation of necessary and sufficient conditions for the strong ellipticity of isotropic hyperelastic materials in plane strain. J. Elasticity **26**, 291–296 (1991).

Davis, S. F. Simplified Second-Order Godunov-Type Methods. SIAM J . Sci. Stat. Comput., **9**, 445–473 (1988)

Dacorogna, B. : Necessary and sufficient conditions for strong ellipticity of isotropic functions in any dimension. Discrete and Continuous Dynamical Systems - Series B, **1**, N 2, 257–263 (2001).

Dafermos, C. M. : Hyperbolic Conservation Laws in Continuum Mechanics, Springer (2000).

De Tommasi, D., Puglisi, G. and Zurlo, G. : A note on the strong ellipticity in two-dimensional isotropic elasticity. J. Elasticity, **109,** 67–74 (2012).

Favrie, N., Gavrilyuk, S. L. and Saurel, R. : Solid-fluid diffuse interface model in cases of extreme deformations. J. Computational Physics, **228**, 6037–6077 (2009).

Favrie, N. and Gavrilyuk, S. L. : Mathematical and numerical model for nonlinear viscoplasticity. Phil. Trans. R. Soc. A, **369**, 2864–2880 (2011).

Favrie, N. and Gavrilyuk, S. L. : Diffuse interface model for compressible fluid-compressible elastic-plastic solid interaction. J. Computational Physics, **231**, 2695–2723 (2012).

Flory, R. J. : Thermodynamic relations for highly elastic materials. Transactions of the Faraday Society, **57**, 829–838 (1961).

Gavrilyuk, S. L., Favrie, N. and Saurel, R. : Modeling wave dynamics of compressible elastic materials. Journal of Computational Physics, **227**, 2941–2969 (2008).

Godunov, S. K. and Romenskii, E. I. : Elements of Continuum Mechanics and Conservation Laws, Kluwer Academic Plenum Publishers, NY (2003).

Hartmann, S. and Neff, P. : Polyconvexity of generalized polynomial-type hyperelastic strain energy functions for nearly incompressibility. Int. J. Solid and Structures, **40,** 2767–2791 (2003).

Horgan, C. O. : Remarks on ellipticity for the generalized Blatz-Ko constitutive model for a compressible nonlinearly elastic solid. J. Elasticity **42,** 165–176 (1995)

Kulikovskii, A. and Sveshnikova, E. Nonlinear waves in Elastic Media, CRC Press (1995)

Le Floch, Ph. G. : Hyperbolic systems of conservation laws : the theory of classical and nonclassical shock waves, Birkhäuser Verlag (2002).

Miller, G. H. and Colella, P. : A high order Eulerian Godunov method for elastic plastic flow in solids, Journal of Computational Physics, **167**, 131–176 (2001).

Ndanou, S., Favrie, N. and Gavrilyuk, S. Criterion of Hyperbolicity in

Hyperelasticity in the Case of the Stored Energy in Separable Form, J. Elasticity, **115**, 1–25 (2014)

Ndanou, S., Favrie, N. and Gavrilyuk, S. The piston problem in hyperelasticity with the stored energy in separable form 2013 http://hal.archives-ouvertes.fr/hal-00917961

Pence, T. J. Distortion of Anisotropic Hyperelastic Solids Under Pure Pressure Loading : Compressibility, Incompressibility and Near-Incompressibility, J. Elasticity, DOI 10.1007/s10659-013-9438-1 (2013)

Titarev, V. A., Romenski, E. and Toro, E.F. MUSTA-type upwind fluxes for nonlinear elasticity, Int. J. Numerical Methods in Engineering, **73**, 897–926 (2008).

Toro, E. Riemann Solvers and Numerical Methods for Fluid Dynamics, Springer Verlag (2009).

Wendroff, B. The Riemann problem for materials with nonconvex equations of state I: Isentropic flow . J. Mathematical Analysis and Applications, **38**, 454–466 (1972).

Appendices

Appendix B

Appendices

B.1 Auto-similar solutions of sub-system 2

Consider smooth auto-similar solutions of sub-system 2 corresponding to non-degenerate eigenfields :

$$\mathbf{W} = \mathbf{U}(\xi), \quad \xi = x/t.$$

The solution satisfies the equation

$$\frac{d\mathbf{U}}{d\xi} = \frac{\mathbf{r}}{\boldsymbol{\nabla}\nu \cdot \mathbf{r}},$$

where ν is an eigenvalue and $\mathbf{r}$ is the corresponding eigenvector. For definiteness consider a simple wave going to the right ($\nu = \nu_2$). We will now calculate explicitly the expression $\boldsymbol{\nabla}\nu \cdot \mathbf{r}$ in the case (6). We have

$$\begin{aligned} S_{12} &= -\frac{\mu\rho}{8\rho_0}\frac{\partial j_2}{\partial \mathbf{a}}\cdot\mathbf{b} = -\frac{\mu\rho}{8\rho_0}\left(\frac{4\left\|\mathbf{a}\right\|^2\mathbf{a} + 4\left(\mathbf{a}\cdot\mathbf{b}\right)\mathbf{b} + 4\left(\mathbf{a}\cdot\mathbf{c}\right)\mathbf{c}}{\Delta^{4/3}} - \frac{4}{3}j_2\frac{\left(\mathbf{b}\wedge\mathbf{c}\right)}{\Delta}\right)\cdot\mathbf{b} \\ &= -\frac{\mu\rho}{2\rho_0}\frac{\left\|\mathbf{a}\right\|^2\mathbf{a}\cdot\mathbf{b} + \left(\mathbf{a}\cdot\mathbf{b}\right)\left\|\mathbf{b}\right\|^2 + \left(\mathbf{a}\cdot\mathbf{c}\right)\left(\mathbf{c}\cdot\mathbf{b}\right)}{\left|\mathbf{a}\cdot\left(\mathbf{b}\wedge\mathbf{c}\right)\right|^{\frac{4}{3}}}. \end{aligned}$$

Hence,

$$\frac{\partial S_{12}}{\partial \mathbf{a}} = -\frac{\mu\rho}{2\rho_0}\left(\frac{\left(\mathbf{b}\cdot\mathbf{c}\right)\mathbf{c} + \left\|\mathbf{b}\right\|^2\mathbf{b} + \left\|\mathbf{a}\right\|^2\mathbf{b} + 2\left(\mathbf{a}\cdot\mathbf{b}\right)\mathbf{a}}{\left|\mathbf{a}\cdot\left(\mathbf{b}\wedge\mathbf{c}\right)\right|^{\frac{4}{3}}}\right)$$

$$-\frac{\mu\rho}{2\rho_0}\left(-\frac{4}{3}\frac{\left\|\mathbf{a}\right\|^2\mathbf{a}\cdot\mathbf{b} + \left(\mathbf{a}\cdot\mathbf{b}\right)\left\|\mathbf{b}\right\|^2 + \left(\mathbf{a}\cdot\mathbf{c}\right)\left(\mathbf{c}\cdot\mathbf{b}\right)}{\left|\mathbf{a}\cdot\left(\mathbf{b}\wedge\mathbf{c}\right)\right|^{\frac{7}{3}}}\left(\mathbf{b}\wedge\mathbf{c}\right)\right).$$

It implies that

$$-\frac{1}{\rho}\frac{\partial S_{12}}{\partial \mathbf{a}}\cdot\mathbf{b}=\frac{\mu}{2\rho_0}\left(\frac{(\mathbf{b}\cdot\mathbf{c})^2+\|\mathbf{b}\|^4+\|\mathbf{a}\|^2\|\mathbf{b}\|^2+2(\mathbf{a}\cdot\mathbf{b})^2}{|\mathbf{a}\cdot(\mathbf{b}\wedge\mathbf{c})|^{\frac{4}{3}}}\right)>0.$$

Further,

$$\boldsymbol{\nabla}_{\mathbf{a}}\nu_2=\frac{\mu}{4\rho_0}\frac{1}{\sqrt{-\frac{1}{\rho}\frac{\partial S_{12}}{\partial \mathbf{a}}.\mathbf{b}}}\boldsymbol{\nabla}_{\mathbf{a}}\left(\frac{(\mathbf{b}\cdot\mathbf{c})^2+\|\mathbf{b}\|^4+\|\mathbf{a}\|^2\|\mathbf{b}\|^2+2(\mathbf{a}\cdot\mathbf{b})^2}{|\mathbf{a}\cdot(\mathbf{b}\wedge\mathbf{c})|^{\frac{4}{3}}}\right)$$

$$=\frac{\mu}{4\rho_0}\frac{1}{\sqrt{-\frac{1}{\rho}\frac{\partial S_{12}}{\partial \mathbf{a}}.\mathbf{b}}}\left(\frac{2\mathbf{a}\|\mathbf{b}\|^2+4(\mathbf{a}\cdot\mathbf{b})\mathbf{b}}{|\mathbf{a}\cdot(\mathbf{b}\wedge\mathbf{c})|^{\frac{4}{3}}}\right)$$

$$+\frac{\mu}{4\rho_0}\frac{1}{\sqrt{-\frac{1}{\rho}\frac{\partial S_{12}}{\partial \mathbf{a}}.\mathbf{b}}}\left(-\frac{4}{3}\frac{(\mathbf{b}\cdot\mathbf{c})^2+\|\mathbf{b}\|^4+\|\mathbf{a}\|^2\|\mathbf{b}\|^2+2(\mathbf{a}\cdot\mathbf{b})^2}{|\mathbf{a}\cdot(\mathbf{b}\wedge\mathbf{c})|^{\frac{7}{3}}}(\mathbf{b}\wedge\mathbf{c})\right).$$

Hence,

$$\boldsymbol{\nabla}\nu_2\cdot\mathbf{r}_2=\boldsymbol{\nabla}_{\mathbf{a}}\nu_2\cdot\mathbf{b}=\frac{3\mu}{2\rho_0}\frac{\|\mathbf{b}\|^2}{|\mathbf{a}\cdot(\mathbf{b}\wedge\mathbf{c})|^{\frac{4}{3}}}\frac{\mathbf{a}\cdot\mathbf{b}}{\sqrt{-\frac{1}{\rho}\frac{\partial S_{12}}{\partial \mathbf{a}}.\mathbf{b}}}. \tag{1}$$

We remark that $\boldsymbol{\nabla}\nu_2\cdot\mathbf{r}_2=0\Leftrightarrow\mathbf{a}\cdot\mathbf{b}=0$, i.e. the inflection point occurs if and only if the vectors $\mathbf{a}$ and $\mathbf{b}$ are orthogonal. For the points which do not belong to the plane $\mathbf{a}\cdot\mathbf{b}=0$, we have :

$$\frac{dv}{d\xi}=\frac{\sqrt{-\frac{1}{\rho}\frac{\partial S_{12}}{\partial \mathbf{a}}\cdot\mathbf{b}}}{\boldsymbol{\nabla}\nu_2\cdot\mathbf{r}_2},$$

$$\frac{da^1}{d\xi}=\frac{b^1}{\boldsymbol{\nabla}\nu_2\cdot\mathbf{r}_2},$$

$$\frac{da^2}{d\xi}=\frac{b^2}{\boldsymbol{\nabla}\nu_2\cdot\mathbf{r}_2},$$

$$\frac{da^3}{d\xi}=\frac{b^3}{\boldsymbol{\nabla}\nu_2\cdot\mathbf{r}_2}.$$

The other relations coming from (12) are :

$$b^\beta = const, \quad c^\beta = const, \quad \eta = const.$$

The last three equations admit two independent first integrals (Riemann invariants) :

$$b^2 a^1 - b^1 a^2 = const, \tag{2}$$

$$b^2 a^3 - b^3 a^2 = const. \tag{3}$$

Finally, one of the variables a^β (for example, a^2) can be choosen as a parameter of the simple wave :

$$\frac{dv}{da^\beta} = \frac{\sqrt{-\frac{1}{\rho}\frac{\partial S_{12}}{\partial \mathbf{a}} \cdot \mathbf{b}}}{b^\beta}.$$

This relation can be integrated to give the last Riemann invariant :

$$v - \int^{a^2} \frac{\sqrt{-\frac{1}{\rho}\frac{\partial S_{12}}{\partial \mathbf{a}} \cdot \mathbf{b}}}{b^2} da^2 = const.$$

Finally, for given b^β and c^β and a^1 and a^3 determined by (2)-(3), the subsystem 2 is reminiscent of the equations of a "barotropic fluid" written in the mass Lagrangian coordinates :

$$\tau_t - v_x = 0,$$

$$v_t + p_x = 0,$$

with the "specific volume" $\tau = -a^2/b^2$, and the 'pressure' $p = -S_{12}/\rho$. The dependence of the 'pressure' p on the 'specific volume' τ is monotonic (to assure the hyperbolicity), but not convex :

$$\frac{\partial^2}{\partial \tau^2}\left(-\frac{S_{12}}{\rho}\right) = \frac{\mu}{8\rho_0}\frac{\partial^2}{\partial \tau^2}\left(\frac{\partial j_2}{\partial \mathbf{a}}\cdot\mathbf{b}\right) = \frac{\mu}{2\rho_0}\frac{\partial^2}{\partial \tau^2}\left(\frac{\|\mathbf{a}\|^2(\mathbf{a}\cdot\mathbf{b}) + (\mathbf{a}\cdot\mathbf{b})\|\mathbf{b}\|^2 + (\mathbf{a}\cdot\mathbf{c})(\mathbf{b}\cdot\mathbf{c})}{(\mathbf{a}\cdot(\mathbf{b}\wedge\mathbf{c}))^{4/3}}\right)$$

$$= \frac{\mu}{2\rho_0}\frac{\partial}{\partial \tau}\left(\frac{\partial}{\partial \mathbf{a}}\left(\frac{\|\mathbf{a}\|^2(\mathbf{a}\cdot\mathbf{b}) + (\mathbf{a}\cdot\mathbf{b})\|\mathbf{b}\|^2 + (\mathbf{a}\cdot\mathbf{c})(\mathbf{b}\cdot\mathbf{c})}{(\mathbf{a}\cdot(\mathbf{b}\wedge\mathbf{c}))^{4/3}}\right)\cdot\frac{d\mathbf{a}}{d\tau}\right)$$

$$= -\frac{\mu}{2\rho_0}\frac{\partial}{\partial \tau}\left(\frac{\partial}{\partial \mathbf{a}}\left(\frac{\|\mathbf{a}\|^2(\mathbf{a}\cdot\mathbf{b}) + (\mathbf{a}\cdot\mathbf{b})\|\mathbf{b}\|^2 + (\mathbf{a}\cdot\mathbf{c})(\mathbf{b}\cdot\mathbf{c})}{(\mathbf{a}\cdot(\mathbf{b}\wedge\mathbf{c}))^{4/3}}\right)\cdot\mathbf{b}\right)$$

$$= -\frac{\mu}{2\rho_0}\frac{\partial}{\partial\tau}\left(\left(\frac{\|\mathbf{a}\|^2\|\mathbf{b}\|^2 + 2(\mathbf{a}\cdot\mathbf{b})^2 + \|\mathbf{b}\|^4 + (\mathbf{b}\cdot\mathbf{c})^2}{(\mathbf{a}\cdot(\mathbf{b}\wedge\mathbf{c}))^{4/3}}\right)\right)$$

$$= \frac{3\mu}{\rho_0}\frac{(\mathbf{a}\cdot\mathbf{b})\|\mathbf{b}\|^2}{(\mathbf{a}\cdot(\mathbf{b}\wedge\mathbf{c}))^{4/3}}.$$

The inflection point is unique. Indeed, (2)–(3) imply $\mathbf{a} = -\mathbf{b}\tau + \mathbf{const}$. Hence, $\mathbf{a}\cdot\mathbf{b} = 0$ gives us a unique value of τ. The solution of the Riemann problem for such a 'barotropic fluid' can be found, in particular, in Wendroff (1972) and Le Floch (2002). The non-convexity of the equation of state implies the existence of 'rarefaction' shocks in a typical solution of the Riemann problem (see Ndanou, Favrie, Gavrilyuk, 2013 for details). These 'rarefaction' shocks are clearly visible in the numerical tests given in the present paper.

B.2 Rankine-Hugoniot relations for sub-system 2

Let D be the velocity of discontinuity. The Rankine-Hugoniot relations are:

$$D[\rho] = 0, \quad D[\rho u] = 0, \quad D[\rho w] = 0, \quad D[b^\beta] = 0, \quad D[c^\beta] = 0,$$

$$[-S_{12}] = D[\rho v], \quad [vb^\beta] = D[a^\beta],$$

$$[-S_{12}v] = D[\rho e^h + \rho e^e + \frac{1}{2}\left(\rho u^2 + \rho v^2 + \rho w^2\right)].$$

Or

$$D[\rho] = 0, \quad D[u] = 0, \quad D[w] = 0, \quad D[b^\beta] = 0, \quad D[c^\beta] = 0,$$

$$[-S_{12}] = D[\rho v], \quad [vb^\beta] = D[a^\beta]$$

$$[-S_{12}v] = D[\rho e^h + \rho e^e + \frac{1}{2}\left(\rho v^2\right)].$$

If $D = 0$, we have: $[S_{12}] = 0$ and $[v] = 0$. If $D \neq 0$ we have the following relations:

$$b^2[a^1] = b^1[a^2], \quad b^2[a^3] = b^3[a^2], \quad b^1[a^3] = b^3[a^1]. \tag{4}$$

We found once again the three Riemann invariants found previously in the studying the simple waves. If we have an initial state, we can parametrize

the state behind the shock by, for example, the variable a^2. Indeed suppose that $[v] \neq 0$, we have:

$$[-S_{12}] = D[\rho v] \Rightarrow [-S_{12}] = D\rho[v] \Rightarrow D = \frac{[-S_{12}]}{\rho[v]}$$

As $[vb^\beta] = D[a^\beta]$, we can choose $[vb^2] = D[a^2]$. As $[b^\beta] = 0$ we can deduce that if $[v] \neq 0$ then $[a^\beta] \neq 0$. With $b^2[v] = D[a^2]$, we have:

$$\rho[a^2]D^2 = b^2[-S_{12}].$$

We can deduce:

$$D_{L,R} = \pm\sqrt{\frac{b^2[-S_{12}]}{\rho[a^2]}},$$

and

$$b^2[v] = D_{L,R}[a^2].$$

Note that the first two independent relations (4) give us a^1 and a^3 as functions of a^2. Since the ratio $-S_{12}/\rho$ does not depend of ρ, it will be only a function of a^2.

B.3 Convexity of a one-parameter family of shear energies

Consider the energy in the form :

$$e^e = \frac{\mu}{4\rho_0}\left(aj_2 + bj_1^2 + c\right) \tag{5}$$

where a and b are constants and the invariants j_1 and j_2 are given explicitly in the form :

$$j_1(\mathbf{a},\mathbf{b},\mathbf{c}) = \frac{\|\mathbf{a}\|^2 + \|\mathbf{b}\|^2 + \|\mathbf{c}\|^2}{\Delta^{2/3}},$$

$$j_2(\mathbf{a},\mathbf{b},\mathbf{c}) = \frac{\|\mathbf{a}\|^4 + \|\mathbf{b}\|^4 + \|\mathbf{c}\|^4 + 2(\mathbf{b}\cdot\mathbf{c})^2 + 2(\mathbf{a}\cdot\mathbf{b})^2 + 2(\mathbf{a}\cdot\mathbf{c})^2}{\Delta^{4/3}}.$$

It is proved in Ndanou, Favrie and Gavrilyuk (2014) that the Hessian matrix of Δj_2 with respect to $\mathbf{a}$ is positive definite. We will establish now the same fact for $E = \Delta j_1^2$. We have

$$E = \frac{\left(\|\mathbf{a}\|^2 + \|\mathbf{b}\|^2 + \|\mathbf{c}\|^2\right)^2}{\Delta^{1/3}}.$$

Then

$$\frac{\partial E}{\partial \mathbf{a}} = \frac{4\mathbf{a}\left(\|\mathbf{a}\|^2+\|\mathbf{b}\|^2+\|\mathbf{c}\|^2\right)}{\Delta^{1/3}} - \frac{1}{3}\frac{\left(\|\mathbf{a}\|^2+\|\mathbf{b}\|^2+\|\mathbf{c}\|^2\right)^2}{\Delta^{4/3}}(\mathbf{b}\wedge\mathbf{c}),$$

$$\begin{aligned}\frac{\partial^2 E}{\partial \mathbf{a}^2} &= \frac{4\left(\|\mathbf{a}\|^2+\|\mathbf{b}\|^2+\|\mathbf{c}\|^2\right)}{\Delta^{1/3}}I + \frac{8(\mathbf{a}\otimes\mathbf{a})}{\Delta^{1/3}} - \frac{4\left(\|\mathbf{a}\|^2+\|\mathbf{b}\|^2+\|\mathbf{c}\|^2\right)}{3\Delta^{4/3}}\mathbf{a}\otimes(\mathbf{b}\wedge\mathbf{c}) \\ &\quad - \frac{4\left(\|\mathbf{a}\|^2+\|\mathbf{b}\|^2+\|\mathbf{c}\|^2\right)}{3\Delta^{4/3}}(\mathbf{b}\wedge\mathbf{c})\otimes\mathbf{a} \\ &\quad + \frac{4}{9}\frac{\left(\|\mathbf{a}\|^2+\|\mathbf{b}\|^2+\|\mathbf{c}\|^2\right)^2}{\Delta^{7/3}}(\mathbf{b}\wedge\mathbf{c})\otimes(\mathbf{b}\wedge\mathbf{c}) \\ &= \frac{4\left(\|\mathbf{a}\|^2+\|\mathbf{b}\|^2+\|\mathbf{c}\|^2\right)}{\Delta^{1/3}}I + \frac{4(\mathbf{a}\otimes\mathbf{a})}{\Delta^{1/3}} \\ &\quad + \frac{4}{\Delta^{1/3}}\left(\mathbf{a} - \frac{\left(\|\mathbf{a}\|^2+\|\mathbf{b}\|^2+\|\mathbf{c}\|^2\right)}{3\Delta}(\mathbf{b}\wedge\mathbf{c})\right)\otimes\left(\mathbf{a} - \frac{\left(\|\mathbf{a}\|^2+\|\mathbf{b}\|^2+\|\mathbf{c}\|^2\right)}{3\Delta}(\mathbf{b}\wedge\mathbf{c})\right).\end{aligned}$$

Hence, E'' is the sum of three positive definite matrices. Now, we have to choose the coefficients a, b, c in (5) such that in the limit of small deformations we have the Hooke law. For that we have to calculate $\mathbf{S}$:

$$\begin{aligned}\mathbf{S} &= -2\rho\frac{\partial e^e}{\partial \mathbf{G}}\mathbf{G} = -\frac{2\mu\rho}{4\rho_0}\left(2bj_1\left(\mathbf{g} - \frac{j_1}{3}\mathbf{I}\right) + 2a\left(\mathbf{g}^2 - \frac{j_2}{3}\mathbf{I}\right)\right) \\ &= -\frac{\mu\rho}{\rho_0}\left(bj_1\left(\mathbf{g} - \frac{j_1}{3}\mathbf{I}\right) + a\left(\mathbf{g}^2 - \frac{j_2}{3}\mathbf{I}\right)\right).\end{aligned}$$

Let $\mathcal{E}$ be the linear deformation tensor, then, neglecting the terms of order $O(\mathcal{E}^2)$ we have :

$$G \approx I - 2\mathcal{E}, \qquad G^2 \approx 1 - 4\mathcal{E}, \qquad |G| \approx 1 - 2tr(\mathcal{E})$$

$$G^2 \approx 1 - 4\mathcal{E}, \qquad \rho = \rho_0(1 - tr(\mathcal{E})),$$

$$g = \frac{G}{|G|^{1/3}} \approx (I - 2\mathcal{E})\left(1 + \frac{2}{3}tr(\mathcal{E})\right) \approx (I - 2\mathcal{E}) + \frac{2}{3}tr(\mathcal{E})I, \qquad j_1 \approx 3,$$

$$g^2 = \frac{G^2}{|G|^{2/3}} \approx (I - 4\mathcal{E})\left(1 + \frac{4}{3}tr(\mathcal{E})\right) \approx \left(1 + \frac{4}{3}tr(\mathcal{E})\right)I - 4\mathcal{E}, \qquad j_2 \approx 3,$$

and

$$\mathbf{S} = -\frac{\mu\rho}{\rho_0}\left(bj_1\left(\mathbf{g} - \frac{j_1}{3}\mathbf{I}\right) + a\left(\mathbf{g}^2 - \frac{j_2}{3}\mathbf{I}\right)\right) \approx 2\mu\left(3b + 2a\right)\left(\mathcal{E} - \frac{tr\left(\mathcal{E}\right)}{3}I\right).$$

Hence, to have Hooke's law, we must have

$$3b + 2a = 1.$$

Finally, a one-parameter family of shear energies satisfying Hooke's law in the limit of small deformations is :

$$e^e = \frac{\mu}{4\rho_0}\left(aj_2 + \frac{1-2a}{3}j_1^2 + 3\left(a-1\right)\right).$$

Here we choose $c = 3\left(a-1\right)$ to have vanishing elastic energy in equilibrium. The equations are then hyperbolic for

$$0 \leq a \leq 0.5$$

B.4 Preservation of curl $\mathbf{e}^\beta$ condition by a Lax-Friedrichs scheme

We will show that the Lax-Friedrichs scheme preserves the discrete representation of curl $\mathbf{e}^\beta$. In $2D$ case, only the third component of curl $\mathbf{e}^\beta$ should be calculated. To discretize the spatial derivatives, we used the centered finite difference. Let us consider a regular Cartesian grid. For any variable f, we denote $f_{i,j}^n$ the value of f in the cell (i,j) at the time instant $n\Delta t$. The components $\left(a^\beta, b^\beta\right)^T$ of the vector $\mathbf{e}^\beta$ gives us only one non-zero component of curl $\mathbf{e}^\beta = \left(0, 0, \frac{\partial \mathrm{b}^\beta}{\partial \mathrm{x}} - \frac{\partial \mathrm{a}^\beta}{\partial \mathrm{y}}\right)^{\mathrm{T}} = (0, 0, \omega_3^\beta)^{\mathrm{T}}$.

Suppose that at the instant $n\Delta t$

$$\left(\omega_3^\beta\right)_{i,j}^n = \frac{\left(b^\beta\right)_{i+1,j}^n - \left(b^\beta\right)_{i-1,j}^n}{2\Delta x} - \frac{\left(a^\beta\right)_{i,j+1}^n - \left(b^\beta\right)_{i,j-1}^n}{2\Delta y} = 0, \quad \forall \quad i,j$$

We need to prove that at the instant $(n+1)\Delta t$

$$\left(\omega_3^\beta\right)_{i,j}^{n+1} = \frac{\left(b^\beta\right)_{i+1,j}^{n+1} - \left(b^\beta\right)_{i-1,j}^{n+1}}{2\Delta x} - \frac{\left(a^\beta\right)_{i,j+1}^{n+1} - \left(b^\beta\right)_{i,j-1}^{n+1}}{2\Delta y} = 0, \quad \forall \quad i,j$$

Consider the Lax-Friedrichs scheme

$$(\mathbf{U})_{i,j}^{n+1} = \frac{1}{4}\left((\mathbf{U})_{i+1,j}^{n} + (\mathbf{U})_{i-1,j}^{n} + (\mathbf{U})_{i,j+1}^{n} + (\mathbf{U})_{i,j-1}^{n}\right)$$

$$-\frac{\Delta t}{\Delta x}\left(\mathbf{F}_{i+\frac{1}{2},j} - \mathbf{F}_{i-\frac{1}{2},j}\right) - \frac{\Delta t}{\Delta y}\left(\mathbf{G}_{i,j+\frac{1}{2}} - \mathbf{G}_{i,j+\frac{1}{2}}\right)$$

discretizing the system of conservation laws :

$$\mathbf{U}_t + \mathbf{F}\left(\mathbf{U}\right)_x + \mathbf{G}\left(\mathbf{U}\right)_y = 0$$

In particular, for variables a^β and b^β we take :

$$\begin{cases} \left(a^\beta\right)_{i,j}^{n+1} = \frac{1}{4}\left(\left(a^\beta\right)_{i+1,j}^{n} + \left(a^\beta\right)_{i-1,j}^{n} + \left(a^\beta\right)_{i,j+1}^{n} + \left(a^\beta\right)_{i,j-1}^{n}\right) \\ -\frac{\Delta t}{\Delta x}\left(u_{i+1,j}^{n}\left(a^\beta\right)_{i+1,j}^{n} + v_{i+1,j}^{n}\left(b^\beta\right)_{i+1,j}^{n} - u_{i-1,j}^{n}\left(a^\beta\right)_{i-1,j}^{n} - v_{i-1,j}^{n}\left(b^\beta\right)_{i-1,j}^{n}\right) \\ \left(b^\beta\right)_{i,j}^{n+1} = \frac{1}{4}\left(\left(b^\beta\right)_{i+1,j}^{n} + \left(b^\beta\right)_{i-1,j}^{n} + \left(b^\beta\right)_{i,j+1}^{n} + \left(b^\beta\right)_{i,j-1}^{n}\right) \\ -\frac{\Delta t}{\Delta y}\left(u_{i,j+1}^{n}\left(a^\beta\right)_{i,j+1}^{n} + v_{i,j+1}^{n}\left(b^\beta\right)_{i,j+1}^{n} - u_{i,j-1}^{n}\left(a^\beta\right)_{i,j-1}^{n} - v_{i,j-1}^{n}\left(a^\beta\right)_{i,j-1}^{n}\right). \end{cases} \tag{6}$$

A simple calculation shows that:

$$\frac{\left(b^\beta\right)_{i+1,j}^{n+1} - \left(b^\beta\right)_{i-1,j}^{n+1}}{2\Delta x} - \frac{\left(a^\beta\right)_{i,j+1}^{n+1} - \left(a^\beta\right)_{i,j-1}^{n+1}}{2\Delta y}$$

$$= \frac{1}{4}\left(\frac{\left(b^\beta\right)_{i+2,j}^{n} - \left(b^\beta\right)_{i,j}^{n}}{2\Delta x} - \frac{\left(a^\beta\right)_{i+1,j+1}^{n} - \left(a^\beta\right)_{i+1,j-1}^{n}}{2\Delta y}\right)$$

$$+\frac{1}{4}\left(\frac{\left(b^\beta\right)_{i+1,j+1}^{n} - \left(b^\beta\right)_{i-1,j+1}^{n}}{2\Delta x} - \frac{\left(a^\beta\right)_{i,j+2}^{n} - \left(a^\beta\right)_{i,j}^{n}}{2\Delta y}\right)$$

$$+\frac{1}{4}\left(\frac{\left(b^\beta\right)_{i,j}^{n} - \left(b^\beta\right)_{i-2,j}^{n}}{2\Delta x} - \frac{\left(a^\beta\right)_{i-1,j+1}^{n} - \left(a^\beta\right)_{i-1,j-1}^{n}}{2\Delta y}\right)$$

$$+\frac{1}{4}\left(\frac{\left(b^\beta\right)_{i+1,j-1}^{n} - \left(b^\beta\right)_{i-1,j-1}^{n}}{2\Delta x} - \frac{\left(a^\beta\right)_{i,j}^{n} - \left(a^\beta\right)_{i,j-2}^{n}}{2\Delta y}\right)$$

$$= \frac{1}{4}\left(\left(\omega_3^{\beta}\right)^{n}_{i,j+1} + \left(\omega_3^{\beta}\right)^{n}_{i,j-1} + \left(\omega_3^{\beta}\right)^{n}_{i+1,j} + \left(\omega_3^{\beta}\right)^{n}_{i-1,j}\right) = 0$$

Hence, the Lax-Friedrichs scheme conserves the discrete version of $\omega_3^{\beta} = 0$.

Chapitre 5

Extension du modèle de l'interaction solide-fluide

Ce chapitre correspond à l'article Ndanou, S., Favrie, N. & Gavrilyuk, S.L. (2014) Multi-solid and multi-fluid diffuse interface model : applications to dynamic fracture and fragmentation soumis à Journal of Computational Physics

5.1 Introduction

Fracture and fragmentation in ductile materials undergoing impact loading is still one of the major theoretical issues in solid mechanics. Since the pioneering works by Taylor [32] and Wilkins [36], few methods were proposed for modelling fracture dynamics in solids undergoing high-velocity impacts. One can mention here an 'Optimal Transportation Mesh Free' method (Li *et al.* [23], [24]) based on the discretization of Hamilton's action for elastic solids where a special failure algorithm is added to describe the fragmentation. Another approach was used, for example, in Barton *et al.* [3] where the fragmentation is governed by regularization in solving the level-set advection equations. We will use a different approach based on the diffuse interface modelling in Eulerian formulation. Such an approach was first proposed by Karni [20], Abgrall [1] and Saurel & Abgrall [29] for modelling interfaces between ideal compressible fluids having different thermodynamic characteristics. With such an approach, the same equations are solved everywhere with the same numerical scheme. This is achieved by adding a

negligible quantity of other phase into pure phases. This kind of model can describe the generation of new interfaces. The main drawback of the Eulerian diffuse interface approach compared to a Lagrangian formulation is that the interfaces are not sharp. Indeed, the 'mixture sells' are always present at the vicinity of moving interfaces. The thickness of 'the mixture region' being increased in time, the method can only be used for short time interval. Hence, a natural application of such methods is high-velocity process (impacts, explosive phase transitions, etc.). This approach has been extended in Saurel *et al.* [30] to fluids exhibiting phase transitions and heat exchanges. Favrie *et al.* [8], and Favrie & Gavrilyuk [10] extended the diffuse interface method to the case of fluid – solid interfaces. The pure solid component was described by a *hyperelastic* model (Miller & Colella [26], Godunov & Romenskii [15], Gavrilyuk *et al.* [14], Godunov & Peshkov [16], Kluth & Després (2008) [21], Barton *et al.* [3] and others). The hyperelastic models have some advantages with respect to conventional *hypoelastic* models [36]. The latter have some drawbacks highlighted, in particular, in [14] and [25] :

- the hypoelastic models are not conservative
- the solution depends on the choice of the objective derivative
- the models are not thermodynamically consistent

In this paper, we extend the diffuse solid-fluid interface model developed in [8], [10] to the case of arbitrary number of interacting hyperelastic solids. Modelling visco-plastic transformations is done by using a Maxwell type model ([15], [16], [9], [3]). In [8] and [10], a special form of the specific energy was used for solids. The energy was the sum of a hydrodynamic part depending only on the density and the entropy, and an elastic part which was unaffected by the volume change. With such an equation of state, the model is hyperbolic under natural convexity conditions. When plastic deformations occurred, the model of [8] and [10] was in agreement with the following requirements :

- Isochoricity of a plastic response (the density did not evolve during the relaxation process)
- Entropy increasing (irreversibility of plastic deformations)
- Shear stresses decreasing (Maxwell type behavior)

- The plasticity yield limit was reached at the end of the relaxation process

Also, the model was able to create cracks and formation of fragments. The cracks formation is due to 'cavitation process' in solids. Indeed, in strong impact-generated tensile waves the model of diffuse interfaces allows gas bubbles growing in the solid under certain conditions. The bubbles will then coalesce to form fractures resulting eventually in solid fragmentation.

The paper is organized as follows. In sections 5.2, 5.3 and 5.4, an extension of a hyperelastic visco-plastic model to an arbitrary number of phases is presented. A numerical algorithm for solving the governing equations is proposed in section 5.5. In section 5.6 we show the capacity of the model to solve problems involving solids under strong solicitations. Technical details (hyperbolicity study, establishment of the Whitham subcharacteristic relations, etc.) are given in Appendices.

5.2 Hyperelastic diffuse interface model for interaction of N solids

We extend first the model of diffuse solid-fluid interfaces to the case of N hyperelastic solids. The model describes, in particular, the evolution of the elastic deformation tensor (Finger tensor) for each solid. The stresses are given by a hyperelastic relation.

5.2.1 Geometric and thermodynamic constraints

Let us denote by ρ_l the density of each solid phase l, and by α_l its volume fraction, $l = 1, ..., N$. The saturation constraint is:

$$\sum_{l=1}^{N} \alpha_l = 1.$$

The mass conservation equations for each component having the average velocity $\mathbf{v}$ is :

$$\frac{\partial \alpha_l \rho_l}{\partial t} + div\left(\alpha_l \rho_l \mathbf{v}\right) = 0.$$

Summing the mass equations for each component, we obtain the equation for the mixture density ρ :

$$\frac{\partial \rho}{\partial t} + div\,(\rho \mathbf{v}) = 0,$$

where

$$\rho = \sum_{l=1}^{N} \alpha_l \rho_l.$$

Defining the mass fraction Y_l of each phase l by:

$$Y_l = \frac{\alpha_l \rho_l}{\rho},$$

we have :

$$\frac{DY_l}{Dt} = 0, \quad \frac{D}{Dt} = \frac{\partial}{\partial t} + \mathbf{v} \cdot \boldsymbol{\nabla}.$$

This equation is a consequence of mass equation of phase l and the equation for the mixture density. Let e_l be the internal energy of phase l. The specific energy of the mixture e is defined as:

$$e = \sum_{l=1}^{N} Y_l e_l.$$

The internal energy e_l is taken in separable form (Flory [13], Hartmann & Neff [17] , Gavrilyuk *et al.* [14]) :

$$e_l = e_l^h\,(\rho_l, \eta_l) + e_l^e\,(\mathbf{g}_l)\,,$$

where η_l is the specific entropy of phase l and

$$\mathbf{g}_l = \frac{\mathbf{G}_l}{|\mathbf{G}_l|^{\frac{1}{3}}}, \qquad |\mathbf{G}_l| = \det\,(\mathbf{G}_l)\,.$$

The Finger tensor $\mathbf{G}_l$ is defined by:

$$\mathbf{G}_l = \mathbf{F}_l^{-T}\mathbf{F}_l^{-1} = \sum_{\beta=1}^{3} \mathbf{e}_l^\beta \otimes \mathbf{e}_l^\beta, \quad \mathbf{F}_l^{-T} = \left(\mathbf{e}_l^1, \mathbf{e}_l^2, \mathbf{e}_l^3\right),$$

$\mathbf{F}_l$ being the deformation gradients, and $\mathbf{e}_l^\beta = \nabla_{\mathbf{x}} X_l^\beta = \left(a_l^\beta, b_l^\beta, c_l^\beta\right)^T$. We will also denote $\mathbf{a}_l = (a_l^\beta)$, $\mathbf{b}_l = (b_l^\beta)$, $\mathbf{c}_l = (c_l^\beta)$, $\beta = 1, 2, 3$. Here $\mathbf{X}_l = (X_l^\beta)$

are the Lagrangian coordinates of particles associated with the solid l. As a consequence, we have the following equations for the the local cobasis $\mathbf{e}_l^\beta$:

$$\frac{\partial \mathbf{e}_l^\beta}{\partial t} + \boldsymbol{\nabla}\left(\mathbf{v}\cdot\mathbf{e}_l^\beta\right) = 0, \quad \mathbf{rot}\left(\mathbf{e}_l^\beta\right) = 0, \quad \beta = 1,2,3. \tag{1}$$

The choice of N local cobasis $\mathbf{e}_l^\beta$ is not natural in the case of a single velocity field. We need just one local cobasis. Indeed, the Lagrangian coordinates are the same, so $\mathbf{e}_l^\beta$ are the same for any l, if they coincide initially. However, further, we will take into account the plasticity effects. Since the relaxation process is specific to each solid and acts on the local cobasis, we need necessarily evolution equations for the local cobasis of each solid. The choice of N local cobasis is also necessary to take into account sliding at the interfaces between solids.

Equations (1) imply:

$$\frac{D\mathbf{G}_l}{Dt} + \left(\frac{\partial \mathbf{v}}{\partial \mathbf{x}}\right)^T \mathbf{G}_l + \mathbf{G}_l \frac{\partial \mathbf{v}}{\partial \mathbf{x}} = 0. \tag{2}$$

The hydrodynamic part of energy e_l^h can be taken, for example, in the following form:

$$e_l^h\left(\rho_l, \eta_l\right) = \frac{p_l + \gamma_l p_{\infty,l}}{\left(\gamma_l - 1\right)\rho_l}, \quad \gamma_l > 1, \quad p_{\infty,l} > 0, \tag{3}$$

with

$$\frac{p_l + p_{\infty,l}}{\rho_l^{\gamma_l}} = A_l\left(\eta_l\right) > 0, \quad \frac{dA_l}{d\eta_l} > 0,$$

The elastic part of the energy e_l^e for isotropic solids is a function of invariants of $\mathbf{g}_l$:

$$e_l^e\left(\mathbf{g}_l\right) = e_l^e\left(j_{1,l}, j_{2,l}\right), \quad j_{1,l} = tr\left(\mathbf{g}_l\right), \quad j_{2,l} = tr\left(\mathbf{g}_l^2\right), \quad i = 1,2.$$

For applications, we take:

$$e_l^e\left(\mathbf{g}_l\right) = \frac{\mu_l}{8\rho_{0,l}}\left(j_{2,l} - 3\right), \tag{4}$$

where μ_l is the shear modulus, and $\rho_{0,l}$ is a constant reference density. More general equations of state can be found in [11]. Let us also remark that the conservation of mass for the solid l can be written in the form:

$$\alpha_l \rho_l = \alpha_{0,l}\left(\mathbf{X}_l\right)\rho_{0,l}\left(\mathbf{X}_l\right)\left|\mathbf{G}_l\right|^{\frac{1}{2}}, \tag{5}$$

where $\rho_{0,l}$ is an initial density (for simplicity, we will take the same reference value as in (4)), and $\alpha_{0,l}$ is an initial volume fraction of the solid l. The equation of mass for the solid l

$$\frac{\partial \alpha_l \rho_l}{\partial t} + div\left(\alpha_l \rho_l \mathbf{v}\right) = 0$$

is a consequence of (5) and the equations (1) for the local cobasis $\mathbf{e}_l^\beta$. Another important remark is that if the shear modulus μ_l vanishes, we recover Euler equations of compressible fluids. So, no need to separate N components into solids and fluids. The fluid component is obtained by just putting to zero the shear modulus.

The elastic energy of each solid in the form (4) satisfies the following properties [27] :

- in the limit of small deformations, Hooke's law is recovered
- the corresponding equation of hyperelastic solids are hyperbolic

We will return later to the notion of hyperbolicity. The Gibbs identity for a solid with the equation of state in separable form is:

$$\theta_l d\eta_l = de_l^h + p_l d\left(\frac{1}{\rho_l}\right), \quad de_l^e = tr\left(\frac{\partial e_l}{\partial \mathbf{G}_l} d\mathbf{G}_l\right), \tag{6}$$

where θ_l are local temperatures. We will also suppose that: $c_l^2 = \frac{\partial p_l}{\partial \rho_l} > 0$ and $\frac{\partial p_l}{\partial \eta_l} > 0$. These inequalities are, in particular, satisfied for the equation of state (3).

5.2.2 Variational principle for a mixture of hyperelastic solids

We use Hamilton's principle of stationary action for a mixture of hyperelastic solids to derive the momentum equation (see [7] for detail). The Lagrangian of the mixture is:

$$L = \int_{\Omega_t} \rho \left(\frac{\mathbf{v}\cdot\mathbf{v}}{2} - e\right) d\Omega,$$

where Ω_t is a material volume. The variation of the Hamilton action can be found under the constraints:

$$\frac{\partial \rho}{\partial t} + div\left(\rho \mathbf{v}\right) = 0,$$
$$\frac{DY_l}{Dt} = 0, \quad l = 1, ..., N,$$
$$\frac{D\eta_l}{Dt} = 0, \quad l = 1, ..., N,$$
$$\frac{\partial \mathbf{e}_l^\beta}{\partial t} + \boldsymbol{\nabla}\left(\mathbf{v}\cdot\mathbf{e}_l^\beta\right) = 0, \quad \mathbf{rot}\left(\mathbf{e}_l^\beta\right) = 0, \quad \beta = 1,2,3, \quad l = 1, ..., N.$$

This implies the momentum equation :

$$\frac{\partial \rho \mathbf{v}}{\partial t} + div\left(\rho \mathbf{v}\otimes\mathbf{v} - \boldsymbol{\sigma}\right) = 0, \tag{7}$$

with $\boldsymbol{\sigma}$ define by:

$$\boldsymbol{\sigma} = \sum_{l=1}^{N} \alpha_l \boldsymbol{\sigma}_l,$$

where the stress tensor $\boldsymbol{\sigma}_l$ of each component is defined by a hyperelastic relation :

$$\boldsymbol{\sigma}_l = -2\rho_l \frac{\partial e_l}{\partial \mathbf{G}_l}\mathbf{G}_l = -p_l\mathbf{I} + \mathbf{S}_l, \tag{8}$$

with $\mathbf{I}$ being the 3×3 identity tensor and:

$$p_l = \rho_l^2 \frac{\partial e_l^h}{\partial \rho_l}, \quad \mathbf{S}_l = -2\rho_l \frac{\partial e_l^e}{\partial \mathbf{G}_l}\mathbf{G}_l = -2\rho_l\left(2\frac{\partial e_l^e}{\partial j_{2,l}}\left(\mathbf{g}_l^2 - \frac{j_{2,l}}{3}\mathbf{I}\right) + \frac{\partial e_l^e}{\partial j_{1,l}}\left(\mathbf{g}_l - \frac{j_{1,l}}{3}\mathbf{I}\right)\right).$$

Also, the pressure equilibrium condition can be derived :

$$p = p_1 = ... = p_N, \tag{9}$$

where p is the mixture pressure :

$$p = \sum_{l=1}^{N} \alpha_l p_l.$$

It implies

$$\boldsymbol{\sigma} = -p\mathbf{I} + \mathbf{S}, \quad \mathbf{S} = \sum_{l=1}^{N} \alpha_l \mathbf{S}_l$$

The equilibrium condition (9) comes from the variation of the Hamilton action with respect to the volume fraction of each component. The proof is exactly the same as in [7].

Finally, the equations describing the interface dynamics of N hyperelastic solids are written as:

$$\begin{cases} \frac{\partial \mathbf{e}_l^\beta}{\partial t} + \boldsymbol{\nabla}\left(\mathbf{v}\cdot\mathbf{e}_l^\beta\right) = 0, \quad rot\left(\mathbf{e}_l^\beta\right) = 0, \quad \beta = 1,2,3, \quad l = 1,...,N, \\ \frac{DY_l}{Dt} = 0, \quad \frac{D}{Dt} = \frac{\partial}{\partial t} + \mathbf{v}\cdot\boldsymbol{\nabla}, \\ p = p_1 = ... = p_N, \\ \frac{\partial \rho}{\partial t} + div\left(\rho\mathbf{v}\right) = 0, \\ \frac{\partial(\rho\mathbf{v})}{\partial t} + div(\rho\mathbf{v}\otimes\mathbf{v} - \boldsymbol{\sigma}) = 0, \\ \frac{D\eta_l}{Dt} = 0. \end{cases} \tag{10}$$

The equation for the local cobasis $\mathbf{e}_l^\beta$ can also be written in nonconservative form :

$$\frac{D\mathbf{e}_l^\beta}{Dt} + \left(\frac{\partial \mathbf{v}}{\partial \mathbf{x}}\right)^T \mathbf{e}_l^\beta = 0.$$

The importance of this nonconservative form for the hyperbolicity study and numerics was discussed in [11] and [27]. Equations for the mixture density, the momentum and the entropy equation for each component l imply the total energy equation:

$$\frac{\partial \rho\left(e + \frac{1}{2}|\mathbf{v}|^2\right)}{\partial t} + div\left(\rho\left(e + \frac{1}{2}|\mathbf{v}|^2\right) - \boldsymbol{\sigma}\mathbf{v}\right) = 0. \tag{11}$$

5.3 Equilibrium visco-plastic model for the interaction of N solids

5.3.1 Governing equations

The model of diffuse interfaces for N hyperelastic solids taking into account plastic transformations is a natural extension of the model developed in [10]

:

$$\begin{cases} \frac{D\mathbf{e}_l^\beta}{Dt} + \left(\frac{\partial \mathbf{v}}{\partial \mathbf{x}}\right)^T \mathbf{e}_l^\beta = \frac{a\mathbf{S}_l \mathbf{e}_l^\beta}{\tau_{rel,l}}, \\ \frac{DY_l}{Dt} = 0, \\ p = p_1 = ... = p_N, \\ \frac{\partial \rho}{\partial t} + div\left(\rho \mathbf{v}\right) = 0, \\ \frac{\partial (\rho \mathbf{v})}{\partial t} + div(\rho \mathbf{v} \otimes \mathbf{v} - \boldsymbol{\sigma}) = 0, \\ \frac{D\eta_l}{Dt} = f_l, \end{cases} \tag{12}$$

Here $\tau_{rel,l}$ are the relaxation times defined by :

$$\frac{1}{\tau_{rel,l}} = \begin{cases} \frac{1}{\tau_{0,l}} \left(\frac{\sum_\alpha \left(S_{\alpha,l}\right)^2 - \frac{2}{3}\sigma_{Y,l}^2}{\mu_l^2} \right)^{n_l}, & \text{if, } \sum_\alpha \left(S_{\alpha,l}\right)^2 - \frac{2}{3}\sigma_{Y,l}^2 > 0, \\ 0 \quad \text{if, } \sum_\alpha \left(S_{\alpha,l}\right)^2 - \frac{2}{3}\sigma_{Y,l}^2 \leq 0, \end{cases} \tag{13}$$

with a being a constant having dimension of stress, $\tau_{0,l}$ and n_l being a characteristic relaxation time and a relaxation exponent, respectively, $\sigma_{Y,l}$ being the yield limit of each solid, and $S_{\alpha,l}$ being the principal values of the deviatoric stress of solid l. To simplify the model presentation, we take in the following $a = 1$ in corresponding physical units. The expression for the relaxation time (13) is an adapted Perzyna' model in visco-plasticity [22]. The right-hand sides f_l must be determined is such a way that:

- they are compatible with the total energy equation
- they are compatible with the entropy inequality

A natural choice of f_l will be proposed below. The equations for the local cobasis $\mathbf{e}_l^\beta$ imply the equation for the Finger tensor $\mathbf{G}_l$:

$$\frac{D\mathbf{G}_l}{Dt} + \left(\frac{\partial \mathbf{v}}{\partial \mathbf{x}}\right)^T \mathbf{G}_l + \mathbf{G}_l \frac{\partial \mathbf{v}}{\partial \mathbf{x}} = 2\frac{\mathbf{G}_l \mathbf{S}_l}{\tau_{rel,l}}. \tag{14}$$

The hyperbolicity of (12) is established in Appendix C.1.

5.3.2 Entropy inequality for the equilibrium visco-plastic model

We will choose f_l of each phase which is compatible with the total energy equation and the entropy inequality. The energy equation has the same form (11). It can be transformed as follows :

$$0 = \frac{\partial\left(\rho\left(e+\frac{1}{2}|\mathbf{v}|^2\right)\right)}{\partial t} + div\left(\rho\mathbf{v}\left(e+\frac{|\mathbf{v}|^2}{2}\right)-\boldsymbol{\sigma}\mathbf{v}\right)$$

$$= \rho\frac{De}{Dt} - tr\left(\boldsymbol{\sigma}\frac{\partial\mathbf{v}}{\partial\mathbf{x}}\right)$$

$$= \sum_{l=1}^{N}\left(\alpha_l\frac{p}{\rho_l}\frac{D\rho_l}{Dt} + \alpha_l\rho_l\theta_l\frac{D\eta_l}{Dt} + \alpha_l\rho_l tr\left(\frac{\partial e_l^e}{\partial\mathbf{G}_l}\frac{D\mathbf{G}_l}{Dt}\right) - \alpha_l tr\left(\boldsymbol{\sigma}_l\frac{\partial\mathbf{v}}{\partial\mathbf{x}}\right)\right).$$

Using the mass conservation law of each component in the form :

$$\frac{D\rho_l}{Dt} = -\frac{\rho_l}{\alpha_l}\frac{D\alpha_l}{Dt} - \rho_l div\left(\mathbf{v}\right),$$

and equation (14), we finally have :

$$\frac{\partial\left(\rho\left(e+\frac{1}{2}|\mathbf{v}|^2\right)\right)}{\partial t} + div\left(\rho\mathbf{v}\left(e+\frac{|\mathbf{v}|^2}{2}\right)-\boldsymbol{\sigma}\mathbf{v}\right) = \sum_{l=1}^{N}\left(\alpha_l\rho_l\theta_l\frac{D\eta_l}{Dt} - \frac{\alpha_l}{\tau_{rel,l}}\mathbf{S}_l:\mathbf{S}_l\right).$$

This equation should be separated into N equations for the entropy evolution of each phase l. It should also respect the entropy inequality. We can use the following separation

$$\alpha_l\rho_l\theta_l\frac{D\eta_l}{Dt} = \frac{\alpha_l}{\tau_{rel,l}}\mathbf{S}_l:\mathbf{S}_l \geq 0, \quad l=1,...,N.$$

We deduce that:

$$f_l = \frac{\mathbf{S}_l:\mathbf{S}_l}{\rho_l\theta_l\tau_{rel,l}}.$$

Finally, with such a choice of f_l the entropy inequality will be satisfied:

$$\frac{\partial\rho\eta}{\partial t} + div\left(\rho\eta\mathbf{v}\right) \geq 0,$$

where η is the mixture entropy defined by:

$$\eta = \sum_{l=1}^{N} Y_l\eta_l.$$

5.4 Non-equilibrium visco-plastic model for the interaction of N solids

The major difficulty with the preceding model comes from the pressure equilibrium conditions (9) which are complemented by the saturation constraint. The numerical resolution of these equations is quite difficult. This is why we replace the equilibrium conditions by ordinary differential equations for the volume fraction, which are relaxation equations. The equilibrium conditions are obtained in the limit case when a characteristic relaxation time goes to zero (see Kapila *et al.* [19] for the fluid case).

5.4.1 Governing equations

The non-equilibrium visco-plastic model can be written as :

$$\begin{cases} \frac{D\alpha_l}{Dt} = \lambda_l \left(p_l - p_I\right), \\ \frac{D\mathbf{e}_l^\beta}{Dt} + \left(\frac{\partial \mathbf{v}}{\partial \mathbf{x}}\right)^T \mathbf{e}_l^\beta = \frac{1}{\tau_{rel,l}} \mathbf{S}_l \mathbf{e}_l^\beta, \\ \frac{\partial \rho}{\partial t} + div(\rho \mathbf{v}) = 0, \\ \frac{\partial \rho \mathbf{v}}{\partial t} + div\left(\rho \mathbf{v} \otimes \mathbf{v} - \boldsymbol{\sigma}\right) = 0, \\ \frac{D\eta_l}{Dt} = f_l, \end{cases} \tag{15}$$

where $\lambda_l > 0$ are large relaxation parameters, and p_I is the interfacial pressure defined as :

$$p_I = \sum_{l=1}^{N} \beta_l p_l, \quad \beta_l > 0, \quad \sum_{l=1}^{N} \beta_l = 1.$$

We will see that in the case of instantaneous relaxation we do not need to know β_l explicitly. The right-hand side f_l , which should be compatible with the entropy inequality, will be chosen later. The model (15) is hyperbolic. The proof is given in Appendix C.2.

5.4.2 Entropy inequality for the non-equilibrium visco-plastic model

We will now choose the right-hand side f_l in the entropy equations of (15) which is compatible with the total energy equation and the entropy inequality. The total energy equation can be transformed as follows:

$$0 = \frac{\partial \rho \left(e + \frac{1}{2}|\mathbf{v}|^2\right)}{\partial t} + div\left(\rho \mathbf{v}\left(e + \frac{|\mathbf{v}|^2}{2}\right) - \sigma \mathbf{v}\right)$$

$$= \rho \frac{De}{Dt} - tr\left(\boldsymbol{\sigma} \frac{\partial \mathbf{v}}{\partial \mathbf{x}}\right)$$

$$= \sum_{l=1}^{N}\left(\alpha_l \rho_l \frac{De_l}{Dt} - \alpha_l tr\left(\boldsymbol{\sigma}_l \frac{\partial \mathbf{v}}{\partial \mathbf{x}}\right)\right)$$

$$= \sum_{l=1}^{N}\left(\alpha_l \rho_l \frac{De_l^h}{Dt} + \alpha_l \rho_l \frac{De_l^e}{Dt} - \alpha_l tr\left(\boldsymbol{\sigma}_l \frac{\partial \mathbf{v}}{\partial \mathbf{x}}\right)\right)$$

$$= \sum_{l=1}^{N}\left(-p_l \frac{D\alpha_l}{Dt} + \alpha_l \rho_l \theta_l \frac{D\eta_l}{Dt} - \frac{\alpha_l}{\tau_{rel,l}} \mathbf{S}_l : \mathbf{S}_l\right).$$

This equation should be separated into N equations for the entropy evolution of each component. However, it should respect the entropy inequality. We can use the following separation (Dell'Isola & Gavrilyuk [7], Favrie & Gavrilyuk [10]) :

$$\alpha_l \rho_l \theta_l \frac{D\eta_l}{Dt} = (p_l - p_I)\frac{D\alpha_l}{Dt} + \frac{\alpha_l}{\tau_{rel,l}} \mathbf{S}_l : \mathbf{S}_l \geq 0, \quad l = 1, ..., N.$$

We then deduce :

$$f_l = \frac{(p_l - p_I)}{\rho_l \theta_l}\frac{D\alpha_l}{Dt} + \frac{\mathbf{S}_l : \mathbf{S}_l}{\rho_l \theta_l \tau_{rel,l}}.$$

Finally, the entropy inequality will be satisfied:

$$\frac{\partial \rho \eta}{\partial t} + div\left(\rho \eta \mathbf{v}\right) \geq 0,$$

where η is the mixture entropy defined by:

$$\eta = \sum_{l=1}^{N} Y_l \eta_l.$$

Remark The sub-characteristic condition (or Whitham condition [35]) states that the characteristic velocities of a relaxed system (12) should be interplaced between the velocities of a relaxing system (15). Such a condition guarantees in a sense a right mathematical modelling of a physical phenomena. The formal proof of this fact is not direct and is always specific to mathematical models under study (see, for example, [12] where this property was established for a class of two-phase fluid models with relaxation). In Appendix C.3 we established a 'weak' sub-characteristic condition : we have proved that both the smallest and the largest sound speeds of the equilibrium system (12) are smaller then the corresponding sound speeds of the non-equilibrium system (15). This condition is important for numerical study when one chooses right-and-left facing shock speeds in the HLLC solver (see section below).

5.5 Numerical resolution of the visco-plastic model

The numerical resolution of the visco-plastic model follows [10] where the fluid-solid diffuse interface model was derived. This procedure consists of three main steps : resolution of hyperbolic part, relaxation of stresses to the yield surface and, finally, the relaxation of pressures. The entropy equations are not numerically solved, they are replaced instead by the evolution equations for the specific hydrodynamic energies of each phase:

$$\frac{\partial \alpha_l \rho_l e_l^h}{\partial t} + div\left(\alpha_l \rho_l e_l^h \mathbf{v}\right) + \alpha_l p_l div\left(\mathbf{v}\right) = -p_I \frac{D\alpha_l}{Dt}, \quad l = 1, ..., N. \qquad (16)$$

5.5.1 Hyperbolic step

A Godunov type method was used for solving the hyperbolic step. To present the method, consider 1D case. The homogeneous equations are :

$$\left\{\begin{array}{l}
\frac{\partial \alpha_l}{\partial t} + u\frac{\partial \alpha_l}{\partial x} = 0, \\
\frac{\partial\left(\alpha_l \rho_l e_l^h\right)}{\partial t} + \frac{\partial\left(\alpha_l \rho_l u e_l^h\right)}{\partial x} + \alpha_l p_l \frac{\partial u}{\partial x} = 0, \\
\frac{\partial(\alpha_l \rho_l)}{\partial t} + \frac{\partial(\alpha_l \rho_l u)}{\partial x} = 0, \\
\frac{\partial a_l^\beta}{\partial t} + \frac{\partial\left(u a_l^\beta\right)}{\partial x} + b_l^\beta \frac{\partial v}{\partial x} + c_l^\beta \frac{\partial w}{\partial x} = 0, \\
\frac{\partial b_l^\beta}{\partial t} + u\frac{\partial b_l^\beta}{\partial x} = 0, \quad \frac{\partial c_l^\beta}{\partial t} + u\frac{\partial c_l^\beta}{\partial x} = 0, \\
\frac{\partial(\rho u)}{\partial t} + \frac{\partial\left(\rho u^2 - \sigma_{11}\right)}{\partial x} = 0, \quad \frac{\partial(\rho v)}{\partial t} + \frac{\partial(\rho uv - \sigma_{12})}{\partial x} = 0, \quad \frac{\partial(\rho w)}{\partial t} + \frac{\partial(\rho uw - \sigma_{13})}{\partial x} = 0, \\
\frac{\partial\left(\rho\left(e+\frac{1}{2}|\mathbf{v}|^2\right)\right)}{\partial t} + \frac{\partial\left(\rho\left(e+\frac{1}{2}|\mathbf{v}|^2\right)u - \sigma_{11}u - \sigma_{12}v - \sigma_{13}w\right)}{\partial x} = 0, \qquad \sigma_{ij} = \sum_{l=1}^{N} \alpha_l \sigma_{ij,l}.
\end{array}\right. \tag{17}$$

The entropy equations are replaced by the equations for the hydrodynamic part of the energy e_l^h. We use the HLLC solver (Toro [33]) because it preserves positivity of the volume fraction and the density, and is able to deal with strong shocks waves. Even if the equations of hyperelasticity contain 7 waves, we will use the solver containing only 3 waves : two waves having the most rapid characteristics (they correspond to longitudinal waves), and the contact characteristics. It was shown in [14] that such a simple solver was able to capture both longitudinal and transverse waves. With such a solver, each wave is considered as a discontinuity and, consequently, jump relations are needed. The system being non-conservative, shock relations are non-conventional.

HLLC type Riemann solver

Consider a cell boundary separating a left state (L) and a right state (R). The left - and right facing wave speeds are obtained following Davis [5] estimates :

$$S_R = \max\left(u_L + c_L, u_R + c_R\right)$$

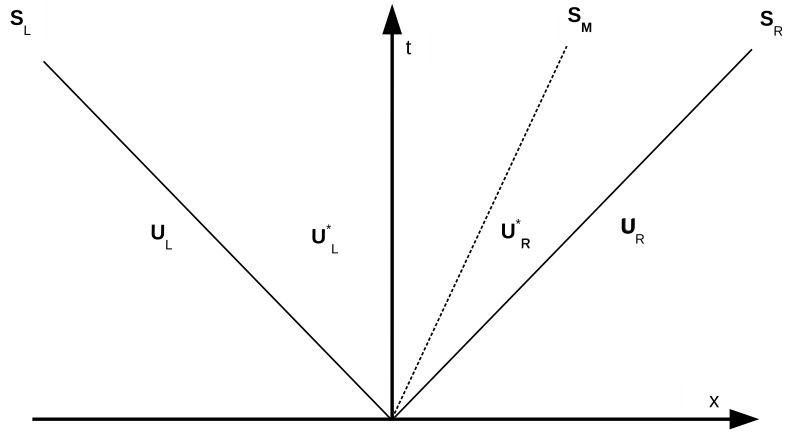

Figure 5.1: HLLC approximate solver. Solution in the 'star' region consists of two constant states separated by a wave of speed S_M.

$$S_L = \min\left(u_L - c_L, u_R - c_R\right)$$

where $c_{L,R}$ are the maximal sound speeds of the system (15) (longitudinal sound speeds). The speed of the contact discontinuity is estimated under HLLC approximation :

$$S_M = \frac{\left(\rho u^2 - \sigma_{11}\right)_L - \left(\rho u^2 - \sigma_{11}\right)_R - S_L\left(\rho u\right)_L + S_R\left(\rho u\right)_R}{\left(\rho u\right)_L - \left(\rho u\right)_R - S_L\rho_L + S_R\rho_R} = u^*,$$

where $\sigma_{11} = \sum_{l=1}^{N} \alpha_l \sigma_{11,l}$ is the mixture normal stress, $\rho = \sum_{l=1}^{N} \alpha_l \rho_l$ is and mixture density as it was previously defined. From these wave speeds **conservative state variables** in the star region (see Figure 5.1) are determined:

$$\left(\alpha_l \rho_l\right)^*_{L,R} = \left(\alpha_l \rho_l\right)_{L,R} \frac{S_{L,R} - u_{L,R}}{S_{L,R} - u^*},$$

$$\sigma^*_{11} = \frac{\left(u_R - S_R\right)\rho_R\sigma_{11L} - \left(u_L - S_L\right)\rho_L\sigma_{11R} + \left(u_L - S_L\right)\rho_L\left(u_R - S_R\right)\rho_R\left(u_R - u_L\right)}{\left(u_R - S_R\right)\rho_R - \left(u_L - S_L\right)\rho_L},$$

$$\sigma_{12}^* = \frac{(u_R - S_R)\,\rho_R\sigma_{12L} - (u_L - S_L)\,\rho_L\sigma_{12R} + (u_L - S_L)\,\rho_L\,(u_R - S_R)\,\rho_R\,(v_R - v_L)}{(u_R - S_R)\,\rho_R - (u_L - S_L)\,\rho_L},$$

$$\sigma_{13}^* = \frac{(u_R - S_R)\,\rho_R\sigma_{13L} - (u_L - S_L)\,\rho_L\sigma_{13R} + (u_L - S_L)\,\rho_L\,(u_R - S_R)\,\rho_R\,(w_R - w_L)}{(u_R - S_R)\,\rho_R - (u_L - S_L)\,\rho_L},$$

$$v_{L,R}^* = v_{L,R} + \frac{\sigma_{12}^* - (\sigma_{12})_{L,R}}{(u_{L,R} - S_{L,R})\,\rho_{L,R}},$$

$$w_{L,R}^* = w_{L,R} + \frac{\sigma_{13}^* - (\sigma_{13})_{L,R}}{(u_{L,R} - S_{L,R})\,\rho_{L,R}}.$$

The right and the left mixture total energies are obtained as :

$$E_{L,R}^* = \frac{\rho_{L,R}E_{L,R}(u_{L,R} - S_{L,R}) - \sigma_{11L,R}u_{L,R} - \sigma_{12L,R}v_{L,R} - \sigma_{13L,R}w_{L,R}}{\rho_{L,R}^*(u^* - S_{L,R})}$$

$$+\frac{+\sigma_{11}^*u^* + \sigma_{12}^*v_{L,R}^* + \sigma_{13}^*w_{L,R}^*}{\rho_{L,R}^*(u^* - S_{L,R})}$$

with

$$E = \sum_{l=1}^{N} Y_l e_l + \frac{1}{2}u^2 + \frac{1}{2}v^2.$$

Then, the **geometric variables** are determined :

$$\left(a_l^\beta\right)_{L,R}^* = \frac{\left(a_l^\beta\right)_{L,R}(u_{L,R} - S_{L,R}) + \left(b_l^\beta\right)_{L,R}\left(v_{L,R} - v_{L,R}^*\right) + \left(c_l^\beta\right)_{L,R}\left(w_{L,R} - w_{L,R}^*\right)}{u^* - S_{L,R}},$$

$$\left(b_l^\beta\right)_{L,R}^* = \left(b_l^\beta\right)_{L,R}, \qquad \left(c_l^\beta\right)_{L,R}^* = \left(c_l^\beta\right)_{L,R}.$$

The **non-conservative variables** are finally determined :

$$(\alpha_l)_{L,R}^* = (\alpha_l)_{L,R},$$

$$(\rho_l)_{L,R}^* = (\rho_l)_{L,R}\,\frac{u_{L,R} - S_{L,R}}{S_M - S_{L,R}}.$$

The phase pressures $(p_l)_{L,R}^*$ are calculated as functions of the densities $(\rho_l)_{L,R}^*$ along their respective Hugoniots by using only the hydrodynamic part of the energy. Indeed, there is no hope to use here a well established 'additivity rule' for the exact Hugoniots for solids with shear that involves automatically the conservation of the total energy. So, an additional step

is thus needed to correct the values of internal energies. These energies are determined as :

$$\left(e_l^h\right)^*_{L,R} = e_l^h((p_l)^*_{L,R}\ , (\rho_l)^*_{L,R}).$$

With the help of this approximate solver, it is possible to derive a Godunov type scheme.

Godunov type scheme

The method used to solve interface problems with the diffuse interface formulation (17) consists in a sequence of steps. The system contains conservative and non-conservative equations, as well as relaxation terms. The algorithm we use follows the one presented in [8] and [10]. It generalizes the case of fluid-fluid interfaces [31].

The conservative part of (17), in absence of relaxation terms, is updated with the conventional Godunov scheme:

$$\mathbf{U}_i^{n+1} = \mathbf{U}_i^n - \frac{\Delta t}{\Delta x}\left(\mathbf{F}_1^*(\mathbf{U}_i^n, \mathbf{U}_{i+1}^n) - \mathbf{F}_1^*(\mathbf{U}_{i-1}^n, \mathbf{U}_i^n)\right), \tag{18}$$

with the vector of conservative variables

$$\mathbf{U} = ((\alpha\rho)_1, ..., (\alpha\rho)_N, \quad \rho u, \quad \rho v, \quad \rho w, \quad \rho E)^T$$

and the flux vector

$$\mathbf{F}_1 = \left((\alpha\rho)_1 u, ..., (\alpha\rho)_N u, \quad \rho u^2 - \sigma_{11}, \rho uv - \sigma_{12}, \rho uw - \sigma_{13}, (\rho E - \sigma_{11})u - \sigma_{12}v - \sigma_{13}w\right)^T$$

The system for non-conservative variables in absence of relaxation terms reads :

$$\frac{\partial \mathbf{G}}{\partial t} + \frac{\partial \mathbf{F}_2}{\partial x} + \mathbf{H}_2\frac{\partial u}{\partial x} + \mathbf{K}_2\frac{\partial v}{\partial x} + \mathbf{M}_2\frac{\partial w}{\partial x} = 0, \tag{19}$$

with

$$\mathbf{G} = \left(\alpha_l, \quad a_l^\beta, \quad b_l^\beta, \quad c_l^\beta, \quad \alpha_l\rho_l e_l^h\right)^T,$$

$$\mathbf{F}_2 = \left(u\alpha_l, \quad ua_l^\beta, \quad ub_l^\beta, \quad uc_l^\beta, \quad \alpha_l\rho_l u e_l^h\right)^T,$$

$$\mathbf{H}_2 = \left(-\alpha_l, \quad 0, \quad -b^\beta, \quad -c^\beta, \quad \alpha_l p_l\right)^T,$$

$$\mathbf{K}_2 = \left(0, \quad b^\beta, \quad 0, \quad 0, \quad 0\right)^T,$$

$$\mathbf{M}_2 = \begin{pmatrix} 0, & c^\beta, & 0, & 0, & 0 \end{pmatrix}^T.$$

The non-conservative equations are solved by the following scheme :

$$\mathbf{G}_i^{n+1} = \mathbf{G}_i^n + \frac{\Delta t}{\Delta x}\left(\mathbf{F}^*_{2,i-1/2} - \mathbf{F}^*_{2,i+1/2} + \mathbf{H}^n_{2,i}\left(u^*_{i-1/2} - u^*_{i+1/2}\right) + \mathbf{K}^n_{2,i}\left(v^*_{i-1/2,R} - v^*_{i+1/2,L}\right)\right)$$

$$+ \frac{\Delta t}{\Delta x}\mathbf{M}^n_{2,i}\left(w^*_{i-1/2,R} - w^*_{i+1/2,L}\right),$$

where $\mathbf{F}^*_{2,i-1/2}$ and $\mathbf{F}^*_{2,i+1/2}$ are the fluxes calculated on each cell boundary with the help of the HLLC solver, $u^*_{i-1/2}$ and $u^*_{i+1/2}$ are normal velocity components at the cell boundaries, $v^*_{i-1/2,R}$, $v^*_{i+1/2,L}$, $w^*_{i-1/2,R}$ and $w^*_{i+1/2,L}$ are the corresponding tangential velocity components.

Regarding the resolution of the non-conservative internal energy equations it is worth to mention that the adopted jump relations used in the Riemann solver will induce entropy jump in each phase in the presence of shocks. However, there is no hope that this jump will be exact.

In order to correct this predicted solution, two extra steps are used. The first one corresponds to a pressure relaxation step, in order to reach the mechanical equilibrium in each computational cell. The second step corresponds to a reset of the internal energies with the help of the total energy conservation equation. These two correction steps are detailed in Section 5.5.2.

5.5.2 Plastic relaxation step

For each cell, we have the conservation equations :

$$\frac{\partial \alpha_l}{\partial t} = 0, \quad \frac{\partial \alpha_l \rho_l}{\partial t} = 0, \quad \frac{\partial \alpha_g \rho_l e_l}{\partial t} = 0,$$

$$\frac{\partial \rho u}{\partial t} = 0, \quad \frac{\partial \rho v}{\partial t} = 0, \quad \frac{\partial \rho w}{\partial t} = 0, \quad \frac{\partial \rho \left(e + \frac{1}{2}\left(u^2 + v^2 + w^2\right)\right)}{\partial t} = 0.$$

The only variables that are changing during this step are the cobasis vectors :

$$\frac{\partial}{\partial t}\mathbf{e}_l^\beta = \frac{\mathbf{S}_l \mathbf{e}_l^\beta}{\tau_{rel}}. \tag{21}$$

This is a system of ordinary differential equations which could be solved by using any integrator. Since this is a system of $9l$ equations, such an

approach will be 'expensive'. A simplified approach was proposed in [15] and was adapted to the case of von Mises yield criterium in [9], [10] . It can be formulated in the following form :

- Apply the singular value decomposition to the matrix $\mathbf{F}_l^{-T} = \mathbf{V}_l \mathbf{K}_l \mathbf{U}_l^T$, where $\mathbf{V}_l$ and $\mathbf{U}_l$ are orthogonal matrices, and $\mathbf{K}_l = diag\,(k_{\beta,l})$, $\beta = 1, 2, 3$, are diagonal matrices. The matrices $\mathbf{V}_l$ and $\mathbf{U}_l$ will stay constant during the plastic relaxation step. Such a transformation diagonalizes also the deviatoric part of the stress tensor.

- Determine the final solution

$$\frac{\partial k_{\beta,l}}{\partial t} = \frac{S_{\beta,l} k_{\beta,l}}{\tau_{rel,l}}, \tag{22}$$

  where $S_{\beta,l}$ are principal values of the deviatoric part of the stress tensor. If the initial conditions are outside of the von Mises yield surface, the solution of the Cauchy problem will be attracted to the yield surface after finite or infinite time (see [9], [10] for details). The proof for the equation of state (4) is in the Appendix C.4.

- Compute a new cobasis matrix $\mathbf{F}_l^{-T}$ using the final diagonal matrix $\mathbf{K}_l$ and the orthogonal matrices computed initially.

5.5.3 Pressure relaxation step

At the end of the plastic step, the N materials have different pressures. In order that mechanical equilibrium be restored in mixture cells, a new relaxation step has to be done for each cell. Following [31], we will propose a simplified approach in the limit of stiff relaxation ($\lambda_l \to +\infty$). The phase energy equation can be rewritten in the following form:

$$\frac{\partial e_l^h}{\partial t} + p_I \frac{\partial \tau_l}{\partial t} = 0, \quad \tau_l = \frac{1}{\rho_l}, \quad l = 1, ..., N.$$

Integrating this equation over the time interval, we can rewrite it in algebraic form:

$$e_{l,e}^h - e_{l,0}^h - \hat{p}_{I,l}\,(\tau_{l,e} - \tau_{l,0}) = 0, \quad l = 1, ..., N, \tag{23}$$

where indices 'e' and '0' mean final equilibrium state, and initial (non-equilibrium one) obtained after the hyperbolic-plastic step. Here $\hat{p}_{I,l}$ is a

new average interface pressure for the phase l. Equation 23 should imply the conservation of the mixture energy. The condition

$$\hat{p}_{I,1} = ... = \hat{p}_{I,N} = \hat{p}_I$$

allows us to conserve the energy. In general, $\hat{p}_I$ is different from p_I. However, if the relaxation parameters λ_l are large, numerical results are insensitive to a particular choice of $\hat{p}_I$. It is convenient to use $\hat{p}_I = p_e$. Thus, using the algebraic energy equation 23 for the stiffened gas EOS, the phase specific volumes become functions only of pressure:

$$\frac{\tau_{l,e}}{\tau_{l,0}} = \frac{p_{l,0} + \gamma_l p_{\infty,l} + p_e\left(\gamma_l - 1\right)}{p_e + \gamma_l p_{\infty,l} + p_e\left(\gamma_l - 1\right)} = \frac{p_{l,0} + \gamma_l p_{\infty,l} + p_e\left(\gamma_l - 1\right)}{\gamma_l\left(p_{\infty,l} + p_e\right)}, \quad l = 1, ..., N.$$

The closure of the model is achieved using the saturation constraint:

$$\sum_{l=1}^{N} \alpha_l = 1,$$

and the relation

$$\alpha_{l,e} = \alpha_{l,0} \frac{\tau_{l,e.}}{\tau_{l,0}}. \tag{24}$$

It is

$$\sum_{l=1}^{N} \frac{\alpha_l}{\gamma_l} \left(\frac{p_{l,0} - p_e}{p_e + p_{\infty,l}} \right) = 0. \tag{25}$$

There is a unique solution of this equation which is always between $min\left(p_{l,0}\right)$ and $max\left(p_{l,0}\right)$. Thus, in the limit $\lambda_l \to \infty, \quad l = 1, ..., N$, one can use the algebraic equation (25) with unknown p_e. Once the relaxed pressure is determined, the phase volume fractions are deduced.

5.5.4 Reinitialization step

Once the volume fractions of each phase are determined, we need to reset the equilibrium pressure to find a new value which is compatible with the energy equation of the mixture. From the total internal mixture energy e, we can find the hydrodynamic part of the mixture internal energy:

$$e^h = \sum_{l=1}^{N} Y_l e_l^h \left(p_l, \rho_l\right) = e - \sum_{l=1}^{N} Y_l e_l^e \left(\mathbf{g}_l\right).$$

Using the pressure equilibrium condition $p = p_1 = ... = p_N$ in the case of the stiffened gas EOS, the mixture EOS now relates the mixture hydrodynamic internal energy, the mixture density and the volume fractions:

$$p\left(\rho, e^h, \alpha_1, ..., \alpha_N\right) = \frac{\rho e^h - \sum_1^N \frac{\alpha_l \gamma_l p_{\infty,l}}{\gamma_l - 1}}{\sum_{l=1}^N \frac{\alpha_l}{\gamma_l - 1}}. \tag{26}$$

Relation (26) is valid in pure phases and in the diffuse interface zone. Once the mixture pressure is determined the internal energies of the phases are reinitialized with the help of their respective EOS:

$$e_l^h = e_l^h \left(p, \frac{(\alpha\rho)_l}{\alpha_l}\right), \quad l = 1, ..., N, \quad e_l^e = e_l^e \left(\mathbf{g}_l\right).$$

5.5.5 Summary of the numerical method

The numerical method can be summarized as follows:

- At each cell boundary solve the Riemann problem for system (17) without relaxation terms with HLLC solver.
- Relax the deviatoric part of the stress tensor to the yield surface.
- Determine the relaxed pressure and the volume fractions by solving equation (25). The Newton method is appropriate for this task.
- Compute the mixture pressure using the equation (26)
- Reset the internal energies with the computed pressure with the help of their respective EOS.
- Start again for the next time step.

5.6 Applications

Propagation and interaction of large amplitude waves in solids (longitudinal, transverse or plastic ones) can cause a lot of damage as, for example, plastic deformations, fracturing and eventually fragmentation. We will show in this section that the diffuse interface model is able to simulate such an irreversible damage.

In the method of diffuse interfaces, an infinitesimal volume fraction of all materials is always present in pure phases. It corresponds to introducing defects in pure materials. For example, in the case of solid-gas interaction, a small gas fraction is always present in the solid. Vice versa, a small amount of solid is present in the gas. The volume fraction of each material dynamically evolves when the waves propagate. For example, infinitesimal gas bubbles may dynamically increase their radius in strong impact-generated tensile waves. The large bubbles may then coalesce and form macroscopic cracks, then fractures and, finally, large fragments.

Let us give a simple analytical explication of the fracturing mechanism in our model. Consider the equilibrium visco-plastic model (12) in a simplified case where only one gas component and one solid component are present. We will use indices g and s for the corresponding unknowns. The entropy equation for each phase reads :

$$\rho_s \theta_s \frac{D\eta_s}{Dt} = \frac{\mathbf{S}_s : \mathbf{S}_s}{\tau_{rel,s}},$$
$$\frac{D\eta_g}{Dt} = 0.$$

Differentiating the pressure equilibrium condition $p_g(\rho_g, \eta_g) = p_s(\rho_g, \eta_g)$ along trajectories, we obtain :

$$\left(\frac{\partial p_g}{\partial \rho_g}\right)_{\eta_g} \frac{D\rho_g}{Dt} + \left(\frac{\partial p_g}{\partial \eta_g}\right)_{\rho_g} \frac{D\eta_g}{Dt} = \left(\frac{\partial p_s}{\partial \rho_s}\right)_{\eta_s} \frac{D\rho_s}{Dt} + \left(\frac{\partial p_s}{\partial \eta_s}\right)_{\rho_s} \frac{D\eta_s}{Dt}.$$

The definitions of sound speeds and the Grüneisen coefficients for each phase enables us to write :

$$\left(\frac{\partial p_k}{\partial \rho_k}\right)_{\eta_k} = c_k^2, \qquad \left(\frac{\partial p_k}{\partial \eta_k}\right)_{\rho_k} = \rho_k \Gamma_k \theta_k.$$

It implies :

$$c_g^2 \frac{D\rho_g}{Dt} + \rho_g \Gamma_g \theta_g \frac{D\eta_g}{Dt} = c_s^2 \frac{D\rho_s}{Dt} + \Gamma_s \rho_s \theta_s \frac{D\eta_s}{Dt}.$$

Material	Gas	Iron	Aluminum	Titanium
γ	1.4	3.9	3.5	2.6
p_∞ (GPa)	0	43.6	32	44
μ (GPa)	0	82	26	42
σ_Y (MPa)	0	200	60	1030
ρ_0 (kg/m^3)	1	7860	2712	4527

Figure 5.2: Table of material parameters used for numerical study. The hydrodynamic parameters (γ and p_∞) are calibrated by using the database [4].

Using the mass conservation equations, we obtain :

$$\left(\frac{\rho_g c_g^2}{\alpha_g} + \frac{\rho_s c_s^2}{\alpha_s}\right) \frac{D\alpha_s}{Dt} = \left(\rho_g c_g^2 - \rho_s c_s^2\right) div(\mathbf{v}) + \Gamma_s \frac{\mathbf{S}_s : \mathbf{S}_s}{\tau_{rel,s}}.$$

It implies :

$$\frac{D\alpha_s}{Dt} = \frac{\rho_g c_g^2 - \rho_s c_s^2}{\frac{\rho_s c_s^2}{\alpha_s} + \frac{\rho_g c_g^2}{\alpha_g}} div(\mathbf{v}) + \frac{\Gamma_s}{\frac{\rho_s c_s^2}{\alpha_s} + \frac{\rho_g c_g^2}{\alpha_g}} \frac{\mathbf{S}_s : \mathbf{S}_s}{\tau_{rel,s}}. \tag{27}$$

In the right-hand side of (27), the first term is negative in tensile waves, while the second one is always positive (the second term is responsible for heating occurring during the plastic transformations). In the case of strong tensile waves, the second term is negligible compared to the first term, and the solid volume fraction will tend to decrease, i.e the gas volume fraction will increase. It produces a bubble growing and results in a cracks formation.

In this section we will first analyze the mechanism of dynamical fracturing of plates having triangular notches. Then, the spallation phenomenon is studied in 1D and 2D cases. Finally, a penetration problem is numerically solved. In all these numerical test cases the considered solid materials (aluminum, titanium (more precisely, Ti-Al6-V4) and iron) are surrounded by air. The material parameters of the corresponding equations of state are given in Table 5.2. The hydrodynamic parameters have been calibrated using the database [4].

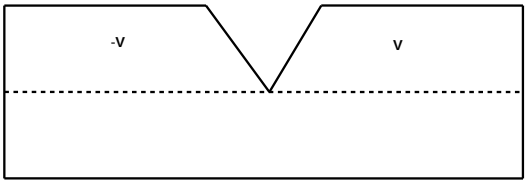

Figure 5.3: A notched iron plate surrounded by a gas is shown. We initially impose a symmetric velocity field $V = \pm 50$ m/s in the upper part of the iron plate delimited by a dashed line, in the other part of the plate the velocity vanishes. null.

5.6.1 Fracturing

Fracturing of an iron plate having a notch

An iron plate of dimension $8\,cm \times 2\,cm$ having a notch is placed in the middle of the calculation domain of dimension $12\,cm \times 4\,cm$. The notch is an isosceles triangle having a base of $1\,cm$ and a height of $1\,cm$ (see Figure 5.3). The density level sets and the evolution of a crack at different time instants are shown in Figure 5.4 for a 1000×1000 cells mesh.

Fracturing with two notches

The same calculation domain and the iron plate of the same dimension surrounded by a gas is considered. However, two symmetric notches are now present (see 5.5). The notches are isosceles triangles of the base $0.6\,cm$ and of the height $0.5\,cm$ (see Figure 5.5). The density levels and the evolution of the crack at different time instants are shown in Figure 5.6 for 1300×1300 cells. In the case where $V = 40\ m/s$, the plate breaks, at the center where the notches are located (see Figure 5.6). It corresponds to the well-known 'principle' in solid mechanics: 'where something is thin, that's where it tears'.

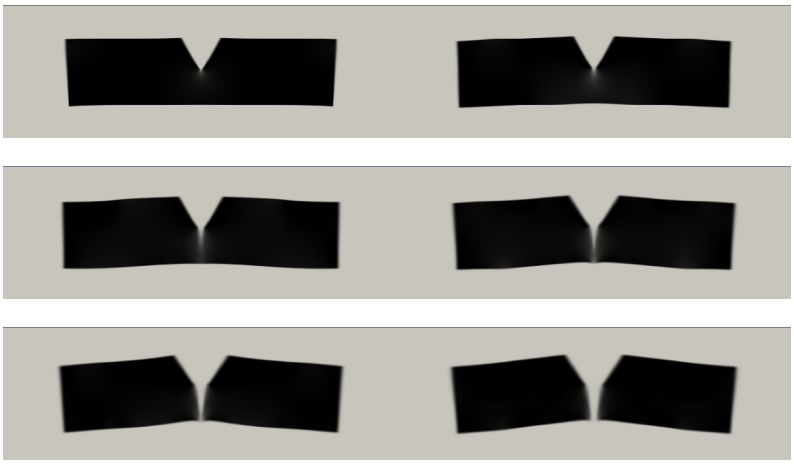

Figure 5.4: One can see appearance and evolution of a crack dividing the plate into two parts. A lighter color corresponds to a lower density. The chosen time instants are : $22 \times 10^{-6}\, s$, $44 \times 10^{-6}\, s$, $66 \times 10^{-6}\, s$, $88 \times 10^{-6}\, s$, $110 \times 10^{-6}\, s$ and $133 \times 10^{-6}\, s$.

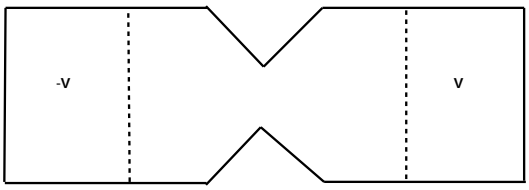

Figure 5.5: An iron plate having two notches is surrounded by a gas. Initially, we impose a symmetric velocity field in a domain delimited by a dashed line. In the other part of the plate the velocity is zero. Two cases are considered with different values of the imposed velocity V : $\pm 40\ m/s$ and $\pm 100\ m/s$.

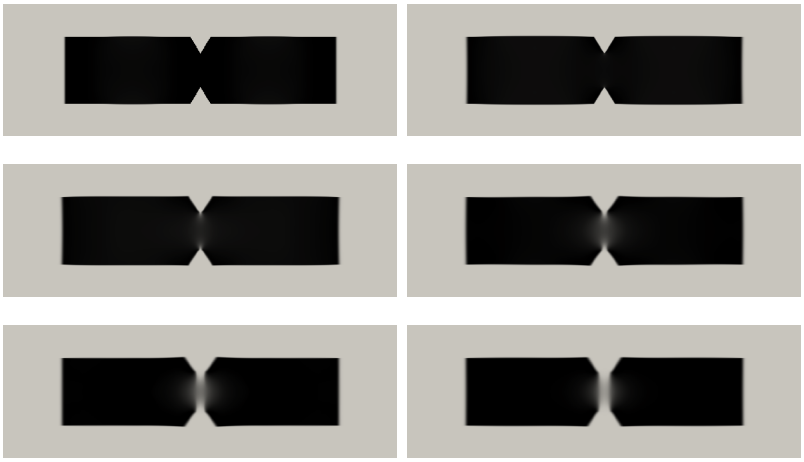

Figure 5.6: The fracture dynamics is shown for $V = \pm 40\ m/s$ for time instants $1.8 \times 10^{-3}s$, $3.6 \times 10^{-3}s$, $5.4 \times 10^{-3}s$, $7.1 \times 10^{-3}s$, $8.9 \times 10^{-3}s$ and $11 \times 10^{-3}s$.

In the case where $V = 100\ m/s$ more complex wave dynamics appears. The results obtained are in contradiction with our physical intuition. Indeed, the plate breaks along the dashed lines where the velocity field is discontinuous, and not in the middle where the plate is thiner (see Figure 5.7). In summary, in dynamics, fractures appear at locations where the tensile stresses are larger, and not necessarily in the thinnest place as it usually happens in statics.

5.6.2 Spallation

Spallation consists in fracturing solids in tensile waves of large amplitude. Such a phenomenon is of great importance in impact engineering. It is a test case for determining mechanical properties of metals. The problem we are studying is a high velocity impact between an aluminum plate (impactor) and a titanium plate (target) (see Figure 5.8). After the impact, two shock waves first appear. One of them propagates in the aluminum plate, and the other one in the titanium plate. The shock wave propagating in the aluminum plate is reflected at the interface between aluminum plate and gas, and propagates then in the aluminum plate. When this wave arrives at the aluminum-titanium interface, another interaction will occur and an rarefaction wave will be transmitted into the titanium plate. On the other hand, the shock wave propagating in the titanium plate will also be reflected from

Figure 5.7: The plate breaking dynamics is shown for $V = \pm 100\ m/s$ for time instants $1.4 \times 10^{-3}\ s$, $2.7 \times 10^{-3}\ s$, $4.0 \times 10^{-3}\ s$, $5.4 \times 10^{-3}\ s$, $6.7 \times 10^{-3}\ s$ and $8.3 \times 10^{-3}\ s$

the free surface. These two rarefaction waves will meet in the titanium plate and will interact at the distance of the free surface which is approximately equal to the thickness of the aluminum plate (see a detailed description in, for example, [2], [6], [18]). A strong tensile stresses appearing during such an interaction will cause spall fracture in the titanium plate. We will show that our model is able to predict this physical phenomenon. First, a $1D$ configuration is considered. We will study the influence of the elastic yield limit on the spallation phenomena. Finally, a $2D$ impact problem will be studied.

Impact problem between an aluminum plate and a titanium plate

Consider a one-dimensional impact between an aluminum plate (projectile) of thickness $2\,mm$, and a titanium (more exactly, Ti-Al6-V4) plate of thickness $9.8\,mm$ (target) surrounded by air. The impact velocity V is 700 m/s (see Figure 5.8). These parameters correspond to experiments of Kanel [18]. The initial density distribution showing the location of interfaces is presented in Figure 5.9. The calculation domain is $1.7\,cm$ long, the mesh grid is composed of 2000 cells.

A typical solution of the Riemann problem is shown in Figure 5.10. The numerical solution is shown in Figure 5.11 at time instant $0.2\mu s$. We will show how to analytically recover the plateau values for the elastic precursor.

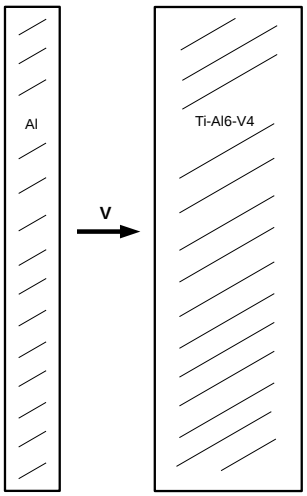

Figure 5.8: Initial configuration for the one-dimensional impact.

Even if the exact solution is useless for practical applications, it is important to validate the numerical scheme. Such calculations have been also made in [28] for the compression of a sphere. They used a different equation of state where the energy is not in separable form.

We rewrite the relations defining the elastic precursor :

$$\rho = \rho_0 a^1 b^2 c^3, \quad e = \frac{p + \gamma p_\infty}{(\gamma - 1)\,\rho} + \frac{\mu}{8\rho_0}\left(\frac{(a^1)^4 + (b^2)^4 + (c^3)^4}{(a^1 b^2 c^3)^{\frac{4}{3}}} - 3\right),$$

$$\sigma_{11} = -p + S_{11}, \quad S_{11} \text{ is defined by:}$$

$$S_{11} = -\frac{\mu}{2\,(a^1 b^2 c^3)^{\frac{1}{3}}}\left((a^1)^4 - \frac{1}{3}\left((a^1)^4 + (b^2)^4 + (c^3)^4\right)\right).$$

Initially $b^2 = 1$ and $c^3 = 1$ and these variables remain constant and equal to 1 in the elastic precursor. Non-diagonal stresses S_{12}, S_{13} and S_{23} are zero in our simplified one-dimensional version. Now, we will suppose that the state after the elastic precursor is at the von Mises yield surface. By symmetry, the constraints S_{22} and S_{33} are equal. The condition $S_{11} + S_{22} + S_{33} = 0$, we

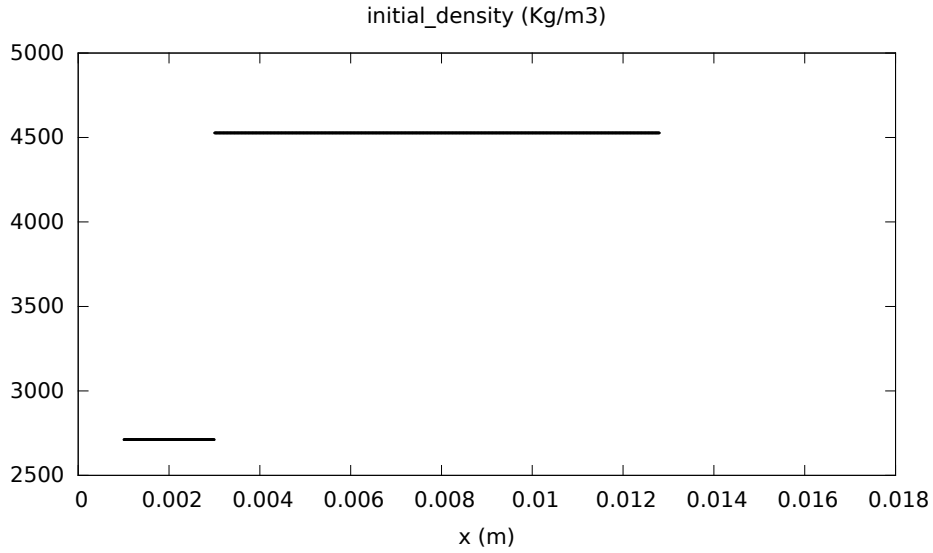

Figure 5.9: The initial density distribution is presented showing, in particular, the location of contact discontinuities. In particular, the contact between plates is at $x = 3\,mm$.

have: $S_{22} = -\frac{1}{2}S_{11}$. The Von Mises yield surface is defined as $S_{11}^2 + S_{22}^2 + S_{33}^2 = \frac{2}{3}\sigma_Y^2$. Or, $S_{11} = -\frac{2}{3}\sigma_Y$. because the elastic precursor is a shock wave. As $\rho = \rho_0^1 b^2 c^3$, $b^2 = 1$ and $c^3 = 1$, then $a^1 = \frac{\rho}{\rho_0}$. S_{11} can also be reduced as follows : $S_{11} = -\frac{\mu}{3}\left((a^1)^4 - 1\right)$. We can now express S_{11} as a function of density:

$$S_{11} = -\frac{\mu}{3\left(\frac{\rho}{\rho_0}\right)^{\frac{1}{3}}}\left(\left(\frac{\rho}{\rho_0}\right)^4 - 1\right).$$

In the elastic precursor, we then have:

$$-\frac{2}{3}\sigma_Y = -\frac{\mu}{3\left(\frac{\rho}{\rho_0}\right)^{\frac{1}{3}}}\left(\left(\frac{\rho}{\rho_0}\right)^4 - 1\right).$$

As $a^1 = \frac{\rho}{\rho_0}$, we obtain the following algebraic equation:

$$\left(a^1\right)^4 - 2\frac{\sigma_Y}{\mu}\left(a^1\right)^{\frac{1}{3}} - 1 = 0.$$

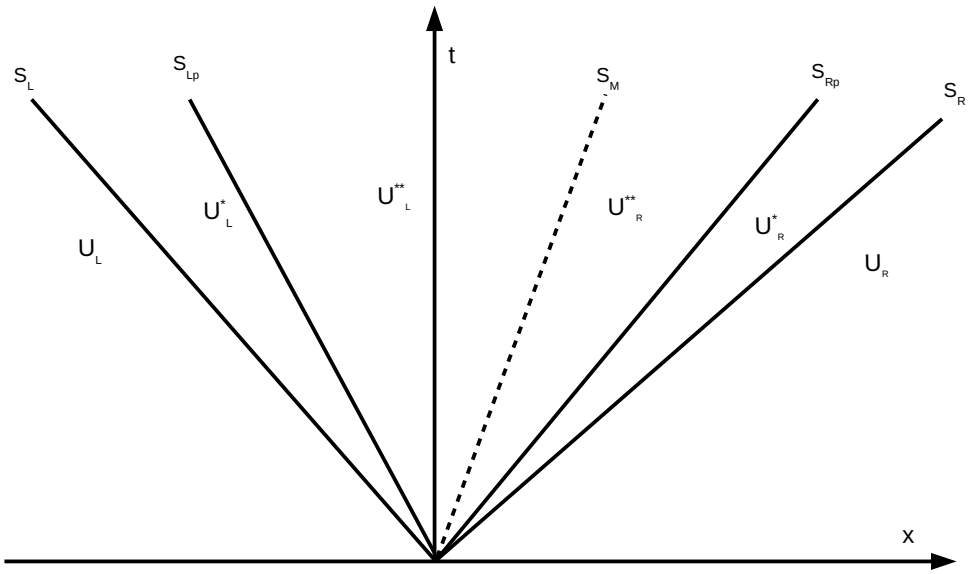

Figure 5.10: Wave's configuration : two left facing waves and two right facing wave are separated by a contact discontinuity. The extreme waves are elastic ones (precursor waves), the intermediate waves are plastic ones.

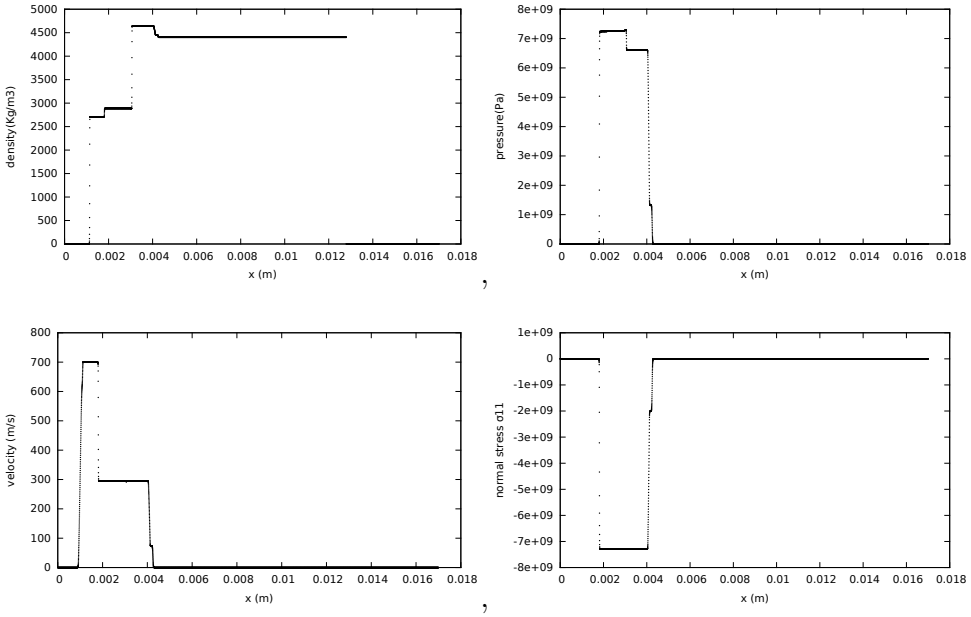

Figure 5.11: The solution of the Riemann problem (the density, pressure, velocity field and the normal stress σ_{11}) resulting from the impact between an aluminum plate and a titanium plate is shown at time $0.2\,\mu s$. The elastic precursor in the titanium plate is clearly visible. However, we can not see the elastic precursor in the aluminum because the yield limit of aluminum is too small. The material velocity and the normal stress are continuous through the interface.

This equation has a unique positive real solution $a_1 > 1$. This allows us to obtain the density in the elastic precursor. Hence, the density in the elastic precursor depends only on the ratio $\frac{\sigma_Y}{\mu}$. Finally, we use the Rankine-Hugoniot relations to find the pressure and the velocity behind the elastic precursor :

$$[e] = \frac{1}{2}(\sigma_{11} - p_0)[\tau].$$
$$[u]^2 = [\sigma_{11}][\tau].$$

The comparison between numerical and analytical results is presented in (28) :

Variables	**Numerical results**	**Analytical results**
Density of aluminum	2715.13 kg/m^3	2715.51 kg/m^3
Density of titanium	4581.73 kg/m^3	4581.90 kg/m^3
Velocity of aluminum	691.57 m/s	691.64 m/s
Velocity of titanium	74.12 m/s	74.58 m/s
Pressure in aluminum	0.13 GPa	0.13 GPa
Pressure in titanium	1.40 GPa	1.41 GPa

(28)

Let us now find the plateau values behind the plastic wave. Now, we do not suppose that $b^2 = 1$. However, we always suppose the symmetry : $b^2 = c^3$ and $S_{22} = S_{33}$. Moreover, we approximately replace the elastic-plastic transition zone by a shock. This allows us to use the jump relations :

$$[u]^2 = [\sigma_{11}][\tau], \qquad [e] = \frac{1}{2}(\sigma_{11} + \sigma_{11,0})[\tau],$$

with

$$\tau = \frac{1}{\rho}, \qquad \rho = \rho_0 a^1 \left(b^2\right)^2,$$

and the fact that in the plastic wave we are always at the yield surface :

$$S_{11} = -\frac{\mu}{3}\frac{\left((a^1)^4 - (b^2)^4\right)}{(a^1)^{\frac{1}{3}}(b^2)^{\frac{2}{3}}} = -\frac{2}{3}\sigma_Y.$$

These relations are completed by the equations of state

$$e = e^h + e^e, \qquad e^h = \frac{p + \gamma p_\infty}{(\gamma - 1)\rho}, \quad e^e = \frac{\mu}{8}\left(\frac{(a^1)^4 + 2(b^2)^4}{(a^1)^{\frac{4}{3}}(b^2)^{\frac{8}{3}}} - 3\right).$$

The comparison between numerical and analytical results are given in the following table :

Variables	**Numerical results**	**Analytical results**
Density of aluminum	2880.6597 kg/m^3	2880.90 kg/m^3
Density of titanium	4783.0544 kg/m^3	4782.80 kg/m^3
Interface velocity	297.2304 m/s m/s	297.149 m/s
Normal stress σ_{11}	-7.50285 GPa	-7.50285 GPa

(29)

The numerical and analytical results shown in (29) are in good agreement. The problem of interaction of rarefaction waves producing spall fractures will be treated numerically in the next section.

Different spallation scenarios

For a given impact velocity, the influence of the yield limit σ_Y on the formation of spall fractures is extremely important. Usually, this value is taken from quasi-static experiments. A mathematical model is needed for evolution of the yield limit (hardening or softening) to describe the spallation phenomena. We will study such an influence only parametrically, by changing the value of the yield limit of titanium. Experimentally, one measures the interface velocity of the target (in our case, the interface velocity between the titanium plate and the air) as a function of time. The behavior of this curve (amplitude and the period of oscillations which appear due to multiple wave interaction inside the titanium plate) can indirectly indicate the structure of the fractured zone. We will reproduce numerically such a curve corresponding to experiments by Kanel [18]. Two values of the yield limit for titanium will be taken : $\sigma_Y = 1030\, MPa$ and $4030\, MPa$. The first value is just a quasistatic one which can be found in the literature. The second value, as we will see later, allows us to reproduce the experimentally observed behavior of the free surface velocity as a function of time. The behavior of the interface velocity as well as the material density (mixture density) are shown in Figures 5.12 and 5.13 for $\sigma_Y = 1030\ MPa$ and $\sigma_Y = 4030\ MPa$, respectively.

Numerical simulation in 2D case

This impact problem generalizes the 1D configuration to the case of the plates of different lengths. Initially, the volume fraction of each phase which

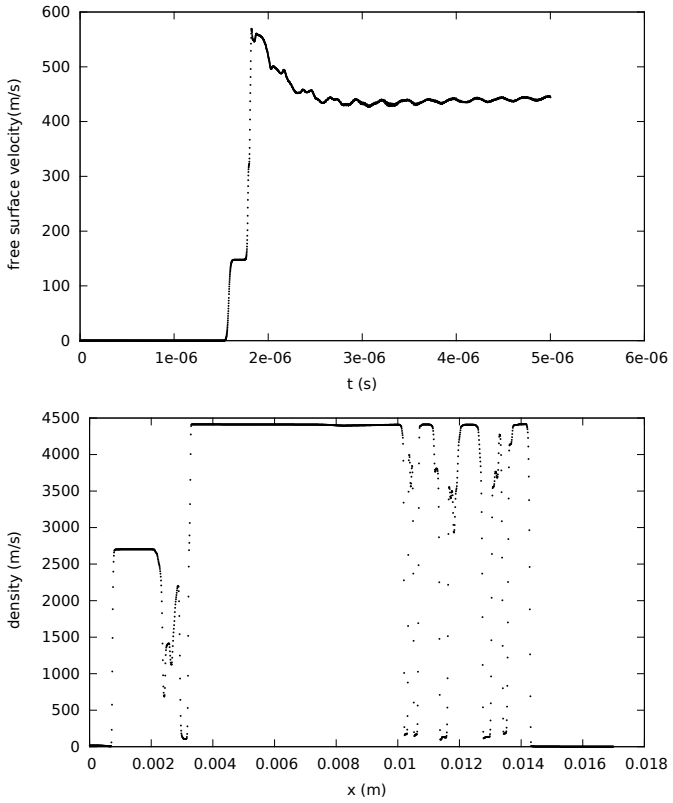

Figure 5.12: An the top, the evolution of interface velocity with respect to time is shown. Approximately, at instant 1.5 μs, the interface suddenly accelerates. It corresponds to the time instant when the elastic precursor arrives at the free surface. The free surface velocity oscillates due to continuously produced wave interaction. At the bottom, the average density distribution is shown at instant 5 μs. We can see 3 spall fractures in the titanium plate where the average density is almost vanishing. So, for small values of Y the dissipation of the elastic energy is more efficient when more spall fractures are formed. As the spall fragments are small, the oscillation amplitude of the free surface velocity is small.

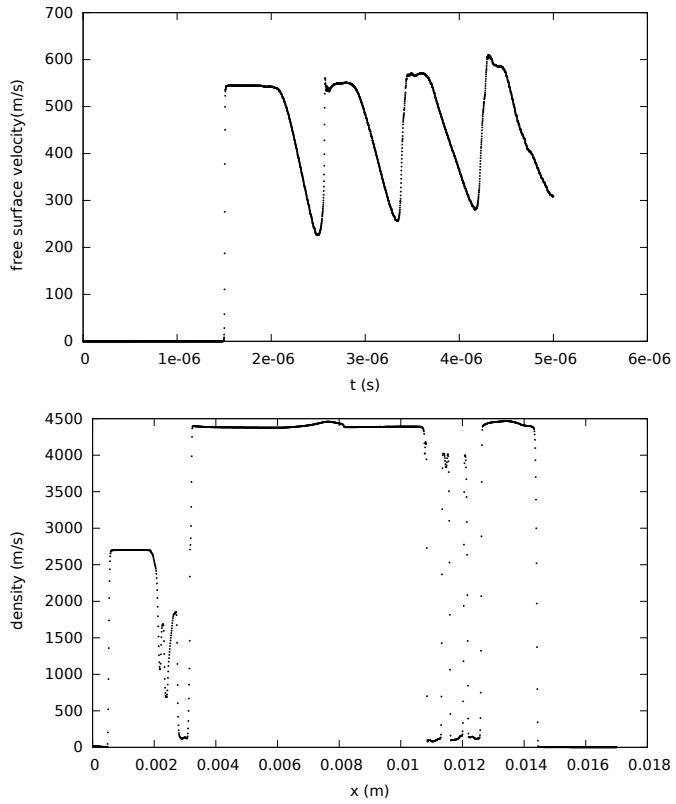

Figure 5.13: At the top, we show the evolution of the free surface velocity with respect to time. We do not exceed the yield elastic limit of our material during the elastic wave formation. The free surface velocity oscillates with a large period. At the botton, the density distribution is shown at time instant of 5 μs. We observe that we have only one spall fracture. Oscillations of the free surface velocity are related to the reflection of waves at the interface of the fragment. As the fragment is large enough, we observe large amplitude oscillations.

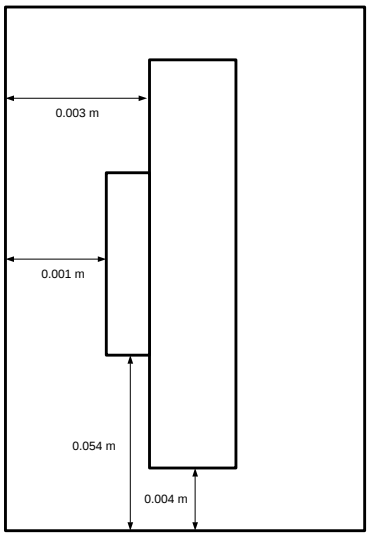

Figure 5.14: An aluminum plate impacts a titanium plate. Geometric characteristics of the calculation domain are shown.

is present in pure phases was 10^{-6}. The initial configuration is shown in Figure 5.14. The computational domain is $0.04\,m \times 0.2\,m$. The aluminum plate has dimension $0.002\,m \times 0.092\,m$. The dimension of the titanium plate is $0.0098\,m \times 0.192\,m$. The velocity impact is $700\,m/s$. Numerical tests were done on a Cartesian mesh of 500×2000 cells. In the case where $\sigma_Y = 1030$ GPa several spall fractures appear as in the 1D case. In the case where $\sigma_Y = 4030$ GPa we observe the formation of a single fracture as in the corresponding 1D case. The main difference between 1D and 2D case is only the topological structure of the spall fracture : in the latter case it as attached to the titanium plate.

5.6.3 High-velocity impact problems

We present here an example of high-velocity impact with penetration. A circular iron disc of $0.01\,m$ radius is normally impacting at $1000\,m/s$ an aluminum plate of dimension $0.16\,m \times 0.02\,m$. Both materials are surrounded by air. The material parameters are given in Table 5.2. Figure 5.17 shows the initial configuration. The volume fraction of the gas α_g initially present in solids is 10^{-6}. The same volume fraction of iron (aluminum) is present in the aluminum (iron) and the gas. The results obtained on a 2000×2000

Figure 5.15: We observe the formation of spall fractures in the impact zone in the titanium plate due to the wave interaction at the time instants $50\mu s$, $100\mu s$, $150\mu s$, $200\mu s$, $250\mu s$ and $320\mu s$.

Figure 5.16: We observe the formation of a single spall fracture in the impact zone at the time instants $50\mu s$, $100\mu s$, $150\mu s$, $200\mu s$, $250\mu s$ and $290\mu s$.

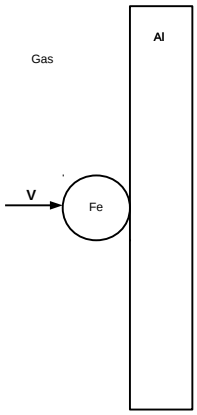

Figure 5.17: Initial configuration for the high-velocity impact problem.

cells mesh are shown in Figure 5.18. At the first time instant, shock waves propagate in the solid. After the wave reflection, the gas volume fraction increases in strong tensile waves, and cracks start to appear. The cracks propagate in the aluminum plate and reach the other side of the material, fragments appear and propagate with their own velocity. The projectile is highly deformed. This kind of problem was also studied in [34] by using Eulerian front tracking, and in [3] by using a level set type method. The first approach is not able to deal with dynamic appearance of interfaces. In particular, it does not allow to study the penetration and fragmentation of solids. In the second approach, the level set regularization brakes the solid filaments produced in the solid stretching.

5.7 Conclusion

A new diffuse interface model for multi-solid and multi-fluid interaction problems is developed. The model is hyperbolic and thermodynamically well posed. Numerous applications are presented as, for example, dynamic fracturing and penetration problems. They show a good qualitative comparison with experiments.

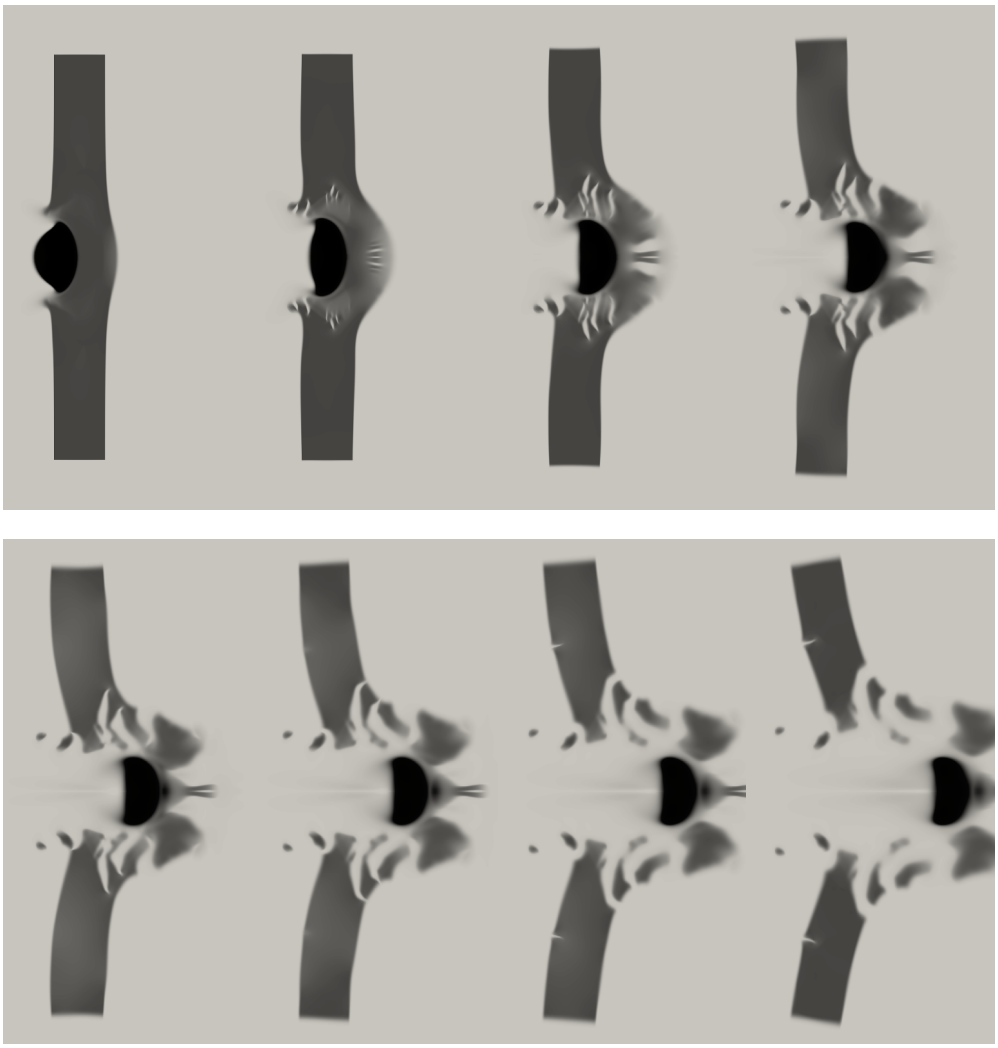

Figure 5.18: An circular iron disc normally impacts an aluminum plate at the velocity of $1000m/s$. Due to large tensile deformations, cracks appear during the penetration of the disc resulting to a final fragmentation of the plate.

5.8 Reference

Bibliography

[1] R. Abgrall How to prevent pressure oscillations in multicomponnet flow calculations : A quasi-conservative approach, *Journal of Computational Physics* 125 (1996) 150-160.

[2] T. Antoun *et al.*, Spall Fracture, *Springer*, 2003.

[3] P. T. Barton, R. Deiterding, D. Meiron and D. Pullin, Eulerian adaptive finite-difference method for high-velocity impact and penetration problems, *Journal of Computational Physics*, 240 (2013), 76-99.

[4] A. V. Bushman, I. V. Lomonosov and K. V. Khishchenko, Shock Wave Database, www.ficp.ac.ru/rusbank/.

[5] S. F. Davis, Simplified second-order Godunov-type methods, *SIAM J . Sci. Stat. Comput*, 9 (1988) 445 - 473.

[6] L. Davison, Fundamentals of Shock Wave Propagation in Solids, *Springer*, 2008.

[7] F. dell'Isola and S. L. Gavrilyuk, Variational Models And Methods In Solid And Fluid Mechanics, *Springer*, 2012.

[8] N. Favrie, S. L. Gavrilyuk and R. Saurel, Solid-fluid diffuse interface model in cases of extreme deformations, *J. Computational Physics*, 228 (2009) 6037 - 6077.

[9] N. Favrie and S. Gavrilyuk, Mathematical and numerical model for nonlinear viscoplasticity, *Phil. Trans. R. Soc. A*, 69 (2011) 2864 - 2880.

[10] N. Favrie and S.L. Gavrilyuk, Diffuse interface model for compressible fluid- compressible elastic-plastic solid interaction, *J. Computational Physics*, 231 (2012) 2696 - 2723.

[11] N. Favrie, S. Gavrilyuk and S. Ndanou, A thermodynamically compatible splitting procedure in hyperelasticity, *J. Computational Physics*, 270 (2014) 300–324.

[12] T. Flåtten and H. Lund, Relaxation two-phase flow models and the subcharacteristic condition, *Mathematical Models and Methods in Applied Sciences*, 21 (2011) 2379 - 2407.

[13] R. J. Flory, Thermodynamic relations for highly elastic materials, *Transactions of Faraday Society*, 57 (1961) 829-838.

[14] S. L. Gavrilyuk and N. Favrie and R. Saurel, Modelling wave dynamics of compressible elastic materials, *J. Computational Physics*, 227 (2008) 2941-2969.

[15] S. K. Godunov and E. I. Romenskii, Elements of Continuum Mechanics and Conservation Laws, *Kluwer Academic Plenum Publishers, NY*, 2003.

[16] S. K. Godunov and I. M. Peshkov, Thermodynamically Consistent Nonlinear Model of Elastoplastic Maxwell Medium, *Computational Mathematics and Mathematical Physics*, 50 (2010), 1409–1426.

[17] S. Hartmann and P. Neff, Polyconvexity of generalized polynomial-type hyperelastic strain energy functions for nearly incompressibility, *Int. J. Solids and Structures,* 40 (2003) 2767 – 2791.

[18] G. I. Kanel, Spall fracture: methodological aspects, mechanisms and governing factors, *International Journal of Fracture*, 163 (2010) 173 - 191.

[19] A. K. Kapila and R. Menikoff, J. B. Bdzil, S. F. Son and D. S. Stewart, Two-phase modeling of deflagration-to-detonation transition in granular materials: Reduced equations, *Physics of Fluids*, 13 (2001) 3002 - 3014.

[20] S. Karni, Multi-component flow calculations by a consistent primitive algorithm, *J. Computational Physics*, 112 (1994) 31-43.

[21] G. Kluth and B. Desprès (2008). Perfect plasticity and hyperelastic models for isotropic materials, *Continuum Mechanics and Thermodynamics*, 20 (2008), 173-192.

[22] J. Lemaitre, J. L. Chaboche, A. Benallal and R. Desmorat, Mécanique des matérieux solides, *Dunod*, 2009.

[23] B. Li, F. Habbal and M. Ortiz, Optimal transportation meshfree approximation schemes for fluid an plastic flows , *International Journal of for Numerical Methods in Engineering*, 83 (2010) 1541-1579.

[24] B. Li, A. Kidane, G. Ravichandran and M. Ortiz, Verification and validation of the Optimal Transportation Meshfree (OTM) simulation of terminal ballistics, *International Journal of Impact Engineering*, 42 (2012) 25-36.

[25] P. H. Maire, R. Abgrall, J. Breil, R. Loubère and B. Rebourcet, A nominally second-order cell-centered Lagrangian scheme for simulating elastic-plastic flows on two-dimensional unstructured grids, *Journal of Computational Physics*, 235 (2013) 626-665.

[26] G. H. Miller and P. Colella, A high order Eulerian Godunov method for elastic plastic flow in solids, *J. Computational Physics*, 167 (2001) 131 - 176.

[27] S. Ndanou and N. Favrie and S. L. Gavrilyuk, Criterion of hyperbolicity in hyperelasticity in the case of the stored energy in separable form, *Journal of Elasticity*, 115 (2014) 1 - 25.

[28] A. L. Ortega, M. Lombardini and D. J. Hill, Converging shocks in elastic-plastic solids, *Physical Review E*, 84 (2011), 056307.

[29] R. Saurel and R. Abgrall, A Multiphase Godunov Method for Compressible Multifluid and Multiphase Flows, *Journal of Computational Physics* 150 (1999) 425-467.

[30] R. Saurel, F. Petitpas and R. Abgrall, Modelling phase transition in metastable liquids: application to cavitating and flashing flows, *Journal of Fluid Mechanics*, 607 (2008) 313-350.

[31] R. Saurel and F. Petitpas and R. A. Berry, Simple and efficient relaxation methods for interfaces separating compressible fluids, cavitating flows and shocks in multiphase mixtures, *Journal of Computational Physics*, 228 (2009) 1678 - 1712.

[32] G.I. Taylor, The use of flat ended projectiles for determining yield stress. I. Theoretical considerations, *Proc. R. Soc. A*, 194 (1948) 289-299.

[33] E.F. Toro, Riemann Solvers and Numerical Methods for Fluid Dynamics: A Practical Introduction (third ed.), *Springer-Verlag*, 2009.

[34] J. Walter, J. Glimm, J. Grove, H. C. Hwang, X. Lin, B. J. Plohr, D. H. Sharp and D. Yu, Eulerian front tracking for solid dynamics, *Proceedings of the 15th US Army Symposium on Solid Mechanics*, 1999, 343 - 366.

[35] G.B. Whitham, Linear and Nonlinear Waves, *John Wiles & Sons*, 1974.

[36] M.L. Wilkins, Calculation of elastic-plastic flow, Methods Comput. Phys., 3 (1964), pp. 211-263

Appendices

Appendix C

Appendices

C.1 Appendix: Hyperbolicity of an equilibrium visco-plastic model

For the hyperbolicity study, we can put zero in the right-hand side of (12) :

$$\begin{cases} \frac{\partial \rho}{\partial t} + div\,(\rho \mathbf{v}) = 0, \\ \\ \frac{D\mathbf{e}_l^\beta}{Dt} + \left(\frac{\partial \mathbf{v}}{\partial \mathbf{x}}\right)^T \mathbf{e}_l^\beta = 0, \\ \\ \rho \frac{D\mathbf{v}}{Dt} + div(-\boldsymbol{\sigma}) = 0, \\ \\ \frac{DY_l}{Dt} = 0, \\ \\ \frac{D\eta_l}{Dt} = 0, \\ \\ p_1 = ... = p_N, \end{cases} \tag{1}$$

with

$$\sum_{l=1}^{N} \alpha_l = 1, \quad \sum_{l=1}^{N} Y_l = 1.$$

These algebraic constraints can be viewed as constraints for initial data: if they are satisfied at $t = 0$, then they are satisfied for all $t > 0$. So, it is more convenient for the study of hyperbolicity to consider all $Y_1, ..., Y_N$ and $\alpha_1, ..., \alpha_N$ as independent variables. The equation for the mixture density is also not independent, it is a consequence of the equations for $\mathbf{e}_l^\beta$. However,

in the following, we will consider ρ as an independent variable for the same raison.

For hyperbolicity, it is sufficient to consider $1D$ case (see [27] for such a justification based on the invariance of the equations under rotation). We choose as independent variables the vector:

$$\mathbf{U} = \left(\rho, \ \mathbf{a}_1, \ \mathbf{b}_1, \ \mathbf{c}_1, \ ..., \ \mathbf{a}_N, \ \mathbf{b}_N, \ \mathbf{c}_N, \ \mathbf{v}, \ Y_1, \ ..., \ Y_N, \ \eta_1, \ ..., \ \eta_N \right)^T.$$

It is convenient to present the pressure equilibrium condition (9) in the following form:

$$p = p_1 \left(\frac{\rho Y_1}{\alpha_1}, \eta_1 \right) = ... = p_N \left(\frac{\rho Y_N}{\alpha_N}, \eta_N \right).$$

These relations are $N-1$ independent relations which allow us to find implicitly all α_l as functions of $\rho, Y_1, ..., Y_N, \eta_1, ..., \eta_N$. As a consequence of the equilibrium condition, we obtain the pressure as a function of $2 \times N + 1$ variables:

$$p = p\left(\rho, Y_1, ..., Y_N, \eta_1, ..., \eta_N\right).$$

Let us denote

$$c_w^2 = \frac{\partial p}{\partial \rho}$$

the Wood sound speed. We have :

$$\boldsymbol{\sigma} = -p\mathbf{I} + \mathbf{S} = -p\mathbf{I} + \sum_{l=1}^{N} \alpha_l \mathbf{S}_l = -p\left(\rho, Y_1, ..., Y_N, \eta_1, ..., \eta_N\right)\mathbf{I} - 2\rho \sum_{l=1}^{N} \left(Y_l \frac{\partial e_l^e}{\partial \mathbf{G}_l} \mathbf{G}_l \right),$$

because $\rho_l = \frac{\rho Y_l}{\alpha_l}$ and $\mathbf{S}_l = -2\rho_l \frac{\partial e_l^e}{\partial \mathbf{G}_l} \mathbf{G}_l$. Hence, we have an explicit dependence of $\boldsymbol{\sigma}$ on ρ, $\mathbf{a}_l$, $\mathbf{b}_l$, $\mathbf{c}_l$, Y_l and η_l. This implies that:

$$\begin{aligned} \frac{\partial \boldsymbol{\sigma}}{\partial x} = & -\sum_{l=1}^{N} \frac{\partial p}{\partial \eta_l} \frac{\partial \eta_l}{\partial x} \mathbf{I} - \sum_{l=1}^{N} \left(\frac{\partial p}{\partial Y_l} \mathbf{I} - \rho \frac{\mathbf{S}_l}{\rho_l} \right) \frac{\partial Y_l}{\partial x} \\ & - \left(c_w^2 \mathbf{I} - \frac{\mathbf{S}}{\rho} \right) \frac{\partial \rho}{\partial x} \\ & + \sum_{\beta=1}^{3} \sum_{l=1}^{N} \alpha_l \left(\frac{\partial \mathbf{S}_l}{\partial a_l^\beta} \frac{\partial a_l^\beta}{\partial x} + \frac{\partial \mathbf{S}_l}{\partial b_l^\beta} \frac{\partial b_l^\beta}{\partial x} + \frac{\partial \mathbf{S}_l}{\partial c_l^\beta} \frac{\partial c_l^\beta}{\partial x} \right). \end{aligned}$$

Thus, we rewrite (1) in non-conservative form:

$$\frac{\partial \rho}{\partial t} + u\frac{\partial \rho}{\partial x} + \rho\frac{\partial u}{\partial x} = 0,$$

$$\frac{\partial a_l^\beta}{\partial t} + u\frac{\partial a_l^\beta}{\partial x} + a_l^\beta\frac{\partial u}{\partial x} + b_l^\beta\frac{\partial v}{\partial x} + c_l^\beta\frac{\partial w}{\partial x} = 0,$$

$$\frac{\partial b_l^\beta}{\partial t} + u\frac{\partial b_l^\beta}{\partial x} = 0, \quad \frac{\partial c_l^\beta}{\partial t} + u\frac{\partial c_l^\beta}{\partial x} = 0,$$

$$\frac{\partial u}{\partial t} + u\frac{\partial u}{\partial x} + \frac{\left(c_w^2 - \frac{S_{11}}{\rho}\right)}{\rho}\frac{\partial \rho}{\partial x}$$

$$-\sum_1^N \frac{\alpha_l}{\rho}\left(\frac{\partial S_{11,l}}{\partial \mathbf{a}_l}\cdot\frac{\partial \mathbf{a}_l}{\partial x} + \frac{\partial S_{11,l}}{\partial \mathbf{b}_l}\cdot\frac{\partial \mathbf{b}_l}{\partial x} + \frac{\partial S_{11,l}}{\partial \mathbf{c}_l}\cdot\frac{\partial \mathbf{c}_l}{\partial x}\right)$$

$$+\frac{1}{\rho}\sum_{l=1}^N\left(\frac{\partial p}{\partial Y_l} - \rho\frac{S_{11,l}}{\rho_l}\right)\frac{\partial Y_l}{\partial x} + \frac{1}{\rho}\sum_{l=1}^N\frac{\partial p}{\partial \eta_l}\frac{\partial \eta_l}{\partial x} = 0,$$

$$\frac{\partial v}{\partial t} + u\frac{\partial v}{\partial x} - \frac{S_{12}}{\rho^2}\frac{\partial \rho}{\partial x}$$

$$-\sum_1^N \frac{\alpha_l}{\rho}\left(\frac{\partial S_{12,l}}{\partial \mathbf{a}_l}\cdot\frac{\partial \mathbf{a}_l}{\partial x} + \frac{\partial S_{12,l}}{\partial \mathbf{b}_l}\cdot\frac{\partial \mathbf{b}_l}{\partial x} + \frac{\partial S_{12,l}}{\partial \mathbf{c}_l}\cdot\frac{\partial \mathbf{c}_l}{\partial x}\right)$$

$$+\rho\sum_{l=1}^N\left(-\frac{S_{12,l}}{\rho_l}\right)\frac{\partial Y_l}{\partial x} = 0,$$

$$\frac{\partial w}{\partial t} + u\frac{\partial w}{\partial x} - \frac{S_{13}}{\rho^2}\frac{\partial \rho}{\partial x}$$

$$-\sum_1^N \frac{\alpha_l}{\rho}\left(\frac{\partial S_{13,l}}{\partial \mathbf{a}_l}\cdot\frac{\partial \mathbf{a}_l}{\partial x} + \frac{\partial S_{13,l}}{\partial \mathbf{b}_l}\cdot\frac{\partial \mathbf{b}_l}{\partial x} + \frac{\partial S_{13,l}}{\partial \mathbf{c}_l}\cdot\frac{\partial \mathbf{c}_l}{\partial x}\right)$$

$$+\rho\sum_{l=1}^N\left(-\frac{S_{13,l}}{\rho_l}\right)\frac{\partial Y_l}{\partial x} = 0,$$

$$\frac{\partial Y_l}{\partial t} + u\frac{\partial Y_l}{\partial x} = 0, \quad l = 1, ..., N,$$

$$\frac{\partial \eta_l}{\partial t} + u\frac{\partial \eta_l}{\partial x} = 0, \quad l = 1, ..., N.$$

Then, the system can be written in vector form :

$$\mathbf{U}_t + \mathbf{D}\mathbf{U}_x = 0,$$

with

$$\mathbf{D} = \begin{pmatrix} \mathbf{A} & \mathbf{T} \\ \mathbf{O}_{2\times N,1+9\times N+3} & u\mathbf{I}_{2\times N} \end{pmatrix},$$

$$\mathbf{T} = \begin{pmatrix} \mathbf{O}_{1+9\times N,2\times N} \\ \mathbf{T}_1 \end{pmatrix},$$

$$\mathbf{T}_1 = \begin{pmatrix} \frac{1}{\rho}\left(\frac{\partial p}{\partial Y_1} - \rho\frac{S_{11,1}}{\rho_1}\right) & \dots & \frac{1}{\rho}\left(\frac{\partial p}{\partial Y_N} - \rho\frac{S_{11,N}}{\rho_N}\right) & \frac{1}{\rho}\frac{\partial p}{\partial \eta_1} & \dots & \frac{1}{\rho}\frac{\partial p}{\partial \eta_N} \\ \left(-\frac{S_{12,1}}{\rho_1}\right) & \dots & \left(-\frac{S_{12,N}}{\rho_N}\right) & 0 & \dots & 0 \\ \left(-\frac{S_{13,1}}{\rho_1}\right) & \dots & \left(-\frac{S_{13,N}}{\rho_N}\right) & 0 & \dots & 0 \end{pmatrix},$$

with

$$\mathbf{A} = \begin{pmatrix} u\mathbf{I}_{1+9\times N} & \mathbf{B}_1 \\ \mathbf{C}_1 & u\mathbf{I}_3 \end{pmatrix}.$$

Here $\mathbf{I}_n$ is the identity matrix of dimension $n \times n$, $\mathbf{O}_{n,m}$ is the null matrix of dimension $n \times m$ (n is the number of lines, and m is the number of columns), $\mathbf{B}_1$ and $\mathbf{C}_1$ are defined as :

$$\mathbf{B}_1 = \begin{pmatrix} \mathbf{m} \\ \mathbf{n}_1 \\ \mathbf{n}_2 \\ \dots \\ \mathbf{n}_N \end{pmatrix}, \quad \mathbf{m} = \begin{pmatrix} \rho, & 0, & 0 \end{pmatrix}, \quad \mathbf{n}_l = \begin{pmatrix} a_l^1 & b_l^1 & c_l^1 \\ a_l^2 & b_l^2 & c_l^2 \\ a_l^3 & b_l^3 & c_l^3 \\ 0 & 0 & 0 \\ 0 & 0 & 0 \\ 0 & 0 & 0 \\ 0 & 0 & 0 \\ 0 & 0 & 0 \\ 0 & 0 & 0 \end{pmatrix},$$

$$\mathbf{C}_1 = \begin{pmatrix} \mathbf{n}, & \mathbf{m}_1, & \mathbf{m}_1, & \dots, & \mathbf{m}_N \end{pmatrix}, \quad \mathbf{n} = \begin{pmatrix} \frac{c_w^2}{\rho} - \frac{S_{11}}{\rho^2} \\ -\frac{S_{12}}{\rho^2} \\ -\frac{S_{13}}{\rho^2} \end{pmatrix},$$

$$\mathbf{m}_l = Y_l \begin{pmatrix} -\frac{1}{\rho_l}\frac{\partial S_{11,l}}{\partial \mathbf{a}_l} & -\frac{1}{\rho_l}\frac{\partial S_{11,l}}{\partial \mathbf{b}_l} & -\frac{1}{\rho_l}\frac{\partial S_{11,l}}{\partial \mathbf{c}_l} \\ -\frac{1}{\rho_l}\frac{\partial S_{12,l}}{\partial \mathbf{a}_l} & -\frac{1}{\rho_l}\frac{\partial S_{12,l}}{\partial \mathbf{b}_l} & -\frac{1}{\rho_l}\frac{\partial S_{12,l}}{\partial \mathbf{c}_l} \\ -\frac{1}{\rho_l}\frac{\partial S_{13,l}}{\partial \mathbf{a}_l} & -\frac{1}{\rho_l}\frac{\partial S_{13,l}}{\partial \mathbf{a}_l} & -\frac{1}{\rho_l}\frac{\partial S_{13,l}}{\partial \mathbf{a}_l} \end{pmatrix}.$$

Hence, the characteristic polynomial is:

$$det\left(\mathbf{D} - \nu\mathbf{I}\right) = (u-\nu)^{2\times N}\, det\left(\mathbf{A} - \nu\mathbf{I}_{1+9\times N+3}\right) = 0. \tag{2}$$

Then we have to solve the characteristic equation:

$$det\left(\mathbf{A} - \nu\mathbf{I}\right) = \begin{pmatrix} (u-\nu)\,\mathbf{I}_{1+9\times N} & \mathbf{B}_1 \\ \mathbf{C}_1 & (u-\nu)\,\mathbf{I}_3 \end{pmatrix} = 0. \tag{3}$$

Let us consider the first case : $\nu = u$. We will show that there are $9 \times N - 2$ linear independent eigenvectors of the matrix $\mathbf{A}$ corresponding to this eigenvalue. Let $\mathbf{r}$ be the right eigenvector of $\mathbf{A}$ corresponding to $\nu = u$:

$$\mathbf{r}^T = \begin{pmatrix} \mathbf{s}^T, & \mathbf{r}_{N+1}^T \end{pmatrix} = \begin{pmatrix} r_0, & \mathbf{r}_1^T, & ..., & \mathbf{r}_N^T, & \mathbf{r}_{N+1}^T \end{pmatrix},$$

with r_0 being a scalar, $\mathbf{r}_l$ being a 9 components vector, and $\mathbf{r}_{N+1}$ a 3 components vector. The equation for the eigenvectors is :

$$\begin{pmatrix} \mathbf{O}_{1+9\times N,1+9\times N} & \mathbf{B}_1 \\ \mathbf{C}_1 & \mathbf{O}_{3,3} \end{pmatrix} \mathbf{r} = \mathbf{0}.$$

Obviously, $\mathbf{r}_{N+1} = 0$, because

$$det\begin{pmatrix} a_l^1 & b_l^1 & c_l^1 \\ a_l^2 & b_l^2 & c_l^2 \\ a_l^3 & b_l^3 & c_l^3 \end{pmatrix} = det\left(\mathbf{F}_l^{-1}\right) > 0.$$

In particular, it implies that $rank\left(\mathbf{B}_1\right) = 3$. To have $9 \times N - 2$ independent eigenvectors $\mathbf{r}$, we need to prove that $rank\left(\mathbf{C}_1\right) = 3$. For this it is sufficient to prove that $rank\left(\mathbf{C}_1\mathbf{B}_1\right) = 3$.

Theorem 1 *If $\nu \neq u$, then the eigenvalues of (3) are given by*

$$\det\left((u-\nu)^2\mathbf{I}_3 - \mathbf{K}\right) = 0,$$

where $\mathbf{K} = \mathbf{C}_1\mathbf{B}_1$. In particular, if $\mathbf{K}$ is symmetric and positive definite, then (3) has $9 \times N - 2 + 2 \times N$ real eigenvalues $\nu \neq u$ corresponding to $9 \times N - 2 + 2 \times N$ linear independent eigenvectors.

Proof. The characteristic polynomial (3) can be transformed as:

$$\det \begin{pmatrix} (u-\nu)\,\mathbf{I}_{1+9\times N} & \mathbf{B}_1 \\ \mathbf{C}_1 & (u-\nu)\,\mathbf{I}_3 \end{pmatrix} =$$

$$\det \left\{ \begin{pmatrix} \mathbf{I}_{1+9\times N} & \mathbf{O}_{1+9\times N,3} \\ \mathbf{C}_1(u-\nu)^{-1} & \mathbf{I}_3 \end{pmatrix} \begin{pmatrix} (u-\nu)\mathbf{I}_{1+9\times N} & \mathbf{B}_1 \\ \mathbf{O}_{3,1+9\times N} & (u-\nu)\mathbf{I}_3 - (u-\nu)^{-1}\mathbf{C}_1\mathbf{B}_1 \end{pmatrix} \right\}$$

$$= \det \begin{pmatrix} (u-\nu)\mathbf{I}_{1+9\times N} & \mathbf{B}_1 \\ \mathbf{O}_{3,1+9\times N} & (u-\nu)\mathbf{I}_3 - (u-\nu)^{-1}\mathbf{C}_1\mathbf{B}_1 \end{pmatrix}$$

$$= (u-\nu)^{9\times N-2} \det \left((u-\nu)^2\mathbf{I}_3 - \mathbf{C}_1\mathbf{B}_1 \right)$$

$$= (u-\nu)^{9\times N-2} \det \left((u-\nu)^2\mathbf{I}_3 - \left(\mathbf{M}_w + \sum_{l=1}^{N} Y_l \mathbf{D}_l \right) \right),$$

where

$$\mathbf{M}_w = \begin{pmatrix} c_w^2 & 0 & 0 \\ 0 & 0 & 0 \\ 0 & 0 & 0 \end{pmatrix}, \quad \mathbf{D}_l = \begin{pmatrix} -\frac{S_{11,l}}{\rho_l} - \frac{1}{\rho_l}\frac{\partial S_{11,l}}{\partial \mathbf{a}_l}\cdot \mathbf{a}_l & -\frac{1}{\rho_l}\frac{\partial S_{11,l}}{\partial \mathbf{a}_l}\cdot \mathbf{b}_l & -\frac{1}{\rho_l}\frac{\partial S_{11,l}}{\partial \mathbf{a}_l}\cdot \mathbf{c}_l \\ -\frac{S_{12,l}}{\rho_l} - \frac{1}{\rho_l}\frac{\partial S_{12,l}}{\partial \mathbf{a}_l}\cdot \mathbf{a}_l & -\frac{1}{\rho_l}\frac{\partial S_{12,l}}{\partial \mathbf{a}_l}\cdot \mathbf{b}_l & -\frac{1}{\rho_l}\frac{\partial S_{12,l}}{\partial \mathbf{a}_l}\cdot \mathbf{c}_l \\ -\frac{S_{13,l}}{\rho_l} - \frac{1}{\rho_l}\frac{\partial S_{13,l}}{\partial \mathbf{a}_l}\cdot \mathbf{a}_l & -\frac{1}{\rho_l}\frac{\partial S_{13,l}}{\partial \mathbf{a}_l}\cdot \mathbf{b}_l & -\frac{1}{\rho_l}\frac{\partial S_{13,l}}{\partial \mathbf{a}_l}\cdot \mathbf{c}_l \end{pmatrix}. \tag{4}$$

For isotropic solids each matrix $\mathbf{D}_l$ is symmetric (see [27] for the proof). If each $\mathbf{D}_l$ is positive definite, the eigenvalues ν are all real. In particular, $\mathbf{D}_l > 0$ for the equation of state (4) (see the proof in [27]). Now, consider the corresponding eigenvectors :

$$\begin{pmatrix} (u-\nu)\,\mathbf{I}_{1+9\times N} & \mathbf{B}_1 \\ \mathbf{C}_1 & (u-\nu)\,\mathbf{I}_3 \end{pmatrix} \mathbf{r} = \mathbf{0}.$$

Then

$$(u-\nu)\,\mathbf{s} + \mathbf{B}_1\mathbf{r}_{N+1} = 0, \qquad \mathbf{C}_1\mathbf{s} + (u-\nu)\,\mathbf{r}_{N+1} = 0.$$

It implies

$$\left((u-\nu)^2\,\mathbf{I} - \left(\mathbf{M}_w + \sum_{l=1}^{N} Y_l \mathbf{D}_l \right) \right) \mathbf{r}_{N+1} = 0. \tag{5}$$

If $\mathbf{M}_w + \sum_{l=1}^{N} Y_l \mathbf{D}_l$ is positive definite, the system has three independent eigenvectors $\mathbf{r}''$. Finally,

$$\mathbf{s} = -\frac{\mathbf{B}_1\mathbf{r}''}{u-\nu}.$$

We obtained a system of 6 linearly independent eigenvectors, because $u-\nu$ can have opposite signs. Hence, the total number of linearly independent vectors is also 6. The theorem is proved.

Remark The fact that the characteristic polynomial (5) depends only on $u-\nu$, is the property of the invariance of the governing equations with respect to the Galilean group of transformations.

If the model for each solid where the internal energy is given in separable form is hyperbolic (i.e. $\mathbf{D}_l > 0$, $l = 1, ..., N$) then the equilibrium visco-plastic model of N solids is hyperbolic.

C.2 Appendix: Hyperbolicity of a non-equilibrium visco-plastic model

As in the case of the equilibrium visco-plastic model, for the hyperbolicity study we consider only a homogeneous system (15) :

$$\begin{cases} \frac{\partial \rho}{\partial t} + div\,(\rho \mathbf{v}) = 0, \\ \frac{D\mathbf{e}_l^\beta}{Dt} + \left(\frac{\partial \mathbf{v}}{\partial \mathbf{x}}\right)^T \mathbf{e}_l^\beta = 0, \\ \rho \frac{D\mathbf{v}}{Dt} + div(-\boldsymbol{\sigma}) = 0, \\ \frac{D\alpha_l}{Dt} = 0, \\ \frac{DY_l}{Dt} = 0, \\ \frac{D\eta_l}{Dt} = 0. \end{cases} \tag{6}$$

It is sufficient to consider $1D$ case. We have:

$$\sum_{l=1}^{N} \alpha_l = 1, \quad \sum_{l=1}^{N} Y_l = 1.$$

These algebraic constraints can be viewed as constraints for initial data : if they are satisfied at $t = 0$, then they are satisfied for all $t > 0$. So, it is more convenient for the study of hyperbolicity to consider all $Y_1, ..., Y_N$ and $\alpha_1, ..., \alpha_N$ as independent variables. We choose as independent variables the vector:

$$\mathbf{U} = \big(\ \rho,\ \ \mathbf{a}_1,\ \ \mathbf{b}_1,\ \ \mathbf{c}_1,\ \ ...,\ \ \mathbf{a}_N,\ \ \mathbf{b}_N,\ \ \mathbf{c}_N,\ \ \mathbf{v}$$

$$\alpha_1,\ \ ...,\ \ \alpha_N,\ \ Y_1,\ \ ...,\ \ Y_N,\ \ \eta_1,\ \ ...,\ \ \eta_N\ \big)^T.$$

We present the stress tensor $\boldsymbol{\sigma}$ in the following form :

$$\boldsymbol{\sigma} = -p\mathbf{I}+\mathbf{S} = \sum_{l=1}^{N}(\alpha_l p_l \mathbf{I} + \alpha_l \mathbf{S}_l) = -\sum_{l=1}^{N}\alpha_l p_l\left(\frac{\rho Y_l}{\alpha_l}, \eta_l\right)\mathbf{I} - 2\rho\sum_{l=1}^{N}\left(Y_l\frac{\partial e_l^e}{\partial \mathbf{G}_l}\mathbf{G}_l\right).$$

We have then an explicit dependence of $\boldsymbol{\sigma}$ on ρ, $\mathbf{a}_l$, $\mathbf{b}_l$, $\mathbf{c}_l$, α_l, Y_l and η_l. This implies that:

$$\frac{\partial \boldsymbol{\sigma}}{\partial x} = -\sum_{l=1}^{N}\left(p_l\left(\frac{\rho Y_l}{\alpha_l}, \eta_l\right) - \rho_l c_l^2\right)\frac{\partial \alpha_l}{\partial x}\mathbf{I} - \rho\sum_{l=1}^{N}\left(c_l^2\mathbf{I} - \frac{\mathbf{S}_l}{\rho_l}\right)\frac{\partial Y_l}{\partial x} - \sum_{l=1}^{N}\alpha_l\frac{\partial p_l}{\partial \eta_l}\frac{\partial \eta_l}{\partial x}\mathbf{I}$$

$$-\left(\sum_{l=1}^{N}Y_l c_l^2\mathbf{I} - \frac{\mathbf{S}}{\rho}\right)\frac{\partial \rho}{\partial x} + \sum_{\beta=1}^{3}\sum_{l=1}^{N}\alpha_l\left(\frac{\partial \mathbf{S}_l}{\partial a_l^\beta}\frac{\partial a_l^\beta}{\partial x} + \frac{\partial \mathbf{S}_l}{\partial b_l^\beta}\frac{\partial b_l^\beta}{\partial x} + \frac{\partial \mathbf{S}_l}{\partial c_l^\beta}\frac{\partial c_l^\beta}{\partial x}\right).$$

Then, we rewrite (6) in non-conservative form:

$$\frac{\partial \rho}{\partial t} + u\frac{\partial \rho}{\partial x} + \rho\frac{\partial u}{\partial x} = 0,$$

$$\frac{\partial a_l^\beta}{\partial t} + u\frac{\partial a_l^\beta}{\partial x} + a_l^\beta\frac{\partial u}{\partial x} + b_l^\beta\frac{\partial v}{\partial x} + c_l^\beta\frac{\partial w}{\partial x} = 0,$$

$$\frac{\partial b_l^\beta}{\partial t} + u\frac{\partial b_l^\beta}{\partial x} = 0, \quad \frac{\partial c_l^\beta}{\partial t} + u\frac{\partial c_l^\beta}{\partial x} = 0,$$

$$\frac{\partial u}{\partial t} + u\frac{\partial u}{\partial x} + \frac{\left(\sum_{l=1}^{N}Y_l c_l^2 - \frac{S_{11}}{\rho}\right)}{\rho}\frac{\partial \rho}{\partial x}$$

$$-\sum_{1}^{N}\frac{\alpha_l}{\rho}\left(\frac{\partial S_{11,l}}{\partial \mathbf{a}_l}\cdot\frac{\partial \mathbf{a}_l}{\partial x} + \frac{\partial S_{11,l}}{\partial \mathbf{b}_l}\cdot\frac{\partial \mathbf{b}_l}{\partial x} + \frac{\partial S_{11,l}}{\partial \mathbf{c}_l}\cdot\frac{\partial \mathbf{c}_l}{\partial x}\right)$$

$$+\frac{1}{\rho}\sum_{l=1}^{N}\left(p_l\left(\frac{\rho Y_l}{\alpha_l}, n_l\right) - \rho_l c_l^2\right)\frac{\partial \alpha_l}{\partial x} + \sum_{l=1}^{N}\left(c_l^2 - \frac{S_{11,l}}{\rho_l}\right)\frac{\partial Y_l}{\partial x} + \frac{1}{\rho}\sum_{l=1}^{N}\alpha_l\frac{\partial p_l}{\partial \eta_l}\frac{\partial \eta_l}{\partial x} = 0,$$

$$\frac{\partial v}{\partial t}+u\frac{\partial v}{\partial x}-\frac{S_{12}}{\rho^2}\frac{\partial \rho}{\partial x}$$
$$-\sum_1^N\frac{\alpha_l}{\rho}\left(\frac{\partial S_{12,l}}{\partial \mathbf{a}_l}\cdot\frac{\partial \mathbf{a}_l}{\partial x}+\frac{\partial S_{12,l}}{\partial \mathbf{b}_l}\cdot\frac{\partial \mathbf{b}_l}{\partial x}+\frac{\partial S_{12,l}}{\partial \mathbf{c}_l}\cdot\frac{\partial \mathbf{c}_l}{\partial x}\right)$$
$$+\sum_{l=1}^N\left(-\frac{S_{12,l}}{\rho_l}\right)\frac{\partial Y_l}{\partial x}=0,$$
$$\frac{\partial w}{\partial t}+u\frac{\partial w}{\partial x}-\frac{S_{13}}{\rho^2}\frac{\partial \rho}{\partial x}$$
$$-\sum_1^N\frac{\alpha_l}{\rho}\left(\frac{\partial S_{13,l}}{\partial \mathbf{a}_l}\cdot\frac{\partial \mathbf{a}_l}{\partial x}+\frac{\partial S_{13,l}}{\partial \mathbf{b}_l}\cdot\frac{\partial \mathbf{b}_l}{\partial x}+\frac{\partial S_{13,l}}{\partial \mathbf{c}_l}\cdot\frac{\partial \mathbf{c}_l}{\partial x}\right)$$
$$+\sum_{l=1}^N\left(-\frac{S_{13,l}}{\rho_l}\right)\frac{\partial Y_l}{\partial x}=0,$$
$$\frac{\partial \alpha_l}{\partial t}+u\frac{\partial \alpha_l}{\partial x}=0,\quad l=1,...,N,$$
$$\frac{\partial Y_l}{\partial t}+u\frac{\partial \alpha_l}{\partial x}=0,\quad l=1,...,N,$$
$$\frac{\partial \eta_l}{\partial t}+u\frac{\partial \eta_l}{\partial x}=0,\quad l=1,...,N.$$

This system can be written as:

$$\mathbf{U}_t+\mathbf{D}\mathbf{U}_x=0.$$

Here

$$\mathbf{D}=\begin{pmatrix}\mathbf{A} & \mathbf{T}\\ \mathbf{O}_{3\times N,1+9\times N+3} & u\mathbf{I}_{3\times N}\end{pmatrix},$$
$$\mathbf{T}=\begin{pmatrix}\mathbf{O}_{1+9\times N,3\times N}\\ \mathbf{T}_1\end{pmatrix},$$

$$\mathbf{T}_1=\begin{pmatrix}\frac{1}{\rho}\left(p_1-\rho_1c_1^2\right) & ... & \frac{1}{\rho}\left(p_N-\rho_Nc_N^2\right) & \left(c_1^2-\frac{S_{11,1}}{\rho_1}\right) & ...\\ 0 & ... & 0 & \left(-\frac{S_{12,1}}{\rho_1}\right) & ...\\ 0 & ... & 0 & \left(-\frac{S_{13,1}}{\rho_1}\right) & ...\end{pmatrix}$$

$$\begin{pmatrix} \left(c_N^2 - \frac{S_{11,N}}{\rho_N}\right) & \frac{\alpha_1}{\rho}\frac{\partial p_l}{\partial \eta_l} & ... & \frac{\alpha_N}{\rho}\frac{\partial p_l}{\partial \eta_l} \\ \left(-\frac{S_{12,N}}{\rho_N}\right) & 0 & ... & 0 \\ \left(-\frac{S_{13,N}}{\rho_N}\right) & 0 & ... & 0 \end{pmatrix},$$

$$c_l^2 = \frac{\partial p_l}{\partial \rho_l} > 0, \quad \frac{\partial p_l}{\partial \eta_l} > 0, \quad l = 1, ..., N,$$

$$\mathbf{A} = \begin{pmatrix} u\mathbf{I}_{1+9\times N} & \mathbf{B}_1 \\ \mathbf{C}_1 & u\mathbf{I}_3 \end{pmatrix}.$$

Here $\mathbf{I}_n$ is the identity matrix of dimension $n \times n$, $\mathbf{O}_{n,m}$ is the null matrix of dimension $n \times m$ (n is the number of lines, and m is the number of columns), $\mathbf{B}_1$ and $\mathbf{C}_1$ are defined as:

$$\mathbf{B}_1 = \begin{pmatrix} \mathbf{m} \\ \mathbf{n}_1 \\ \mathbf{n}_2 \\ ... \\ \mathbf{n}_N \end{pmatrix}, \quad \mathbf{m} = \begin{pmatrix} \rho, & 0, & 0 \end{pmatrix}, \quad \mathbf{n}_l = \begin{pmatrix} a_l^1 & b_l^1 & c_l^1 \\ a_l^2 & b_l^2 & c_l^2 \\ a_l^3 & b_l^3 & c_l^3 \\ 0 & 0 & 0 \\ 0 & 0 & 0 \\ 0 & 0 & 0 \\ 0 & 0 & 0 \\ 0 & 0 & 0 \\ 0 & 0 & 0 \end{pmatrix},$$

$$\mathbf{C}_1 = \begin{pmatrix} \mathbf{n}, & \mathbf{m}_1, & \mathbf{m}_1, & ..., & \mathbf{m}_N \end{pmatrix}, \quad \mathbf{n} = \begin{pmatrix} \frac{c_f^2 - \frac{S_{11}}{\rho}}{\rho} \\ -\frac{S_{12}}{\rho^2} \\ -\frac{S_{13}}{\rho^2} \end{pmatrix},$$

$$\mathbf{m}_l = Y_l \begin{pmatrix} -\frac{1}{\rho_l}\frac{\partial S_{11,l}}{\partial \mathbf{a}_l} & -\frac{1}{\rho_l}\frac{\partial S_{11,l}}{\partial \mathbf{b}_l} & -\frac{1}{\rho_l}\frac{\partial S_{11,l}}{\partial \mathbf{c}_l} \\ -\frac{1}{\rho_l}\frac{\partial S_{12,l}}{\partial \mathbf{a}_l} & -\frac{1}{\rho_l}\frac{\partial S_{12,l}}{\partial \mathbf{b}_l} & -\frac{1}{\rho_l}\frac{\partial S_{12,l}}{\partial \mathbf{c}_l} \\ -\frac{1}{\rho_l}\frac{\partial S_{13,l}}{\partial \mathbf{a}_l} & -\frac{1}{\rho_l}\frac{\partial S_{13,l}}{\partial \mathbf{b}_l} & -\frac{1}{\rho_l}\frac{\partial S_{13,l}}{\partial \mathbf{c}_l} \end{pmatrix},$$

where

$$c_f^2 = \sum_{l=1}^{N} Y_l c_l^2.$$

Hence, the characteristic polynomial is:

$$det\,(\mathbf{D}-\nu\mathbf{I}) = (u-\nu)^{3\times N}\, det\,(\mathbf{A}-\nu\mathbf{I}_{1+9\times N+3}) = 0.$$

Then we have to solve the characteristic equation:

$$det\,(\mathbf{A}-\nu\mathbf{I}) = \begin{pmatrix} (u-\nu)\,\mathbf{I}_{1+9\times N} & \mathbf{B}_1 \\ \mathbf{C}_1 & (u-\nu)\,\mathbf{I}_3 \end{pmatrix} = 0. \tag{7}$$

Let us consider the first case : $\nu = u$. We will show that there are $9\times N-2$ linear independent eigenvectors of the matrix $\mathbf{A}$ corresponding to this eigenvalue. Let $\mathbf{r}$ be a right eigenvector of $\mathbf{A}$ corresponding to $\nu = u$:

$$\mathbf{r}^T = \begin{pmatrix} \mathbf{s}^T, & \mathbf{r}_{N+1}^T \end{pmatrix} = \begin{pmatrix} r_0, & \mathbf{r}_1^T, & ..., & \mathbf{r}_N^T, & \mathbf{r}_{N+1}^T \end{pmatrix}$$

with r_0 being a scalar, $\mathbf{r}_l$ being a 9 components vector and $\mathbf{r}_{N+1}$ a 3 components vector. The equation for the eigenvectors is :

$$\begin{pmatrix} \mathbf{O}_{1+9\times N,1+9\times N} & \mathbf{B}_1 \\ \mathbf{C}_1 & \mathbf{O}_{3,3} \end{pmatrix} \mathbf{r} = \mathbf{0}.$$

Obviously, $\mathbf{r}_{N+1} = 0$, because

$$det \begin{pmatrix} a_l^1 & b_l^1 & c_l^1 \\ a_l^2 & b_l^2 & c_l^2 \\ a_l^3 & b_l^3 & c_l^3 \end{pmatrix} = det\left(\mathbf{F}_l^{-1}\right) > 0.$$

In particular, it implies that $\mathrm{rank}\,(\mathbf{B}_1) = 3$. To have $9\times N-2$ linear independent eigenvectors $\mathbf{r}$, we need to prove that $\mathrm{rank}\,(\mathbf{C}_1) = 3$. For this it is sufficient to prove that $rank\,(\mathbf{C}_1\mathbf{B}_1) = 3$.

Theorem 2 *If $\nu \neq u$, then the eigenvalues of (7) are given by*

$$\det\left((u-\nu)^2\mathbf{I}_3 - \mathbf{K}\right) = 0,$$

where $\mathbf{K} = \mathbf{C}_1\mathbf{B}_1$**.** *In particular, if $\mathbf{K}$ is symmetric and positive definite, then (7) has $9\times N-2+3\times N$ real eigenvalues $\nu \neq u$ corresponding to $9\times N-2+3\times N$ independent eigenvectors.*

Proof. *Consider now the case where $\nu \neq u$. The characteristic polynomial (7) can be transformed as :*

$$\det \begin{pmatrix} (u-\nu)\,\mathbf{I}_{1+9\times N} & \mathbf{B}_1 \\ \mathbf{C}_1 & (u-\nu)\,\mathbf{I}_3 \end{pmatrix} =$$

$$\det \begin{pmatrix} \mathbf{I}_{1+9\times N} & \mathbf{O}_{1+9\times N,3} \\ \mathbf{C}_1(u-\nu)^{-1} & \mathbf{I}_3 \end{pmatrix} \begin{pmatrix} (u-\nu)\mathbf{I}_{1+9\times N} & \mathbf{B}_1 \\ \mathbf{O}_{3,1+9\times N} & (u-\nu)\mathbf{I}_3 - (u-\nu)^{-1}\mathbf{C}_1\mathbf{B}_1 \end{pmatrix}$$

$$= \det \begin{pmatrix} (u-\nu)\mathbf{I}_{1+9\times N} & \mathbf{B}_1 \\ \mathbf{O}_{3,1+9\times N} & (u-\nu)\mathbf{I}_3 - (u-\nu)^{-1}\mathbf{C}_1\mathbf{B}_1 \end{pmatrix}$$

$$= (u-\nu)^{9\times N-2} \det\left((u-\nu)^2\mathbf{I}_3 - \mathbf{C}_1\mathbf{B}_1\right)$$

$$= (u-\nu)^{9\times N-2} \det\left((u-\nu)^2\mathbf{I}_3 - \left(\mathbf{M}_f + \sum_{l=1}^{N} Y_l\mathbf{D}_l\right)\right),$$

where

$$\mathbf{M}_f = \begin{pmatrix} c_f^2 & 0 & 0 \\ 0 & 0 & 0 \\ 0 & 0 & 0 \end{pmatrix}, \quad \mathbf{D}_l = \begin{pmatrix} -\frac{S_{11,l}}{\rho_l} - \frac{1}{\rho_l}\frac{\partial S_{11,l}}{\partial \mathbf{a}_l}\cdot\mathbf{a}_l & -\frac{1}{\rho_l}\frac{\partial S_{11,l}}{\partial \mathbf{a}_l}\cdot\mathbf{b}_l & -\frac{1}{\rho_l}\frac{\partial S_{11,l}}{\partial \mathbf{a}_l}\cdot\mathbf{c}_l \\ -\frac{S_{12,l}}{\rho_l} - \frac{1}{\rho_l}\frac{\partial S_{12,l}}{\partial \mathbf{a}_l}\cdot\mathbf{a}_l & -\frac{1}{\rho_l}\frac{\partial S_{12,l}}{\partial \mathbf{a}_l}\cdot\mathbf{b}_l & -\frac{1}{\rho_l}\frac{\partial S_{12,l}}{\partial \mathbf{a}_l}\cdot\mathbf{c}_l \\ -\frac{S_{13,l}}{\rho_l} - \frac{1}{\rho_l}\frac{\partial S_{13,l}}{\partial \mathbf{a}_l}\cdot\mathbf{a}_l & -\frac{1}{\rho_l}\frac{\partial S_{13,l}}{\partial \mathbf{a}_l}\cdot\mathbf{b}_l & -\frac{1}{\rho_l}\frac{\partial S_{13,l}}{\partial \mathbf{a}_l}\cdot\mathbf{c}_l \end{pmatrix}. \tag{8}$$

In the case of isotropic solids each matrix $\mathbf{D}_l$ is symmetric (see [27] for the proof). If each $\mathbf{D}_l$ is positive definite, the eigenvalues ν are all real. This is the case, in particular, for the equation of state (4) (see the proof in [27]). Now, consider the corresponding eigenvectors.

$$\begin{pmatrix} (u-\nu)\,\mathbf{I}_{1+9\times N} & \mathbf{B}_1 \\ \mathbf{C}_1 & (u-\nu)\,\mathbf{I}_3 \end{pmatrix} \mathbf{r} = \mathbf{0}.$$

Then

$$(u-\nu)\,\mathbf{s} + \mathbf{B}_1\mathbf{r}_{N+1} = 0, \qquad \mathbf{C}_1\mathbf{s} + (u-\nu)\,\mathbf{r}_{N+1} = 0.$$

It implies

$$\left((u-\nu)^2\,\mathbf{I} - \left(\mathbf{M}_f + \sum_{l=1}^{N} Y_l\mathbf{D}_l\right)\right)\mathbf{r}_{N+1} = 0. \tag{9}$$

If $\mathbf{M}_f + \sum_{l=1}^{N} Y_l\mathbf{D}_l$ is positive definite, the system has three independent eigenvectors $\mathbf{r}''$. Finally,

$$\mathbf{s} = -\frac{\mathbf{B}_1\mathbf{r}''}{u-\nu}.$$

We obtained a system of 6 linearly independent eigenvectors, because $u-\nu$ can have opposite signs. Hence, the total number of linearly independent vectors is also 6. The theorem is proved.

In conclusion, if the visco-plastic model for each solid with the energy in separable form is hyperbolic (i.e. $\mathbf{D}_l = \mathbf{D}_l^T > 0$, $l = 1, ..., N$) then (15) is hyperbolic.

C.3 Weak sub-characteristic condition

The sub-characteristic condition (or Whitham condition [35]) states that the characteristic velocities of a relaxed system should be interplaced between the velocities of a relaxing system. Such a condition guarantees in a sense a right mathematical modelling of a physical phenomena. The formal proof of this fact is not direct and is always specific to mathematical models under study (see, for example, [12] where this property was established for a class of two-phase fluid models with relaxation). In this section, we will establish a weak sub-characteristic condition. We will show that the longitudinal waves of the equilibrium visco-plastic model (12) are not faster than the longitudinal waves of the non-equilibrium visco-plastic model (15). A similar result will be proved for the slowest transverse wave.

The expressions for the equilibrium' sound speed (Wood sound speed) and the 'frozen' sound speed are given by:

$$\frac{1}{\rho c_w^2} = \sum_{l=1}^{N} \frac{\alpha_l}{\rho_l c_l^2}, \qquad c_f^2 = \sum_{l=1}^{N} Y_l c_l^2, \qquad c_w^2 \leq c_f^2.$$

Let us consider first the case of longitudinal waves. Let λ_f^{max} and λ_w^{max} being the biggest eigenvalue of the matrix $\mathbf{N}_f = \mathbf{M}_f + \sum_{l=1}^{N} Y_l \mathbf{D}_l$ and $\mathbf{N}_w = \mathbf{M}_w + \sum_{l=1}^{N} Y_l \mathbf{D}_l$, respectively (see for definitions (4), (8)). We need to prove that: $\lambda_w^{max} \leq \lambda_f^{max}$. Let $\mathbf{r}$ be an eigenvector of norm 1 associated with the eigenvalue λ_w^{max}. Then, we have:

$$\lambda_w^{max} = \mathbf{r}^T \mathbf{N}_w \mathbf{r} = \mathbf{r}^T \mathbf{M}_w \mathbf{r} + \mathbf{r}^T \left(\sum_{l=1}^{N} Y_l \mathbf{D}_l \right) \mathbf{r} \leq \mathbf{r}^T \mathbf{M}_f \mathbf{r} + \mathbf{r}^T \left(\sum_{l=1}^{N} Y_l \mathbf{D}_l \right) \mathbf{r}$$

$$= \mathbf{r}^T \mathbf{N}_f \mathbf{r} \leq \lambda_f^{max} ||\mathbf{r}||^2 = \lambda_f^{max}.$$

Finally, we consider the case of transverse waves. Let $\lambda_f^{\min}$ and $\lambda_w^{\min}$ being the smallest eigenvalue of the matrix $\mathbf{N}_f$ and $\mathbf{N}_w$, respectively. We need to prove that: $\lambda_w^{\min} \leq \lambda_f^{\min}$. Let $\mathbf{r}$ be an eigenvector of norm 1 associated with the eigenvalue $\lambda_f^{\min}$. Then, we have:

$$\lambda_w^{\min} = \lambda_w^{\min} ||\mathbf{r}||^2 \leq \mathbf{r}^T \mathbf{N}_w \mathbf{r} = \mathbf{r}^T \mathbf{M}_w \mathbf{r} + \mathbf{r}^T \left(\sum_{l=1}^{N} Y_l \mathbf{D}_l \right) \mathbf{r} \leq \mathbf{r}^T \mathbf{M}_f \mathbf{r} + \mathbf{r}^T \left(\sum_{l=1}^{N} Y_l \mathbf{D}_l \right) \mathbf{r}$$

$$= \mathbf{r}^T \mathbf{N}_f \mathbf{r} = \lambda_f^{\min}.$$

It was thus shown that:

- $\lambda_w^{\min} \leq \lambda_f^{\min}$.
- $\lambda_w^{\max} \leq \lambda_f^{\max}$.

C.4 Lyapunov function

The purpose of this part is to show that

$$L_l = \mathbf{S}_l : \mathbf{S}_l$$

is a Lyapunov function for system (22). In particular, it implies that our solution attains the von Mises yield surface given by :

$$\mathbf{S}_l : \mathbf{S}_l = \frac{2}{3}\sigma_{Y,l}^2,$$

where $\mathbf{S}_l$, $\sigma_{Y,l}$ are the deviatoric part of the stress tensor, and the yield elastic limit of phase l, respectively. Since the proof is the same for any l, we will simplify the notations by deleting the index 'l'. Equations (22) are

$$\frac{dk_\beta}{dt} = \frac{S_\beta k_\beta}{\tau_{rel}}.$$

They admit the first integral

$$k_1 k_2 k_3 = const.$$

It implies that the density $\rho = \rho_0 k_1 k_2 k_3$ is conserved during this relaxation step. In the case of the equation of state (4) we have :

$$S_\beta = -\frac{\mu}{2}\frac{\rho}{\rho_0}\left(\frac{k_\beta^4}{(k_1k_2k_3)^{\frac{4}{3}}} - \frac{1}{3}\sum_\alpha \frac{k_\alpha^4}{(k_1k_2k_3)^{\frac{4}{3}}}\right).$$

Hence

$$\frac{dL}{dt} = \frac{d}{dt}\sum_\beta S_\beta^2 = 2\sum_\beta S_\beta \frac{dS_\beta}{dt} = -\mu\frac{\rho}{\rho_0}\sum_\beta S_\beta\left(\frac{4k_\beta^3}{(k_1k_2k_3)^{\frac{4}{3}}}\frac{dk_\beta}{dt} - \frac{4}{3}\sum_\alpha \frac{k_\alpha^3}{(k_1k_2k_3)^{\frac{4}{3}}}\frac{dk_\alpha}{dt}\right)$$

$$= -\mu \frac{\rho}{\rho_0} \sum_\beta S_\beta \frac{4k_\beta^3}{(k_1 k_2 k_3)^{\frac{4}{3}}} \frac{dk_\beta}{dt}$$

$$= -\frac{4\mu}{\tau_{rel}} \frac{\rho}{\rho_0} \sum_\beta S_\beta^2 \frac{k_\beta^4}{(k_1 k_2 k_3)^{\frac{4}{3}}} < 0.$$

The yield surface is attained in finite or infinite time depending on the exponent n_l in (13). This completes the proof.